A LARGE SCALE GENOMIC SCREEN REVEALS MECHANISMS OF YEAST POSTREPLICATION REPAIR IN *SACCHAROMYCES CEREVISIAE*

A Thesis Submitted to the College of

Graduate Studies and Research

In Partial Fulfillment of the Requirements

For the Degree of Doctor of Philosophy

In the Department of Microbiology and Immunology

University of Saskatchewan

Saskatoon, SK. CANADA

LINDSAY GAIL BALL

PERMISSION TO USE

In presenting this thesis in partial fulfilment of the requirements for a Postgraduate degree from the University of Saskatchewan, I agree that the libraries of this University may make it freely available for inspection. I further agree that permission for copying of this thesis in any manner, in whole or in part, for scholarly purposes may be granted by the professor or professors who supervised my thesis work or, in their absence, by the Head of the Department or the Dean of the College in which my thesis work was done. It is understood that any copying or publication or use of this thesis or parts thereof for financial gain shall not be allowed without my written permission. It is also understood that due recognition shall be given to me and to the University of Saskatchewan in any scholarly use which may be made of any material in my thesis.

Requests for permission to copy or to make other use of material in this thesis in whole or part should be addressed to:

Head of the Department of Microbiology and Immunology
University of Saskatchewan
Health Science Building
107 Wiggins Road, Room A302
Saskatoon, Saskatchewan.
S7N 5E5
CANADA

ABSTRACT

In *Saccharomyces cerevisiae* DNA postreplication repair (PRR) functions to bypass replication-blocking lesions to prevent damage-induced cell death. PRR employs two different mechanisms to bypass damaged DNA. While translesion synthesis (TLS) has been well characterized, little is known about the molecular events involved in error-free bypass although it has been assumed that homologous recombination (HR) is required for such a mode of lesion bypass. We undertook a genome-wide, synthetic genetic array (SGA) screen for novel genes involved in PRR and observed evidence of genetic interactions between error-free PRR and HR. We were screening for synthetic lethality which occurs when the combination of two mutations leads to an inviable organism, however, either single mutation allows for cell viability. In addition, we screened for conditionally synthetic lethal interaction which occurs when the combination of two mutations is inviable only in the presence of a DNA-damaging agent. This screen identified and assigned four genes, *CSM2, PSY3, SHU1* and *SHU2*, whose products form a stable Shu complex, to the error-free PRR pathway. Previous studies have indicated that the Shu complex is required for efficient HR and that inactivation of any one of these genes is able to suppress the severe phenotypes of *top3* and *sgs1*. We confirmed and further extended some of the reported observations and demonstrated that error-free PRR mutations are also epistatic to *sgs1*. Based on the above analyses, we

propose a model in which error-free PRR utilizes the Shu complex to recruit HR to facilitate template switching, followed by double-Holliday junction resolution by Sgs1-Top3.

Null mutations of HR genes including *rad51, 52, 54, 55* and *57* are known to confer characteristic synergistic interactions with TLS mutations. To our surprise, null mutations of genes encoding the Mre11-Rad50-Xrs2 (MRX) complex, which is also required for HR, are epistatic to TLS mutations. The MRX complex confers an endo/exonuclease activity required for the detection and processing of DNA double-strand breaks (DSBs). Our results suggest that the MRX complex functions in both TLS and error-free PRR and that this function requires the nuclease activity of Mre11. This is in sharp contrast to other known HR genes that only function downstream of error-free PRR. Furthermore, we found that inactivation of *SGS1* significantly inhibits proliferating cell nuclear antigen (PCNA) monoubiquitination and is epistatic to mutations in TLS, suggesting that Sgs1 also functions at earlier steps in DNA lesion bypass. We also examined the roles of Sae2 and Exo1, two accessory nucleases involved in DSB resection, in PRR. We found that while Sae2 is primarily required for TLS, Exo1 is exclusively involved in error-free PRR. In light of the distinct and overlapping activities of the above nucleases in the resection of DSBs, we propose that the distinct single-strand nuclease activities of MRX, Sae2 and Exo1 dictate the preference between TLS and error-free PRR for lesion bypass.

While both PRR pathways are dependent on the ubiquitination of PCNA, error-free PRR utilizes non-canonical Lys63-linked polyubiquitinated PCNA to signal lesion

bypass. This mechanism is dependent on the Mms2-Ubc13 complex being in close proximity to PCNA, a process thought to be dependent on Rad5. Rad5 is a member of the SWI/SNF family of ATPases that contains a RING finger motif characteristic of an E3 Ub ligase. Previous *in vitro* experiments demonstrated the ability of Rad5 to promote replication fork regression, a function dependent on its helicase/ATPase activity. We therefore created site-specific mutants defective in either Rad5 RING finger or helicase/ATPase activity, or both, in order to examine their genetic interactions with known TLS and error-free PRR genes. Our results indicate that both the Rad5 RING finger motif and the helicase/ATPase activity are exclusively involved in error-free PRR. To our surprise, like the Rad5 RING finger, lack of the helicase/ATPase activity also abolishes the Lys63-linked PCNA polyubiquitin chain formation, suggesting that either the Rad5 helicase/ATPase-promoted replication fork regression signals PCNA polyubiquitination or this domain has a yet unidentified activity.

In summary, results obtained from this thesis dissertation have revealed novel mechanisms of yeast PRR in *S. cerevisiae*, a mechanism that appears to be evolutionarily conserved throughout eukaryotes, from yeast to humans.

ACKNOWLEDGMENTS

There are many people to whom I am eternally grateful to for their guidance, support, friendship and love while I worked towards achieving my Ph.D. I would not be where I am today without you, so Thank you!

I would like to thank my supervisor, Dr. Wei Xiao. Thank you for allowing me the opportunity to work and learn in your laboratory. Your knowledge, enthusiasm, and devotion to research are inspiring and infectious. You have opened doors for me that I didn't know existed, and for that I am eternally grateful for all that you have done for me, Thank you!

I would like to thank my committee members for their support and guidance during my graduate studies, Dr. Peter Bretscher, Dr. Michel Desautels, Dr. Ron Geyer, Dr. Troy Harkness, and to Dr. Linda Reha-Krantz for agreeing to be my external examiner.

To those that I have had the privilege of collaborating with during my graduate studies, Dr. Charles Boone, Dr. Jennifer Cobb, Dr. Barry Ziola and Renee Brost, Thank you!

Thank you to ALL the members of Wei Xiao laboratory, both past and present, that I have had the pleasure of working with! Especially; Parker Andersen, Audesh Bhat, Leslie Barbour, Michael Biss, Hania Dworaczek, Yu Fu, Li Jia, Landon Pastushok, and

Rui Wen. To Ke Zhang, Michelle Hanna, and Amanda Lambrecht Thank you not only for your technical assistance in accomplishing this body of work, but also for your friendship! To Lindsay Pelzer your friendship both inside and outside the lab means the world to me, Thank you!

To the department of Microbiology and Immunology, and now Biomedical sciences, Thank you! A special Thank you to Mary, Dawn, Vern, Katie, Sherry, and Evelyn.

To my Family and Friends, THANK YOU! Your love, support and friendship has given me the strength to finish my thesis! I am eternally grateful to all of you, and truly blessed to have you in my life! To my Mom and Dad, the words Thank you are not enough to tell you how grateful I am to the two of you! Thank you for your never ending, never wavering love and support! Thank you for never letting me give up, and for teaching me to believe that I can accomplish anything that I set my mind to. Thank you for giving me wings to fly! I am truly blessed to call the two of you Mom and Dad!

Thank you!

TABLE OF CONTENTS

LIST OF TABLES

Table **Page number**

LIST OF FIGURES

Figure **Page number**

LIST OF ABBREVIATIONS

Abbreviation

°C .....Degrees celsius, a unit of measurement for temperature
Δ .....Deletion mutant (null mutation)
•OH .....Hydroxyl radical
% .....Percentage
3-AT.....3-amino triazole
3-meA 3-methyl-adenine
4-NQO 4-Nitroquinoline
6-4 PP.....6-4 photoproducts
8-oxoG 7, 8-dihydro-8-oxoguanine
A.....Adenine
aa.....Amino acids
Ade.....Adenine
ADP .....Adenosine diphosphate
Amp .....Ampicillin
AP .....Apurinic or apyrimidinic site
APS .....Ammonium persulfate
ATP.....Adenosine triphosphate
ATPase.....An enzyme that catalyzes ATP to ADP
BER.....Base excision repair
BIR.....Break-induced repair
C.....Cytosine
CPD.....Cyclobutane pyrimidine dimer
CSM2 .....Chromosome segregation in meiosis
ddH_2O .....Double-distilled sterile water (or reversed osmosed)
DDT .....DNA damage tolerance
dHJ.....Double-Holliday junction
DMA .....Deletion mutant array
DMSO.....Dimethyl sulfoxide
DNA.....Deoxyribonucleic acid
DSBR .....Double-strand break repair
DSB.....Double-strand breaks
DTT.....Dithiothreitol
E1, E2, E3, ...Ub-activating enzyme, Ub-conjugating enzyme, Ub-ligase
EDTA.....(Ethylenedinitrilo)tetraacetic Acid

EMS .....Ethyl methanesulfonate
ENU .....Ethylnitrosourea
FOA .....5-Fluoroorotic acid
g .....Gram, a unit of mass
G.....Guanine
G418.....Kanamycin resistance
Gal_{AD} .....Galactose activating domain
Gal_{BD} .....Galactose binding domain
GCR .....Gross chromosomal rearrangement
GST .....Glutathione-S-transferase
HCl.....Hydrochloric acid
His .....Histidine
HR.....Homologous recombination
HU.....Hydroxyurea
HUH.....*hisG-URA-HisG*
I .....Isoleucine
IPTG.....Isopropylthio-b-D-galactoside
IR .....Ionizing radiation
K.....Lysine
kan^R .....Kanamycin resistance/G418 resistance
L .....Litre
LB .....Luria broth
Leu .....Leucine
LiOAc .....Lithium acetate
Lys .....Lysine
mAb .....Monoclonal antibody
µL.....Microlitre
mL .....Millilitre
MMC.....Mitomycin C
MMR.....Mismatch Repair
MMS .....Methyl methanesulfonate
MNNG .....*N*-methyl-*N*'-nitro-*N*-nitrosoguanidine
MNU .....Methylnitrosourea
MRX Mre11-Rad50-Xrs2
mSv .....Millisievert, a measurement of radiation dose
nat^R.....ClonNAT resistance
NEM.....N-ethylmaleimide
NER .....Nucleotide excision repair
NHEJ.....Non-homologous end joining
O^6-meG .....O^6-methylguanine
OD.....Optical density
ORF.....Open reading frame
PBS .....Phosphate buffered saline
PBST.....PBS with 0.05% Tween 20 polyoxyethylene 20 sorbitan monolaurate

PCNA.....Proliferating cell nuclear antigen
PCR.....Polymerase chain reaction
PEG.....Polyethylene glycol
PIP.....PCNA interacting protein
PMSF .....Phenylmethylsulfonyl fluoride
Polζ.....Polymerase ζ
PPCB.....Protease cleavage buffer
PRR.....Postreplication repair
psi.....Pounds per square inch (unit of measure for pressure)
PSY3.....Platinum sensitivity
PVDF .....Polyvinylidene difluoride
R.....Arginine
Rad.....Radiation
RING.....Really interesting new gene
ROS.....Reactive oxygen species
RPA.....Replication protein A
rpm.....Revolutions per minute
RSA.....Random spore analysis
S .....Serine
SD .....Synthetic dextrose
SDS .....Sodium dodecyl sulfate
SDSA .....Synthesis-dependent strand annealing
SDS-PAGE .....SDS-polyacrylamide gel electrophoresis
SDSA .....Synthesis-dependent strand annealing
SHU1.....Suppressor of *sgs1* HU sensitivity
SHU2.....Suppressor of *sgs1* HU sensitivity
SGA .....Synthetic genetic array
SGD .....Saccharomyces genome database
SMC.....Structural maintenance of chromosomes
SOC.....Super optimal broth with catabolite repression
SSA .....Single-strand annealing
ssDNA.....Single-strand DNA
SSB .....ssDNA break
SUMO.....Small ubiquitin-like modifier
T .....Thymine
TAE.....Tris-acetate EDTA buffer
TCA .....Trichloracetic acid
TE.....Tris EDTA buffer
TEMED.....N,N,N’,N’–Tetramethylethylenediamine
TLS .....Translesion synthesis
Trp.....Tryptophan
TSS.....Transformation and storage solution
UBM .....Ub-binding motifs
Ura .....Uracil

USD .....Unscheduled DNA synthesis
UV.....Ultraviolet
Ub.....Ubiquitin
V.....Volt
v/v .....Volume/volume
w/v .....Weight/volume
XP .....Xeroderma pigmentosum
XPV .....Xeroderma pigmentosum variant
Y2H.....Yeast two-hybrid
YPD .....Yeast-extract peptone dextrose
YPAD.....YPD with adenine added

CHAPTER ONE

INTRODUCTION

Deoxyribonucleic acid (DNA) contains the instructions for life, and as such must be preserved. At the core of the DNA helix structure are two nucleotides joined together by hydrogen bonds which align in a Watson-Crick base pairing scheme where A aligns with T, and C aligns with G in a stepwise manner. External to the DNA nucleotides are two phosphate-deoxyribose backbones upheld by phosphodiester bonds. DNA is organized into chromosomes that must be correctly duplicated before cellular division may occur. During normal DNA replication DNA fidelity is maintained by the polymerase selection of correct base pairing and an associated 3`-5` proofreading exonuclease. Although DNA mutations are required for evolutionary changes a balance between genomic stability and instability must be maintained for cell survival and inheritance. Cellular DNA is quite dynamic and is subject to constant assault as it readily reacts with a variety of agents both internal and external to the cell. Therefore, in order to maintain genomic integrity living organisms have developed a comprehensive set of highly conserved mechanisms to deal with DNA damage. Depending on the source, DNA damage can be predominantly divided into two categories: endogenous DNA damage referring to damage occurring from within the cell, while the second category pertains to both physical and chemical DNA damage originating from outside the cell.

1.1 – DNA Damage

1.1.1 – Spontaneous DNA Damage

Cellular metabolism, although vital to cell survival also results in accidental spontaneous DNA damage from a variety of sources. DNA constantly reacts with oxygen, water, and UV radiation from the sun, all essential requirements to life, but have the potential devastating ability to alter and spontaneously damage DNA. Oxygen is one trigger of spontaneous DNA damage. Although oxygen is required for life, reactive oxygen species (ROS) formed as byproducts of aerobic metabolism are highly toxic to cells as they readily react with DNA at an estimated rate of 10^4-10^6 oxidized adducts/cell/day (Ames and Gold, 1991). Such adducts may occur on any of the four DNA nucleotides and on deoxyribose. Predominantly, intracellular ROS emanate from errors in the electron transport chain during mitochondrial respiration (Friedberg *et al.*, 2006). However, additional ROS may originate from extracellular sources such as radiation, redox cycling compounds, various drugs and chemicals. ROS are a major source of spontaneous DNA damage in numerous intracellular macromolecules including proteins, lipids, carbohydrates, and nucleic acids (Friedberg *et al.*, 2006), and are known to cause more than 80 products of DNA nucleotide damage (Bjelland and Seeberg, 2003).

The leading source of DNA damage caused by ROS is thought to be the formation of Fenton oxidants that are the result of H_2O_2 reacting with iron-complexed DNA (Fenton, 1894; Friedberg *et al.*, 2006). It was later confirmed that the oxidant produced in this reaction was indeed the hydroxyl radical ($\bullet$OH) (Haber and Weiss, 1939; Koppenol, 2001). Once the reactive hydrophilic hydroxyl radicals are formed near DNA

they are highly reactive (Breen and Murphy, 1995), and as such predominantly add excessive hydrogen atoms to the double-bonds of DNA nucleotides, or remove hydrogen from the deoxyribose sugar in DNA resulting in fragmentation, nucleotide loss, and or single- and double-strand breaks .

Not only is genomic DNA subject to hydroxyl radicals, but also its precursors. The ROS induced lesion 7, 8-dihydro-8-oxoguanine (8-oxoG) is one such example. 8-oxoG can be incorporated into the parent strand of DNA following oxidation, but additionally the daughter strand can have a precursor 8-oxoG incorporated. 8-oxoG is usually incorrectly base-paired with an A residue resulting in a transverse mutation (Cheng *et al.*, 1992; Kuchino *et al.*, 1987; Shibutani *et al.*, 1991). Should these mutations not be removed subsequent rounds of replication can incorporate the error thereby compounding the initial DNA damage (Friedberg *et al.*, 2006). Cells typically maintain a balance between biochemical antioxidants and enzymes to breakdown ROS; however, if the balance is upset by an increase in ROS, redox active chemicals, or oxygen availability the results can be devastating.

Cells have multiple mechanisms to protect against reactive oxygen species. These mechanisms include maintaining a decreasing oxygen gradient from extracellular to intracellular levels, compartmentalization of DNA to the nucleus away from oxygen metabolism, DNA protection via histones, the ability to trigger cell cycle arrest, degradation of damaged macromolecules, and induction of apoptosis in eukaryotes, all of which contribute to the cells ability to protect against spontaneous DNA damage via reactive oxygen species. Despite the vast ability of cells to protect against damage,

spontaneous DNA damage by oxygen and cellular metabolism is still inevitable. In humans, oxidative stress has been implicated in neurodegenerative disorders, atherosclerosis, cancer, alcohol-induced liver damage, as well as a contributing factor to the ageing process (Friedberg *et al.*, 2006). Although potentially devastating, cells have the ability to use ROS to their advantage in the innate immune response against bacterial pathogenesis (Segal and Shatwell, 1997; Vazquez-Torres *et al.*, 2001).

In addition to ROS, deamination, or loss of an exocyclic amino group from cytosine, adenine, guanine, or 5-methylcytosine, which readily occurs at physiological pH and temperature, results in the affected nucleotide being converted to uracil, hypoxanthine, xanthine or thymine, respectively, and is a prevalent form of spontaneous DNA damage. Mammalian cells under physiological conditions reportedly deaminate cytosine residues to uracil at a rate of 100-500 times/day (Adelman *et al.*, 1988; Albert and Burns, 1977; Ames *et al.*, 1993; Friedberg *et al.*, 2006).

DNA nucleotides are continually lost from nucleic acids resulting in abasic sites. Abasic, or AP (apurinic or apyrimidinic) sites can be spontaneously formed when the N-glycosyl bond between the DNA nucleotide and sugar is cleaved leaving behind an intact sugar-phosphate chain. Spontaneous depurination in human cells is thought to occur at a rate of approximately 9,000 bases/cell/day (Prise *et al.*, 1994), and even cells maintained at a physiological temperature reportedly lose 18,000 purine residues everyday due to hydrolysis of the N-glycosyl bond in DNA (Allen and Tresini, 2000; Alvarez *et al.*, 1998; Friedberg *et al.*, 2006). Fortunately, repair of the damage caused by depurination is quickly initiated by ubiquitous AP endonucleases at a rate that is greater than the

spontaneous damage can occur (Lindahl, 1993). However, AP sites also arise as an intermediate during base excision repair (BER) (discussed later). Although AP sites formed in this manner are short lived, deficiencies in BER will result in the accumulation of AP sites (Friedberg *et al.,* 2006). Cells completely lacking AP repair enzymes in *S. cerevisiae* are rendered inviable (Guillet and Boiteux, 2003).

It has also been stated that DNA replication alone introduces enough spontaneously induced errors to overwhelm a cell with potentially devastating outcomes (Friedberg *et al.,* 2006). This may be the result of a misinsertion of nucleotides during syntheses, which is a plausible result even though replicative DNA polymerases typically function with high fidelity. Although errors introduced during replication are generally resolved immediately by associated exonucleases, should errors persist beyond this point they are excised and corrected post-replicatively by mismatch repair.

There are a seemingly overwhelming number of ways in which DNA can be spontaneously damaged, and the above sources are only a portion of ways by which DNA can be damaged. Exogenous DNA damage is also a major contributing factor to cellular DNA damage.

1.1.2 – Exogenous DNA Damage

1.1.2.1 – Physical DNA-damaging Agents

Ionizing radiation (IR) is a naturally occurring external source of physical damage to DNA, and results in excited and ionized molecules that have the ability to randomly cause damage to all cellular components, including DNA lesions (Friedberg *et al.*, 2006).

Typically people living in the United States of America are exposed to 1-2 mSv per year, with an additional dose of 0.5 mSv possibly due to artificial radiation sources utilized in the medical profession for diagnostics and treatment such as X-rays (Friedberg *et al.*, 2006). In addition, elevation and time spent at high-altitudes can greatly increase exposure to IR, suggesting that individual exposures can vary considerably. IR has the ability to physically damage DNA both directly and indirectly. Direct damage is a result of the absorption of radiation by DNA and results in the ionization of DNA nucleotides and sugars, whereas species formed from the radiolysis of water are a major source of indirect DNA damage by IR. However, both direct and indirect damage may result in the same intermediate reactive products, and one of the reactive intermediates is the hydroxyl radical. Hence, DNA damage as a result of IR can be deemed similar to that of ROS to a certain extent. However, the most lethal affects caused by IR result from single and double-strand breaks (DSBs) (Friedberg *et al.,* 2006). Single-strand breaks can result from the abstraction of a hydrogen atom from deoxyribose and may occur either directly from IR, or indirectly from hydroxyl radicals formed from IR exposure (Friedberg *et al.*, 2006). DSBs resulting from IR are an important example of multiple damage sites, and may result because a single track of IR produces a cluster of ionizations allowing two or more hydroxyl radicals to abstract hydrogen atoms from both DNA strands (Friedberg *et al.*, 2006). Therefore, oxidative damage can also result from an exogenous source like IR, in addition to the endogenous sources mentioned earlier. However, exogenous oxidative damage may also result from metal ions and barbiturates for example (Buonocore and

Bellieni, 2010). Nonetheless, it is the cellular response to DNA damage that determines the lethality of DNA damage.

In addition to IR, DNA is also damaged by Ultraviolet (UV) radiation. UV radiation can be divided by three wavelength ranges: UV-A (320 to 400 nm), UV-B (295-320 nm), and UV-C (100-295 nm), where solar radiation consists mainly of UV-A and UV-B waves as UV-C waves are filtered out by the ozone (Friedberg *et al.*, 2006). However, in seeming contrast, most UV radiation studies in laboratories involve the study of UV-C radiation for ease of treatment. However, UV-C radiation does induce the same lesions as UV-A and UV-B, but is slightly more specific for DNA specific lesions. One of the major lesions induced by UV radiation is cyclobutane pyrimidine dimers (CPD), a phenomenon where adjacent pyrimidines become covalently linked by a four-member ring structure (Friedberg *et al.*, 2006). 6-4 photoproducts (6-4 PP) are another major form of UV-induced lesions. 6-4 PP link the C6 position of the 5' pyrimidine to an adjacent C4 position of the 3' pyrimidine and thus distort the DNA helix. UV radiation may also result in spore photoproducts, photoinduced lesions involving purines, pyrimidine hydrates, thymine glycol lesions, crosslinking of DNA to proteins, and strand breaks most likely caused from the biological processing of the UV radiation-induced damage (Friedberg *et al.*, 2006). UV-induced lesions are typically repaired by nucleotide excision repair (NER) (discussed later) before they hinder DNA replication.

1.1.2.2 – Chemical DNA-damaging Agents

Alkylating agents include a wide variety of chemicals, most of which are suspected carcinogens and can cause such extreme consequences as death. For example, mustard gas has been used in chemical warfare in World Wars. However, alkylating agents also have the ability to act as anticancer chemotherapeutic drugs. All four DNA nucleotides have been shown to have reactive sites for alkylating agents, albeit to varying degrees (Friedberg *et al.*, 2006). The two major consequences of alkylating agents are replication blocks (3-methyladenine for example (3-meA), and mutagenesis (O^6-methylguanine (O^6-meG)) (Friedberg *et al.*, 2006). However, to a lesser extent, alkylation of DNA nucleotides may weaken the N-glycosyl bond, and result in alkali-labile AP sites (Friedberg *et al.*, 2006; Loeb and Preston, 1986). Alkylating agents can be either monofunctional and covalently bound with one nucleophilic center in DNA, or bifunctional and react with two sites in DNA, which forms crosslinks. In the laboratory the most commonly used monofunctional alkylating agents for studying DNA repair include methylnitrosourea (MNU), *N*-methyl-*N*'-nitro-*N*-nitrosoguanidine (MNNG), methyl methanesulfonate (MMS), ethylnitrosourea (ENU) and ethyl methanesulfonate (EMS).

Crosslinking agents are important components to chemical DNA damage as well. Crosslinking agents have the ability to construct complete blocks in DNA hindering both DNA replication and transcription, and crosslinks formed by alkylating agents are virtually irreversible (Kozekov *et al.*, 2003). The ability of a bifunctional alkylating agent to bind to two nucleophilic centers on opposing DNA strands results in an interstrand

crosslink. However, if the nucleophilic centers are on the same DNA strand it is referred to as an intrastrand crosslink. Notable crosslinking agents include nitrogen mustard, cisplatin and mitomycin C (MMC); the latter two are employed as chemotherapeutic agents (Kozekov *et al.*, 2003). Crosslinking can refer to DNA-DNA crosslinking, but evidence has shown that DNA-protein crosslinks by aldehydes such as formaldehyde are also plausible (Kurtz and Lloyd, 2003). We are continually exposed to aldehydes and related compounds via tobacco smoke, car exhaust and endogenously from oxidative degradation of unsaturated lipids (Friedberg *et al.*, 2006). In addition to the chemicals that can cause DNA crosslinks, IR (Love *et al.*, 1986; Marmur and Grossman, 1961) and UV radiation (Lett *et al.*, 1961) also have the ability to form intermolecular DNA crosslinks (Friedberg *et al.*, 2006).

Crosslinks may also be formed during photosensitized reactions. For example, psoralenes can intercalate into DNA upon exposure to UV-A radiation thereby producing covalent adducts to pyrimidines (Hearst *et al.*, 1984), typically across the 5-6 double-bond of thymine, and also cause helix distortion and unwinding of the DNA (Friedberg *et al.*, 2006; Pearlman *et al.*, 1985). Although potentially harmful, psoralenes provide a mechanism for studying the repair of interstrand DNA crosslinks, as well as a treatment for patients suffering from psoriasis, a skin disease (Friedberg *et al.*, 2006).

In addition to the chemical damage discussed so far, canonical cellular metabolism has the ability to create DNA-damaging agents. A variety of relatively unreactive chemical compounds readily undergo metabolic activation by enzymes attempting to protect the cell from cytotoxic agents and potentially detrimental effects by

breaking down these chemicals to water-soluable excretable forms. Unfortunately, sometimes this results in an activated electrophilic form that may readily react with DNA, which converts these cytotoxic chemicals into genotoxic compounds. Well known chemicals that act in this manner are *N*-2-Acetyl-2-Aminofluorene, Benzo[*a*]pyrene, aflatoxins, MNNG, and 4-Nitroquinoline 1-Oxide (4-NQO). Benzo[*a*]pyrene is one of the most carcinogenic compounds known and is readily found in cigarette smoke, vehicle exhaust, and charred foods. While aflatoxins are mycotoxins produced by certain fungi and contaminate cereal grains consumed by humans, alfatoxin-B_1 is taken up into the cell by passive diffusion and metabolized to aflatoxin B_1-8,9-epoxide, which then attacks certain guanine residues in duplexed DNA, resulting in a weakened N-glycosyl bond and AP sites (Friedberg *et al.*, 2006). In addition to the above chemicals, metabolism of the natural hormone estrogen can result in reactive electrophilic metabolites. The consequences can be DNA adducts, AP sites, ROS, oxidized DNA nucleotides and DNA strand breaks, to name a few.

DNA damage from DNA strand breaks can be induced by chemicals such as bleomycin, IRs, as well as from alteration of enzymatic activities in the cell such as topoisomerase inhibitors. Bleomycin, although used as an antitumor antibiotic, abstracts hydrogen from DNA, resulting in nucleotide modification, AP sites and strand breaks (Friedberg *et al.*, 2006; Povirk, 1996). DNA strand breaks may also result from topoisomerases. Topoisomerases are nicking and closing enzymes that function while covalently attached to DNA ends. DNA ends are subsequently re-joined when the topoisomerase is released from the DNA. However, in the presence of a topoisomerase

inhibitor (camptothecin for example), the topoisomerase remains covalently attached to the broken DNA end resulting in DSBs with DNA-protein crosslinks (Ferguson and Baguley, 1996; Froelich-Ammon and Osheroff, 1995). Human cells resolve such DNA-protein crosslinks with the enzyme *TDP1* (Friedberg *et al.*, 2006).

Although many forms of DNA damage have been mentioned thus far, it should be noted that DNA damage is also dependent on the higher order structure of DNA organization into nucleosomes and chromosomes. For example, CPD DNA damage has no preferential distribution in chromatin. Alternatively, 6-4 PP accumulate in the linker region and distribute randomly in the nucleosome core to a lesser extent (Friedberg *et al.*, 2006).

It is easy to see that DNA damage is an inevitable component to life, and as such poses a major challenge to the cell to be able to identify many types of DNA damage. The devastating results from spontaneous DNA damage alone has the potential to overwhelm a cell, not to mention DNA damage induced by environmental factors. It is no wonder why cells have evolved numerous mechanisms to repair and bypass DNA damage.

1.2 – DNA Repair Pathways

Given the multitude of mechanisms that constantly assault cellular DNA, it is no surprise that cells have responded with an equally large array of mechanisms to not only repair but also bypass DNA damage to allow for cell survival. In the strict sense of the term, as defined by Friedberg *et al.* 2006, DNA repair is defined as "*cellular responses to*

DNA damage that result in the restoration of normal nucleotide sequence and DNA structure.", and as such two mechanisms exist for DNA repair, reversal and excision of DNA damage (Friedberg *et al.*, 2006). In addition to the DNA repair and tolerance mechanisms discussed below it should be mentioned that cell cycle progression and transcription also play important roles in responding to DNA damage for the preservation of genomic stability.

1.2.1 – Direct Reversal of Damage

Direct reversal of DNA damage is thought to be the simplest, most efficient, most direct, and most accurate way to repair DNA damage, and is typically thought to be error-free. Reversal of DNA damage is thought to be efficient as only a single gene product is required resulting in a presumably rapid repair mechanism; however, the repercussion is a requirement of high energy (Friedberg *et al.*, 2006). Although direct reversal occurs in a very limited manner by photoreactivation or methyl transfer, it was the discovery of photoreactivation in 1949 (Kelner, 1949) that initiated the field of DNA repair. Photoreactivation, a one-step enzymatic reaction by a photolyase, is a light requiring reaction (Cleaver, 2003; Sancar, 2003) that reverses covalently joined adjacent pyrimidines characterized by both CPDs and 6-4 PPs. In addition to photoreactivation other forms of direct reversal are available to cells to deal with at least four different kinds of alkylation base damage which are regulated by the adaptive response to alkylation damage (Friedberg *et al.*, 2006). Therefore, mutagenic alkylating agents such as MNNG, MNU, and to a smaller extent, MMS, which react with DNA to produce many

O-alkylated and *N*-alkylated products are reversed. In addition to photoreactivation and direct reversal of alkylation damage single-strand DNA (ssDNA) breaks (SSBs), without end group damage, may be repaired in a direct reversal mechanism via the enzyme DNA ligase in which the ends are simply rejoined (Jacobs *et al.*, 1972).

1.2.2 – Base Excision Repair (BER)

BER is thought to be the most utilized mechanism of DNA repair in nature, and it is conserved from bacteria to humans (Friedberg *et al.*, 2006). BER is defined and initiated by the presence of DNA glycosylases. DNA glycosylases are found in bacteria, yeast and human cells, and typically maintain function specificity for a particular class of base damage such as inappropriate base incorporation, or mispairing (Friedberg *et al.*, 2006).

The essential component of a DNA glycosylase is the catalytic release of free bases as a product of their reaction with DNA (Friedberg *et al.*, 2006). Many DNA glycosylases are categorized in the helix-hairpin-helix superfamily. These DNA glycosylases have a helix-hairpin-helix DNA binding motif found in many DNA binding proteins (Doherty *et al.*, 1996). There are six families under the helix-hairpin-helix superfamily which are defined by the modified nucleotide they excise. They are: alkyladenine-DNA glycosylase, *N*-methylpurine-DNA glycosylase II, A/G specific adenine glycosylase/mismatch glycosylase, endonuclease III, 8-oxoG-DNA glycosylase I, and 8-oxoG-DNA glycosylase II. In addition to the helix-hairpin-helix superfamily, uracil-DNA glycosylase has the ability to remove uracil from DNA (Friedberg *et al.*,

2006). Although the specificity that DNA glycosylases maintain is a great benefit to BER, it would be a daunting task for the cell to maintain DNA glycosylases specific for each plausible type of DNA damage; instead DNA glycosylases with broader catalytic selectivity are also present in the cell, some of which are able to remove alkylation damage for example. Unfortunately, the consequence of utilising less specific enzymes is a more energy exhaustive repair mechanism. Glycosylases typically function by dispersing along the minor groove of DNA until DNA damage is encountered. The DNA glycosylase then compresses the DNA backbone and the abnormal nucleoside is flipped out to allow for specific recognition of the altered nucleotide and subsequent cleavage by hydrolysis of the N-glycosyl bond that links the damaged or altered nucleotide to the DNA backbone. The result is an AP site. DNA glycosylases may be monofunctional, and result in an AP site, or bifunctional as some of them also cleave the backbone 3' end of the AP site; the latter class is designated DNA glycosylase/AP lyases. Regardless, the resultant AP sites must be repaired by AP endonucleases and finally correct nucleotides are incorporated via DNA polymerases through a "short patch" (often one nucleotide) or a "long patch" (two to eight nucleotides) BER pathway. Finally joining of DNA ends by DNA ligases, as in other forms of DNA repair and recombination processes, complete BER (Friedberg *et al.*, 2006). Because BER is a multistep process, the intermediates formed have the potential to be either mutagenic or reactive if BER is initiated and subsequently left incomplete. Results have shown that repair of single or clustered DNA lesions by DNA glycosylases that are initiated but either aborted or failed result in lethal

DSBs (Blaisdell and Wallace, 2001; Demple and DeMott, 2002; Sutherland *et al.*, 2002; Wallace, 2002).

1.2.3 – Mismatch Repair (MMR)

Mismatched DNA nucleotides may arise from the misincorporation of DNA nucleotides during canonical DNA replication, from insertion of an extra nucleotide, deletion of a nucleotide, formation of a heteroduplex, and deamination of 5-methylcytosine, to name a few. MMR functions to correct nucleotide errors that arise during DNA replication and have escaped the proofreading activity of DNA polymerases. MMR repairs mismatched or unpaired nucleotides, mispairings arising during replication, and mispairings that result from the incorporation of damaged nucleotide precursors (Earley and Crouse, 1998), for example the incorporation of d8oxoGTP resulting in DNA damage. In additional nucleotides being incorporated or deleted due to replication slippage. MMR is similar to BER and NER, discussed below, in terms of their molecular mechanisms of functioning. MMR functions by recognizing the lesion, discriminating between the newly synthesized DNA strand containing an error and the parental strand, excision, and finally ligation. Although MMR may remove DNA damage in the example of 8oxoG-A mismatches in yeast, in the case of O6meG-T mismatches, dTMP is removed and the DNA damage remains (Friedberg *et al.*, 2006).

In *Escherichia coli*, MMR distinguished the parent strand from the daughter strand by the methylation state of adenine in a d(GATC) sequence (Modrich and Lahue, 1996), and although MMR is highly conserved from prokaryotes to eukaryotes, it has not

yet been determined how this distinction is made in eukaryotes. Regardless of the organism MMR is initiated by MutS, or MutS homologue, binding to DNA mismatches via a conserved DNA binding domain. In prokaryotes this is achieved via the MutS homodimer, while *S. cerevisiae* encodes six MutS homologues Msh1-6 (Friedberg *et al.*, 2006). Msh1 in *S. cerevisiae* is thought to function independently as a homodimer (Chi and Kolodner, 1994) in the repair of mitochondrial DNA (Dzierzbicki *et al.*, 2004; Reenan and Kolodner, 1992) while Msh2, Msh3, and Msh6 function to maintain the nuclear genome (Johnson *et al.*, 1996; Marsischky *et al.*, 1996) leaving Msh4 and Msh5 to function during meiotic recombination (Friedberg *et al.*, 2006; Hollingsworth *et al.*, 1995; Ross-Macdonald and Roeder, 1994). MutS and MutS homologs undergo an ATP-dependent conformation change allowing MutS to move along the DNA backbone *in vitro* (Blackwell *et al.*, 1998; Gradia *et al.*, 1999; Iaccarino *et al.*, 2000). Subsequently, MutS binds to MutL at the site of mismatch (Grilley *et al.*, 1989) in a second ATP-dependent step (Friedberg *et al.*, 2006). MutL, a homodimer in prokaryotes, is comprised of the heterodimer Mlh1-Pms1 (Prolla *et al.*, 1994a; Prolla *et al.*, 1994b; Wang *et al.*, 1999) in *S. cerevisiae*. *S. cerevisiae* encodes a total of four MutL orthologues; however, the heterodimers of Mlh1-Mlh3, Mlh1-Mlh2 are thought to play more specialized roles, for example in the repair of frameshift mutations (Flores-Rozas and Kolodner, 1998; Harfe *et al.*, 2000). In *E. coli* subsequent steps involve recruitment of MutH opposite a *dam* methylated GATC parent DNA sequence. Alternatively, in *Bacillus subtilis*, which does not have *dam*-directed methylation, MutS has been shown to colocalize with replication foci. Yet, in mammalian cells studies have suggested the involvement of

proliferating cell nuclear antigen (PCNA) (Friedberg *et al.*, 2006). Subsequently four exonucleases have been implicated for MMR in *E. coli*, while Exo1 has been demonstrated to be involved in MMR in *S. cerevisiae* and demonstrated co-localization with PCNA (Tishkoff *et al.*, 1997). During meiosis in *S. cerevisiae* MMR also maintains an antirecombinational function thereby preventing heteroduplex formation particularly between divergent DNA sequences (Alani *et al.*, 1994; Borts *et al.*, 2000). Defects in MMR are thought to cause an increase in the spontaneous mutation rate by up to a 1000-fold, and in humans it is associated with cancer thus signifying the importance of MMR in maintaining genomic stability.

1.2.4 – Nucleotide Excision Repair (NER)

Alternative to BER and MMR, DNA repair may also be accomplished by nucleotide excision repair. Following the discovery of enzymatic photoreactivation DNA repair was differentiated as either light dependent repair (photoreactivation) or dark repair (repair independent of light and photoreactivation), which led to the discovery of NER by autoradiographic experiments in *E. coli*. NER is defined as a process where damaged nucleotides are excised from the genome as part of an oligonucleotide (Friedberg, 1988), and should not be confused with BER that excises damaged nucleotides from the genome. Although a complex process, NER can simply be explained as the recognition of a damaged nucleotide, incision on either side of the affected DNA nucleotide, excision of the oligonucleotide, DNA synthesis to fill the DNA gap, and finally DNA ligation.

In *E. coli*, NER is carried out by three proteins, UvrA, UvrB and UvrC that act in a sequential manner (collectively referred to as UvrABC endonuclease). *UvrAB* genes are under the control of the SOS regulon and as such are DNA damage inducible genes. In addition, UvrB appears to have an SOS-independent induction mechanism as well. Mutations in any one of the *uvrABC* endonuclease genes render *E. coli* cells sensitive to UV radiation and numerous chemical agents including nitrogen mustard and MNNG. UvrA is an ATPase and a dimeric DNA binding protein, and recognizes various types of DNA nucleotide damage. Following UV radiation the UvrABC endonuclease generally hydrolyses the eighth phosphodiester bond 5' to CPD or 6-4 PP; however, the 3' incision is more variable, and is surmised to account for the variability in DNA conformation as a result of different nucleotide damage allowing NER to handle numerous types of DNA damage (Friedberg *et al.*, 2006).

In eukaryotes inactivation of *RAD1*, *RAD2*, *RAD3*, *RAD4* and *RAD10* genes causes an increased sensitivity to UV radiation and chemicals which produce bulky nucleotide adducts, and renders NER completely defective *in vivo* (Friedberg *et al.*, 2006). Humans defective in NER suffer from xeroderma pigmentosum (XP), a condition in which the repair of UV damage from sunlight is inadequate, and typically results in skin cancer at a young age (Friedberg *et al.*, 2006).

1.2.5 – Homologous Recombination (HR)

In 1974 Game and Mortimer published a paper establishing the X-ray sensitivity of the *rad50-rad57* mutants (Game and Mortimer, 1974), and since then mutations of the

RAD50-RAD59 genes have been shown to have a characteristic sensitivity to ionizing radiations and chemicals that cause strand breaks (Friedberg *et al.*, 2006). Strand breaks, specifically unrepaired DSBs are thought to be the main reason for cell killing following IR. However, DSBs may also arise endogenously during cellular metabolism or exogenously as a result of exposure to DNA-damaging chemicals. Regardless of how they arise, DSBs must be repaired to avoid mutations, loss or rearrangement of chromosomes, cell death and, in higher eukaryotes cancer. DSBs are essentially repaired by one of two mechanisms; non-homologous end joining (NHEJ), or HR.

Homologous recombination is accomplished by the *RAD52* epistasis group (Table 1.1) in *S. cerevisiae* and is known to play several vital roles in maintaining genomic stability by removing DSBs and interstrand crosslinks in both prokaryotes and eukaryotes. In addition, HR functions in preserving replication forks, telomere maintenance and chromosome segregation in meiosis I (Friedberg *et al.*, 2006). Because HR requires an extensive region of DNA homology from undamaged sister chromatid or homologous chromosomes in order to function it is thought to be largely an error-free process. HR is characterized by the requirement of recombinases, of which there are two in eukaryotes, Rad51 (which shares 30% sequence identity with the bacterial RecA protein (Symington, 2002)) and Dmc1. While Dmc1 functions only in meiosis Rad51 is required for mitotic and meiotic events requiring HR. Deletion of *RAD51* renders *S. cerevisiae* cells highly sensitive to DNA-damaging agents, while in higher eukaryotes deletion of *RAD51* renders cells inviable and in vertebrates, as studied in mice causes embryonic lethality (Symington, 2002; Tsuzuki *et al.*, 1996). In *S. cerevisiae* DSBs are

detected and bound by the MRX complex, which is required for efficient DSB resection. Mutants of the MRX complex maintain persistent strand breaks that are not processed appropriately (Friedberg *et al.*, 2006). The ssDNA left behind is rapidly bound by RPA (replication protein A) allowing Rad52 to recruit Rad51 to the RPA-ssDNA complex. It is thought that RPA binding to ssDNA is inhibitory to Rad51 binding, therefore Rad52 and the Rad55-Rad57 heterodimer function to recruit and stabilize Rad51 binding to ssDNA (Fung *et al.*, 2009). Rad51 is known to self-interact as well as interact with Rad52, Rad54, Rdh54/Tid1 and Rad55 (Symington, 2002). Although the interaction between Rad51 and Rad52 is quite stable in yeast, the interactions between Rad51, Rad52 and Rad54 are thought to be highly dynamic in higher eukaryotes. The Rad51 nucleofiliment protein initiates strand invasion into a homologous sequence to form a D-loop. Antagonistic to HR is the Srs2 protein which contains both helicase and ATPase activities *in vitro* (Rong and Klein, 1993). Srs2 disassembles the Rad51 presynaptic filament allowing for the ssDNA to once again be coated with RPA and abolishing further Rad51 binding (Krejci *et al.*, 2003; Veaute *et al.*, 2003). It is thought that Rad54 promotes chromatin remodeling, DNA unwinding and strand annealing between the donor DNA and the incoming Rad51-nucleofiliment protein (Friedberg *et al.*, 2006). By displacing the original paired DNA strands a Holliday junction intermediate is formed that must be resolved. Two scenarios exist for HR, one in which the second DNA end is captured resulting in two Holliday junctions being formed (Double-strand break repair or DSBR), and the second where synthesis-dependent strand annealing (SDSA) is required

(Figure 1.1). Depending on how the double-Holliday junction is resolved in DSBR, it may result in crossover or non-crossover events.

In addition to HR and NHEJ cells can utilize several other mechanisms to survive DSB that are alternative to HR, yet still require some form of homologous pairing to function. One such mechanism is single-strand annealing (SSA) (Figure 1.1), a result of the annealing of direct repeats that were revealed by resection of the DSB to ssDNA. The genetic requirements for SSA differ from HR in that in *S. cerevisiae* Rad51 is dispensable whereas Rad52 and its homolog Rad59 are required (Friedberg *et al.*, 2006). Although SSA can repair DSBs the unfortunate consequence is the deletion of what can be a large portion of DNA. In addition to SSA is the break-induced repair (BIR) of DSBs. BIR also assumes the invasion of a 3` ssDNA overhang; however, as in SDSA the displaced strand does not pair back but instead serves as the lagging-strand template of a newly formed replication fork (Friedberg *et al.*, 2006).

NHEJ acts directly on the ends of DSBs allowing for the direct ligation of the ends (Figure 1.1). Various studies have suggested the existence of two NHEJ pathways. One NHEJ pathway is dependent on DNA end binding protein Ku which prevents the DNA ends from degradation (Feldmann *et al.*, 2000; Gottlich *et al.*, 1998; Liang and Jasin, 1996), while the second is Ku-independent and mutagenic. In contrast to the error-free mechanisms of HR, NHEJ is typically thought of as mutagenic due to the potential loss of DNA at free DNA ends since the two DSBs may be reannealed by NHEJ whether their ends are complimentary or not. Free DNA ends are susceptible to nuclease degradation and this method is therefore error prone as some genetic material may be lost

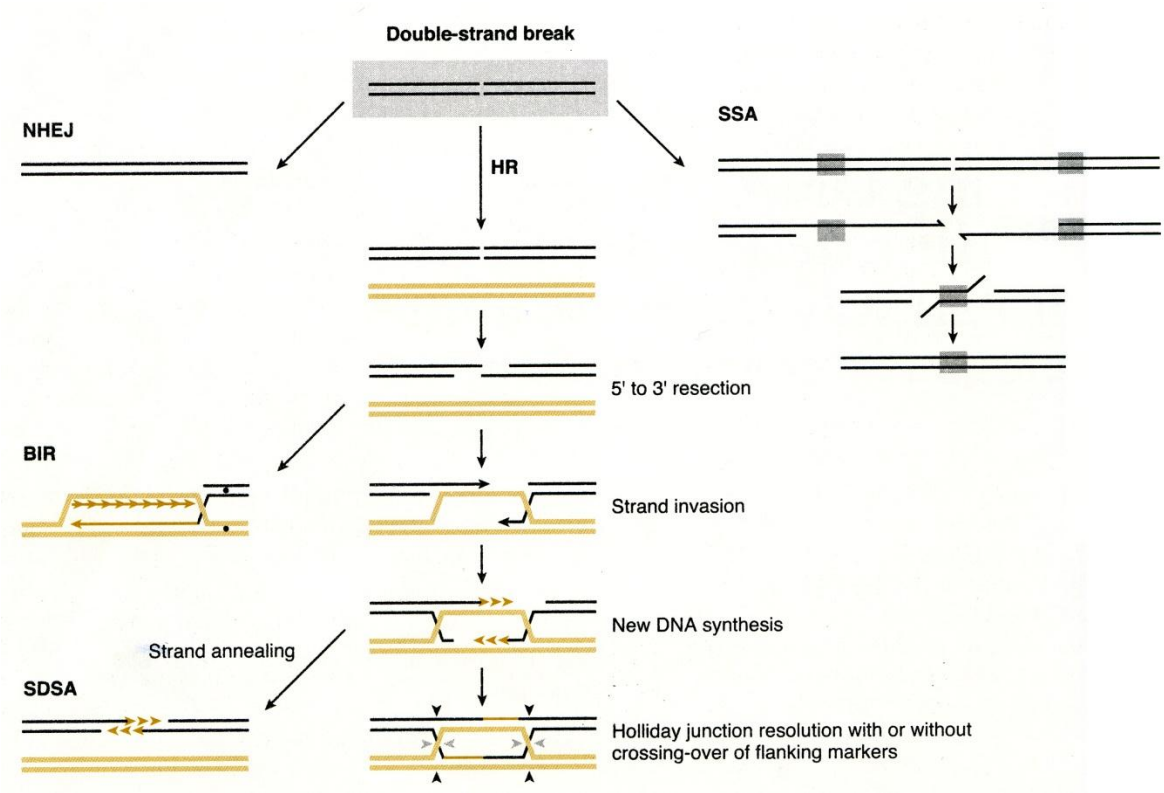

Figure 1.1 – Overview of Eukaryotic DSB Repair Pathways. DSBs may be resealed by NHEJ, or alternatively DSB may be resected to form 3`overhangs thus initiating HR. Strand invasion can result in the formation of a replication fork and an extended gene conversion tract for break induced repair (BIR). Following limited DNA synthesis (shown in gold) the invading strand may reanneal without crossover events which is referred to as synthesis dependent strand annealing (SDSA). Should HR continue following strand invasion Holliday junctions are formed and subsequently resolved. Alternatively single-strand annealing (SSA) results from the annealing of direct repeats. Friedberg *et al*., 2006 (Copyright granted for republish or display in a thesis/dissertation).

(Pfeiffer, 1998). Although NHEJ and HR occur in all eukaryotes, yeast cells prefer HR, while mammalian somatic cells prefer NHEJ.

Studies in *S. cerevisiae* have shown that BER, NER, and HR have overlapping functions in repairing spontaneous and exogenous oxidative DNA damage (Doetsch *et al.*, 2001; Gellon *et al.*, 2001; Swanson *et al.*, 1999; Vance and Wilson, 2001). However, should these mechanisms fail, DNA damage tolerance functions to maintain cell survival.

1.3 – DNA Damage Tolerance

Although most DNA damage can be removed and repaired by BER, MMR, NER, HR and NHEJ as previously discussed, certain damage may elude DNA repair, overwhelm DNA repair mechanisms, or present a replication blockage thus hindering replicative DNA polymerases. Therefore, in order to preserve genomic stability and viability, cells possess mechanisms that allow the cell to tolerate DNA damage, these mechanisms are thought to be as biologically significant as DNA repair mechanisms (Friedberg *et al.*, 2006). This is collectively termed DNA damage tolerance (DDT).

1.3.1 – DNA Damage Tolerance and Translesion DNA Synthesis in *E. coli*

The notion that cells produce physiological responses to DNA damage was initially discovered in *E. coli*. The majority of cellular responses to DNA damage in *E. coli* are centrally controlled by the SOS regulatory network. During the early phases of the SOS response accurate DNA repair is achieved; however, should these mechanisms fail or damage exceeds repair, the SOS response is activated to initiate a series of DNA

damage tolerance mechanisms. The SOS regulon genes respond to ssDNA. The RecA protein recognizes ssDNA and thus promotes two parallel pathways; recombination-mediated bypass which constitutes the majority of lesion bypass in *E. coli*, and TLS. Current ideology suggests that it is ssDNA generated from attempted replication of damaged template DNA or as a result of interrupted DNA replication that serves as a DNA damage signal. It is the ternary complex formed amongst the RecA protein, a nucleoside triphosphate, and ssDNA (also referred to as a RecA nucleoprotein filament) that activates the RecA protein (Craig and Roberts, 1980; Little *et al.*, 1981). It is these nucleoprotein filaments, or active RecA that interact with LexA and induce autocleavage of the LexA protein, a homodimer repressor of the SOS regulon at the SOS boxes, thus allowing for transcriptional activation of more than 40 genes required for DNA repair and cell survival (Courcelle *et al.*, 2001; Friedberg *et al.*, 2006; Little, 1984). In particular the SOS response induces both *DinB* and *UmuDC* that encode polymerases PolIV and PolV, respectively, both of which are involved in TLS. Activated RecA has the ability to facilitate UmuD self-cleavage and the resulting product forms an active heterotrimer UmuD'$_2$C (Bruck *et al.*, 1996; Woodgate *et al.*, 1989), which is the highly mutagenic form of PolV. PolV is thought to replace the replicative polymerase (PolIII) and allow for lesion bypass. Although DNA repair and DNA damage tolerance in *E. coli* seem to be centered on RecA, this mechanism does not appear to be evolutionarily conserved in eukaryotes.

1.3.2 – Radiation Repair Epistasis Groups in *S. cerevisiae*

The yeast genome was first suggested to be a radiation-sensitive target in the late 1940's (Laterjet and Ephrussi, 1949); however, it was in the late 1960's (Nakai and Matsumoto, 1967) that the first investigation for radiation-sensitive yeast mutants began (Friedberg, 1988). Since then over 30 *RAD* (*RAD*iation sensitive) genes have been identified that contribute to the resistance of killing by UV and/or IR. Subsequently many *rad* mutants have been shown to display enhanced sensitivity to other chemicals (Friedberg, 1988). Since then *RAD* genes have been organized into essentially three epistasis groups representing three classes of cellular responses to DNA damage in *S. cerevisiae*. An epistatic interaction can be operationally defined as the presence of two mutations in different genetic loci resulting in a phenotype quantitatively equal to one of the single mutations. An epistatic interaction thus suggests that the genes being studied are involved in sequential steps of a multistep biochemical pathway or their products are in the same multimeric complex. Alternatively, if the two mutations produce an additive or synergistic phenotype, they are placed in different epistasis groups (Friedberg *et al.*, 2006). In *S. cerevisiae* the *RAD3* epistasis group and *RAD52* group consist of NER and HR genes, respectively, and repair the majority of radiation-induced DNA lesions. In addition, lesions induced by oxidative and alkylating agents may be dealt with by BER. Should any or all of the above pathways fail the third radiation repair epistasis group, represented by *RAD6*, is thought to function by reinitiating replication without removing the lesion itself. This is termed, though somewhat misleadingly, DNA PRR. The genes that are known to be allocated to each epistasis group are listed in Table 1.1.

Table 1.1 - *S. cerevisiae* Radiation Repair Epistasis Groups

RAD3 group	*RAD52* group	*RAD6* group
RAD1	*RAD50*	*RAD5 (REV2)*
RAD2	*RAD51*	*RAD6*
RAD3	*RAD52*	*RAD18*
RAD4	*RAD54*	*REV1*
RAD7	*RAD55*	*REV3*
RAD10	*RAD56*	*REV7*
RAD14	*RAD57*	*MMS3*
SSL1	*RAD59*	*UBC13*
SSL2 (RAD25)	*XRS2*	
TFB1	*MRE11*	
RAD16		
RAD23		
MMS19		

Friedberg *et al*. 2006, and Friedberg *et al*. 1991.

1.3.3 – DNA Postreplication Repair (PRR) in Yeast

The *RAD6* epistasis group is one of the initial radiation repair epistasis groups found in *S. cerevisiae*. Historically, genes that were not assigned to either the *RAD3* or *RAD52* epistasis groups were placed into the *RAD6* group. While the first two epistasis groups remove and repair DNA-damaging lesions, PRR functions to allow replication to bypass lesions without removing the lesion itself. Consequently, PRR functions to avoid potentially lethal effect with or without increased mutagenesis. Genes required for PRR were initially identified by alkaline sucrose gradients that demonstrated the inability of yeast mutants to fill single-stranded gaps following UV radiation in an NER deficient background (di Caprio and Cox, 1981; Prakash, 1981). Experimental results showed that ssDNA gaps persisted in *rad6* and *rad18* mutants (Prakash, 1981). Since then, the stable complex formed by Rad6 and Rad18 have been shown to centrally control the PRR pathways, and while Rad6 has diverse functions outside of PRR, Rad18 functions exclusively in PRR. Like *E. coli,* PRR in *S. cerevisiae* can be subdivided into two pathways. However, in *S. cerevisiae* it is the sequential ubiquitination of PCNA that satisfactorily explains the current genetic observations with regards to how the *RAD6* pathway operates to bypass DNA damage in eukaryotes and shuffles DNA lesion bypass to either a TLS (error-prone) or an error-free pathway.

1.3.3.1 – Ubiquitination

Ubiquitin (Ub) is a 76 amino acid protein which can be found either freely or covalently attached to a substrate in the cell. Conjugation of Ub to other proteins occurs

through a cascade of reactions as depicted in Figure 1.2 (adapted from (Matyskiela *et al.*, 2009)). Ubiquitination is known to be highly conserved among diverse eukaryotes. To begin, the α-carboxyl group of Ub, which is essential for all Ub-dependent processes, must be activated. This allows for Ub to be linked to an E1 (Ub-activating) enzyme in an ATP-dependent fashion. Following ATP hydrolysis a thioester bond is formed between Ub and the E1. In the second step Ub is passed from the E1 to an E2 (Ub-conjugating) enzyme via transthiolation (Hochstrasser, 1996). The E2 family of enzymes is defined by a conserved catalytic core (Ubc) domain that contains an active-cysteine residue. From the E2, Ub may then be transferred to an E3 (Ub-ligase), however this step is not essential and ubiquitination may occur in the absence of an E3. Regardless, the final step creates an isopeptide bond between the C-terminal glycine residue of Ub and a lysine residue on the target protein, resulting in a monoubiquitinated substrate. It is also possible that substrates can be monoubiquitinated at several lysine residues resulting in a multiubiquitinated substrate. In addition, covalently bound Ub can be further modified by the sequential addition of Ub resulting in polyubiquitin chains. In 1980 it was proposed that selective conjugation of Ub to proteins marked these substrates for degradation (Hershko *et al.*, 1980), and in 1987 Hough *et al.* purified a protease capable of degrading a multiubiquitin-protein substrates (Hough *et al.,* 1987). Subsequently Ub has become best known for its role in covalent modification of substrates to signal them for degradation by the 26S proteasome (Hochstrasser, 1996), which breaks down the substrate but recycles the Ub protein. Predominantly short-lived regulatory proteins are

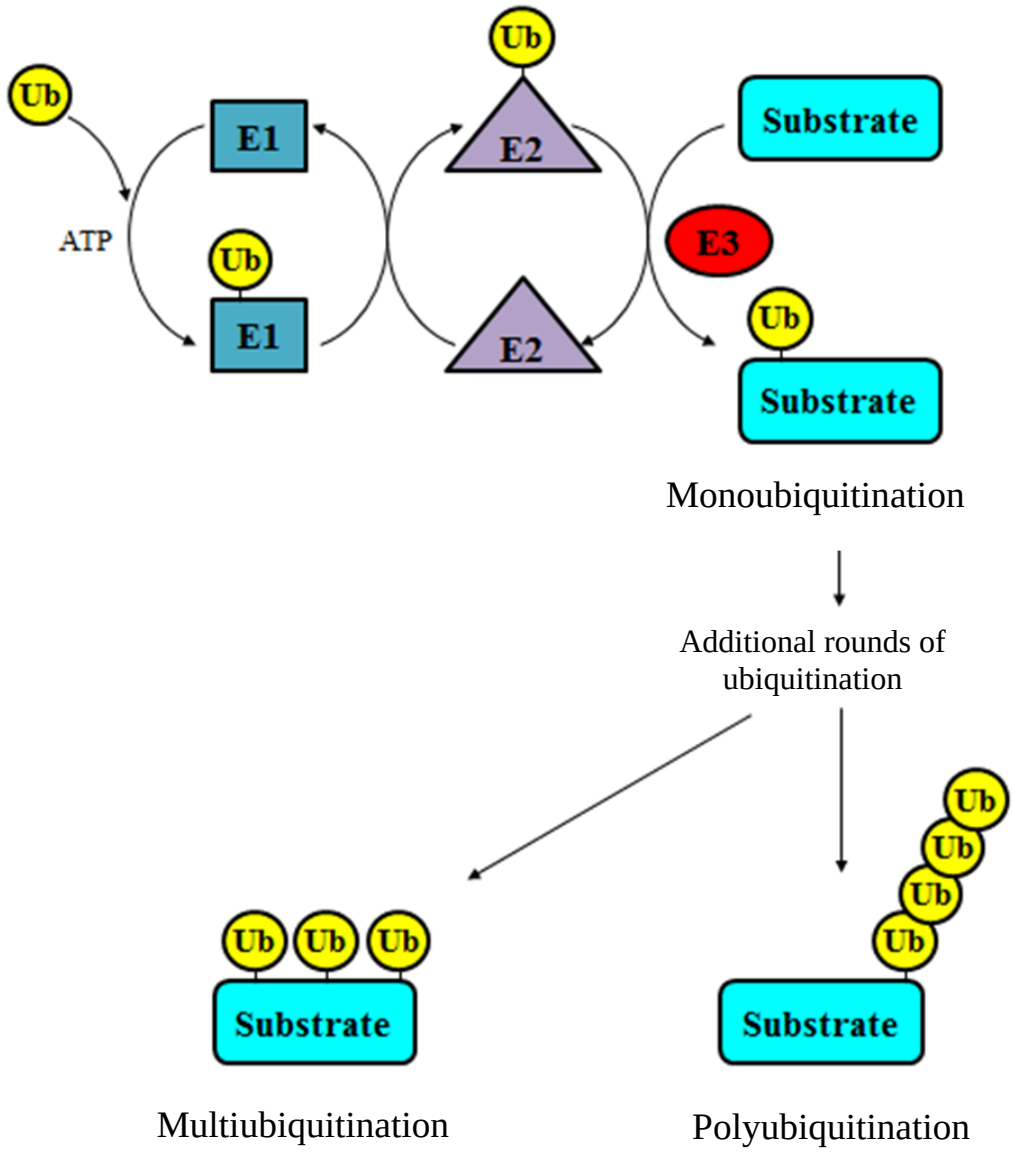

Figure 1.2 – Ubiquitination. Ubiquitination occurs via a cascade of reactions. An E1 (ubiquitin-activating) enzyme is attached to a Ub moiety by a thioester bond in an ATP-dependent manner. The Ub is then transferred from the E1 to an E2 (Ub-conjugating) enzyme, and subsequently, Ub is transferred to an E3 (Ub-ligase) enzyme, although not absolutely required. In a final step Ub is attached to a substrate. The final result is a monoubiquitinated substrate. Subsequent rounds of ubiquitination may allow for the substrate to be multiubiquitinated at several lysine residues. In addition, covalently bound ubiquitin can be further modified by the sequential addition of ubiquitin resulting in polyubiquitin chains. Ub chains may be formed in a Lys48-dependent manner and signal for proteosomal degradation, or in a non-canonical Lys63-dependent manner and signal for DNA damage response.

degraded via the Ub-dependent proteasome pathway (Pickart, 1997). Substrates that are best recognized by the 26S proteasome are typically those conjugated to Lys48 polyubiquitin chains, a signal which has an affinity for the specific length of the Lys48 chain. Since intracellular proteolysis is essential for all organisms, including bacteria, the importance of the Lys48 chains is only further exemplified by the finding that the Ub-K48R point mutation causes lethality in *S. cerevisiae* (Finley *et al.*, 1994). However, substrates covalently modified by a single Ub or unmodified substrates have also been shown to be degraded by the 26S proteasome. It should also be noted that Ub can target proteins for degradation by the lysozyme. Although Lys48-linked Ub chains may be the most abundant it has become clear that there are additional Ub chain modifications found *in vivo*. Studies have shown that polyubiquitination can occur on seven Lys sites on Ub itself; Lys48, Lys63, Lys11, Lys29, Lys33, Lys27, and Lys6 (Arnason and Ellison, 1994; Peng *et al.*, 2003).

A study which examined all six Lys residues on Ub found that it was a Ub-K63R mutant that showed sensitivity to DNA-damaging agents such as MMS and UV but did not affect protein turnover, therefore suggesting that this Lys63 residue was not involved in degradation and instead functioned in the DNA repair pathway (Spence *et al.*, 1995). Since then the Lys63-linked chains have been linked to DNA damage tolerance (Hofmann and Pickart, 1999; Ulrich, 2002), the inflammatory response (Sun and Chen, 2004), protein trafficking (Hicke and Dunn, 2003) and ribosomal protein synthesis (Spence *et al.*, 2000). It is the monoubiquitination, and non-canonical Lys63-linked

polyubiquitin chains that play a vital role in PRR, both TLS and error-free PRR, respectively.

1.3.3.2 – Translesion DNA Synthesis (TLS)

Post-translational modification of PCNA by Ub plays a vital role in coordinating DNA damage tolerance processes in yeast. The Rad6-Rad18 complex is a characteristic E2-E3 complex that is responsible for the monoubiquitination of PCNA which allows for TLS lesion bypass. In eukaryotes DNA lesions that stall replication are bypassed by TLS polymerases, specifically the Y family of DNA polymerases and DNA polymerase ζ (Polζ) (a member of the B family of polymerases). The TLS pathway was first identified by a genetic screen for mutants incapable of reverting the *arg4-17* and *lys1-1* alleles following exposure to UV irradiation (Lemontt, 1971a, b). It has since become accepted that TLS is comprised of *REV1*, *REV3*, and *REV7* (Figure 1.3). The TLS polymerases are known to have a relaxed fidelity for nucleotide incorporation, a function that is required to promote DNA synthesis in the presence of DNA damage, and as such results in a bypass mechanism that is highly mutagenic. *REV1* is known to have deoxycytidyl transferase activity (Nelson *et al.*, 1996a), and is known to have separate PCNA- and Ub-interacting domains. Rev1 is thought to function as a scaffolding protein for TLS independent of its terminal transferase activity. Rev3 and Rev7 form the non-essential DNA polymerase ζ (Polζ), which interacts with Rev1; all three *REV* genes are required for the characteristic mutagenesis induced by UV irradiation lesions or other

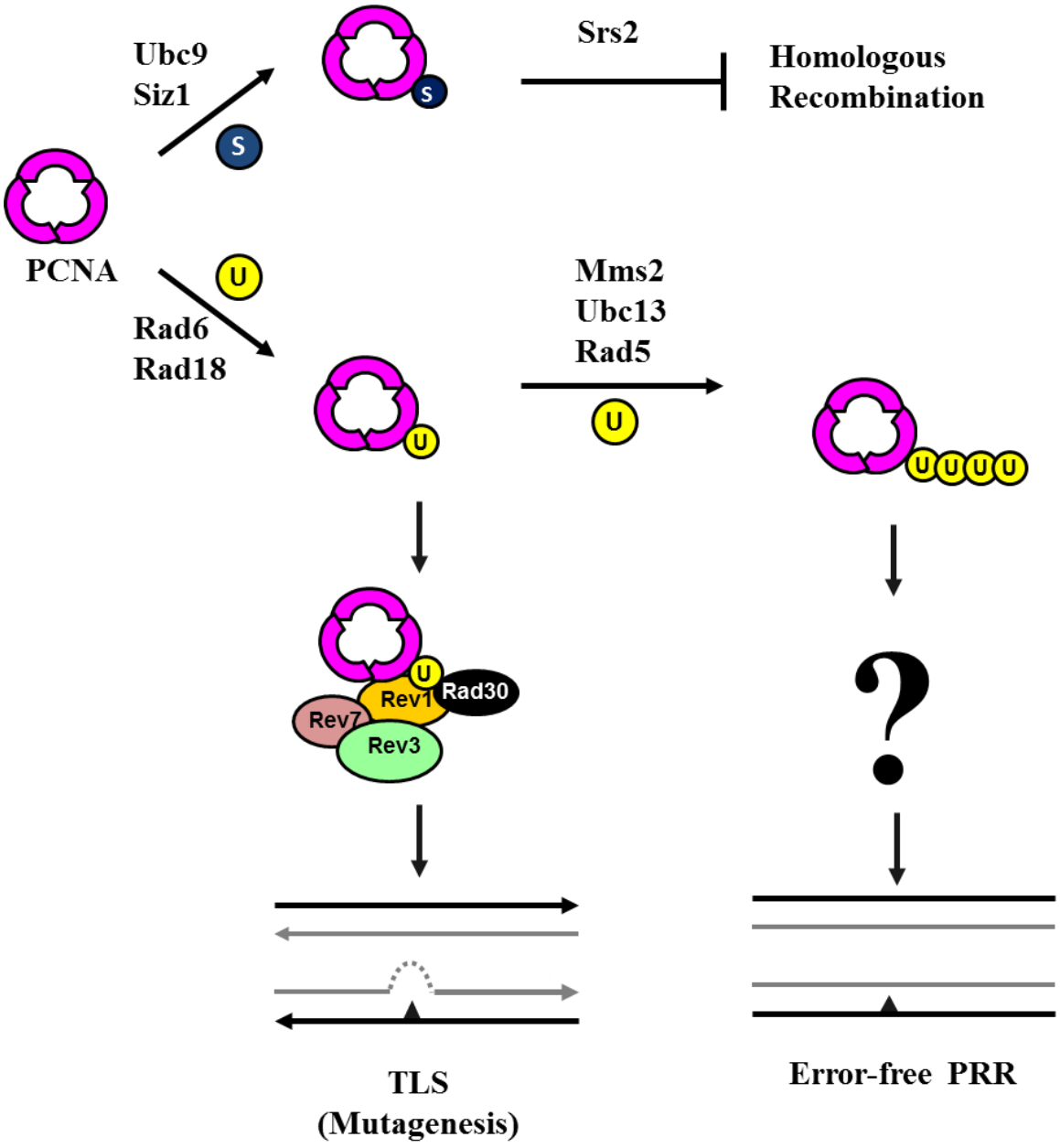

Figure 1.3 – Model Depicting the Budding Yeast DNA Damage Tolerance Pathways Mediated by Covalent Modifications of PCNA. Covalent modification of PCNA at K164 allows for the monoubiquitination of PCNA and in combination with Rev1, Rev3 and Rev7 allows for TLS, or error-prone lesion bypass. The sequential polyubiquitination of PCNA by Rad5–Ubc13–Mms2 results in an error-free mechanism of lesion bypass. Although some form of a homologous chromatid template is thought to be required for error-free lesion bypass the exact mechanisms involved remain unknown. It is therefore the hypothesis of this body of work that additional genes and proteins are involved in error-free PRR, and thus we intend to identify them.

chemical carcinogens (Johnson *et al.*, 1998). PCNA provides the main scaffold to which TLS polymerases bind to in order to execute their role. Rev3, which is the catalytic subunit of Polζ, is not essential for cell growth or viability in yeast cells; however, deletion of *Rev3l* in mice results in embryonic lethality (Bemark *et al.*, 2000; Esposito *et al.*, 2000; Wittschieben *et al.*, 2000). Evidence also suggests that abasic lesions on DNA induce PCNA ubiquitination because TLS DNA polymerases are required for proficient replication through abasic sites in yeast and mammalian cells (Pages *et al.*, 2008b).

Underscoring the significance of TLS process is the finding that mutations of the XPV/*POLH* gene, which encodes Polη in humans, results in a modified form of XP, xeroderma pigmentosum variant (XPV). Patients with XPV are hypersensitive to UV damage and are predisposed to cancer. However, while TLS is well characterized, relatively little is known about error-free PRR.

1.3.3.3 – Error-free PRR

The existence of the error-free PRR branch under the *RAD6* pathway is suspected because the *rad6* or *rad18* mutant is extremely sensitive to killing by DNA-damaging agents while the *rev* mutants are not (Lawrence, 1994; Prakash *et al.*, 1993). Perhaps the first firm demonstration of the existence of error-free PRR was through genetic characterization of the *mms2* mutant (Broomfield *et al.*, 1998; Xiao *et al.*, 1999). The *mms2* mutant displays moderate sensitivity to killing by a variety of DNA-damaging agents and the gene is thus assigned to the *RAD6* pathway. The characteristic features of *mms2* include its strong synergistic interaction with *rev3* and its *REV3*-dependent

increase in spontaneous mutagenesis. Since then Mms2, Ubc13, and Rad5 have all be allocated to the *RAD6* error-free PRR pathway through genetic and epistatic analysis. *MMS2* encodes a Ubc-like protein but does not contain an active-site Cys residue. It turns out that Mms2 forms a stable complex with Ubc13, and this complex specifically promotes the non-canonical Lys63-linked Ub chain formation (Figure 1.3) (Hofmann and Pickart, 1999). Indeed *ubc13* is epistatic to *mms2* and the two mutants share all characteristic features as described above (Brusky *et al.*, 2000). Furthermore, Rad5, a member of the SWI/SNF family of ATPases with a C_3HC_4 RING finger motif, is capable of interacting with Pol30 (PCNA), Ubc13 and Rad18 and may serve as an E3 for Ubc13–Mms2 (Ulrich and Jentsch, 2000). Thus, it is thought that Rad5 functions to recruit the Mms2–Ubc13 complex in close proximity to PCNA and facilitate the Lys63-linked polyubiquitination of PCNA. However, this is thought to be merely a signalling mechanism, and does not directly facilitate error-free lesion bypass. Additional genes are therefore required for error-free lesion bypass.

During normal DNA synthesis DDT is thought to occur at sites of DNA damage, which has stalled the replication fork machinery. While replication may restart downstream of the DNA lesion, if synthesis continues on the undamaged strand there becomes two plausible mechanisms for error-free lesion bypass (Figure 1.4). One possible model is that stalled replication forks can be processed by fork reversal (or a chicken-foot model) a possible Rad51-independent template switching mechanism which allows for synthesis to continue after the unfolding of the template switch resulting in an error-free lesion bypass mechanism. Alternatively, template switching by HR in a Rad51-

dependent manner may allow for strand invasion to occur thereby using an intact sister chromatid strand as template for DNA synthesis, resulting in error-free lesion bypass (Figure 1.4) following resolution of the intermediate structures. Although, these two mechanisms may not be mutually exclusive, either model allows for lesion bypass however leaving behind the original replication blocking lesion to be repaired later. Alternative to the error-free mechanisms, TLS and the associated low-fidelity polymerases may synthesize DNA across from the DNA lesion allowing for lesion bypass to occur, although it does so in a largely error-prone manner.

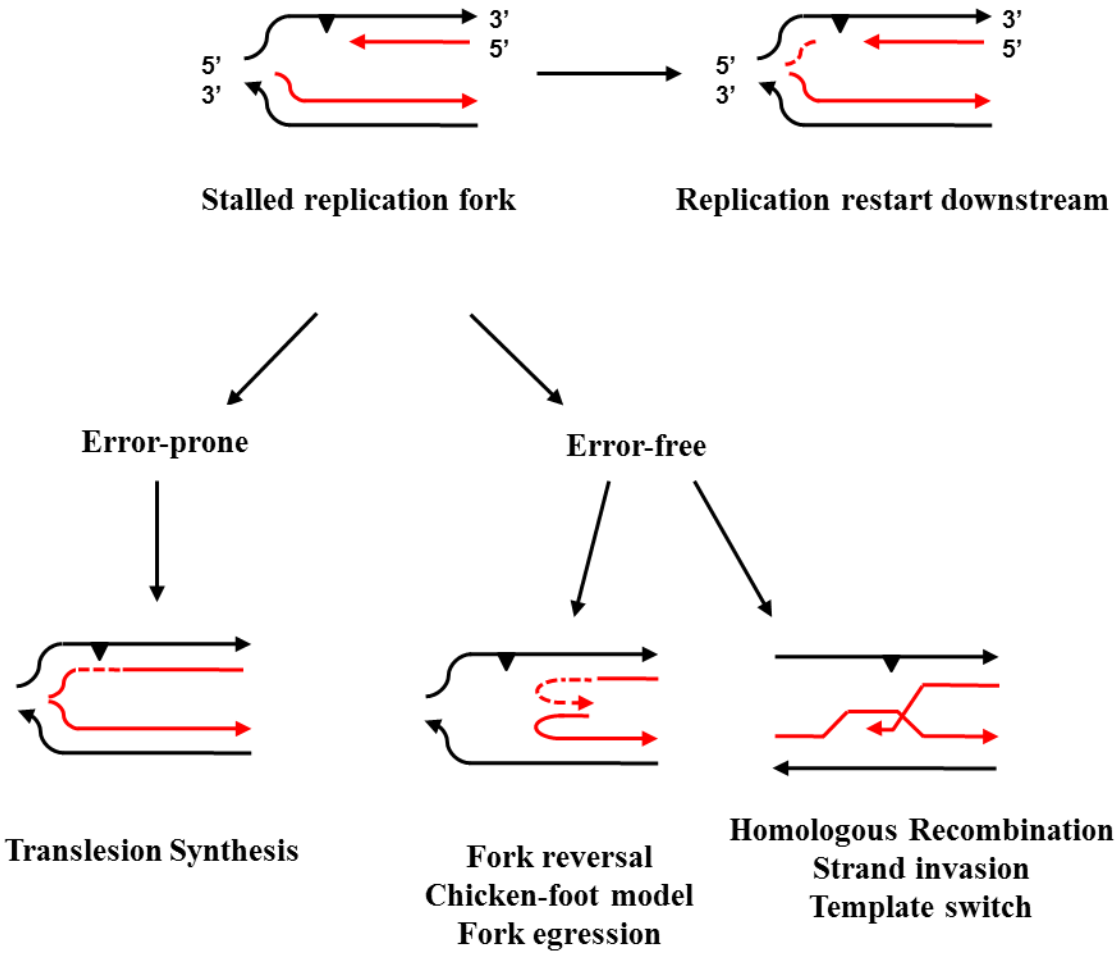

Figure 1.4 – Mechanisms of Lesion Bypass at Stalled Replication Forks. Possible means of lesion bypass include replication restart, translesion DNA synthesis and two alternate error-free lesion bypass mechanisms. While fork reversal is one error-free model for lesion bypass template switching in a Rad51-dependent manner is a possibility too, however, the two might not be mutually exclusive. (Modified with permission from Parker Andersen, (Andersen, 2009)).

1.4 – Rationale for This Study

Although the mechanisms of TLS have been well characterized and the existence of error-free pathway has been definitively demonstrated, relatively little was known about the detailed molecular mechanism of error-free PRR. Previous reports have proposed that some form of a homologous chromatid template was required (Broomfield *et al.*, 2001; Li *et al.*, 2002; Zhang and Lawrence, 2005); however, the exact mechanism of error-free lesion bypass remained uncertain. It is henceforth the ambition of this body of work to find novel genes and proteins involved in PRR, specifically error-free PRR, in hopes of expounding the current understanding of error-free PRR mechanisms and subsequently lesion bypass.

By taking advantage of the synergism between the TLS and error-free PRR pathways it is possible to search for novel genes involved in both PRR pathways. Synthetic lethal screening is a powerful genetic technique available to search for mutants in related pathways. The theory being that when either individual gene is deleted the cell is viable, as the alternative pathway can functionally compensate for the deletion; however, if both genes are deleted, thus eliminating both pathways, the cells become sick or inviable. To begin this study, a screen of the non-essential genes in the *S. cerevisiae* genome was initiated utilising synthetic genetic array (SGA) analysis with the help of Dr. Charles Boone at the University of Toronto. In addition, because we are searching for novel genes involved in a DNA damage tolerance mechanism, by conducting a conditional synthetic lethal screen (by adding a DNA-damaging agent to the SGA screen) we may broaden our search to identify genetic interactions that occur only in the presence

of DNA damage and may therefore give us a better understanding of the genetic interactions occurring in the PRR or DNA damage tolerance pathways. Initial screening results are presented here, and novel findings are explored to gain further insight into PRR.

It is technically difficult and laborious to study DNA repair pathways in humans; therefore, this study utilizes a model eukaryotic organism, namely haploid *S. cerevisiae* yeast strains, which have a fast doubling time (approximately 1.5 hour) and an easily manipulated genome which are vital to studying DNA repair mechanisms. As many of these genes have known human homologues, it is hopeful that by gaining further insight into the yeast PRR, this study will provide insight into how these similar functions are conserved in higher eukaryotes to prevent the hallmark of genomic instability, namely cancer.

CHAPTER TWO

MATERIALS AND METHODS

2.1 – Molecular Biology Techniques

2.1.1 – Bacterial Culture and Storage

The *E. coli* strains DH10B and DH5α (Gibco BRL, Grand Island, NY USA) were used for bacterial transformations, while BL21 (DE3)-RIL (Strategene, # 230245) cells were utilized for protein overexpression of pGEX-Pol30. Unless otherwise noted bacterial strains were incubated at 37 ºC in Luria Broth (LB) (US Biological L1505) (10 g Tryptone, 5 g yeast extract, 5 g NaCl in a total of 1 L ddH_2O (double-distilled sterile or reverse osmosized H_2O)). LB agar plates were made by resuspending the desired amount of LB agar powder (US Biological L1500) in ddH_2O, autoclaving, and pouring approximately 25 mL into each Petri dish. Plasmid selection was maintained by the addition of Ampicillin (Amp) to a final concentration of 50 μg/mL. For long term storage transformed cells were grown overnight in 900 μL of LB + Amp at 37 ºC to which 100 μL of dimethyl sulfoxide (DMSO. EMD Chemicals, MX1485-6) was added, and cells were subsequently frozen at -70 ºC.

2.1.2 – Preparation of Competent Cells

2.1.2.1 – Competent Cells for Chemical Transformation

Competent cells for chemical transformation were grown in the LB medium to an OD_{600} of 0.3-0.4, diluted 1:1 in transformation solution storage (TSS) solution (LB with 10 %

polyethylene glycol$_{8000}$ (PEG)$_{8000}$, 5 % DMSO, 50 mM Mg^{2+} ($MgSO_4$ or $MgCl_2$), and pH 6.5), aliquoted 50 μL/tube and stored at -70 ºC. This protocol was previously described (Chung *et al.*, 1989).

2.1.2.2 – Competent Cells for Electroporation

Competent cells were prepared as outlined in the Bio-Rad *E. coli* Pulser manual. *E. coli* cells were grown to an OD_{600} of 0.6 in 1 L of LB media. Cells were collected by centrifugation at 3500 rpm and the pellet was resuspended in 10 % sterile, cold glycerol. Centrifugation was repeated 4x, each time reducing the resuspension volume, with a final volume of 4 mL. Cells were then aliquoted, 25 μL/tube and quickly frozen at -70 ºC for long term storage.

2.1.3 – Bacterial Transformation

2.1.3.1 – Transformation by Electroporation

Transformation of electroporation competent cells was achieved by thawing cells on ice, to which 1-2 μL of 0.1-0.2 μg/μL DNA sample was added, and transferred to a GenePulser Cuvette (Bio-Rad, # 165-2089). The cuvette was then loaded into a Bio-Rad *E. coli* Pulser and treated with a 1.8 V electric pulse. 200 μL of super optimal broth with catabolite repression (SOC) media (SOC Broth. American Biorganics, Inc., Niagra Falls N.Y., Catalog No. A19-8445. Containing 20 g peptone C, 5 g yeast extract, 0.585 g NaCl, 0.9523 g $MgCl_2$, 1.204 g $MgSO_4$, 0.1864 g KCl and 3.603 g glucose per litre) was added to the cuvette to remove the cells and placed in a 37 ºC water bath for 45 minutes. 50 – 200 μL (volume was dependent on the predicted efficiency of the transformation) of cell suspension was then plated on LB + drug selection agar plates, and incubated at 37 ºC overnight.

2.1.3.2 – Chemical Transformation

Chemical transformations were achieved by thawing chemical competent cells on ice, adding DNA (no more than 10 % the final volume) and incubated on ice for 30 minutes. Cells were then heat shocked for 1 minute at 42 ºC, resuspended in 450 μL SOC media and incubated at 37 ºC before being plated on LB + drug selective media and incubated at 37 ºC.

2.1.4 – Plasmid DNA Isolation

2.1.4.1 – Plasmid DNA Isolation by Quantum Prep® Kit

The majority of plasmid DNA isolation was achieved by using the Quantum Prep® Plasmid Miniprep kit purchased from Bio-Rad (Catalogue #732-6100) and utilising the protocol provided with the kit, with one slight modification: the last step was repeated twice, resulting in a total volume of 200 μL of plasmid DNA obtained instead of the suggested 100 μL.

2.1.4.2 – The Boiling Method

Plasmid isolation via the boiling method was performed as previously described (Maniatis *et al.*, 1982). Bacterial cells were grown in 1.5 mL LB + drug selection media overnight at 37 ºC, collected by centrifugation and resuspended in 350 μL of STET (0.1 M NaCl, 10 mM Tris-HCl pH 8.0, 1 mM (Ethylenedinitrilo)tetraacetic Acid (EDTA. EMD Chemicals, EX0539-1) pH 8.0, 5 % Triton X-100). 25 μL of lysozyme (10 mg/mL, Sigma, L-6876) was added to the eppendorf tube, which was briefly vortexed and placed in boiling water for 45 seconds. Cells were then centrifuged for 10 minutes and the pellet was removed by a toothpick. 8 μL 5 M NaCl and 2 volumes of cold 95 % ethanol were added to the supernatant followed by

incubation at -20 ºC for 30 minutes. Samples were then centrifuged for 15 minutes at top speed (13,200 rpm) before the dried pellet was resuspended in sterile ddH_2O, and stored at -20 ºC.

2.1.4.3 – Alkaline-Lysis Method

Alkaline-lysis was achieved as previously described (Maniatis *et al.*, 1982). In short, a single bacterial colony was used to inoculate 2 mL LB + drug selection media and incubated overnight. Next morning 1.5 mL of cells were collected by centrifugation and resuspended in 100 μL of ice-cold solution I (50 mM glucose, 25 mM Tris-HCl pH 8.0, 10 mM EDTA pH 8.0) vigorously vortexed, followed by the addition of 200 μL freshly prepared solution II (0.2 N NaOH, 1 % sodium dodecyl sulfate (SDS. J.T. Baker, Phillipsburg, N.J. 4095-02). The tube was inverted several time and 150 μL of ice-cold solution III (5 M potassium acetate, 11 % glacial acetic acid in ddH_2O) was added. Again, the tube was inverted several times and incubated on ice for 3-5 minutes and centrifuged at 12,000 rpm for 5 minutes. The supernatant was then transferred to a new tube and the DNA was precipitated with 8 μL 5 M NaCl, and 2 volumes of cold 95 % ethanol. Samples were then centrifuged for 15 minutes at top speed before being resuspended in sterile ddH_2O, and stored at -20 ºC.

2.1.5 – Polymerase Chain Reaction (PCR)

PCR was completed based on the instructions from the protocol for Platinum® *Taq* DNA polymerase purchased from Invitrogen (Carlsbad CA., USA. Cat. No. 10966-034). In short a typical PCR reaction mixture was composed of the following; 5 μL of 10x PCR buffer (provided with purchase of Platinum® *Taq*), 1.0 μL of 50 mM $MgCl_2$, 1.8 μL of 2.5 mM dNTPs (made from the 100 mM dNTP set, Invitrogen, Cat. No. 10297-018), 0.5 μL Patinum® *Taq* DNA

polymerase, 0.5 μL of each primer (primers were ordered from Integrated DNA Technologies and were specific to each PCR run) (See Table 2.1 for a full list of oligonucleotides used in this study), 0.5 μL of template DNA, and sterile ddH_2O to a total volume of 50 μL. A standard PCR amplification was cycled as follows; initial denature at 94 ºC for 2 minutes, denature 94 ºC for 30 seconds, annealing 55 ºC for 30 seconds, extension at 72 ºC for 1 minute/kb of the expected amplified fragment, a final extension of 72 ºC for 10 minutes followed by holding temperature at 4 ºC until the samples were removed. Denaturation, annealing and extension steps were cycled 30 times. Samples were stored at -20 ºC until they were analysed by an agarose gel electrophoresis.

Table 2.1 – Oligonucleotides Used in This Study.

Oligonucleotide	Sequence (5'-3')
EXO1-1	CTT ACG CGT CTT TAG CAA AGG C
EXO1-2	GTG AAT TGC ACA TGC CCA GCG
MMS2-2	CGT AGA AGA AAG CAG CG
MMS2-9	GGG TCG ACA AAG GTT TCT CCT TCC TTC
MRE11-7	GAG TTC ACA AGC AAG CCT G
MRE11-8	GAA TGC AAA TTT GCT CCT CTC
POL30-1	CCG GAT CCA AAT GTT AGA AGC AAA ATT TGA AG
POL30-2	GGC TCG AGT TAT TCT TCG TCA TTA AAT TTG A
PSY3-1	CCT AAC TTA AAG AAT TCC
PSY3-2	GGT AAG GGA GGA TCC GTT TC
PSY3-3	CCC GGA TCC ATG GAA GTT TTA
RAD51-1	GGT GGG ACC ATA AAGG GGG AAT AG
RAD51-2	GCA GTA GGG TTG CGA GGT ATA TG
REV3-2	CTT AGA GGA TAC GAA GAT TCC TC
REV3-3	AAT ACC CGT CAA ATT TGG GG
SAE2-1	GGG CTG CAG TGT ACT TAG CCG TTC
SAE2-2	GCG AAA ATA ACG TCG CAG TTC
SGS1-1	CAA GAA ACT CGA GCC TG
SGS1-2	GAT TTC ACC ACT GCA GG
SIZ1-3	CAG AAA GAA TGA ACC TTT GCC
SIZ1-4	GTG GAA GGA AAG GAC ATA TCC

2.1.6 – Agarose Gel Electrophoresis and DNA Fragment Isolation

Analysis of DNA samples (plasmid or genomic origin) was achieved by agarose gel electrophoresis. 0.7 % agarose (UltraPure™ Agarose. Invitrogen, Cat No. 15510-027) gels were made in 1xTAE (Tris-acetate EDTA) (50x TAE stock was made with 2.42 g Tris base, 57.1 mL glacial acetic acid, 150 mL EDTA pH 8.0 to a total volume of 1L) and run at 88 V before being stained with ethidium bromide to visualize DNA bands. To purify DNA from an agarose gel, the DNA band was cut out and places into a small 0.5 μL microcentrifuge tube that contained a small amount of cheese cloth and a small hole in the bottom, which was then placed inside a 1.5 mL tube. The sample was frozen at -70 ºC for a minimum of 20 minutes before being centrifuges at top speed for 10 minutes. The flow through was treated with phenol and chloroform, and the DNA was precipitated by ethanol before being resuspended in sterile water.

2.2 – Recombinant Protein Overexpression and Purification

The pGEX-*POL30* construct was created by amplifying the *POL30* ORF (utilizing the *POL30-1* and *POL30-2* primers) with the addition of *Bam*H1 and *Xho*1 restriction sites at 5' and 3', respectively. This fragment was then cloned into the *Bam*H1-*Sal*1 sites of pGEX6p to form pGEX-*POL30*. The plasmid DNA was then transformed into *E. coli* BL21(DE3)-RIL cells and selected for on LB + Amp plates. To overexpress pGEX-*POL30* 10 mL liquid medium was inoculated from a single colony. In the morning the 10 mL culture was used to inoculate 300 mL of fresh LB + Amp media and allowed to grow to an $OD_{600\ nm}$ of 0.6 - 0.8 (approximately 3 hours). Cells were then induced with 0.1 mM UltraPure™ IPTG (Isopropylthio-b-D-galactoside. Invitrogen, Cat. No. 15529-019) for 1 hour at 30 ºC. Following inductions cells were pelleted and resuspended in 90 mL phosphate buffered saline (PBS) before being French pressed twice at

10,000 psi. The supernatant was then collected by centrifugation at 15,000 rpm for 10 minutes and passed through a 0.45 μm filter (Acrodisc® 25mm Syringe Filter w/ 0.45 μm Supor® Membrane. Pall Corporation, Ann Arbor, MI. PN:4614). A 5 mL sample was then loaded onto a pre-packed 5 mL GSTrap column (GE Healthcare, #17-5131-01), and repeated several times before the sample was washed with 5 column volumes of PBS, and eluted with fresh reduced glutathione elution buffer (10 mM reduced glutathione (L-Glutathione reduced. Sigma, G4251) in 50 mM Tris-HCl, and pH 8.0). Eluted samples containing purified GST-Pol30 protein) were then collected and subjected to a buffer exchange into PreScission™ Protease Cleavage Buffer (PPCB) (50 mM Tris, 100 mM NaCl, 1 mM EDTA, and pH 8.0 adjusted with HCl) using an Amicon® Ultra-15 Centrifugal Filter Device (Millipore, Cat. No. UFC901024). This was accomplished first by concentrating the protein sample, adding 10 mL of PPCB, concentrating again, and repeating a minimum of four times. The final result was a concentrated sample in PPCB (Figure 2.2 (A), Lane 1) that was run on a 12% resolving and 5% stacking SDS-PAGE (SDS-polyacrylamide gel electrophoresis) gel for visualization as described on page 18.52 of (Maniatis *et al.*, 1989). The protein concentration was determined using a BCA™ Protein Assay Kit (Pierce, Prod# 23227), and the GST-Pol30 fusion protein was then cleaved with PreScission™ Protease (Amersham Pharmacia Biotech Inc., 27-0843-01) at 1 μL/100 μg protein (Figure 2.2A, Lane 2). Following cleavage samples were then once again subjected to buffer exchange, this time into PBS (Figure 2.2B, Lane 1), and re-run through the GST column to eliminate GST from the sample. This time the initial flow-through was collected, concentrated, and the protein concentration was determined (Figure 2.2B, Lane 3). These protein sample was given to Dr. Barry Ziola whose laboratory raised polyclonal antibodies against Pol30, and subsequently screened for monoclonal antibodies against Pol30.

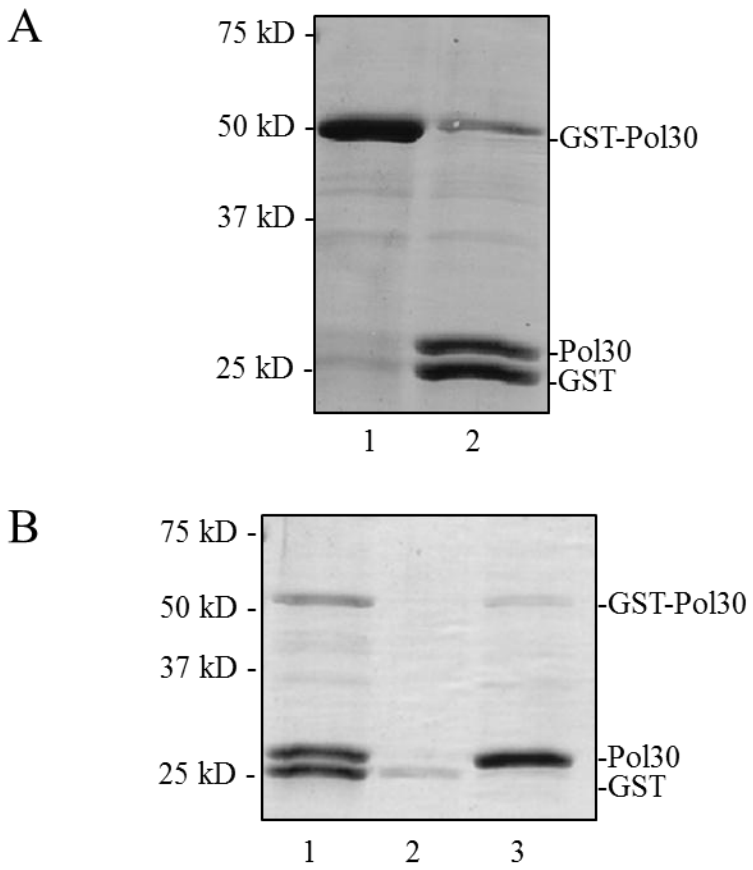

Figure 2.1 – Purification of Pol30 Protein. *E. coli* BL21(DE3)-RIL cells transformed with pGEX-*POL30* were subjected to IPTG induction, lysis, and GST purification. Samples taken during the experiment were run on SDS-PAGE gels for visualization and verification. (A) Lane 1 is purified GST-Pol30 protein that resulted from the first round of GST purification. Lane 2 shows the result of PreScission™ Protease cleavage of the GST-Pol30 protein shown in lane 1. (B) Lane 1 is the same as lane 2 in (A) following buffer exchange into PBS. Lanes 2 and 3 are samples taken during the second round of GST purification which was carried out to separate the GST and Pol30 proteins. The sample in Lane 2 were taken while washing the GST column just before GST elution (Note; this lane is sequentially out of order and should follow Lane 3). Lane 3 contained the sample collected from the flow through during the loading step of the second round of GST purification. The predominant protein present in lane 3 is Pol30, and is the sample that was used to raise and screen antibodies against Pol30.

2.3 – Yeast Genetics

2.3.1 – Yeast Cell Culture

Yeast cells were cultured at 30 °C in either rich yeast-extract peptone dextrose (YPD) broth medium containing 1 % Bacto-yeast extract, 2 % Bacto-peptone, and 2 % glucose (YPD broth traditional formulation with peptone purchased from US Biological, C7062642) or YPD agar media (YPD agar traditional formulation with peptone (powder) purchased from US Biological, C9031173). Synthetic dextrose (SD) medium (0.67 % Bacto-yeast nitrogen base without amino acids (aa), carbohydrate and with ammonium sulphate, US Biological, C7082704), 2 % glucose, with or without 2 % bacto-agar (Becton, Dickinson and Company. REF # 214010)) was used for selection and supplemented with various amino acids as required (Sherman *et al.*, 1983). In certain cases 5-Fluoroorotic acid (FOA, US Biological, F5050; 0.67 % yeast nitrogen base, 0.1 % FOA, 2 % glucose, plus required amino acids and 2x uracil) was used for the selection of appropriate genomic pop-outs. For long term storage, yeast cells were grown on agar plates (YPD or SD) at 30 ºC for 2-3 days. Cells were then removed from the plate using a sterile toothpick, and resuspended in 1.0 mL of sterile 15 % (v/v) glycerol. Cells were subsequently stored at -70 ºC.

2.3.2 – Yeast Strains

The yeast strains used in this study are listed in Table 2.2. All of the strains used are isogenic derivatives of DBY747, HK578 or BY4741. HK578 is a derivative of W303 corrected for the *RAD5* gene by Dr. H. Klein (New York University), while the ORF deletion strains of BY4741 were created by the *Saccharomyces* Genome Deletion Project Consortium and purchased from Research Genetics (Invitrogen). DBY747 is from D. Botstein (Stanford

University). Additional strains used in this study are isogenic derivatives of the above strains and were created by gene disruption, or were the result of synthetic genetic array (SGA) crosses. See Table 2.2 for genotypes and modifications to the strain background. Newly created strains were confirmed by phenotypic changes when possible, and by PCR of genomic DNA.

Table 2.2 – Haploid *Saccharomyces cerevisiae* Strains Used in This study

Strain	Genotype	Source
Y5565	*MAT*α *can1* Δ::*MFA1pr-HIS3mfa1* Δ::*MF* α*1pr-LEU2 lyp1* Δ *his3* Δ*1 leu2* Δ*0 ura3* Δ*0 met15* Δ*0*	C. Boone
Y8389	Y5565 with *rev1* Δ::nat^R *lys2* Δ+	C. Boone
Y8388	Y5565 with *rad6* Δ::nat^R *lys2* Δ+	C. Boone
Y8426	Y5565 with *ubc13* Δ::nat^R *lys2* Δ+	C. Boone
Y8621	Y5565 with *rev3* Δ::nat^R *lys2* Δ+	C. Boone
Y8622	Y5565 with *rad30* Δ::nat^R *lys2* Δ+	C. Boone
Y9897	Y5565 with *mms2* Δ::nat^R *lys2* Δ+	C. Boone
Deletion mutant array	BY4741 *MAT***a** *can1* Δ::*MFA1pr-HIS3 lrp1* Δ	C. Boone
WXY2491	DMA with *rev3* Δ::nat^R *mre11* Δ::kan^R	This Study
WXY2493	DMA with *mms2* Δ::nat^R *mre11* Δ::kan^R	This Study
WXY2460	DMA with *rev3* Δ::nat^R *rad50* Δ::kan^R	This Study
WXY2462	DMA with *mms2* Δ::nat^R *rad50* Δ::kan^R	This Study
WXY2219	DMA with *rev3* Δ::nat^R *rad51* Δ::kan^R	This Study
WXY2416	DMA with *mms2* Δ::nat^R *rad52* Δ::kan^R	This Study
WXY2032	DMA with *rev3* Δ::nat^R *rad52* Δ::kan^R	This Study
WXY2417	DMA with *mms2* Δ::nat^R *rad54* Δ::kan^R	This Study
WXY2555	DMA with *rev3* Δ::nat^R *rad54* Δ::kan^R	This Study
WXY2419	DMA with *mms2* Δ::nat^R *rad55* Δ::kan^R	This Study
WXY2020	DMA with *rev3* Δ::nat^R *rad55* Δ::kan^R	This Study
WXY2420	DMA with *mms2* Δ::nat^R *rad57* Δ::kan^R	This Study
WXY2421	DMA with *rev3* Δ::nat^R *rad57* Δ::kan^R	This Study
WXY2477	DMA with *rev3* Δ::nat^R *xrs2* Δ::kan^R	This Study
WXY2479	DMA with *mms2* Δ::nat^R *xrs2* Δ::kan^R	This Study
BY4741	*MAT***a** *his3* Δ1 *leu2* Δ0 *met15* Δ0 *ura3* Δ0	Invitrogen
BY4741 *trp1* Δ	BY4741 with *trp1* Δ::kan^R	SGD Consortium
BY4741 *psy3* Δ	BY4741 with *psy3* Δ::kan^R	SGD Consortium
BY4741 *shu1* Δ	BY4741 with *shu1* Δ::kan^R	SGD Consortium
BY4741 *shu2* Δ	BY4741 with *shu2* Δ::kan^R	SGD Consortium
BY4741 *csm2* Δ	BY4741 with *csm2* Δ::kan^R	SGD Consortium
BY4741 *sgs1* Δ	BY4741 with *sgs1* Δ::kan^R	SGD Consortium
BY4741 *rad51* Δ	BY4741 with *rad51* Δ::kan^R	SGD Consortium
BY4741 *rad9* Δ	BY4741 with *rad9* Δ::kan^R	SGD Consortium
BY4741 *rev3* Δ	BY4741 with *rev3* Δ::kan^R	SGD Consortium
BY4741 *xrs2* Δ	BY4741 with *xrs2* Δ::kan^R	SGD Consortium
BY4741 *mre11* Δ	BY4741 with *mre11* Δ::kan^R	SGD Consortium
BY4741 *mms2* Δ	BY4741 with *mms2* Δ::kan^R	SGD Consortium
BY4741 *rad50* Δ	BY4741 with *rad50* Δ::kan^R	SGD Consortium
BY4741 *rad52* Δ	BY4741 with *rad52* Δ::kan^R	SGD Consortium
BY4741 *rad54* Δ	BY4741 with *rad54* Δ::kan^R	SGD Consortium
BY4741 *rad55* Δ	BY4741 with *rad55* Δ::kan^R	SGD Consortium

Table 2.2 Continued

Strain	Genotype	Source
BY4741 *rad57* Δ	BY4741 with *rad57* Δ::*kan*^{R}	SGD Consortium
BY4741 *exo1* Δ	BY4741 with *exo1* Δ::*kan*^{R}	SGD Consortium
BY4741 *sae2* Δ	BY4741 with *sae2* Δ::*kan*^{R}	SGD Consortium
WXY1353	BY4741 with *sgs1* Δ::*kan*^{R} *psy3* Δ::*LEU2*	This Study
WXY2469	BY4741 with *mms2* Δ::*kan*^{R} *rad51* Δ::*LEU2*	This Study
WXY2531	BY4741 *psy3* Δ::*kan*^{R} *rad54* Δ::*HIS3*	This Study
WXY2533	BY4741 with *rad54* Δ::*HIS3*	This Study
WXY2534	BY4741 *psy3* Δ::*kan*^{R} *rad51* Δ::*LEU2*	This Study
WXY2546	BY4741 with *sae2* Δ::*kan*^{R} *rev3* Δ::*LEU2*	This Study
WXY2547	BY4741 with *sae2* Δ::*kan*^{R} *mms2* Δ::*LEU2*	This Study
WXY2550	BY4741 with *sae2* Δ::*kan*^{R} *rev3* Δ::*LEU2 mre11* Δ::*HIS3*	This Study
WXY2551	BY4741 with *rev3* Δ::*kan*^{R} *exo1* Δ::*LEU2*	This Study
WXY2904	BY4741 *rad9* Δ::*kan*^{R} *psy3* Δ::*LEU2*	This Study
WXY2949	BY4741 with *mms2* Δ::*kan*^{R} *exo1* Δ::*LEU2*	This Study
WXY2950	BY4741 with *sae2* Δ::*kan*^{R} *exo1* Δ::*LEU2*	This Study
PJ69-4a	*MAT***a** *trp1-901 leu2-3,112 ura3-52 his3-200 gal4* Δ *gal80* Δ *Met2::GAL7-lacZ LYS2::GAL1-HIS3 GAL2-ADE2*	P. James
DBY747	*MAT***a** *his3* -Δ1 *leu2-3,112 trp1-289 ura3-52*	D. Botstein
WXY664	DBY747 with *mms2* Δ::*URA3*	Lab Stock
WXY667	DBY747 with *rev3* Δ::*hisG-URA3-hisG*	Lab Stock
WXY731	DBY747 *rad5* Δ::*HUH*	Lab Stock
WXY1164	DBY747 with *rad51* Δ::*HIS3*	This Study
WXY1323	DBY747 with *psy3* Δ::*kan*^{R}	This Study
WXY1324	DBY747 with *rev3* Δ::*hisG-URA3-hisG psy3* Δ::*kan*^{R}	This Study
WXY1325	DBY747 with *mms2* Δ::*URA3 psy3* Δ::*kan*^{R}	This Study
WXY2379	DBY747 with *mre11* Δ::*HIS3*	This Study
WXY2384	DBY747 with *pol30-K164R*	This Study
WXY2389	DBY747 with *mre11* Δ::*HIS3 pol30-K164R*	This Study
WXY2390	DBY747 with *mre11* Δ::*HIS3 rev3* Δ::*LEU2*	This Study
WXY2392	DBY747 with *sgs1* Δ::*HIS3*	This Study
WXY2393	DBY747 with *rev3* Δ::*HUH sgs1* Δ::*HIS3*	This Study
WXY2394	DBY747 with *sae2* Δ::*LEU2*	This Study
WXY2917	DBY747 with *exo1* Δ::*LEU2*	This Study
WXY2918	DBY747 with *mms2* Δ::*URA3 exo1* Δ::*LEU2*	This Study
WXY2974	DBY747 *rad5-I916A*	This Study
WXY2991	DBY747 with *exo1* Δ::*LEU2 rev3* Δ::*hisG-URA3-hisG*	This Study
WXY2990	DBY747 *rad-IAA*	This Study
WXY2900	DBY747 *rad5-AA*	This Study
HK578-10A	*MAT***a** *ade2-1 can1-100 his3-11,15 leu2-3,112 trp1-1 ura3-1*	H. Klein
HK578-10D	*MAT*α *ade2-1 can1-100 his3-11,15 leu2-3,112 trp1-1 ura3-1*	H. Klein
HK590-10A	HK578-10A with *srs2* Δ::*HIS3*	H. Klein

Table 2.2 Continued

Strain	Genotype	Source
HK578-2C	10A *rad5* Δ::*URA3*	H. Klein
HK579-10A	10A *mms2* Δ::*HIS3*	H. Klein
HK810	HK578-10A with *rev3* Δ::*LEU2*	H. Klein
LSY396	HK578-10A with *rad50* Δ::*hisG-URA3-hisG*	L. Symington
LSY402	HK578-10A with *rad51* Δ::*LEU2*	L. Symington
LSY386	HK578-10A with *rad52* Δ::*TRP1*	L. Symington
LSY403	HK578-10A with *rad54* Δ::*LEU2*	L. Symington
WXY902	HK578-10D *mms2* Δ::*HIS3*	Lab Stock
WXY920	HK578-10A *mms2* Δ::*HIS3 rev3* Δ*::HUH*	Lab Stock
WXY930	HK578-10D with *rad18* Δ::*LEU2*	Lab Stock
WXY919	HK578-10A with *ade2-1 ade3* Δ::*hisG mrell* Δ::*HIS3*	Lab Stock
WXY956	HK578-10D *rev3* Δ::*LEU2*	Lab Stock
WXY963	HK578-10A with *psy3* Δ::*HIS3 rad52* Δ::*LEU2*	This Study
WXY964	HK578-10A with *psy3* Δ::*HIS3 rad51* Δ::*LEU2*	This Study
WXY965	HK578-10A with *psy3* Δ::*HIS3 rad50* Δ::*hisG-URA3-hisG*	This Study
WXY966	HK578-10D with *psy3* Δ::*HIS3 rad54* Δ::*LEU2*	This Study
WXY970	HK578-10A with *sgs1* Δ::*LEU2*	This Study
WXY989	HK578-10D with *pol30* Δ::*HIS 3* / YCpL-*Pol30*/ pGBT*RAD18* /YEp*RAD6*	Lab Stock
WXY990	HK578-10D with *pol30* Δ::*HIS 3* / YCpL-*pol30-K164R* /pGBT*RAD18* /YEp*RAD6*	Lab Stock
WXY994	HK578-10A with *pol30-K164R*	Lab Stock
WXY1328	HK578-10D with *psy3* Δ::*LEU2*	This Study
WXY1329	HK578-10D with *mms2* Δ::*HIS3 psy3* Δ::*LEU2*	This Study
WXY1330	HK578-10A with *rev3* Δ::*LEU2 psy3* Δ::*HIS3*	This Study
WXY1334	HK578-10A with *rev3* Δ::*LEU2 psy3* Δ::*HIS3 srs2* Δ::*TRP1*	This Study
WXY1342	HK578-10A with *psy3* Δ::*HIS3 srs2* Δ::*LEU2*	This Study
WXY1358	HK578-10A with *psy3* Δ::*HIS3 sgs1* Δ::*LEU2*	This Study
WXY2959	HK578-10A with *siz1* Δ::*HIS3*	This Study
WXY2960	HK578-10A with *mms2* Δ::*URA3 siz1* Δ::*HIS3*	This Study
WXY2962	HK578-10A with *siz1* Δ::*HIS3 sae2* Δ::*LEU2*	This Study
WXY2963	HK578-10A with *siz1* Δ::*HIS3 exo1* Δ::*URA3*	This Study
WXY2964	HK578-10A *rad5* Δ::*URA3 siz1* Δ::*LEU2*	This Study
WXY2965	HK578-10A *rad5-AA siz1* Δ::*LEU2*	This Study
WXY2966	HK578-10A *rad5-IAA siz1* Δ::*LEU2*	This Study
WXY2969	HK578-10A with *sgs1* Δ::*LEU2 siz1* Δ::*URA3*	This Study
WXY2975	HK578-10A with *sae2*Δ*::LEU2*	This Study
WXY2981	HK578-10A *rad5 -AA*	This Study
WXY2982	HK578-10A *rad5 -IAA*	This Study
WXY2983	HK578-10A *rad5-I916A rev3* Δ::*LEU2*	This Study
WXY2985	HK578-10A *rad5* Δ::*URA3 rev3* Δ*::LEU2*	This Study

Table 2.2 Continued

Strain	Genotype	Source
WXY2994	HK578-10A with *siz1* Δ::*HIS3 rad51* Δ::*LEU2*	This Study
WXY2995	HK578-10A with *mre11* Δ::*HIS3 siz1* Δ::*LEU2*	This Study
WXY2996	HK578-10A *rad5 -AA rev3* Δ::*LEU2*	This Study
WXY2997	HK578-10A *rad5 -IAA rev3* Δ::*LEU2*	This Study
WXY2998	HK578-10A *rad5 -AA mms2* Δ::*URA3*	This Study
WXY2999	HK578-10A *rad5 -IAA mms2* Δ::*URA3*	This Study
WXY3001	HK578-10A *rad5- I916A*	This Study
WXY3002	HK578-10A *rad5- I916A mms2* Δ::*LEU2*	This Study
WXY3007	HK578-10A with *pol30-K164R sae2*Δ*::LEU2*	This Study
WXY3008	HK578-10D with *rad18* Δ::*TRP1 sae2* Δ::*LEU2*	This Study

2.3.3 – Yeast Transformation

Yeast cells were transformed using a modified lithium acetate method (Ito *et al.*, 1983). Overnight, 2 mL of yeast cultures were incubated at 30 ºC in appropriate liquid media (either YPD or SD minimal medium with required aa). The next morning cells were sub-cultured into 5 mL of fresh media and allowed to grow until a mid-logarithmic growth phase was achieved. 1 mL of yeast culture was then pelleted by centrifugation for each transformation being prepared, and subsequently washed in 500 µl LiOAc solution (0.1 M lithium acetate (LiOAc), 10 mM Tris-HCl; pH 8.0, 1 mM EDTA. Finally the pellet was resuspended in 100 µL LiOAc. 4 µL of carrier DNA (single-stranded salmon sperm) and 5 µL of transforming DNA (See Table 2.3 for a full list of plasmids used in this study) were added to the resuspended yeast cells and allowed to sit at room temperature for 5 minutes. 280 µL of 50 % PEG_{4000} was added and the contents of the tube were mixed by inverting the tube 8-10 times, and incubated at 30 ºC for 45 minutes. Following incubation 39 µL of DMSO was added to each transformation, mixed by inverting the tube 8-10 times and heat shocked at 42 ºC for 5 minutes. Yeast cells were then pelleted by centrifugation at top speed for 30 seconds, washed in 500 µL of sterile ddH_2O before finally being resuspended in 100 µL sterile ddH_2O and plated on appropriate minimal media and allowed to grow for 3-5 days at 30 ºC.

Table 2.3 – Plasmids Used in This Study.

Plasmid	Source	Reference
YCp50-*MAT* ***a***	F. Fabre	Heude and Fabre, 1993
YCp50-*MAT* α	F. Fabre	Heude and Fabre, 1993
YCpL-*Pol30*	Lab stock	
YCpL-*pol30-K164R*	Lab stock	
pGBT *RAD18*	Lab stock	
YEp*RAD6*	D. Gietz	
p*exo1* Δ::*LEU2*	This study	This study
p*exo1* Δ::*URA3*	This study	This study
p*mms2* Δ::*HIS3*	Lab Stock	Barbour *et al* ., 2006
p*mms2* Δ::*LEU2*	Lab Stock	Broomfield et al., 1998
p*mms2* Δ::*URA3*	Lab Stock	Broomfield *et al* ., 1998
p*mre11* Δ::*HIS3*	W. Xiao	Barbour *et al* ., 2000
p*psy3* Δ::*HIS3*	W. Xiao	Ball *et al* ., 2009
p*psy3* Δ::*Kan* ^{R}	W. Xiao	Ball *et al* ., 2009
p*psy3* Δ::*LEU2*	W. Xiao	Ball *et al* ., 2009
p*rad51* Δ::*LEU2*	W. Xiao	Ball *et al* ., 2009
p*rad52* Δ::*LEU2*	Lab Stock	Xiao *et al* ., 1996
p*rad54* Δ::*HIS3*	W. Xiao	Ball *et al* ., 2009
pDG347 (p*rev3* Δ::*hisG-URA3-hisG*)	D. Gietz	Roche *et al* ., 1994
p*rev3* Δ::*LEU2*	Lab Stock	Xiao *et al* ., 1996
p*sae2* Δ::*LEU2*	This study	This study
p*siz1* Δ::*HIS3*	This study	This study
p*siz1* Δ::*URA3*	This study	This study
pPWΔSGS1	I. Hickson	Watt *et al* ., 1995
p*sgs1* Δ::*HIS3*	This study	This study
pFP56 (p*srs2* Δ::*TRP1*)	H. Klein	
pGAD424 *SHU1*	T. Ito	Ito *et al* ., 2001
pGAD424 *SHU2*	T. Ito	Ito *et al* ., 2001
pGAD424 *CSM2*	T. Ito	Ito *et al* ., 2001
pGBKT7 *SHU1*	T. Ito	Ito *et al* ., 2001
pGBKT7 *SHU2*	T. Ito	Ito *et al* ., 2001
pGBKT7 *CSM2*	T. Ito	Ito *et al* ., 2001
pGAD424 *PSY3*	W. Xiao	Ball *et al* ., 2009
pGBT9 *PSY3*	W. Xiao	Ball *et al* ., 2009
pGAD424	D. Gietz	
pGBT9	D. Gietz	
pGBKT7	Clontech	
pGEX6-POL30	W. Xiao	This study

2.3.4 – Targeted Gene Disruption

Yeast strains created by one-step targeted gene deletion using a disruption cassette were introduced to the cells via yeast transformation following appropriate restriction digestion of the disruption cassette. Disruption cassettes used in this study are explained below.

2.3.4.1 – Disruption Cassettes Created for this Study

2.3.4.1.1 – *EXO1* Disruption Cassettes

The 2.1 kb *EXO1* open reading frame (ORF) was cloned into pBluescript and the 1.3 kb *Nde*I-*Bsa*BI fragment within the *EXO1* ORF was deleted and replaced by a *Bam*HI linker, which was then used to clone either a 1.6 kb *Bam*HI fragment containing *LEU2* from YDp-L or a 1.1 kb *Bam*HI fragment containing *URA3* from YDp-U (Berben *et al.*, 1991). The *exo1*Δ*::LEU2* disruption cassette was released by *Bgl*II-*Pst*I digestion and the *exo1*Δ*::URA3* disruption cassette was released by *Bgl*II-*Sna*BI digestion prior to yeast transformation. Following gradient plate analysis, putative mutants were further screened by PCR using primers *EXO1-1* and *EXO1-2* (See Table 2.1).

2.3.4.1.2 – *PSY3* Disruption Cassettes

DBY747 strains containing the *psy3*Δ::*kan*^{R} allele were created by transforming cells with a DNA fragment obtained from PCR amplification of the BY4741 *psy3*Δ::*kan*^{R} allele by primers *PSY3-1* and *PSY3-2* (See Table 2.1). To construct plasmids containing the *psy3*Δ disruption cassettes, a 1.8 kb genomic DNA fragment containing the *PSY3* ORF and its flanking sequences were PCR amplified using *PSY3-1* and *PSY3-2*, from which a 1.7 kb *Bam*HI fragment

was cloned into pTZ19R. A 0.6 kb *Eco*47–*Spe*I fragment containing the vast majority of the *PSY3* ORF was deleted and replaced with a *Bgl*II linker. A *Bam*HI fragment containing either a 1.6 kb *LEU2* fragment from YDp-L or a 1.16 kb *HIS3* fragment from YDp-H (Berben *et al.*, 1991) was cloned into the *Bgl*II site to form p*psy3*Δ*::LEU2* or p*psy3*Δ*::HIS3*, respectively. These disruption cassettes were released by *Bam*HI digestion prior to transformation. Following gradient plate analysis, putative mutants were further screened by PCR using primers *PSY3-2* and *PSY3-3* (See Table 2.1).

2.3.4.1.3 – *RAD5* Point Mutations

To create *RAD5* site-specific mutants, a 3.5 kb *Pml*I-*Sal*I yeast genomic fragment containing *RAD5* ORF but missing the N-terminal 100 aa coding region was cloned into plasmid YIplac211 (*URA3*) (Gietz and Sugino, 1988) to form YIpU-Rad5ΔN, which was used to create *rad5-I916A* and *rad5-AA* (D681A+E682A) mutations. Site-specific mutagenesis was performed by a mega-primer approach (Ke and Madison, 1997) using mutagenic primers that also create diagnostic restriction sites. The cloned site-specific mutations were screened by restriction analysis and further confirmed by sequencing. The resulting YIp plasmids were linearized by *Nru*I cleavage prior to yeast transformation and the confirmed transformants were subject to 5-FOA selection for the appropriate genomic pop-outs that only contain the desired point mutation(s) at the *RAD5* locus.

2.3.4.1.4 – *RAD51* Disruption Cassette

To construct a plasmid containing the *rad51* disruption cassette, a 3.7 kb *Bam*HI fragment containing *RAD51* and its flanking sequences was cloned and a 1.25 kb *Spe*I–*BstE*II fragment containing essentially the entire *RAD51* ORF was deleted and replaced with a *Bgl*II linker, which allowed us to clone the 1.6 kb *Bam*HI fragment from YDp-L containing *LEU2*. The resulting plasmid was cleaved by BamHI to release the *rad51*Δ*::LEU2* cassette.

2.3.4.1.5 – *RAD54* Disruption Cassette

To construct a plasmid containing the *rad54* disruption cassette, the 2.7 kb *RAD54* ORF was amplified as an *Eco*RI–*Sal*I fragment and cloned into pTZ19R. The 1.9 kb *Bam*HI fragment within the *RAD54* ORF was then deleted and replaced with the 1.16 kb *HIS3* fragment from YDp-H. The *rad54*Δ*::HIS3* disruption cassette was released by *Stu*I–*Eco*RV digestion.

2.3.4.1.6 – *SAE2* Disruption Cassette

A 1.7 kb yeast genomic DNA fragment containing the *SAE2* ORF and flanking regions was amplified by primers *SAE2-1* and *SAE2-2* (See Table 2.1) and cloned into pGEM-T. A 1.0 kb *Hin*dIII-*Bsi*WI fragment containing essentially the entire *SAE2* ORF was deleted and replaced by a *Bam*HI linker, which was used to clone the 1.6 kb *Bam*HI fragment containing *LEU2* from YDp-L (Berben *et al.*, 1991) to form p*sae2*Δ::*LEU2*. The *sae2*Δ*::LEU2* disruption cassette was released by *Pst*I-*Sal*I digestion prior to yeast transformation.

2.3.4.1.7 – *SIZ1* Disruption Cassette

A 2.0 kb yeast genomic DNA fragment within the *SIZ1* ORF was amplified by primers *SIZ1-3* and *SIZ1-4* (See Table 2.1) and cloned into pGEM-T. A 1.4 kb *Bam*HI fragment was deleted and replaced by either a 1.16 kb *Bam*HI fragment containing *HIS3* from YDp-H or a 1.1 kb *Bam*HI fragment containing *URA3* from YDp-U (Berben *et al.*, 1991). The *siz1*Δ*::HIS3* disruption cassette was released by *Apa*LI-*Eco*RV digestion and the *siz1*Δ*::URA3* disruption cassette was released by *Bgl*II-*Cla*I digestion prior to yeast transformation. Following gradient plate analysis, putative mutants were further screened by PCR using primers *SIZ1-3* and *SIZ1-4* (See Table 2.1).

2.3.4.1.8 – *SGS1* Disruption Cassette

The 4.4 kb *SGS1* ORF was PCR amplified and cloned into pGEM-T. A 1.3 kb *Cla*I-*Hin*dIII fragment within *SGS1* ORF was deleted and replaced with a *Bam*HI linker, which was used to clone a 1.16 kb *Bam*HI fragment containing *HIS3* from YDp-H (Berben *et al.*, 1991) to form p*sgs1*Δ::*HIS3*. The *sgs1*Δ*::HIS3* cassette was released by *Afl*II-*Bsr*GI digestion prior to yeast transformation. Following gradient plate analysis, putative mutants were further screened by PCR using primers *SGS1-1* and *SGS1-2* (See Table 2.1).

2.3.4.2 – Other Disruption Cassettes Used in this Study

Sources and use of *rad52*Δ*::LEU2* (Xiao *et al.*, 1996), *rev3*Δ::*hisG-URA3-hisG* (Roche *et al.*, 1994), *rev3*Δ::*LEU2* (Xiao *et al.*, 1996) *mms2*Δ::*HIS3* (Barbour *et al.*, 2006), *mms2*Δ::*LEU2* (Broomfield *et al.*, 1998), *mms2*Δ::*URA3* (Broomfield *et al.*, 1998) and *mre11*Δ::*HIS3* (Barbour

et al., 2000) disruption cassettes have been previously described. Plasmid pPWΔ*SGS1* containing the *sgs1*Δ*::LEU2* disruption cassette was received from Dr. I. Hickson (University of Oxford, UK), and the *sgs1*Δ*::LEU2* cassette was released by *Nco*I–*Pst*I. Plasmid pFP56 (which contains *srs2*Δ*::TRP1*) was received from Dr. H. Klein and the *srs2*Δ*::TRP1* cassette was released by *Sac*I–*Cla*I digestion.

2.3.5 – Isolation of genomic DNA

A 2 mL overnight culture of yeast cells was grown in appropriate media before being pelleted by centrifugation in a 2 mL screw cap tube. The pellet was resuspended in 230 μL of yeast DNA extraction buffer to each tube. Alternatively yeast colonies can be scraped directly from a plate and resuspended in the yeast DNA extraction solution (however, this should not be done with a toothpick). Once the cells are resuspended, 100 μL of phenol, 100 μL of chloroform, and one scoop (approximately 0.3 g) of acid washed beads were added to each tube. Samples were then vigorously vortexed at top speed for 3 minutes, and centrifuged for 5-6 minutes at top speed. The supernatant was carefully removed and transferred to a new tube, to which 4 μL of 5 M NaCl and 600 μL of cold 95 % ethanol was added, the tube was inverted several times and then placed in the -20 ºC freezer for a minimum of 20 minutes. Samples were then removed from the freezer and centrifuged at top speed for 15 minutes. The remaining pellet was dried, resuspended in 200 μL of TE (10 mM Tris-HCl, 1 mM EDTA, pH 8.0) and incubated with 5 μL of 10 mg/mL RNaseA at 37 ºC for 10 minutes. To each tube 8 μL 5M NaCl and two volumes 95% cold ethanol were added, followed by incubation at -20 ºC for a minimum of 20 minutes before being centrifuged at top speed for 15 minutes. The supernatant was removed, the samples were dried, and finally resuspended in 50 μL sterile ddH_2O (Hoffman and Winston, 1987).

2.3.6 – Testing for Sensitivity to DNA-Damaging Agents

2.3.6.1 – Serial Dilution Plates

Serial dilution assays were used as a semi-quantitative means to determine MMS (Aldrich, 129925), hydroxyurea (HU, Sigma, H8627) and UV sensitivity as previously described (Barbour *et al.*, 2006). 2 mL overnight yeast cell cultures were grown in YPD (or selective medium if necessary) at 30 ºC, subcultured the next morning into 3 mL of fresh media and allowed to grow to a mid-logarithmic phase. Cell density was determined by a hemocytometer and adjusted to 2 x 10^6 cells/mL. 10-fold dilutions were then made in sterile ddH_2O and 8 μL aliquots of each dilution were spotted onto YPD and YPD + drug plates. MMS and HU were added to sterile, molten YPD agar once it had cooled to 55 ºC and just before the agar plates were poured. UV plates were spotted on YPD agar plates just like the control plates, but were subsequently exposed to 254-nm UV light in a UV crosslinker (Fisher Sci. model FB-UVXL at approximately 2400 mW/cm^2) at specific doses. It should be noted that Petri dish lids must be removed during UV treatment, and any plates treated with UV require incubation in the dark to prevent photoreactivation. Once serial dilution plates were spotted they were incubated for 2 days at 30 ºC, photographed, and the results were analysed.

2.3.6.2 – Gradient plate analysis of MMS sensitivity

The gradient plate assay was used as a semi-quantitative measurement of relative MMS sensitivity as previously described (Barbour *et al.*, 2006). 30 mL of sterile molten YPD agar cooled to 55 ºC was mixed with an appropriate amount of MMS and poured into a square Petri dish to form the bottom layer of a gradient plate. The gradient was formed by allowing the bottom layer to solidify while the plate was tilted (Figure 2.2, Step 1). After the first layer had

solidified, the Petri dish was returned to a flat surface (Figure 2.2, Step 2) and an additional 30 mL of sterile molten YPD agar without MMS was added to each plate to form the top layer (Figure 2.2, Step 3). The control plate, which contains no MMS, was made by simply pouring 60 mL of sterile molten YPD agar into a square Petri dish and allowed to solidify while remaining level. To print the cultures on the gradient plates 400 μL of sterile water was warmed to 55 ºC and combined with 500 μL of sterile molten YPD agar and kept at 55 ºC until ready to use. Once ready, 100 μL of a 2 mL overnight yeast culture was added to the pre-warmed water/molten YPD agar mixture and gently poured out over a sterile microscope slide. The long edge of a second sterile microscope slide was then dipped into the culture/water/molten YPD agar mixture and imprinted on one gradient plate (Figure 2.2, Step 4). The same microscope slide was repeatedly dipped into the same mixture and imprinted on the control plate and subsequently on the desired MMS plates. This process was then repeated for each strain required for analysis. Plates were then incubated at 30 ºC for two days before being photographed, and the results were then analysed.

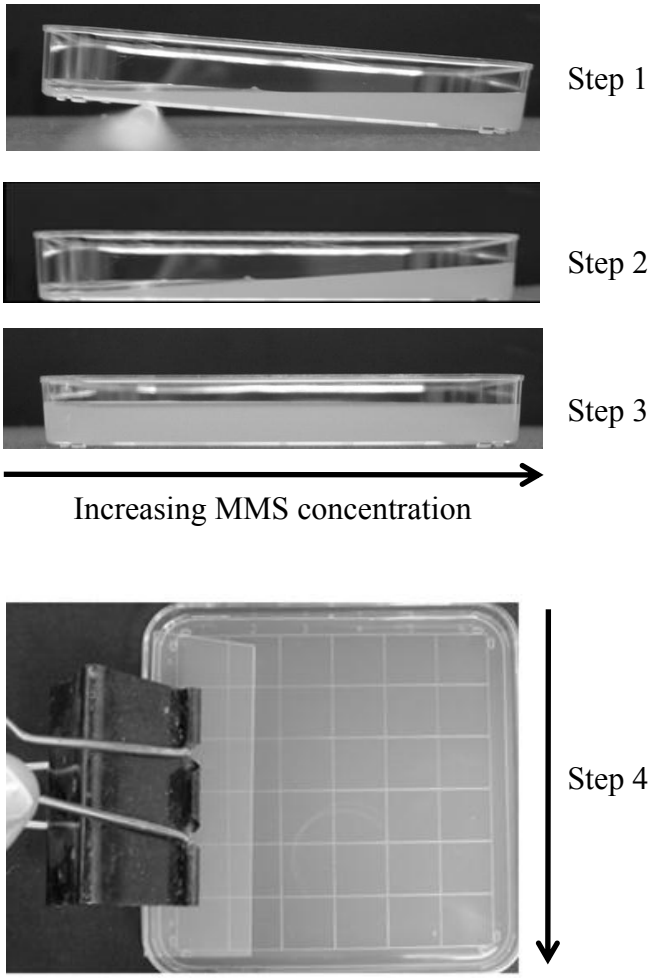

Figure 2.2 – Making Gradient Plates for the Semi-Quantitative Analysis of MMS Sensitivity. Step 1 (side view): The bottom 30 mL of YPD sterile molten agar (containing the desired percentage of MMS) is poured into the bottom of a square Petri dish while the dish is slanted. Step 2 (side view): Once the bottom layer of agar has solidified the plate is returned to a flat surface. Step 3 (side view): The top 30 mL of YPD sterile molten agar is poured on top of the bottom layer to achieve an overall level surface, and allowed to solidify. Step 4 (top view): Plates were then imprinted with yeast cultures using the long edge of a microscope slide, and incubated at 30 ºC for two days before results are photographed and analysed. Arrows represent increasing MMS concentration gradient.

2.3.6.3 – Quantitative Assessment of Sensitivity by a Liquid Killing Experiment

MMS-induced liquid killing was conducted as previously published (Xiao *et al.*, 1996). Briefly, overnight yeast cultures were used to inoculate fresh YPD and allowed to grow until a cell count of approximately 2 x 10^7 cells/mL was reached. MMS was added to the liquid culture and samples were withdrawn at indicated times. Cells were then harvested by centrifugation, washed, diluted if necessary, and plated onto YPD agar plates. Colonies were counted after 3 days of incubation at 30 ºC and scored as a percentage of cell survival against untreated cells.

2.3.7 – Spontaneous Mutagenesis Assay

The spontaneous mutation rate was measured by monitoring the Trp^+ reversions of the *trp1-289* allele in the DBY747 strain via a modified Luria and Delbruck fluctuation test, as previously described (Broomfield *et al.*, 1998). An overnight yeast culture was subcultured into five (therefore each experiment contained five independent cultures for each strain) 10 mL YPD test tubes to a final cell count of 20 cells/mL and allowed to grow at 30 ºC for 3 days. Cells were then collected, washed, resuspended, diluted if required, and plated. Each strain was plated onto YPD (to score total survivors), and onto SD-Trp to score the Trp^+ revertants. Spontaneous mutation rates were calculated as previously described (Williamson *et al.*, 1985) , and calculated by the following formulas:

$$Frequency = \frac{total\ cell\ number\ of\ Trp+\ cells}{total\ number\ of\ viable\ cells}$$

$$Rate = \frac{0.4343 * Frequency}{\log(total\ cell\ number) - \log(initial\ cell\ number)}$$

* Where 0.4343 is approximately $\log_{10}e$.

2.3.8 – Mating-Type Heterozygosity

The mating-type heterozygosity assay was performed as previously described (Barbour and Xiao, 2006). Essentially the mating-type heterozygosity assay was accomplished by transforming a control YCp-*MAT***a** or YCp-*MAT*α plasmid (Heude and Fabre, 1993; Watt *et al.*, 1995) into a yeast strain containing a null mutation in the gene of interest. Yeast strains were then compared for their sensitivity to MMS via gradient plate analysis.

2.3.9 – Yeast Two-Hybrid (Y2H) Analysis

pGBKT7 and pGAD424 plasmids containing *CSM2*, *SHU1* or *SHU2* ORFs were received from Dr T. Ito (Kanazawa University, Japan). The original *PSY3* genes from the above collection contained sequence errors. The *PSY3* ORF was PCR amplified as a *Bam*HI–*Sal*I fragment, cloned into pGBT9 and pGAD424, and the cloned insert sequences were confirmed. Y2H was first described in 1989 by Fields and Song (Fields and Song, 1989), and performed by transforming the yeast strain PJ69-4a (James *et al.*, 1996) with various combinations of the Gal_{BD} and Gal_{AD} plasmids. The transformants were selected on SD-Trp-Leu agar, and subsequently restreaked. Liquid cultures were grown overnight before being scored for growth on selective media. Alternatively, cells

were taken directly from selective agar plates, resuspended in sterile ddH_2O and spotted on Y2H selective plates. SD-Trp-Leu-His and SD-Trp-Leu-His + various concentrations of 3-amino triazole (3-AT) were used to test for activation of the P_{GAL1}-*HIS3* reporter gene, and SD-Trp-Leu-Ade screened for activation of the P_{GAL1}-*ADE* reporter. At least three independent transformation colonies were selected and compared for each Y2H interaction tested. Plates were photographed following minimum 3 day incubation at 30 °C.

2.3.10 – Synthetic Genetic Array (SGA) Analysis

The query genes chosen for SGA were *RAD30*, *RAD6*, *UBC13*, *MMS2*, *REV1*, and *REV3*. BY4741 yeast strains containing null mutation of these genes were used to create the query strains required for SGA. The query strains were created by a non-essential gene switching method using the strain Y5565 from Dr. Charles Boone (University of Toronto). The query strains were then crossed with the deletion mutant array and analysed in triplicate by SGA as previously described (Tong and Boone, 2006; Tong *et al.*, 2001). SGA screens were performed in Dr. Charles Boone's laboratory. In addition to the standard SGA screen a conditionally synthetic lethal screen was run by adding 0.004 % MMS to the final *MAT***a**-kan^R-nat^R double mutant selection plates and scored for fitness. Thus, we expanded our search to include putative genetic interactions occurring in the presence of a DNA-damaging agent. The result was 407 putative genetic interactions which were then subsequently screened by random spore analysis (RSA).

2.3.11 – Random Spore Analysis (RSA)

RSA was performed on putative interactions that appeared at least twice in the three rounds of SGA screening. During the initial steps in SGA diploid cells are plated onto sporulation medium to allow for subsequent selection of *MAT*a meiotic progeny. These sporulation plates were sent to us from Dr. Boone's lab, and used to perform RSA analysis on putative genetic interactions found during SGA screening. In short, spores were resuspended in 500 μL of sterile water and an aliquot was plated onto selective media with or without 0.004 % MMS as follows: 20 μL onto SD-His/Arg/Lys + canavanine/thialysine, 40 μL onto SD-His/Arg/Lys + canavanine/thialysine/G418, 40 μL onto SD-His/Arg/Lys + canavanine/thialysine/clonNAT and 80 μL onto SD-His/Arg/Lys + canavanine/thialysine/G418/clonNAT (Tong and Boone, 2006). The plates were incubated at 30 °C for 3 days before they were photographed and scored for synergistic interactions.

2.3.12 – Flow Cytometry Analysis

A 50 mL culture was grown overnight at 30 °C in YPAD (YPD supplemented with 20 mg/L Ade from Sigma, A9126), diluted into 50 mL of warm YPAD to a cell count of 5 x 10^6 cells/mL, and allowed to grow to 1 x 10^7 cells/mL (approximately 2 hours). Cells were then collected by centrifugation, washed twice with sterile water and resuspended in 50 mL of warm YPAD at pH 5. α-Factor was added at a dose at which >90 % of cells were arrested, which took approximately 2 hours. Cells were then centrifuged and vigorously washed three times in sterile water before being resuspended

in 20 mL of YPAD and divided into two 10 mL cultures. MMS (0.02 %) was added to one of the cultures and incubation continued at 30 °C. Culture (600 μL) was taken at each time point, added to 1.4 mL of 100 % ethanol and stored at 4 °C until all samples were ready to be analysed. Samples were then spun down and resuspended in 500 μL of 50 mM sodium citrate (pH 7). 2.5 μL of 10 mg/mL RNaseA was added and the samples were incubated at 50 °C for 1 hour. 20 μL of 10 mg/mL Proteinase K was added, and each sample was vortexed and returned to 50 °C for another hour. Cells were collected by centrifugation and resuspended in 500 μL of 50 mM sodium citrate (pH 7) containing propidium iodide (Fluka) by vortex. Samples were then briefly sonicated and subjected to analysis at the Flow Cytometry Core Facility at the University of Calgary.

2.3.13 – Detection of PCNA Ubiquitination

2.3.13.1 – Yeast Cell Preparation

Detection of ubiquitinated PCNA was adapted from a previous report (Knop *et al.*, 1999). Two 10 mL overnight cultures were grown at 30 °C in YPAD for each strain being tested. The two cultures were then combined; cells were counted with a haemocytometer and diluted to $0.3x10^{-7}$ in a total volume of 100 mL (in a 250 mL flask) of pre-warmed YPAD and allowed to grow for an additional 2 hours. Cultures were then split in two; one was treated with 0.05 % MMS while the other remained untreated and both cultures were then returned to 30 °C for 90 minutes. 20 mL of culture was pelleted (2 minutes at 4300 rpm at 4 °C), the supernatant was immediately discarded, and the pellet was quickly frozen in liquid nitrogen for 10 minutes. The pellet was then

resuspended in cold sterile ddH_2O containing 25 mM N-ethylmaleimide (NEM) (Sigma, E1271) (made fresh in 95 % cold ethanol) and 1 mM phenylmethylsulfonyl fluoride (PMSF) (Sigma, P-7626) (made fresh in 95 % cold ethanol) and transferred to a 1.5 mL screw cap tube that had been pre-chilled on ice. 150 μL of a 1.85 M NaOH solution with 7.5 % β-mercaptoethanol was then added to each tube, mixed by inverting the tube several times, and incubated on ice at 4 °C for 15 minutes. Next, 150 μL of 55 % w/v TCA (trichloracetic acid), made fresh in cold ddH_2O, was added, mixed by inverting the tube. Samples were then incubated on ice at 4 °C for 10 minutes before samples were centrifuged at 13,200 rpm at 4 °C for 10 minutes. The supernatant was discarded and the pellet was resuspended in a modified, freshly made HU buffer; 8 M urea, 5 % SDS, 200 mM Tris-HCl pH 6.8, 1 mM EDTA, 0.025 % bromophenol blue (Sigma, B5525), 1.5 % dithiothreitol (DTT) (EMD Chemicals, 3860), 25 mM NEM, 1 mM PMSF, and 0.5 % Triton-X-100 (Sigma). 12 μL of a 2 M Tris-base solution was added to each sample, and the protein was denatured for 10 minutes at 65 °C while shaking at 1400 rpm (initial pellet should be completely dissolved at this point and purple in colour). Samples were then centrifuged at room temperature for 30 seconds at 13,200 rpm, and 50 μL of the supernatant was removed and added to 50 μL of Bio-Rad laemmli sample buffer (catalogue #161-0737), and frozen overnight at -20 °C. Samples should not be boiled at any subsequent step as urea can induce carbamylation which can interfere with antibody binding (Kaiser and Tagwerker, 2005). Samples were then analysed by SDS-PAGE (Laemmli, 1970), followed by immunoblotting.

2.3.13.2 – SDS-PAGE Gel

40 μLs of each sample was run on a 1.5 mm 13 % SDS-PAGE gel; 4.5 mL sterile ddH_2O, 6.45 mL 30 % acrylamide (acrylamide/bis-acrylamide 37:1 ratio. Sigma, A6050), 3.75 mL 1.5 M Tris pH 8.8 (Tris Amino ultra pure. Angus Buffers & Biochemicals, Niagra, NY, Cat # 15-40500), 150 μL of 10 % ammonium persulfate (APS, Sigma, A-9164), 150 μL of 10 % SDS, and finally 6 μL of N,N,N',N'–Tetramethylethylenediamine (TEMED, Sigma, T-9281) resulting in a final volume of 15 mL which is sufficient for two gels. SDS-PAGE gels were made with a 4 % stacking layer; 5.375 mL sterile ddH_2O, 1.0015 mL 30 % acrylamide, 0.975 mL 1.5 M Tris pH 6.8, 75 μL of 10 % SDS, 75 μL of 10 % APS, and 7.5 μL TEMED. Gels were run at 128V until the 25 kDa marker (Precision plus protein standards from Bio-Rad cat. # 161-0374) had run to the bottom of the gel. The gels were then soaked in transfer buffer (6.07 g Tris-base, 28.5 g glycine, 150 mg SDS, 150 mL methanol, and ddH_2O up to 1L) for 10 minutes before being transferred to a polyvinlyidene fluoride (PVDF) transfer membrane.

2.3.13.3 – Western Blot

Proteins from SDS-PAGE gels were transferred to the Polyscreen (R) PVDF transfer membrane (Perkin Elmer NEF1002001PK) by wet transfer. TCA-treated samples reportedly require a longer blotting transfer time (Wright *et al.*, 1989); therefore a wet transfer system (Bio-Rad) was used for 4 hours at 100 V at 4 °C on ice. The transfer buffer (as previously described) and ice packs were changed every hour. Membranes

were then blocked overnight in 10 % skim milk (Carnation instant skim milk powder) in PBST (phosphate buffered saline (PBS, 8 g NaCl, 0.2 g KCL, 1.44 g Na_2HP0_4, 0.24 g KH_2P0_4 add ddH_2O up to 1L and pH 7.4 with hydrochloric acid) plus 0.05 % Tween 20 (Tween®20 Polyoxyethylene 20 Sorbitan Monolaurate. EMD Chemicals, 9480)), before the primary antibody was added at a 1:2000 dilution in 1 % skim milk (in PBST) for 2 hours. We raised monoclonal antibodies in mice against yeast PCNA from bacterial overexpressed pGST-*POL30* with the help of Dr. Barry Ziola (University of Saskatchewan). Membranes were vigorously washed for 10 minutes in PBST three times before incubating with the secondary antibody (Bio-Rad goat α mouse HRP, catalogue # 172-1011) at a 1:8000 dilution. The membrane was incubated for an hour with the secondary antibody before being washed for 10 minutes with PBS, and repeated three times. Results were visualized by Western Lightning Plus-ECL (Perkin and Elmer Life Sciences, NEL #104) and developed on HyBlot CL autoradiograph film from Denville Scientific, Inc. (Cat. No. E3018) with appropriate exposure times.

CHAPTER THREE

THE YEAST Shu COMPLEX COUPLES ERROR-FREE POSTREPLICATION REPAIR TO HOMOLOGOUS RECOMBINATION

This chapter is essentially as published in Ball *et al*. 2009.

3.1 – Abstract

DNA postreplication repair functions to bypass replication-blocking lesions and prevent damage-induced cell death. PRR employs two different mechanisms to bypass damaged DNA. While translesion synthesis has been well characterized, little is known about the molecular events involved in error-free bypass, although it has been assumed that homologous recombination is required for such a mode of lesion bypass. We undertook a genome-wide synthetic genetic array screen for novel genes involved in error-free PRR and observed evidence of genetic interactions between error-free PRR and HR. Furthermore, this screen identified and assigned four genes, *CSM2*, *PSY3*, *SHU1* and *SHU2*, whose products form a stable Shu complex, to the error-free PRR pathway. Previous studies have indicated that the Shu complex is required for efficient HR and that inactivation of any of these genes is able to suppress the severe phenotypes of *top3* and *sgs1*. We confirmed and further extended some of the reported observations and demonstrated that error-free PRR mutations are also epistatic to *sgs1*. Based on the above analyses, we propose a model in which error-free PRR utilizes the Shu complex to recruit

HR to facilitate template switching, followed by double-Holliday junction resolution by Sgs1-Top3. This mechanism appears to be conserved throughout eukaryotes.

3.2 – Introduction

Cellular DNA is dynamic and subject to constant assault as it readily reacts with a variety of agents that can lead to genomic instability. Genomic instability may also occur during replication, recombination and repair itself. Most lethal replication-blocking lesions are repaired by two radiation repair epistasis groups in *S. cerevisiae*, namely NER and HR. In addition, lesions induced by oxidative and alkylating agents are often dealt with by BER (Friedberg *et al.*, 2006). If these pathways are unable to function or the damage exceeds repair capacity, cell death may occur. In order to avoid such severe consequences, replication may be reinitiated at blocks without removing the lesion itself (Ganesan, 1974; Sarasin and Hanawalt, 1980; Walker, 1995). The third radiation repair epistasis group in *S. cerevisiae*, represented by *RAD6*, is presumed to mediate this process and has been termed PRR (Broomfield *et al.*, 2001; Prakash *et al.*, 1993). PRR is defined as a cellular process that converts low-molecular-weight genomic fragments into high-molecular-weight DNA in the presence of DNA damage, which can be detected by an alkaline sucrose gradient assay (di Caprio and Cox, 1981; Prakash, 1981).

PRR is centrally controlled by a stable complex formed between Rad6 and Rad18 (Bailly *et al.*, 1994), which possesses ATPase, ssDNA-binding and ubiquitination activities (Bailly *et al.*, 1997a). Rad6, which has diverse functions beyond PRR (Broomfield *et al.*, 2001), encodes a Ub-conjugating enzyme (Ubc or E2) (Jentsch *et al.*,

1987) that is essential for all of its known biological functions (Sung *et al.*, 1990). Rad18 is a ssDNA-binding protein (Bailly *et al.*, 1994) that appears to function exclusively in PRR and contains a Rad6-binding domain (Bailly *et al.*, 1997b), a really interesting new gene (RING) finger domain characteristic of a Ub-ligase (E3), and a putative Zn-finger DNA-binding domain (Jones *et al.*, 1988).

The PRR pathway is subdivided into two parallel pathways: error-prone (TLS or mutagenesis) represented by *REV1, REV3* and *REV7*, and error-free PRR represented by *MMS2, UBC13* and *RAD5* (Barbour and Xiao, 2003; Broomfield *et al.*, 2001). It is now clear that the entire *RAD6* pathway is dependent on the sequential ubiquitination of PCNA, a DNA polymerase sliding clamp encoded by the *POL30* gene in budding yeast (Hoege *et al.*, 2002). Monoubiquitination of PCNA at the K164 residue by the Rad6–Rad18 complex (Hoege *et al.*, 2002) allows for lesion bypass, which requires Rev1, a member of the Y-family of DNA polymerases, and the non-essential B-family DNA polymerase Polξ, comprised of Rev3 and Rev7 (Nelson *et al.*, 1996a, b; Stelter and Ulrich, 2003). Inactivation of the *REV* genes causes only a moderate level of sensitivity to killing by a variety of DNA-damaging agents, but confers major defects in UV-induced mutagenesis (Lawrence, 2004). Rev1 contains a PCNA interacting domain (Guo *et al.*, 2006) and Ub-binding motifs (UBM) (Bienko *et al.*, 2005), as well as a Polζ-interacting domain (Acharya *et al.*, 2005; Acharya *et al.*, 2006; Guo *et al.*, 2003), suggesting Rev1 functions as a scaffold for TLS.

While TLS is well characterized, relatively little is known about error-free PRR. The existence of this branch under the *RAD6* pathway was initially surmised because the

rad6 or *rad18* mutant is extremely sensitive to killing by DNA-damaging agents while the *rev* mutants are not (Lawrence, 1994; Prakash *et al.*, 1993). Perhaps the first firm demonstration of the existence of error-free PRR was through genetic characterization of the *mms2* mutant (Broomfield *et al.*, 1998; Xiao *et al.*, 1999). The *mms2* mutant displays moderate sensitivity to killing by a variety of DNA-damaging agents and the gene is assigned to the *RAD6* pathway. The characteristic features of *mms2* include its strong synergistic interaction with *rev3* and its *REV3*-dependent increase in spontaneous mutagenesis. *MMS2* encodes a Ubc-like protein but does not contain an active-site Cys-residue. It turns out that Mms2 forms a stable complex with Ubc13, and this complex specifically promotes the non-canonical Lys63-linked Ub chain formation (Hofmann and Pickart, 1999). Indeed *ubc13* is epistatic to *mms2* and the two mutants share all characteristic features as described above (Brusky *et al.*, 2000). Furthermore, Rad5, a member of the SWI/SNF family of ATPases with a C_3HC_4 RING finger motif, is capable of interacting with Pol30, Ubc13 and Rad18 and may serve as an E3 for Ubc13–Mms2 (Ulrich and Jentsch, 2000). Thus, it is thought that Rad5 functions to recruit the Mms2–Ubc13 complex in close proximity to PCNA and facilitate the Lys63-linked polyubiquitination of PCNA.

The above sequential PCNA ubiquitination model satisfactorily explains the current genetic observations with regard to how the *RAD6* pathway operates to tolerate DNA damage. However, while it becomes apparent that the error-free mode of lesion bypass requires the completion of sister chromatid synthesis past the replication blocking lesion and that it most likely employs some form of homologous chromatid as a template

(Broomfield *et al.*, 2001; Li *et al.*, 2002; Zhang and Lawrence, 2005), exactly how this is achieved is currently unclear. Furthermore, we argue that, analogous to the role of PCNA monoubiquitination in TLS, PCNA polyubiquitination following DNA damage only serves as a signal for error-free PRR and hence additional members of this pathway may be present to couple PCNA polyubiquitination to the error-free bypass. In order to understand how this pathway operates, we undertook a large-scale genomic screen to search for additional components of error-free PRR and report here the identification and genetic characterization of four genes that form a complex to function in coupling error-free PRR to HR. This study also allows us to demonstrate that error-free PRR utilizes HR proteins to form a recombinant intermediate that requires helicase-topoisomerase activities to complete the error-free bypass process.

3.3 – Results

3.3.1 – Identification of Novel Error-Free PRR Genes

One method to identify novel genes and their putative function is synthetic lethal screening. Synthetic lethality occurs when the combination of two mutations leads to a inviable organism, but either single mutant is viable (Guarente, 1993). Synthetic lethal interactions most likely occur if the two genes are in distinct pathways and one is capable of functionally compensating for defects in the other (Hartman *et al.*, 2001). In the past, we have adapted the synthetic lethal screening protocol to isolate novel genes whose inactivation demonstrated synergistic interaction with yeast error-free PRR mutations (Barbour *et al.*, 2006; Barbour and Xiao, 2006). With the completion of the yeast genome

sequence and the establishment of genome-wide SGA (Tong *et al.*, 2001), we attempted to search for novel non-essential genes involved in both error-free PRR and TLS pathways.

A typical SGA screen involves a query mutation being crossed to an ordered array of approximately 5000 nonessential gene deletions (Tong *et al.*, 2001) allowing meiotic progeny containing both mutations to be scored for fitness. Our design for this genetic screen was based on the initial discovery of dramatic synergism between error-free PRR (*MMS2* and *UBC13*) and TLS (*REV1*, *REV3* and *REV7*) pathway mutations (Broomfield *et al.*, 1998; Xiao *et al.*, 1999). For example, on a plate containing 0.005% MMS, the growth of wild-type and each of the above single mutants is not inhibited, while simultaneous inactivation of both error-free PRR and TLS pathways results in complete inhibition of growth (Barbour *et al.*, 2006). Quantitative analysis indicates that the synergism is greater than 103-fold (Broomfield *et al.*, 1998). Hence, we reasoned that if an SGA screen was performed in the presence of a very low-dose of MMS using a TLS mutant as the query strain, we would be able to preferentially identify candidate genes involved in error-free PRR, and vice versa.

Two query mutants from each pathway (*mms2*, *ubc13*, *rev1* and *rev3*), as well as *rad30* and *rad6* were utilized as query strains for SGA. The initial screens resulted in 407 potential genetic interactions, and subsequent random spore analysis (RSA) confirmed 108 putative genetic interactions (Table 3.1). While *rad6* resulted in identifying many synthetic lethal genetic interactions, there are likely due to the functions Rad6 has outside of its function in PRR. In addition the *RAD30* query mutant only identified *RAD5*, an

Table 3.1 – Putative Genetic Interactions Confirmed by SGA and RSA

ubc13Δ	*mms2Δ*	*mms2Δ cont.*	*rev1Δ*	*rev3Δ*	*rad30Δ*	*rad6Δ*
YML012C-A	***RIM8***	*RAD24*	***SIC1***	*YPL144W*	*RAD5*	***KEM1***
YPR101W	***MGA2***	*RAD17*	*FMP35*	*THP1*		***SWC5***
MNN10	*MNN10*	*BIM1*	*ASF1*	*RAD54*		***SWR1***
VID21	*YKL069W*	*RLF2*	*MPH1*	*MMS2*		***SWC3***
MAG1	*YML096W*	*POL32*	*CTF4*	*SHU1*		***MRE11***
RAD9	*PSY2*	*HSL1*	*PSY3*	*PSY3*		***CTG4***
REV3	*VID21*	*ELM1*	*SIC1*	*CSM2*		***MMS22***
REV1	*BRE1*	*CKB1*	*DDC1*	*RAD55*		***XRS2***
REV7	*MRC1*	*RTS1*	*RAD55*	*RAD17*		***RAD50***
MSI1	*PAT1*	*RIM13*	*RAD17*	*RAD24*		***CSF1***
REV1	*CHL1*	*VPS9*	*RAD24*	*UBC13*		***SWI4***
HUR1	*MAG1*	*HSP26*	*DCC1*	*RAD57*		***MSC1***
RVS167	*RAD1*	*TPS1*	*UBC13*	*RAD51*		***BUB3***
SCS7	*CAC2*	*HSP26*	*RAD51*	*RAD52*		***NUP133***
VPS8	*RAD9*	*DEG1*	*RAD57*			***AAT2***
CIK1	*MSI1*	*LSM1*	*MMS2*			***STO1***
DDC1	*REV3*	*PMR1*				***BUB1***
RAD24	*REV1*	*RIM9*				***CLA4***
NUP133	*REV7*	*RIM21*				***RPL27A***
POL32	*HUR1*	*SRB2*				***VPS72***
CKB1	*VPS21*	*UMP1*				***ARP6***
ELM1	*RVS167*	*YNL171C*				***VPS71***
VPS9	*HIR3*	*YLR358C*				***DEP1***
VPS9	*CLB2*	*YGL046W*				***DEG11***
KCS1	*SGF29*	*YML102C-A*				***UME6***
DEG1	*RIM20*	*YML012C-A*				***CYS3***
RIM9	*VPS8*	*CIK1*				***PGD1***
YML012C-A	*RIM8*	*KAP122*				***FUR4***
						YLR358C
						YNL171C

* This table shows the SGA query strains across the top, and all of the synthetic lethal relationships (in bold type) and conditionally synthetic lethal interactions that were confirmed by RSA analysis.

already known PRR gene. Additional results included the identification of *REV1*, *REV3* and *REV7* via the *mms2* and *ubc13* query strains, while *MMS2* and *UBC13* were identified using *rev1* and *rev3* query strains. As expected, all four screens identified damage checkpoint genes, further supporting the notion that DNA damage checkpoints form a third alternative pathway for damage tolerance (Barbour *et al.*, 2006) and validating this screen. Here we report the genetic characterization of four genes, *CSM2*, *PSY3*, *SHU1* and *SHU2*, three of which were identified in this study using *rev1* and *rev3* query strains, and the involvement of HR and Sgs1-Top3 in error-free PRR. Other putative genes will be further investigated and reported elsewhere.

3.3.2 – HR is Involved in Error-Free PRR

Of the RSA-confirmed genetic interactions, we noticed that both *rev1* and *rev3* identified HR genes, including *RAD51*, *RAD52*, *RAD54*, *RAD55* and *RAD57*. In contrast, neither *mms2* nor *ubc13* identified any of the above genes. A serial dilution assay demonstrates that all HR mutations are indeed synergistic to *rev1* (data not shown) or *rev3* (Figure 3.1) with respect to killing by MMS or UV irradiation, whereas when these mutations were combined with *mms2* (Figure 3.1) or *ubc13* (data not shown), the double mutants only displayed slightly more sensitivity than either of corresponding single mutants.

It has been previously argued that the error-free and error-prone pathways within PRR deal with similar lesions, namely a stalled replication fork facing a replication block on the template strand (Broomfield *et al.*, 2001; Xiao *et al.*, 1999). If one assumes that

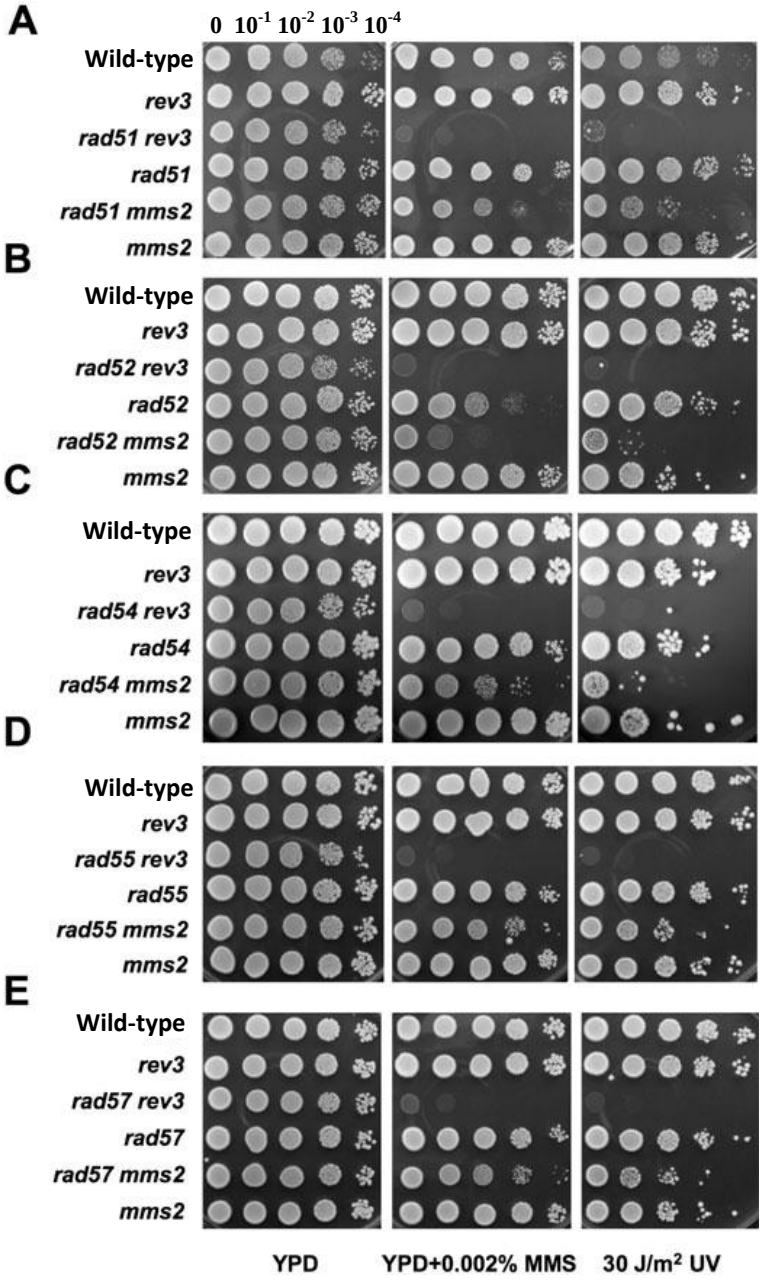

Figure 3.1 – Differential Genetic Interactions Between *REV3* or *MMS2* and Homologous Recombination Genes with Respect to MMS and UV Sensitivity. All the strains were in the BY4741 background and created by crossing Y8621 (*rev3*Δ::*nat*^{R}) or Y9897 (*mms2*Δ::*nat*^{R}) with the yeast deletion mutant array. (A) *rad51*Δ; (B) *rad52*Δ; (C) *rad54*Δ; (D) *rad55*Δ; and (E) *rad57*Δ. Cells grown overnight were spotted on YPD or YPD plus 0.002 % MMS. For UV treatment, spotted plates were exposed to the UV does as indicated. The plates were then incubated at 30 ºC for 2 days before being photographed. Results were observed a minimum of three times. Results contributed by Ke Zhang.

TLS and HR pathways function independently, an obvious conclusion would be that error-free PRR and HR functions overlap so that the double mutant is not as sensitive as that of the TLS–HR double mutant. As a matter of fact, it has been proposed for decades that the presumed error-free PRR pathway must utilize some means of homologous search for newly synthesized sister chromatid as a template to complete error-free bypass (Prakash *et al.*, 1993), and it has been reported recently that error-free PRR does employ homologous sister chromatid exchange (Zhang and Lawrence, 2005). Our observations provide direct evidence for the involvement of HR proteins and indicate that even the accessory HR proteins like Rad55 and Rad57 play pivotal roles in this process.

3.3.3 – *CSM2, PSY3, SHU1* and *SHU2* Act in the Same Pathway and Their Products Form a Stable Complex

In this study, we argued that there must be a cellular component that links error-free PRR to HR and further proposed that inactivation of this component would result in epistatic interactions with both error-free PRR and HR. In the subsequent sections, we describe the characterization of a Shu complex consisting of Csm2, Psy3, Shu1 and Shu2 (Shor et al., 2005) in support of our claim that the Shu complex fulfills the role of coupling error-free PRR to HR. *PSY3* was identified in the SGA and RSA screens via both *rev1* and *rev3* query strains. Figure 3.2 shows genetic interaction between *psy3* and *rev3* in a typical RSA experiment. In this case, all wild-type, single and double mutants grew well on minimal media; however, in the presence of 0.004% MMS, growth of the *psy3 rev3* double mutant is inhibited, indicating that the interaction between *psy3* and

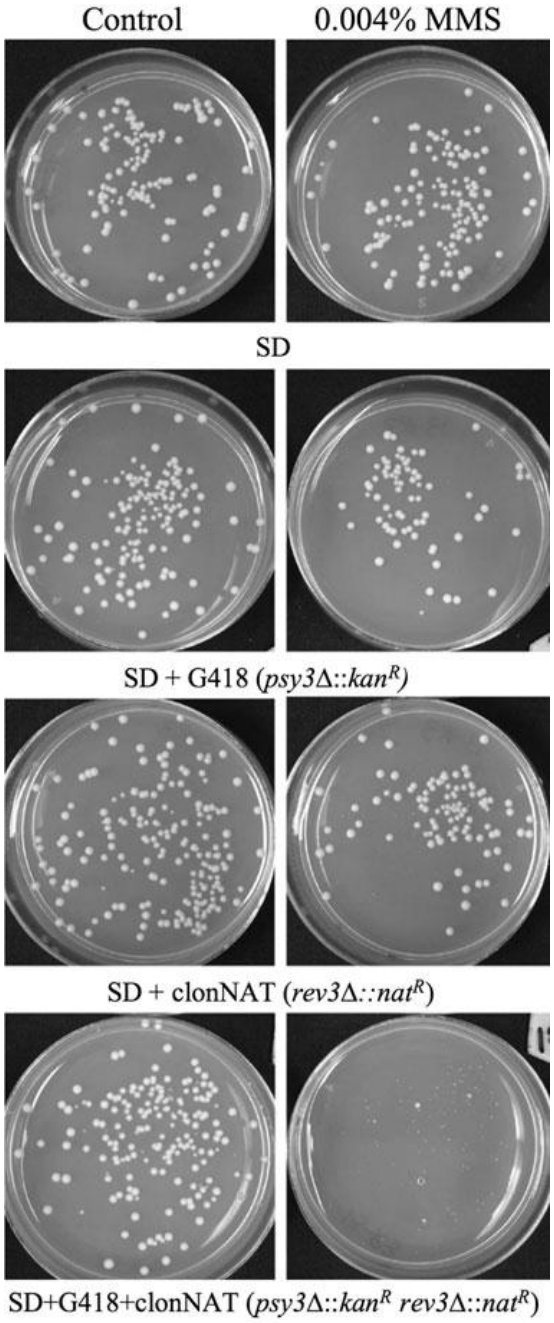

Figure 3.2 – Genetic Interaction Between *REV3* and *PSY3* as Demonstrated via RSA. The Y8621 strain (*rev3*Δ::*nat*^{R}) was crossed with the deletion mutant array and the relevant diploids carrying a *psy3*Δ::*kan*^{R} allele were analysed using RSA. Meiotic progeny derived from the sporulation of heterozygous diploids were selected on media for either the single or double mutants, with or without 0.004 % MMS, as indicated. The plates were incubated at 30 ºC for 3 days and photographed.

rev3 is synergistic with respect to MMS sensitivity. In addition, *CSM2* and *SHU1* were also identified through this screen. *PSY3* (*p*latinum *s*ensitivity) was initially identified as part of a genome-wide screen for mutants sensitive to platinum (Wu *et al.*, 2004). *CSM2* (*c*hromosome *s*egregation in *m*eiosis) was initially discovered as part of a genome-wide screen for mutations affecting chromosome segregation in meiosis (Rabitsch *et al.*, 2001), while *SHU1* and *SHU2* (*s*uppressor of *sgs1HU* sensitivity) were identified by a screen for non-*sgs1*Δ suppressors of the *top3*Δ slow-growth phenotype and thought to be part of HR (Shor *et al.*, 2005). Indeed, deletion of any of the four genes results in a similar level of MMS sensitivity and the double mutants did not further enhance sensitivity phenotypes (Figure 3.3A) (Shor *et al.*, 2005). Furthermore, a genome-wide Y2H experiment indicated physical interaction among these four proteins (Ito *et al.*, 2001). Therefore, we obtained these Y2H clones, made sequence corrections wherever necessary as the initial Y2H clones contained point mutations, and cloned the correct ORF in both Y2H vectors. Our Y2H analysis (Figure 3.3B) confirmed the previously reported interactions (Ito *et al.*, 2001; Shor *et al.*, 2005) and allowed us to create an interaction map, in which Psy3 not only interacts with Csm2, Shu1 and Shu2, but Shu1 and Shu2 also bind to each other (Figure 3.3C). All the interactions are deemed to be strong since they survived the most stringent test on SD-Ade plate (James *et al.*, 1996). In this study *psy3* was primarily used to study the Shu complex because it was identified by both *rev1* and *rev3* query mutants, and it is the only component of the Shu to interact with all other three members (Figure 3.3C).

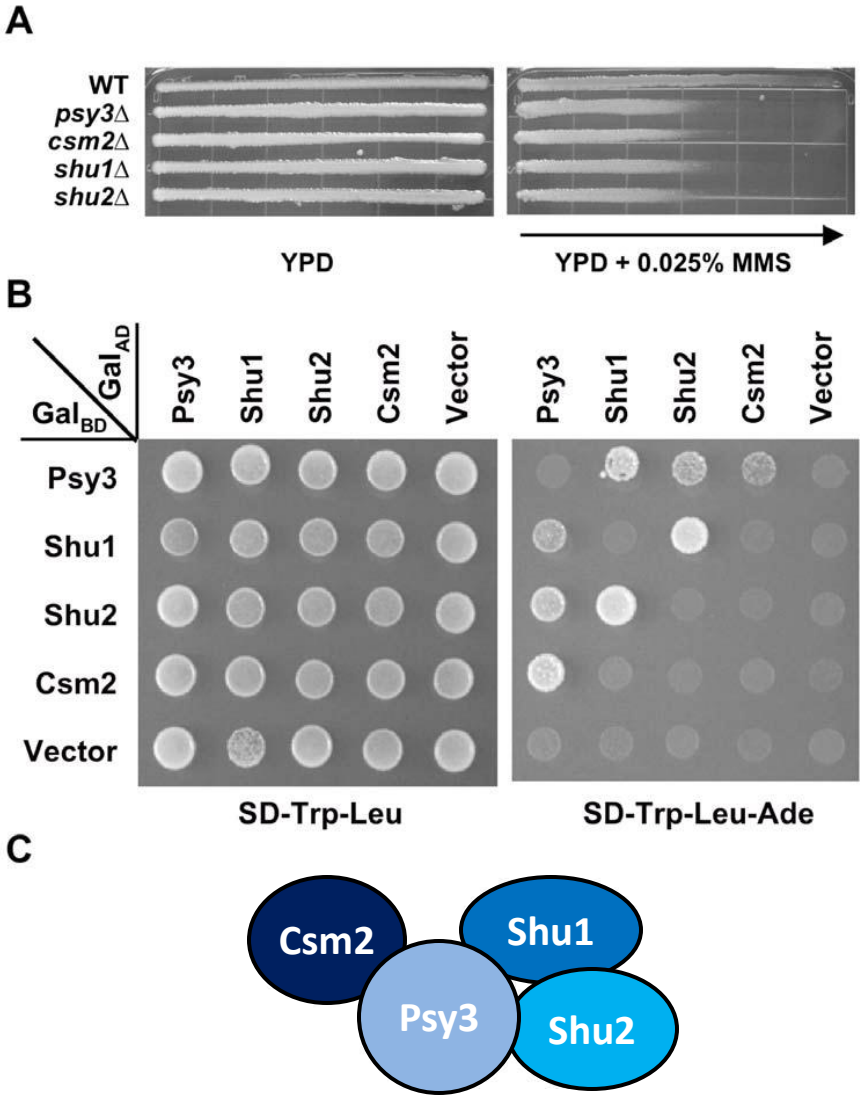

Figure 3.3 – Functional and Physical Interactions Amongst Members of the *S. cerevisiae* Shu Complex. (A) All four null mutants, *csm2*Δ, *psy3* Δ, *shu1* Δ and *shu2* Δ display a similar level of sensitivity to MMS. Overnight cell cultures were imprinted on YPD or YPD + 0.025 % MMS gradient plates. Plates were incubated at 30 ºC for 2 days and then photographed. The arrow indicates the increasing gradient of MMS. Strains used were isogenic to BY4741 (Table 2.2). Results were observed a minimum of three times. (B) Yeast two-hybrid analysis demonstrates the physical interaction between Psy3, Shu1, Shu2 and Csm2. The yeast strain PJ69-4a was co-transformed with various combinations of the Gal_{BD} and Gal_{AD} plasmids before being scored for growth on selective media. Plates were photographed following 3 days of incubation at 30 ºC. Results were observed from a minimum of three independently transformed cells. These results are consistent with previous reports (Ito *et al.*, 2001; Shor *et al.*, 2005). (C) A schematic diagram of the Shu complex illustrating the involved physical interactions.

3.3.4 – HR Repair Mutations are Epistatic to *shu* Mutations

It has been reported that *rad52* is epistatic to *shu* mutations (Shor *et al.*, 2005). However, *rad52* is extremely sensitive to MMS and, under the above experimental conditions, the *shu* single mutants do not display apparent sensitivity. We combined *psy3* with *rad51*, *rad52* and *rad54*, among which *rad51* and *rad54* are relatively less sensitive to MMS than *rad52* and are primarily involved in HR (Paques and Haber, 1999). Both the gradient plate assay (Figure 3.4A–C) and the quantitative liquid killing experiment (Figure 3.5) showed that the *hr* mutations are epistatic to *psy3* regardless of the level of *hr* mutant sensitivity. These observations are consistent with a recent report (Mankouri *et al.*, 2007) employing *rad51* and *rad54*. It was also reported that in the presence of a low-dose of MMS, inactivation of *RAD52* results in delayed S-phase progression (Oakley *et al.*, 2002). We found that although *psy3* is much less sensitive to MMS than *rad51*or *rad54* (Figure 3.4), he progression through S-phase in the presence of 0.02% MMS is delayed to the same extent as *rad51* and *rad54* (Figure 3.6). More importantly, the *psy3 hr* double mutants do not further delay the progression (Figure 3.6). Together, we confirm that the *SHU* genes belong to the *HR* pathway and may have a specific function during S-phase.

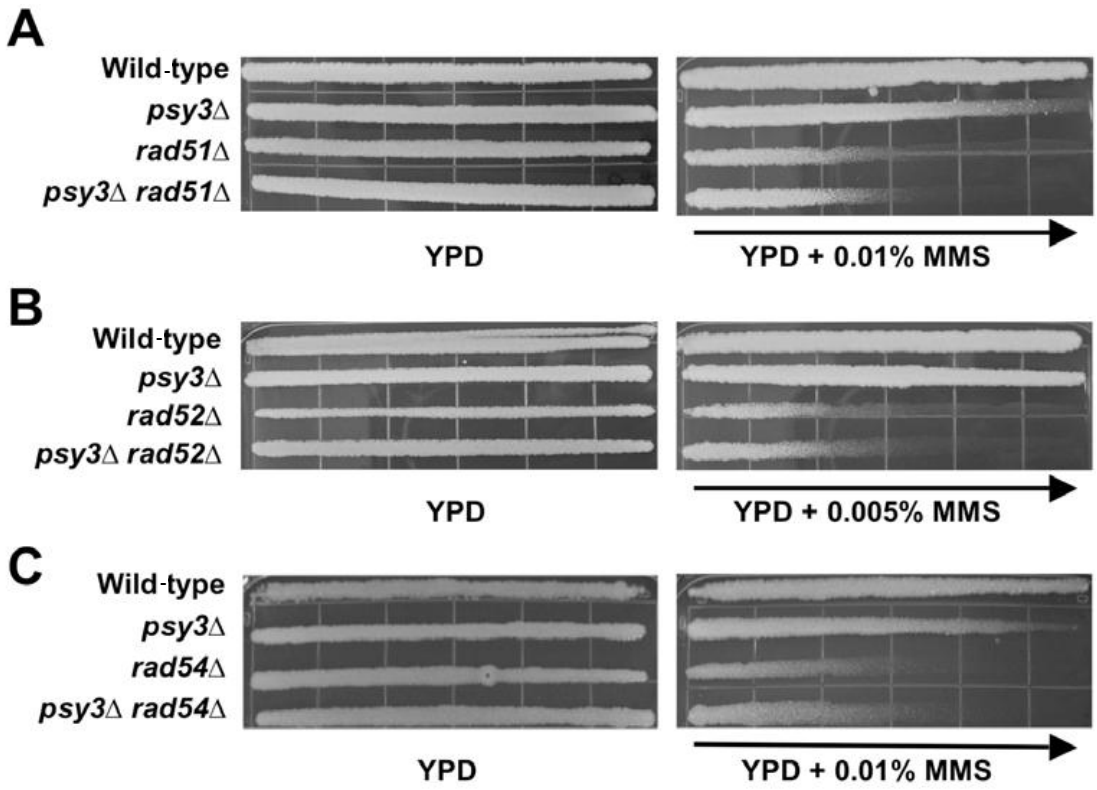

Figure 3.4 – Gradient Plate Assays Explore Genetic Interactions Between *psy3* and Selected *hr* Mutations. (A-C) Gradient plate assays. Overnight cell cultures were imprinted on YPD or YPD + MMS gradient plates at the indicated concentrations and incubated at 30°C for two days before being photographed. Arrows indicate the increasing concentration of MMS. Results were observed a minimum of three times.

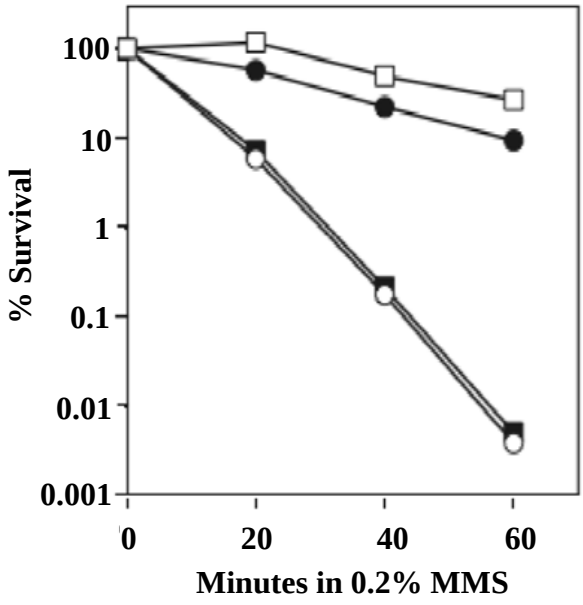

Figure 3.5 – Quantitative Assessment of the Genetic Interactions Between *psy3* and *rad51* by a 0.2 % MMS-Induced Liquid Killing Experiment. All strains used were isogenic derivatives of HK578; (□) HK578-10A (wild-type), (○) WXY402 (*rad51*Δ), (●) WXY1328 (*psy3*Δ) and (■) WXY964 (*psy3*Δ*rad51*Δ). Results are the average of three independent experiments.

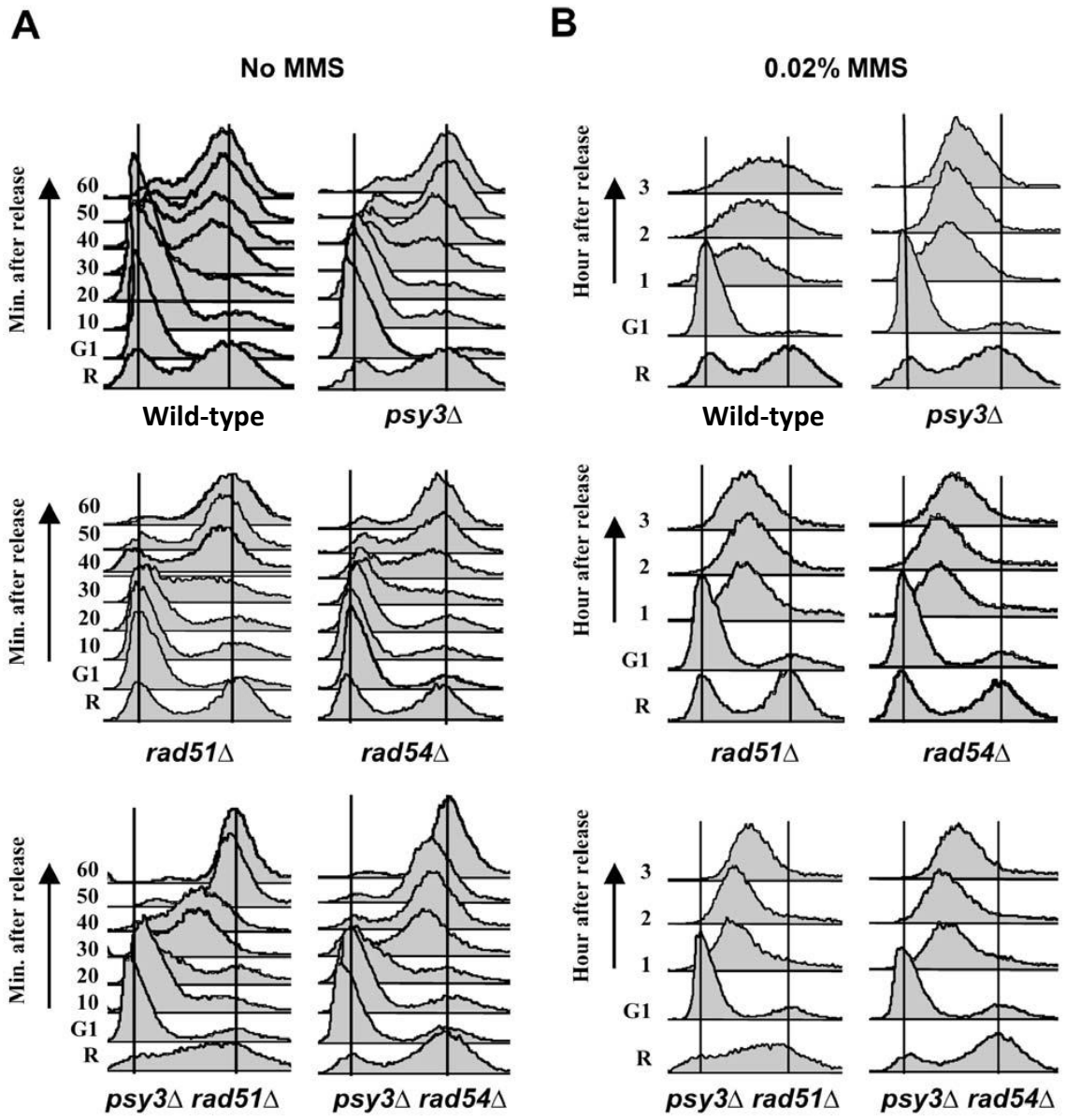

Figure 3.6 – *psy3* is Epistatic to *rad51* and *rad54* with Respect to MMS-Induced Cell Cycle Delay. α-factor arrested G1 cells were released into either (A) rich YPAD or (B) YPAD + 0.02% MMS. Samples were taken at the indicated time points and analysed by flow cytometry. Vertical lines in each graph indicate (from left to right) G1, mid-S and G2 phases. All strains used were isogenic to BY4741. Results were observed by three independent experiments.

3.3.5 – *shu* Mutations Suppress *sgs1* Phenotypes

All four *SHU* genes were isolated by their mutational phenotype to suppress the HU sensitivity of *top3* and *sgs1* (Shor *et al.*, 2005). However, the authors reported that *shu* mutations are additive to *sgs1* with respect to killing by MMS. We examined the genetic interactions between *psy3* and *sgs1* in three different strain backgrounds (W303, BY4741 and DBY747) and in each case, deletion of *PSY3* was able to suppress the severe *sgs1* sensitivity to HU and MMS (e.g. Figure 3.7). In contrast, neither single nor the double mutant displayed enhanced sensitivity to UV. This observation differs from that of Shor *et al*. (2005) but agrees with a recent report by Mankouri *et al*. (2007), who also found that deletion of *SHU* genes can reduce MMS-induced X-molecules accumulated in the absence of *SGS1*.

To further address whether deletion of *SHU* suppresses the *sgs1* mutant phenotypes, especially during S-phase, we took advantage of the knowledge that *SGS1* confers an S-phase checkpoint function (Frei and Gasser, 2000). In our experimental setting and as reported (Frei and Gasser, 2000), wild-type cells complete S-phase within 1 h in the absence of MMS, and *psy3*, *sgs1* single and the *psy3 sgs1* double mutants do not display apparent differences (Figure 3.8). In the presence of low-dose MMS, cell cycle progression through S-phase is delayed in wild-type cells, which do not complete S-phase in 3 h, whereas deletion of *SGS1* results in an accelerated progression through S-phase, which is completed by 3 h (Figure 3.8). In contrast, in the presence of MMS, *psy3* cells further delay S-phase progression compared to wild-type cells as shown 3 h after release from α-factor, the majority of *psy3* cells remain in

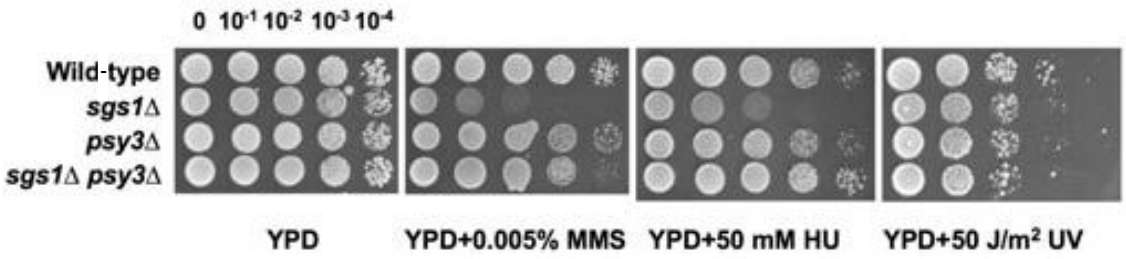

Figure 3.7 – Deletion of *PSY3* Suppresses the *sgs1* Mutant Phenotype. Relative sensitivity of *psy3* and *sgs1* mutants to MMS, HU and UV by 10-fold serial dilution assays. Cells grown overnight were spotted on YPD or YPD plus DNA-damaging agents at indicated concentrations. For UV treatment, spotted plates were exposed to the UV dose as indicated. The plates were then incubated at 30 ºC for 2 days before being photographed. All strains used were isogenic to BY4741. Results were observed a minimum of three times.

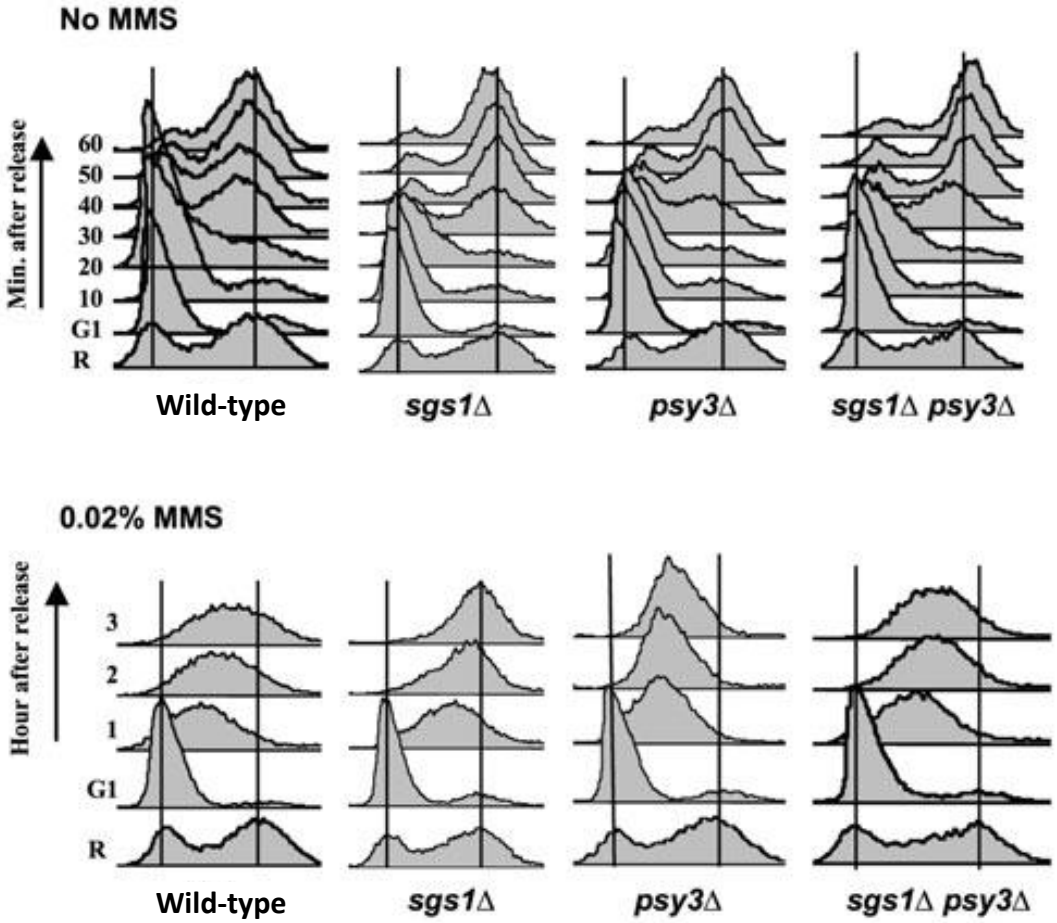

Figure 3.8 – Deletion of *PSY3* Suppresses the *sgs1* S-phase Checkpoint Defect. α-factor arrested G1 cells were released into rich YPAD or YPAD + 0.02 % MMS. Samples were taken at the indicated time points and analysed by flow cytometry. Vertical lines in each graph indicate (from left to right) G1 and G2 phases. R stands for random, or an asynchronous sample of cells. All strains used were isogenic to BY4741. Results were observed in three independent experiments.

mid-S-phase. Interestingly, deletion of *PSY3* completely suppresses the *sgs1* cell cycle checkpoint so that in the presence of 0.02% MMS, the *sgs1 psy3* double mutant progresses through S-phase at a rate nearly indistinguishable from that of the *psy3* single mutant (Figure 3.8). Taken together, we are able to confirm previous reports that *shu* mutations are indeed epistatic to *sgs1*, indicating that the Shu complex functions upstream of the Sgs1-Top3-Rim1 pathway as *shu* mutations are able to reduce the severe sensitivity of an *SGS1* mutant.

3.3.6 – *SHU* Belongs to the Error-Free PRR Pathway

The synergistic interaction between *shu* and *rev* mutations does not necessarily place *SHU* genes in the error-free PRR pathway. A good example is that mutations in the DNA damage checkpoint genes display synergistic interactions with both error-free and TLS PRR mutations (Barbour *et al.*, 2006). However, none of the *SHU* genes were identified by the *mms2* or *ubc13* query strains. To further determine genetic interactions between *shu* and *mms2/ubc13*, isogenic single and double mutants were created and their various phenotypes examined with respect to their involvement in the error-free PRR pathway. First of all, both plate-based (Figure 3.9A) and quantitative liquid killing (Figure 3.9B) experiments demonstrate that *psy3* is epistatic to *mms2* while synergistic to *rev3*, and that the synergism is over 103-fold, which is reminiscent of the genetic interaction between *mms2* and *rev3* (Broomfield *et al.*, 1998). Second, error-free PRR is characterized by its enhanced spontaneous mutagenesis in a *REV3*-dependent manner

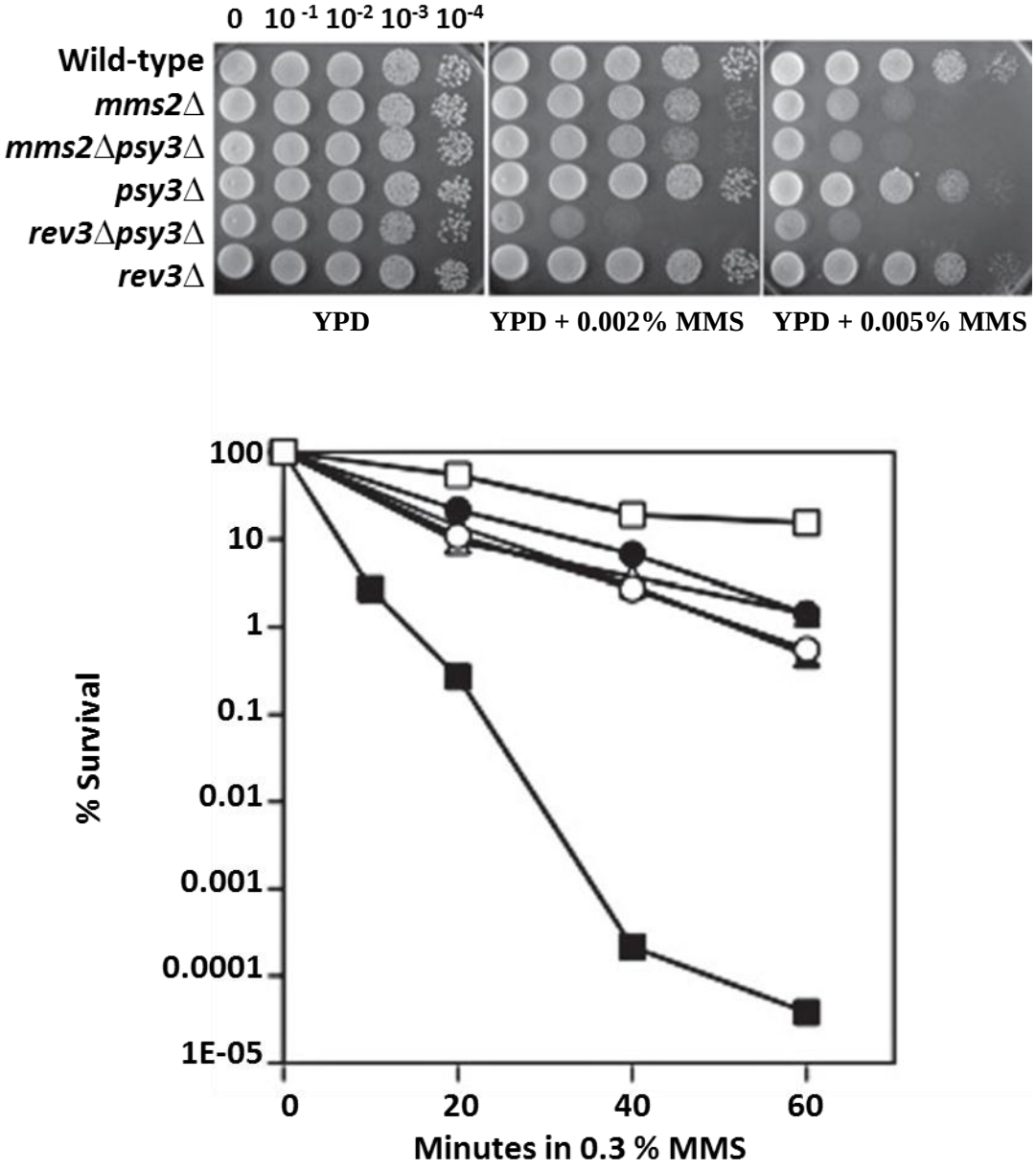

Figure 3.9 – Sensitivity of *mms2*, *psy3* and *rev3* Mutants to MMS. (A) A 10-fold serial dilution assay on rich media with or without MMS at concentrations as indicated. The plates were incubated at 30 °C for 2 days before being photographed. Strains used were HK578-10A and its isogenic derivatives. Results were observed a minimum of three times. (B) Cell survival in the presence of 0.3 % MMS by a liquid-killing assay. The results are the average of four independent experiments. Strains used were isogenic to DBY747. (□) DBY747 (wild-type), (●) WXY1323 (*psy3*Δ), (Δ) WXY667 (*rev3*Δ), (○) WXY644 (*mms2*Δ), (■) WXY1324 (*rev3*Δ*psy3*Δ) and (▲) WXY1325 (*mms2*Δ *psy3*Δ).

(Broomfield *et al.*, 1998). We found that deletion of *PSY3* resulted in a 10-fold increase in the spontaneous *trp1-289* reversion rate over wild-type cells, which is *REV3* dependent (Table 3.2). As previously reported (Broomfield *et al.*, 1998), deletion of *MMS2* results in a nearly 20-fold increase in spontaneous mutation rate. Importantly, we found in this study that deletion of *PSY3* in the *mms2* strain only enhances spontaneous mutagenesis slightly (Table 3.2), indicating that *PSY3* and *MMS2* function in the same pathway. Third, the *psy3* mutant displayed MMS-induced mutagenesis in a *REV3*- dependent manner and at the level comparable to that of *mms2*, which was higher than wild-type cells (data not shown). Finally, we also found that *rad5* and *rad18* are epistatic to *psy3* with respect to MMS-induced killing (data not shown), further confirming that *PSY3*, and hence the *SHU* complex, belongs to the error-free branch of the *RAD6* epistasis group.

Table 3.2 – *S. cerevisiae* Spontaneous Mutation Rates to Examine *psy3*

Strain[a]	Key alleles	Rate (x 10^{-8})[b]	Fold[c]
DBY747	Wild-type	1.12 ± 0.3	1
WXY667	*rev3* Δ	0.31 ± 0.14	0.3
WXY644	*mms2* Δ	19.8 ± 1.4	17.6
WXY1323	*psy3* Δ	11.8 ± 3.9	10.5
WXY1324	*psy3* Δ*rev3* Δ	0.98 ± 0.34	0.9
WXY1325	*psy3* Δ*mms2* Δ	25.3 ± 0.8	22.6

a. All strains are isogenic derivatives of DBY747.

b. The spontaneous mutation rates are the average of at least three independent experiments with standard deviation.

c. Relative to the wild-type mutation rate.

3.3.7 – Additional Evidence that the *SHU* Genes are Novel Members of the *RAD6* Epistasis Group

Currently, there are no direct assays to determine whether a gene is involved in error-free PRR. In addition to the above standard genetic analyses initially employed to define error-free PRR, there are three other phenotypes that appear to be unique to the *RAD6* group of genes. First, only mutations in the *RAD6* epistasis group are suppressed by inactivation of *SRS2* (Broomfield and Xiao, 2002; Ulrich, 2001). *SRS2* encodes a 3′-5′ DNA helicase that inhibits Rad51-ssDNA filament formation and was initially isolated by its ability to suppress the severe DNA damage sensitivity of *rad6*. Indeed, we found that *srs2* is epistatic to *psy3* (Figure 3.10A). Furthermore, deletion of *SRS2* is able to completely suppress the severe sensitivity of the *psy3 rev3* double mutant to killing by MMS (Figure 3.10A). We noticed that the *psy3 rev3 srs2* triple mutant is even more resistant to MMS than the *srs2* single mutant. This phenotype has been repeatedly observed in several independent strains and the mechanism remains to be investigated. Second, we previously reported that mating-type heterozygosity enhances tolerance to a wide range of DNA-damaging agents, an effect that is unique to mutations in the *RAD6* pathway (Barbour and Xiao, 2006). Here we demonstrate that the MMS sensitivity of a *psy3* single mutant is partially rescued in a pseudodiploid with opposite mating types, an effect that is not observed when cells carry two copies of the same mating-type gene (Figure 3.10B). Third, we recently reported that the damage checkpoint pathway mutations are synergistic to mutations in both PRR branches (Barbour *et al.*, 2006).

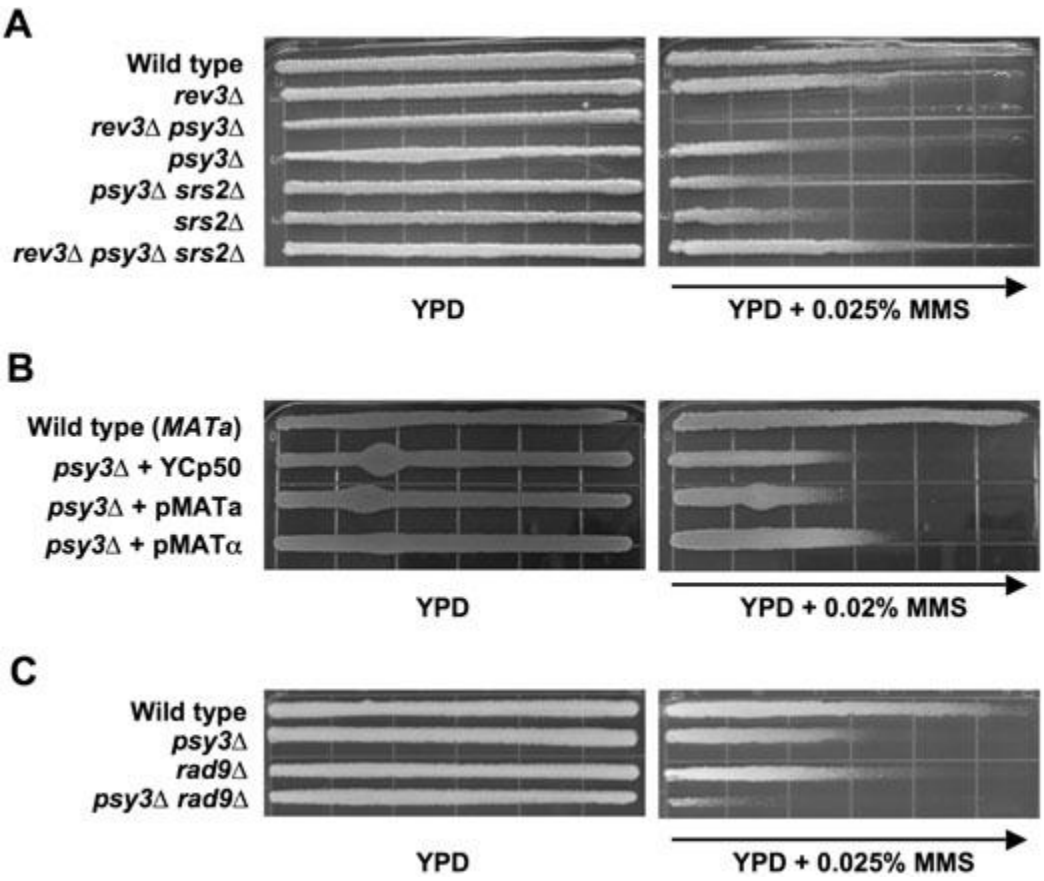

Figure 3.10 – Additional Phenotypes of *psy3* are Indicative of a Member of the Error-Free PRR Pathway. (A) Suppression of the *psy3* sensitivity to MMS by the *srs2* mutation. (B) Effects of mating-type heterozygosity on *psy3* sensitivity to MMS. (C) The genetic interaction between *psy3* and *rad9*. Overnight cell cultures were imprinted on YPD or YPD + MMS and incubated at 30 °C for 2 days before being photographed. Arrows indicate the increasing concentration of MMS. Strains used in (A) and (B) were isogenic to HK578-10A and strains used in (C) were isogenic to BY4741. Cells carrying the YCp50 vector, YCp50-*MAT***a** (p*MAT***a**) or YCp50-*MAT*α (p*MAT*α) are indicated in (B). Figure 3.10B contributed by Ke Zhang. Results were observed a minimum of three times.

Indeed, the *rad9psy3* double mutant appears to be much more sensitive to killing by MMS than either of the corresponding single mutants (Figure 3.10C). In summary, all of the above results are consistent with the notion that *SHU* genes are novel members of the error-free PRR pathway.

3.3.8 – *mms2* is Epistatic to *sgs1* with Respect to MMS Sensitivity

If Sgs1-Top3 indeed acts downstream of the error-free PRR-Shu-HR pathway to resolve stalled replication forks, one would predict that *mms2/ubc13* mutations will be epistatic to *sgs1*. Indeed we found that in a strain in which *mms2* is slightly less sensitive to MMS than *sgs1*, the *mms2 sgs1* double mutant is indistinguishable from *mms2* (Figure 3.11A), indicating that *mms2* suppresses the *sgs1* sensitivity. We also examined the effect of *mms2* and *mms2 sgs1* mutations on the cell cycle progression in the presence of MMS. Like wild-type, *mms2* cells accumulate at S-phase in the presence of 0.02% MMS even after 3 h of incubation. In contrast, most *sgs1* cells pass through S-phase rapidly within 2 h after release from G1.The *sgs1 mms2* double mutant cells progress through S-phase much slower than *sgs1* cells and do not complete the progress even 3 h after release (Figure 3.11B). Hence, we are able to conclude that error-free PRR mutations are epistatic to *sgs1* for MMS-induced DNA damage.

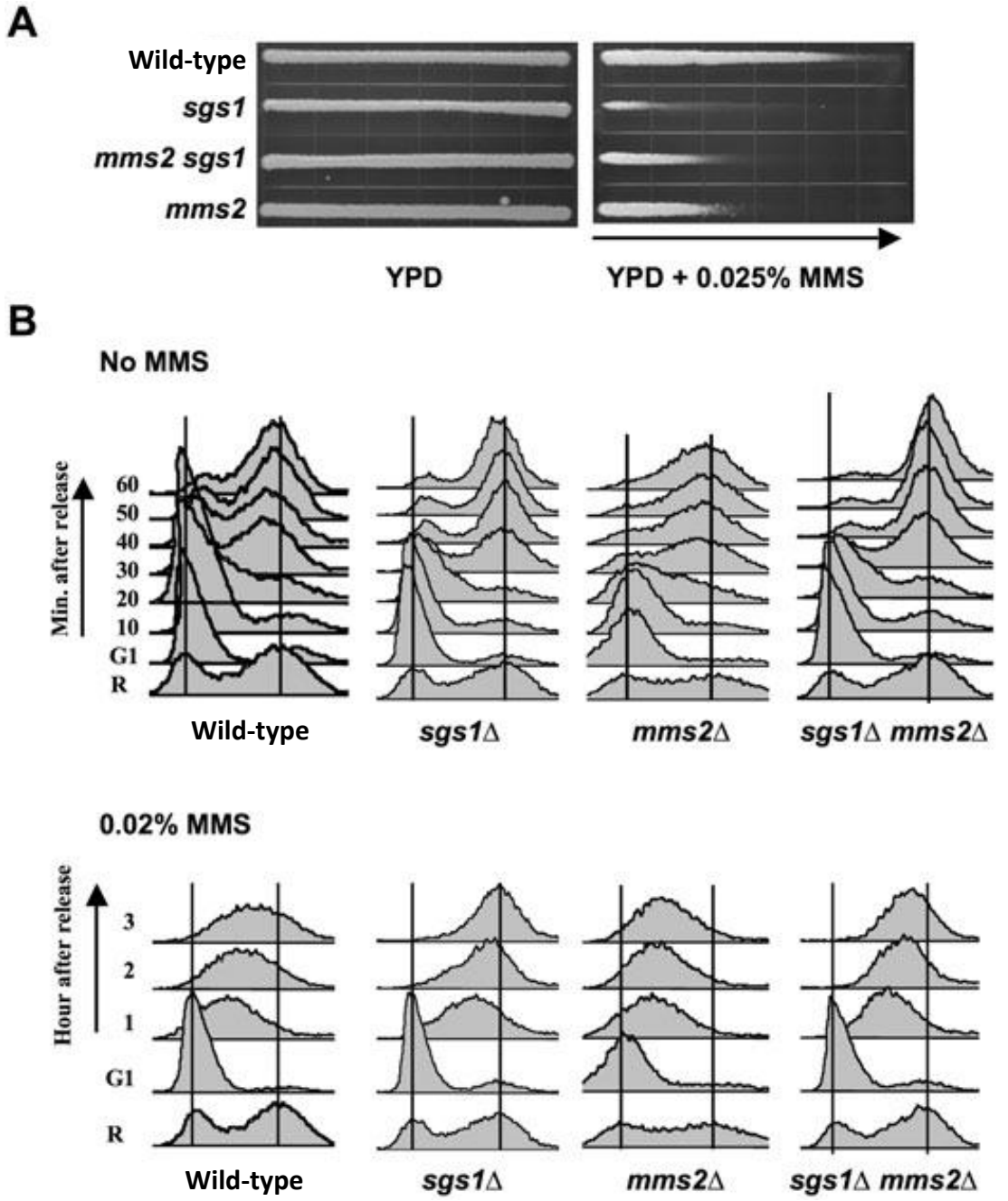

Figure 3.11 – Deletion of *MMS2* Suppresses *sgs1* Mutant Phenotypes. (A) *mms2* suppresses *sgs1* for MMS sensitivity. A gradient plate assay was performed as described and the plates were incubated at 30 °C for 2 days before being photographed. Arrows indicate the increasing concentration of MMS. Results were observed a minimum of three times. (B) *mms2* suppresses the *sgs1* S-phase checkpoint defect. Experimental conditions were as described in Figure 3.8 legend. All strains used were isogenic to BY4741. Results were observed in three independent experiments.

3.4 – Discussion

By employing a modified SGA screen protocol, we identified three out of four genes known to form the Shu complex. Our screening protocol was set strictly to aim at identifying genes within the *RAD6* pathway and subsequent genetic analyses demonstrate that *SHU* genes indeed belong to the error-free branch of PRR. First of all we show, as previously reported, that the single mutants of the *SHU* genes have indistinguishable phenotypes and that the four gene products form a stable complex. Second, *shu* is epistatic to *mms2/ubc13* with respect to killing by MMS, a genetic definition that the corresponding genes belong to the same pathway. Third, *shu* is synergistic to *rev3* with respect to MMS-induced killing, and the level of synergism is characteristic of two branched pathways handling the same substrate. Fourth, *shu* mutants display a mutator phenotype characteristic of error-free PRR defects, and this increase in spontaneous mutagenesis is dependent on functional *REV3*. Finally, *shu* mutations also confer phenotypes only observed with defects in typical error-free PRR genes, such as suppression by the *srs2* mutation (Broomfield and Xiao, 2002) or mating-type heterozygosity (Barbour and Xiao, 2006), as well as the synergistic interaction with damage checkpoint (Barbour *et al.*, 2006). These phenotypes collectively place *SHU* genes as members of error-free PRR in a most stringent manner.

Members of *SHU* genes have also been identified through several previous genetic screens, including increase in gross chromosomal rearrangement (GCR) (Huang *et al.*, 2003; Smith *et al.*, 2004), suppression of slow growth and HU sensitivity of *top3* (Shor *et al.*, 2005) and alleviation of synergistic phenotypes of *sgs1 mms4/mus81* or

mph1 mms4/mus81 (St Onge *et al.*, 2007). These phenotypes can be attributed to the role of Shu complex in promoting certain aspect(s) of HR mediated by Rad51 and Rad54 (Mankouri *et al.*, 2007). Based on previous reports and results presented in this study, we argue that the Shu complex plays a unique role in S-phase and is probably responsible for converting stalled replication forks into HR intermediates, which are subsequently resolved by Sgs1-Top3. First, *rad52* in general and *rad51*, *rad54* more specifically are epistatic to *shu* in response to killing by MMS, suggesting that the Shu complex functions only in the presence of HR. Second, inactivation of *SHU* effectively suppresses HU and MMS sensitivity seen in the *sgs1* mutant, as well as other phenotypes associated with *top3* (Mankouri *et al.*, 2007; Shor *et al.*, 2005), suggesting that it functions upstream of Sgs1-Top3-Rim1. This is reminiscent of *hr* mutations that also suppress *sgs1* and *top3* phenotypes (Shor *et al.*, 2002). Third, although *shu* mutants are much less sensitive to MMS than *hr* mutants, they have a similar effect in delaying S-phase progression in the presence of MMS, and the *shu hr* double mutation has the same effect as corresponding single mutations, suggesting that the Shu complex plays an important role in this particular aspect of HR. Fourth, *shu* mutations have an opposite effect to *sgs1* on S-phase progression in the presence of MMS, while *shu* is epistatic to *sgs1*. This observation supports more direct evidence that inactivation of *HR* (Liberi *et al.*, 2005) or *SHU* genes (Mankouri *et al.*, 2007) inhibits MMS-induced X-molecules, which represent abnormal DNA replication intermediates, from accumulating in the *sgs1* mutant. Since X-molecules have been implied to be a recombinant intermediate derived from sister chromatid invasion at the stalled replication fork, a model is conceivable (Figure 3.12) in

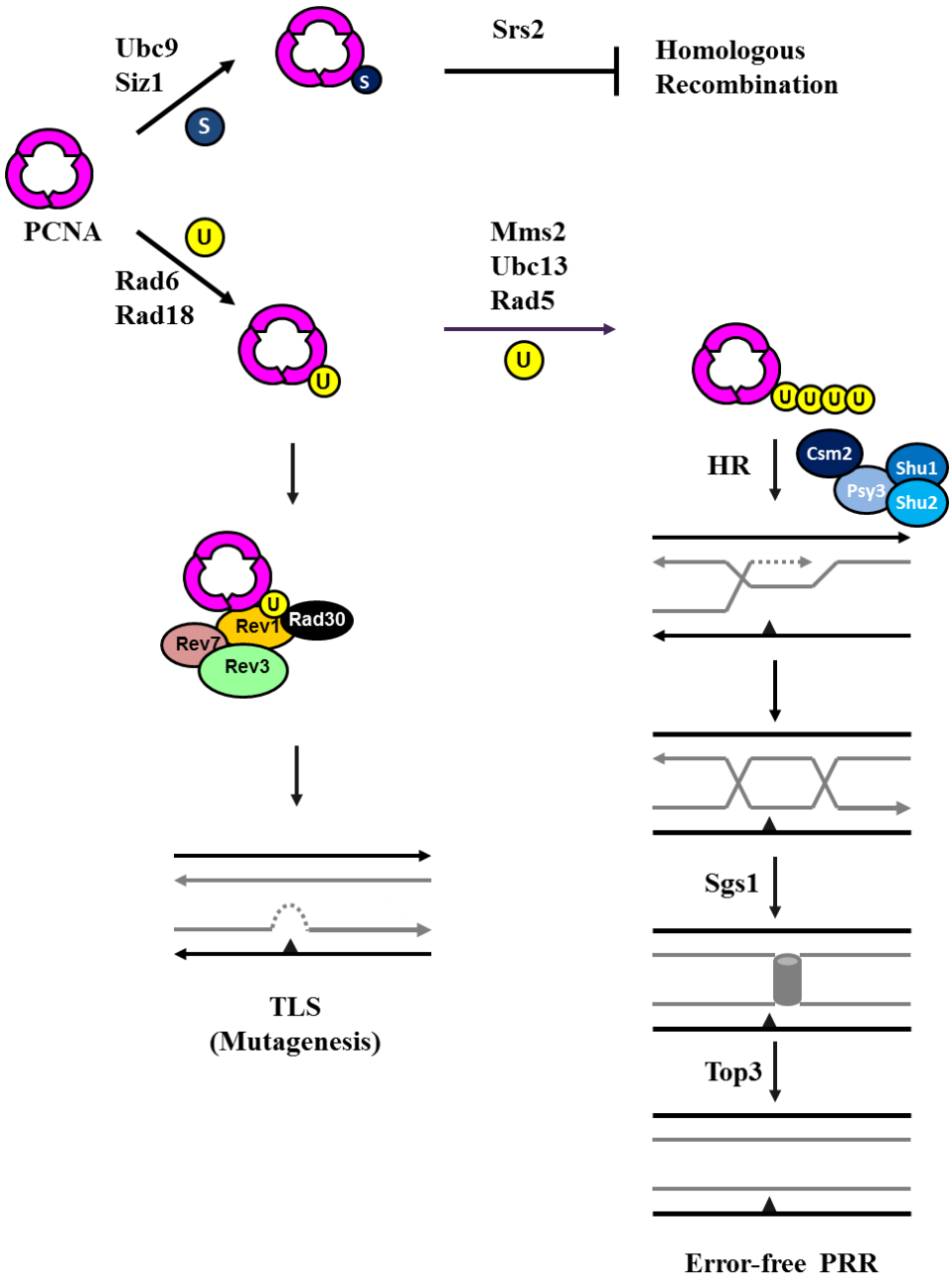

Figure 3.12 – A Proposed Model Depicting the Budding Yeast DNA Damage Tolerance Pathways Mediated by Covalent Modifications of PCNA, Paying Special Attention to the Error-Free PRR Pathway. It is proposed that after PCNA polyubiquitination by Rad5–Ubc13–Mms2, the Shu complex helps to recruit homologous recombination proteins to the site of a stalled replication fork, resulting in the invasion and utilization of the newly synthesized sister chromatid for translesion synthesis. Continual template switching and replication creates a double-Holliday junction, which requires the Sgs1 helicase for branch migration and the Top3 topoisomerase to resolve the resulting hemicatenane structure without crossing over. Essentially as published in Ball *et al*. 2009.

which the Shu complex channels blocked replication forks to undergo HR-mediated DNA synthesis, or template switching, resulting in the formation of a double-Holliday junction (dHJ) that requires the Sgs1 helicase for strand migration and the Top3 topoisomerase to resolve the Sgs1 product to avoid crossing over (Wu and Hickson, 2003). Finally, to confirm that the Shu complex indeed couples error-free PRR to HR-Sgs1, we observed phenotypes indicative of functional overlap between the two pathways and more strikingly the phenotypic suppression of *sgs1* phenotypes by *mms2*. While this study demonstrates firmly that error-free PRR employs HR and Sgs1-Top3 resolution to bypass replication blocks arising during S-phase, a recent report also demonstrated an *in vitro* assay where Rad5, through its intrinsic helicase activity, promotes replication fork regression (Blastyak *et al.*, 2007). Although fork regression and template switching are two proposed models of error-free bypass (Broomfield *et al.*, 2001), they are not necessarily mutually exclusive. One possibility is the fork regression followed by sister chromatid invasion and resolution. Alternatively, it remains possible that error-free PRR employs both modes of bypass. Consistent with the latter possibility is the fact that Rad5 is a multifunctional protein (Ahne *et al.*, 1997; Chen *et al.*, 2005; Johnson *et al.*, 1992) and that the *rad5* mutant is much more sensitive to DNA-damaging agents than a typical error-free PRR pathway mutant such as *mms2* or *ubc13* (Xiao *et al.*, 2000). Nevertheless, the template switch model is supported by an observation using a carefully designed damage substrate that mimics UV-induced lesions on both DNA strands (Zhang and Lawrence, 2005).

Although *SHU* genes are assigned to the error-free PRR pathway through this study, we notice some differences between *mms2/ubc13* mutants and *shu* mutants. First, while *hr* mutations are epistatic to *shu*, they are additive to *mms2/ubc13*. Second, while *mms2/ubc13* are synergistic with *rev3* to essentially any DNA-damaging agents examined (Broomfield *et al.*, 1998; Xiao *et al.*, 1999), the strong synergism between *shu* and *rev3* appears to be limited to MMS (L.G. Ball and W. Xiao, data not shown). Third, *mms2* or *ubc13* mutant is slightly more sensitive to MMS than *shu* mutants (e.g. Figure 3.9A). Finally, the *mms2* mutant consistently displays a higher spontaneous mutation rate than *psy3* in the *trp1-289* reversion assay. Interestingly, *SHU* genes have been identified in the screen for GCR suppressors, whereas neither *mms2* nor *ubc13* came out of these screens (Huang *et al.*, 2003; Smith *et al.*, 2004). Collectively, we interpret these differences as an indication that the Shu complex may inherit a subset of error-free PRR activities, most likely during S-phase, and respond to lesions induced by agents like MMS.

PSY3 and *SHU2* appear to have homologues in *Schizosaccharomyces pombe* (*rld1* and *swi1* respectively) and human cells (*RAD51D* and *SWI1* respectively), and their functions are reminiscent of *SHU* with respect to promoting HR and suppressing RecQ family mutant phenotypes (Martin *et al.*, 2006). Given that Mms2–Ubc13-mediated DNA damage tolerance pathway is also conserved in eukaryotes (Andersen *et al.*, 2005; Brown *et al.*, 2002; Li *et al.*, 2002), it would be of great interest to examine whether these homologues also function in a similar manner.

CHAPTER FOUR

DNA ENDO/EXONUCLEASES AND THE Sgs1 HELICASE ARE REQUIRED FOR YEAST DNA POSTREPLICATION REPAIR

4.1 – Abstract

Yeast DNA PRR functions to bypass replication-blocking lesions in order to prevent damage-induced cell death. PRR employs two different mechanisms to bypass damaged DNA, namely TLS and error-free PRR. We recently demonstrated that error-free PRR utilizes homologous recombination and the Sgs1 helicase to facilitate template switching. To our surprise, *sgs1* and null mutations of genes encoding the Mre11-Rad50-Xrs2 (MRX) complex, which are also required for HR, are epistatic to TLS mutations. Further genetic analyses indicated that two other nucleases involved in double-strand end resection, Sae2 and Exo1, are also variably required for efficient lesion bypass. The modes of their involvement in different branches of PRR were further confirmed by mutagenesis assay and their effects on the inhibition of PCNA ubiquitination. In light of the distinct and overlapping activities of the above nucleases in the resection of double-strand breaks, we propose that the interplay among Sgs1 and distinct single-strand nuclease activities of MRX, Sae2 and Exo1 dictate the preference between TLS and error-free PRR for lesion bypass.

4.2 – Introduction

In order to maintain genomic integrity, living organisms have developed a set of highly conserved mechanisms to deal with spontaneous and induced DNA damage. DNA lesions that result in stalled replication apparatus are among the most dangerous and result in genomic instability, a well-known hallmark of cancer. DNA repair and replication checkpoints act to prevent the collapse of blocked replication apparatus, while HR acts to rescue DSBs induced by collapsed replication forks (Friedberg *et al.*, 2006). To prevent detrimental outcomes, the budding yeast *Saccharomyces cerevisiae RAD6* DNA PRR epistasis group functions to bypass replication blocks (Barbour and Xiao, 2003). Within this pathway, Rad6 is known to have diverse functions outside of PRR, while Rad18 functions exclusively in a stable complex with Rad6 to monoubiquitinate PCNA. PCNA is encoded by the essential gene *POL30* in budding yeast and is a DNA polymerase sliding clamp. It is generally believed that upon exposure to DNA damage, PCNA is monoubiquitinated at the K164 residue (Hoege *et al.*, 2002) and that this monoubiquitination promotes TLS. The TLS pathway is represented by *REV3* and *REV7*, which encode the catalytic and regulatory subunits of DNA Polζ, and *REV1*; inactivation of any one of the above genes results in severely compromised induction of mutagenesis after DNA damage treatment and a reduction in spontaneous mutagenesis (Lawrence, 2004).

Monoubiquitinated PCNA can be further polyubiquitinated by Mms2-Ubc13-Rad5 to form non-canonical K63-linked Ub chains, which leads to an error-free mode of PRR (Hoege *et al.*, 2002). An *mms2* null mutation causes moderate sensitivity to killing

by numerous DNA-damaging agents, strong synergistic interaction with *rev3*, and a *REV3*-dependent increase in spontaneous mutagenesis (Broomfield *et al.*, 1998; Xiao *et al.*, 1999). Similar phenotypes have been observed for the *ubc13* null mutant as well (Brusky et al., 2000; Hofmann and Pickart, 1999). It has long been proposed that error-free PRR utilizes some form of HR to bypass replication-blocking lesions (Prakash *et al.*, 1993); however, direct evidence only emerged recently for the involvement of HR in error-free PRR (Chapter 3) (Ball *et al.*, 2009). In this report, genes required for HR, including *RAD51*, *RAD52*, *RAD54*, *RAD55* and *RAD57*, were placed downstream of *MMS2* and *UBC13* within the error-free branch of PRR. However, other genes involved in HR, including *MRE11*, *RAD50* and *XRS2*, whose products form a stable complex known as the MRX complex (Krogh and Symington, 2004), have not been characterized with respect to PRR.

The MRX complex binds DNA and is known to be involved in numerous activities such as telomere length, damage recognition and processing following DSBs, non-homologous end joining, cell cycle checkpoint activation, meiosis and most recently BER (D'Amours and Jackson, 2002; Daley et al., 2005; Grenon et al., 2001; Ivanov et al., 1994; Lisby et al., 2004; Steininger et al.; Steininger et al., 2008; Tsukuda et al., 2005). Mre11 is also known to function as both a ssDNA endonuclease and a 3'-5' exonuclease (Paull and Gellert, 1998, 1999). Phenotypically, the null mutant of any one of the MRX components exhibits extreme sensitivity to ionizing radiation and other DNA-damaging agents (Krogh and Symington, 2004). Rad50 belongs to the structural maintenance of chromosomes (SMC) family of proteins and contains two heptad repeats in its center that

fold into a coiled-coil (de Jager *et al.*, 2001). Mre11 binds to the base of the coiled-coil (Mre11-Rad50), while at the very tip a conserved Cys-X-X-Cys motif is found to form a hook-shaped domain allowing dimerization with another Mre11-Rad50 dimer resulting in an $Mre11_2Rad50_2$ heterotetramer (Anderson *et al.*, 2001; Hopfner *et al.*, 2002). Xrs2, the third component of MRX, binds to Mre11 via its conserved C-terminal domain; the interaction between Mre11 and Xrs2 is essential for all known Mre11 functions (Tsukamoto *et al.*, 2005).

Here we report our investigation of novel functions of the MRX complex in both TLS and error-free PRR. Two relevant nucleases Exo1 and Sae2 were also characterized in this study. In addition we examined the role of the Sgs1 helicase in the early steps of lesion bypass. These studies unexpectedly revealed the involvement of the MRX complex and Sgs1 in regulating PRR pathways.

4.3 – Results

4.3.1 – The MRX Complex Functions in Both TLS and Error-free PRR

Previous work in our laboratory (Chapter 3) utilized an SGA screen (Tong *et al.*, 2001) of all non-essential genes in *S. cerevisiae* to identify novel genes involved in TLS and error-free PRR (Ball *et al.*, 2009). Both *rev1* and *rev3* query strains identified HR genes including *RAD51*, *RAD52*, *RAD54*, *RAD55*, and *RAD57* (Ball *et al.*, 2009). Mutations of all the above genes conferred characteristic synergistic interactions with *tls* mutations (Figure 4.1 and data not shown), while neither the *mms2* nor *ubc13* mutation displayed

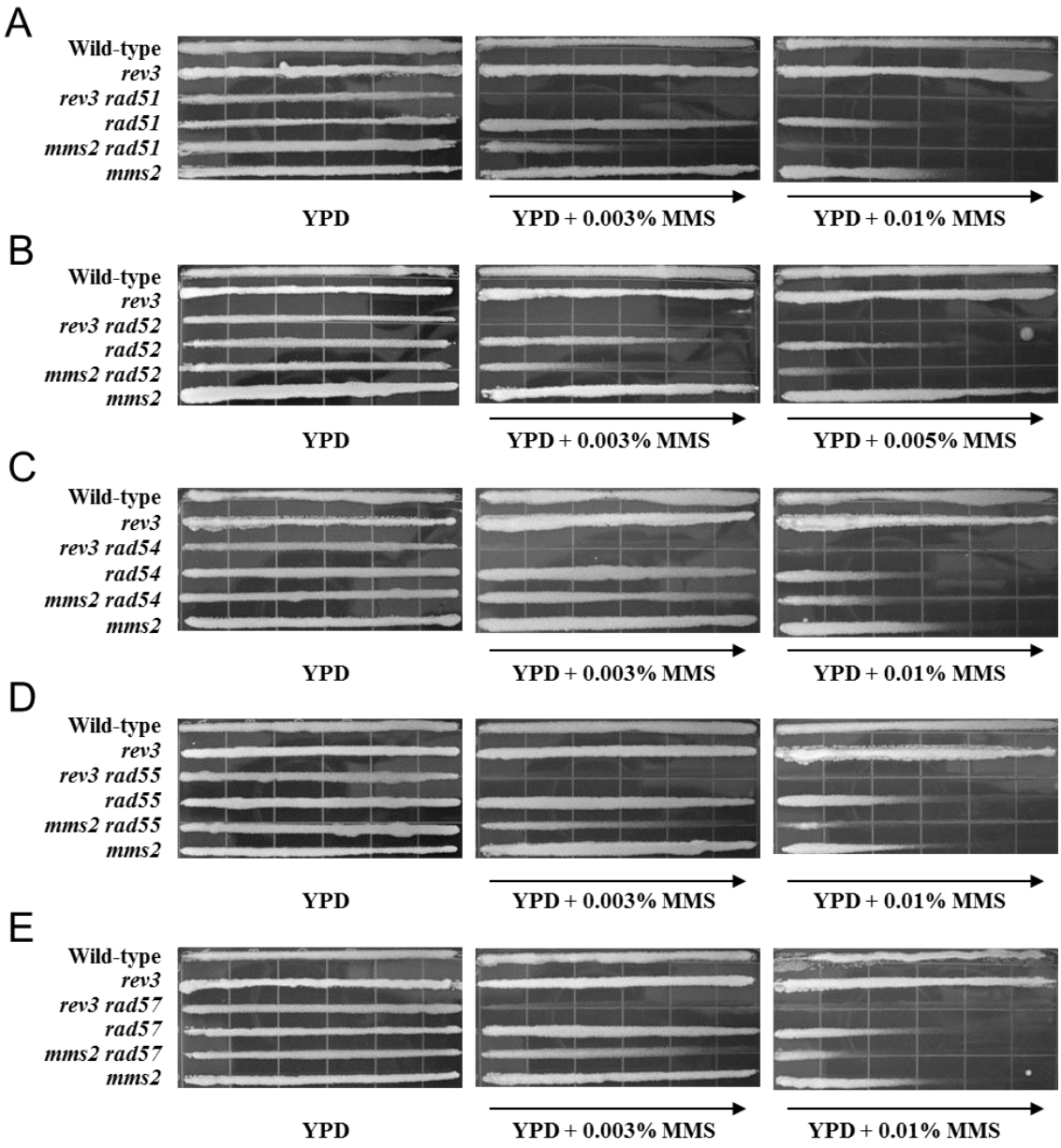

Figure 4.1 – Differential Genetic Interactions between *REV3* or *MMS2* and Homologous Recombination Genes with Respect to MMS Sensitivity by a Gradient Plate Assay. Overnight cell cultures were imprinted on YPD or YPD + MMS at the concentration indicated and incubated at 30 °C for 2 days before being photographed. The arrows indicate the increasing MMS concentration. All strains used were isogenic to BY4741. (A) *rad51*Δ *vs. rev3*Δ or *mms2*Δ. (B) *rad52*Δ *vs. rev3*Δ or *mms2*Δ. (C) *rad54*Δ *vs. rev3*Δ or *mms2*Δ. (D) *rad55*Δ *vs. rev3*Δ or *mms2*Δ. (E) *rad57*Δ *vs. rev3*Δ or *mms2*Δ. Results were observed a minimum of three times.Results contributed by Ke Zhang.

synergistic interaction with the above HR mutations (Figure 4.1 and data not shown). To our surprise, none of the *MRX* genes were pulled out in the above SGA screens, suggesting that *mrx* mutations may have unexpected genetic interactions with *tls* mutations. Upon further screening and characterization of the MRX complex, we found that null mutations of *mre11* (Figure 4.2A), *rad50* (Figure 4.2B), and *xrs2* (Figure 4.2C) are essentially epistatic to *rev3* with respect to killing by the alkylating agent MMS that specifically causes replication-blocking lesions, which was in sharp contrast to the synergistic interactions between *hr rev3* double mutants (Figure 4.1). On the other hand, genetic interactions between *mrx* and *mms2* are essentially identical to that of *hr* and *mms2* (Figure 4.2A, B, C, and Figure 4.1). To further illustrate differences between *mrx* and *hr* with respect to their genetic interactions with TLS mutations, we performed quantitative liquid killing experiments to compare *rad51* and *mre11*. While *rad51* is indeed synergistic with *rev3* (Figure 4.3A), the *mre11 rev3* double mutant is barely more sensitive to 0.1% MMS than the *mre11* single mutant (Figure 4.3B). In addition, while the *mms2 rad51* double mutant is more sensitive to MMS-induced killing than either of the corresponding single mutants (Figure 4.3A), the *mms2 mre11* double mutant is again barely more sensitive to 0.1% MMS than the *mre11* single mutant (Figure 4.3B). Similar results were also obtained after UV irradiation (Figure 4.4). Together these observations suggest that the MRX complex does not function exclusively in error-free PRR like other known HR genes, and instead functions in both the TLS and error-free PRR pathways.

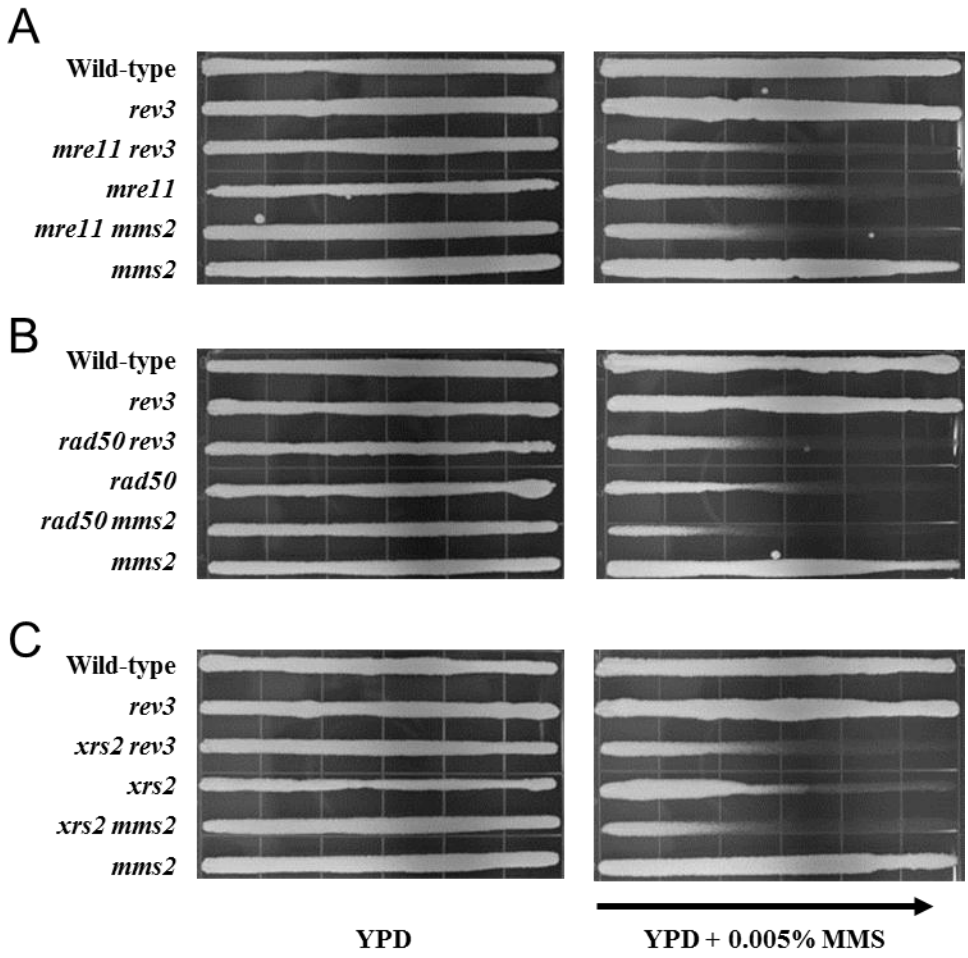

Figure 4.2 – Genetic Interactions Between *REV3* or *MMS2* and the MRX Complex Genes with Respect to MMS Sensitivity. (A-C) Cell survival in a gradient plate assay. Overnight cell cultures were imprinted on YPD or YPD + 0.005 % MMS and incubated at 30 °C for 2 days before being photographed. The arrow indicates the increasing MMS concentration. All strains used were isogenic to BY4741. (A) *mre11*Δ *vs. rev3*Δ or *mms2*Δ; (B) *rad50*Δ *vs. rev3*Δ or *mms2*Δ; (C) *xrs2*Δ *vs. rev3*Δ or *mms2*Δ. Results were observed a minimum of three times. Results contributed by Ke Zhang.

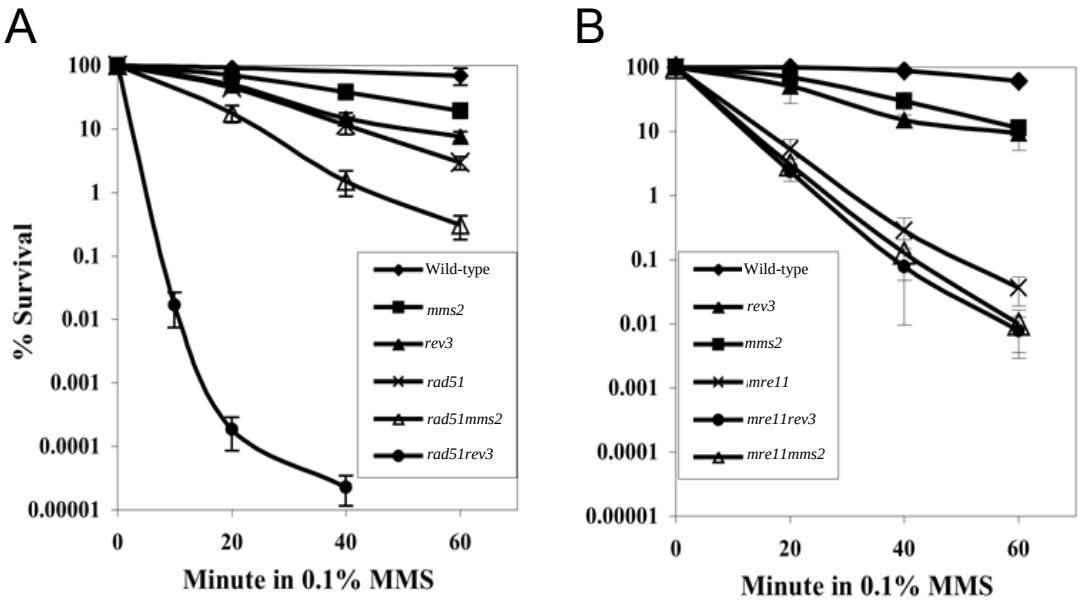

Figure 4.3 – Cell Survival in a Liquid Killing Assay to Explore the Genetic Interactions Between *REV3* or *MMS2* and the MRX Complex. These results are the average of three independent experiments with standard deviations indicated by error bars. All strains used were isogenic to BY4741. (A) *rad51*Δ *vs. rev3*Δ or *mms2*Δ; (B) *mre11*Δ *vs. rev3*Δ or *mms2*Δ. Results contributed by Ke Zhang.

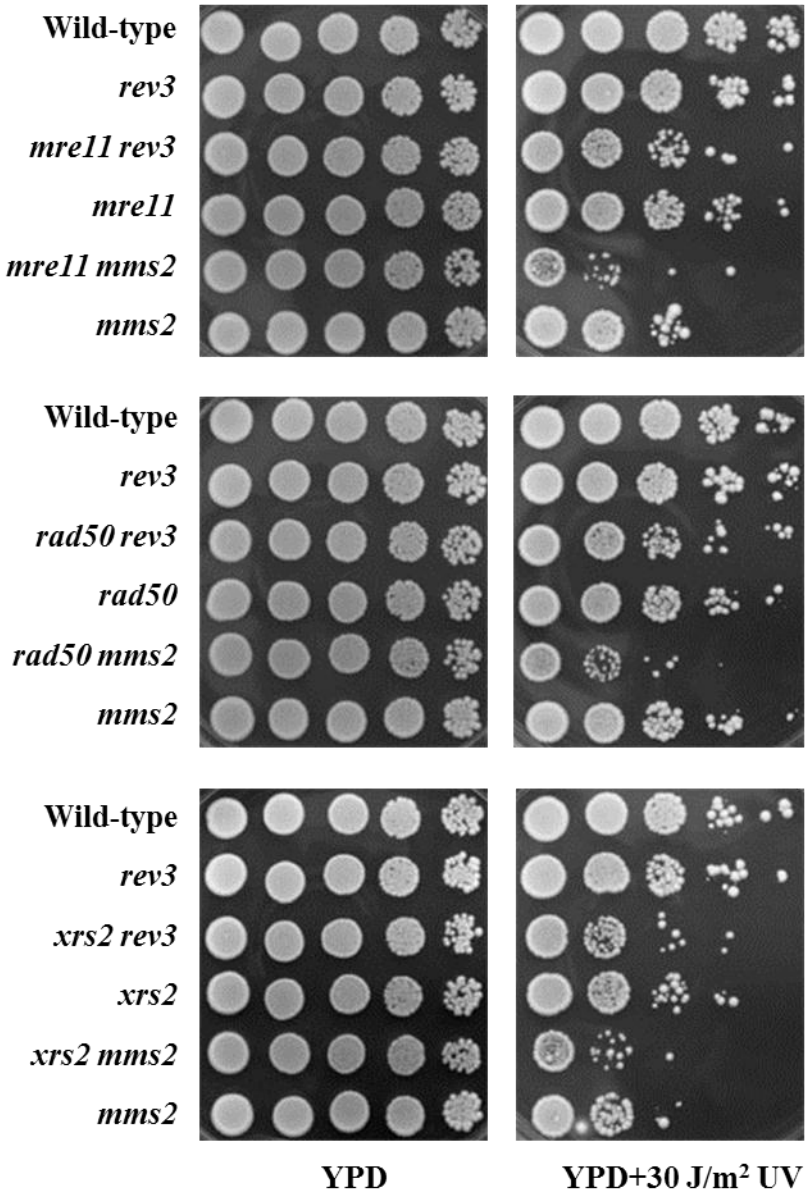

Figure 4.4 – Genetic Interactions Between *REV3* or *MMS2* and the MRX Complex Genes with Respect to UV Sensitivity. Overnight cell cultures were used to make a series of 10-fold dilutions, spotted and the plates were then exposed to the UV dose as indicated and incubated at 30 °C for 2 days before being photographed. All strains used were isogenic to BY4741. Results were observed a minimum of three times. Results contributed by Ke Zhang.

4.3.2 – Genetic Interactions Between MRX and PCNA Modifications

It is the sequential ubiquitination of PCNA that satisfactorily explains the current genetic observations with regard to how the *RAD6* pathway operates to tolerate and bypass replication-blocking lesions. To critically determine whether MRX genes are involved in the PRR pathways, we combined the *mre11* null mutation with a *pol30-K164R* point mutation that abolishes ubiquitination of PCNA (Hoege *et al.*, 2002). Our prediction was that if the increased sensitivity conferred by *mre11* were due to its involvement in PRR, the *mre11 pol30-K164R* double mutant would be as sensitive as one of the single mutants. Indeed, while *mre11* appears slightly more sensitive to MMS than the *pol30-K164R* single point mutation, the *mre11 pol30-K164R* double mutant is less sensitive than the *mre11* single mutant and more like the *pol30-K164* single mutant (Figure 4.5). This result further supports the notion that Mre11 functions in the same pathway as PCNA posttranslational modifications at the K164 residue.

The epistatic genetic relationship between *mre11* and *pol30-K164R* does not necessarily indicate whether the MRX complex acts upstream or downstream of PCNA ubiquitination. To answer this question, we set out to determine if deletion of *MRX* genes could alter the relative level of ubiquitinated PCNA. To achieve this objective, we raised polyclonal antibodies against purified Pol30 expressed from bacterial cells. When it was realized that cross reactions to other yeast proteins became a concern, we screened a large number of monoclonal antibodies and obtained functional monoclonal antibodies (mAbs) for this study. We were able to verify monoubiquitinated PCNA in the wild-type yeast

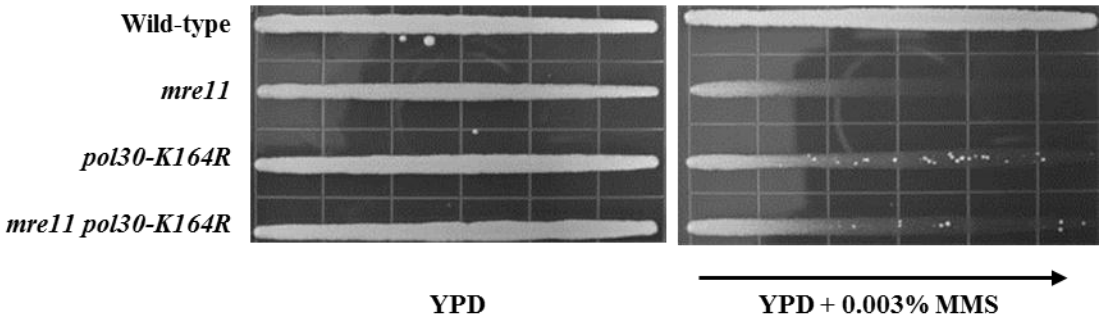

Figure 4.5 – *MRE11* and Belongs to the Yeast PRR Pathway. Overnight cell cultures were imprinted on YPD or YPD + MMS gradient plates at the given concentrations, and incubated at 30 °C for 2 days before being photographed. The arrow indicates the increasing MMS concentration. *pol30-K164R* is epistatic to *mre11*. Strains used were DBY747 (Wild-type) and its isogenic derivatives WXY2379 (*mre11*Δ), WXY2384 (*pol30-K164R*) and WXY2389 (*mre11*Δ *pol30-K164R*). Results were observed a minimum of three times. Results contributed by Ke Zhang.

whole cell extracts without the need for His_n-affinity purification, and notably this modification was absent in a strain containing a genomic integration of the *pol30-K164R* point mutation (Figure 4.6A, lanes 3 and 4), and was not detected in the absence of MMS treatment (cf. lanes 1, 2 vs. 5, 6). The fact that this band was slightly shifted up in the strain containing the *POL30*-His_7 allele compared to the native Pol30 allele (cf. lanes 5 and 6) further confirms that this band is PCNA modification. It was previously reported that overexpression of *RAD18* alone can enhance PCNA ubiquitination (Davies *et al.*, 2008). Our laboratory also found that simultaneous overexpression of both *RAD6* and *RAD18* could enhance Rad17 monoubiquitination (Fu *et al.*, 2008). In this study, we found that overexpressing *RAD18* alone or *RAD6+RAD18* was able to enhance the visualization of monoubiquitinated PCNA, although it is not required (Figure 4.6B). In addition, as expected, a null mutation of *rad18* abolishes monoubiquitinated PCNA (Figure 4.7, lane 5). In addition, we found that deletion of *mre11* visually reduced the level of monoubiquitinated PCNA (Figure 4.14). Together our results clearly demonstrate that the MRX complex is a novel member of the PRR pathway functioning upstream of PCNA modification.

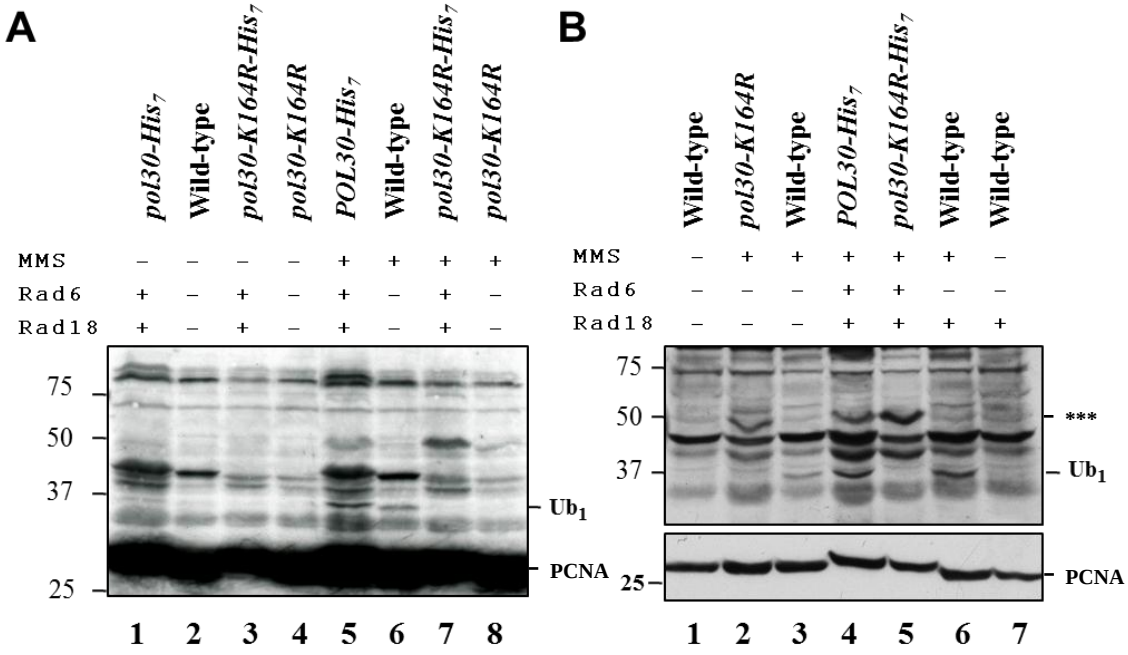

Figure 4.6 – Characterization of Monoubiquitinated PCNA. (A) Detection of monoubiquitinated PCNA. (B) Overexpression of *RAD6 +RAD18* or *RAD18* alone improves the detection of PCNA in whole cell extracts. Overnight cultures were subcultured and allowed to grow to a cell count of approximately $1x10^7$ cells/mL before being treated with 0.05 % MMS for 90 minutes or remained untreated. Total cell extracts were subject to SDS-PAGE and western blot analyses with an in-house anti-Pol30 monoclonal antibody. Strains used were HK578-10A (wild-type), WXY994 (*pol30-K164R*), WXY989 (*Pol30-His$_7$*), and WXY990 (*pol30-K164R-His$_7$*). Molecular size markers are labeled on left (in kD). Unmodified Pol30 protein is indicated by PCNA, and monoubiquitinated PCNA is indicated by Ub_1. *** An unknown band that appears only in a *pol30-K164R* point mutation after MMS treatment, and may represent a different modification of PCNA. The lower box in Figure B resulted from a shorter exposure time of the same western depicted above it. Results were observed a minimum of three times.

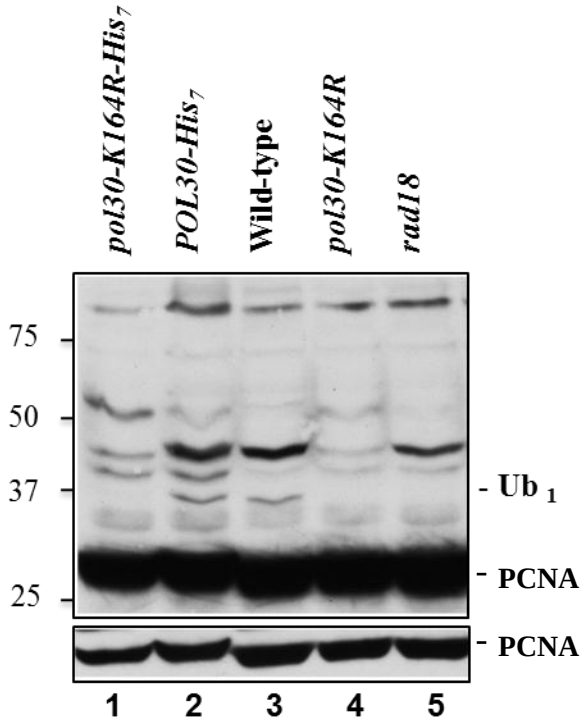

Figure 4.7 – PCNA Monoubiquitination is Dependent on *RAD18*. Overnight cultures were subcultured and allowed to grow to a cell count of approximately $1x10^7$ cells/mL before being treated with 0.05 % MMS for 90 minutes. Total cell extracts were subject to SDS-PAGE and western blot analyses with an in-house anti-Pol30 monoclonal antibody. Strains used were HK578-10A (wild-type), WXY994 (*pol30-K164R*), WXY989 (*POL30-His$_7$*), WXY990 (*pol30-K164R-His$_7$*) and WXY930 (*rad18*Δ). Molecular size markers are labeled on left (in kD). Unmodified Pol30 protein is indicated by PCNA, and monoubiquitinated PCNA is indicated by Ub_1. The lower box resulted from a shorter exposure time of the same western shown above. Results were observed a minimum of three times.

4.3.3 – Involvement of Two Nucleases, Sae2 and Exo1, in PRR

The MRX complex is rapidly recruited to DSBs, signals checkpoint activation and regulates 5'-3' resection of the DNA ends (Lee *et al.*, 1998; Lisby *et al.*, 2004; Nelms *et al.*, 1998). MRX is also known to interact with Sae2/CtIP/Ctp1 (Clerici *et al.*, 2005; Limbo *et al.*, 2007; Sartori *et al.*, 2007). Sae2 was initially discovered in two genetic screens designed to isolate mutants defective in the steps following the initiation of Spo11-induced DSBs but functioning before resolution of the recombination intermediates (McKee and Kleckner, 1997; Prinz *et al.*, 1997). Since then Sae2 has been deemed the "unofficial fourth member" of the MRX complex (Mimitou and Symington, 2009). However, the function of the MRX complex in cooperation with Sae2 in processing DSBs is partly redundant with the 5'-3' exonuclease Exo1 (Tran *et al.*, 2004). Exo1 has been implicated in mismatch repair, telomere integrity (Liberti and Rasmussen, 2004; Tran *et al.*, 2004), error-free PRR (Tran *et al.*, 2007) and most recently long-range resection of DSBs together with MRX and Sae2 (Bonetti *et al.*, 2009; Mimitou and Symington, 2008; Zhu *et al.*, 2008). Therefore, it is necessary to investigate the roles of Sae2 and Exo1 in relation to PRR.

The genetic interaction between *sae2* and both *mms2* and *rev3* resulted in double mutations that were only slightly more sensitive than their respective single mutants (Figure 4.8A), making it difficult to specifically place *SAE2* in one of the two PRR pathway. This result is also reminiscent of the genetic interaction between *mrx* and both PRR pathways (Figure 4.2 and 4.3). To determine whether *SAE2* plays a role in PRR, we

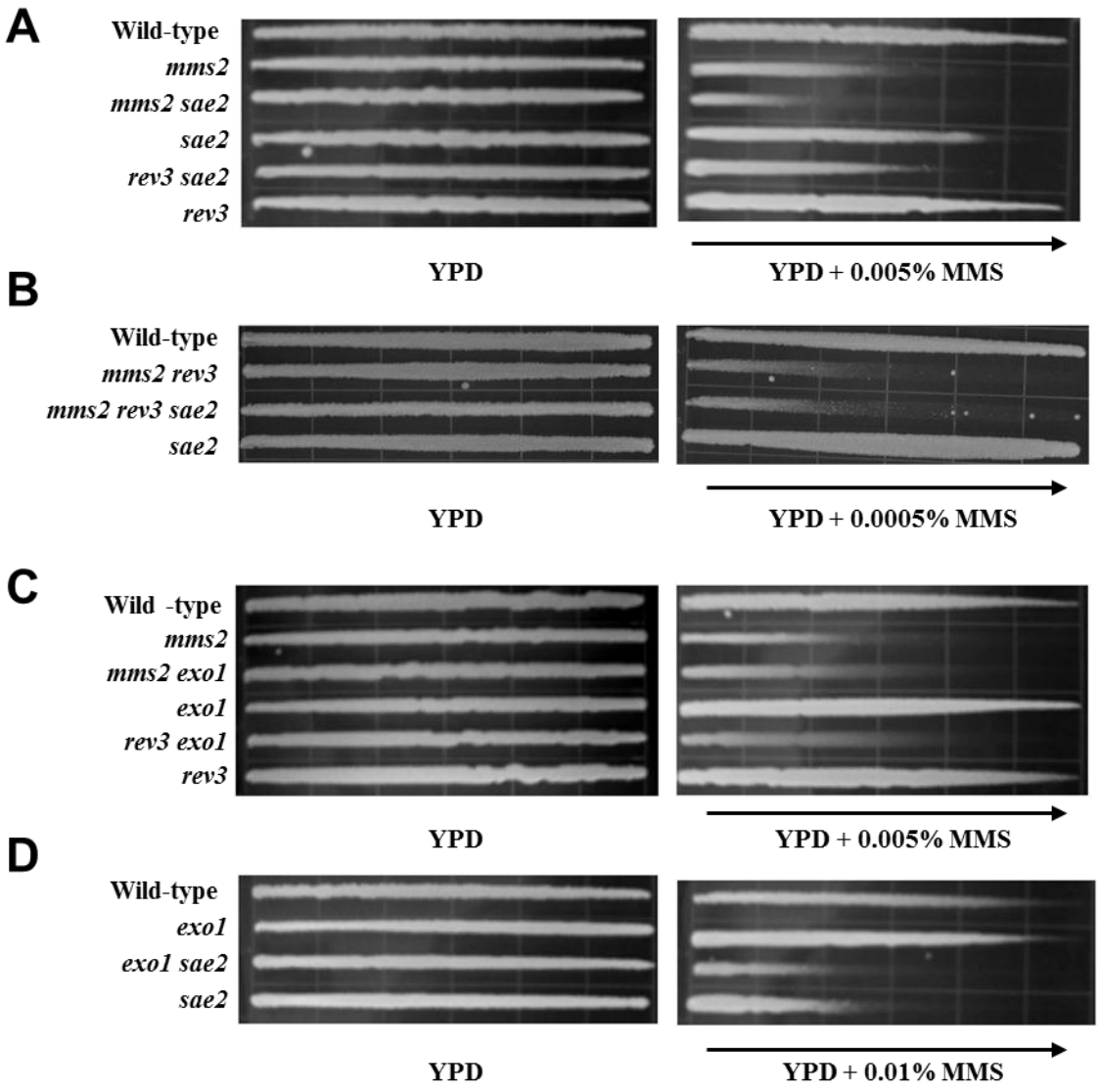

Figure 4.8 – Genetic Interactions Between *SAE2*, *EXO1*, and *REV3* or *MMS2*. Overnight cell cultures were imprinted on YPD or YPD + MMS gradient plates at the given concentrations, and incubated at 30°C for 2 days before being photographed. Arrows indicate the increasing MMS concentration. All strains used were isogenic to BY4741. (A) *sae2*Δ vs. *mms2*Δ or *rev3*Δ. (B) *sae2*Δ vs. *mms2*Δ *rev3*Δ. (C) *exo1*Δ vs. *mms2*Δ or *rev3*Δ. (D) *exo1*Δ *vs. sae2*Δ. Results were observed a minimum of three times.

deleted *SAE2* in the *mms2 rev3* double mutant and found that the resulting triple mutant was as sensitive to MMS as the *mms2 rev3* double mutant (Figure 4.8B), suggesting that *SAE2* plays partial roles in both TLS and error-free PRR. To further address whether the increased MMS sensitivity of the *sae2* mutant is due to its role within the PRR pathway, we combined *sae2* with either *rad18* or the *pol30-K164R* mutation and in both cases the double mutants were as sensitive to MMS as the corresponding single mutants (Figure 4.9A and B). These observations clearly place *SAE2* within the yeast PRR pathway with respect to MMS sensitivity.

The *exo1* single mutant does not display noticeable sensitivity to MMS-induced killing (Figure 4.8C), making it difficult to determine its epistatic relationship with other gene mutations. However, the *exo1 rev3* double mutant displays a much greater sensitivity to MMS than either corresponding single mutant (Figure 4.8C), suggesting that *EXO1* functions in a pathway distinct from TLS. In sharp contrast, the *exo1 mms2* double mutant is as sensitive to MMS as the *mms2* single mutant (Figure 4.8C), indicating that *EXO1* functions in the error-free PRR pathway. This observation agrees with a recent report (Tran *et al.*, 2007). We also examined the genetic interaction between *SAE2* and *EXO1* and found that the *exo1 sae2* double mutant is as sensitive to MMS as the *sae2* single mutant (Figure 4.8D). Given the fact that the *exo1* mutation could enhance *rev3* sensitivity, this observation indicates that *sae2* is epistatic to *exo1*, or that, like *EXO1*, *SAE2* also functions in the error-free PRR pathway.

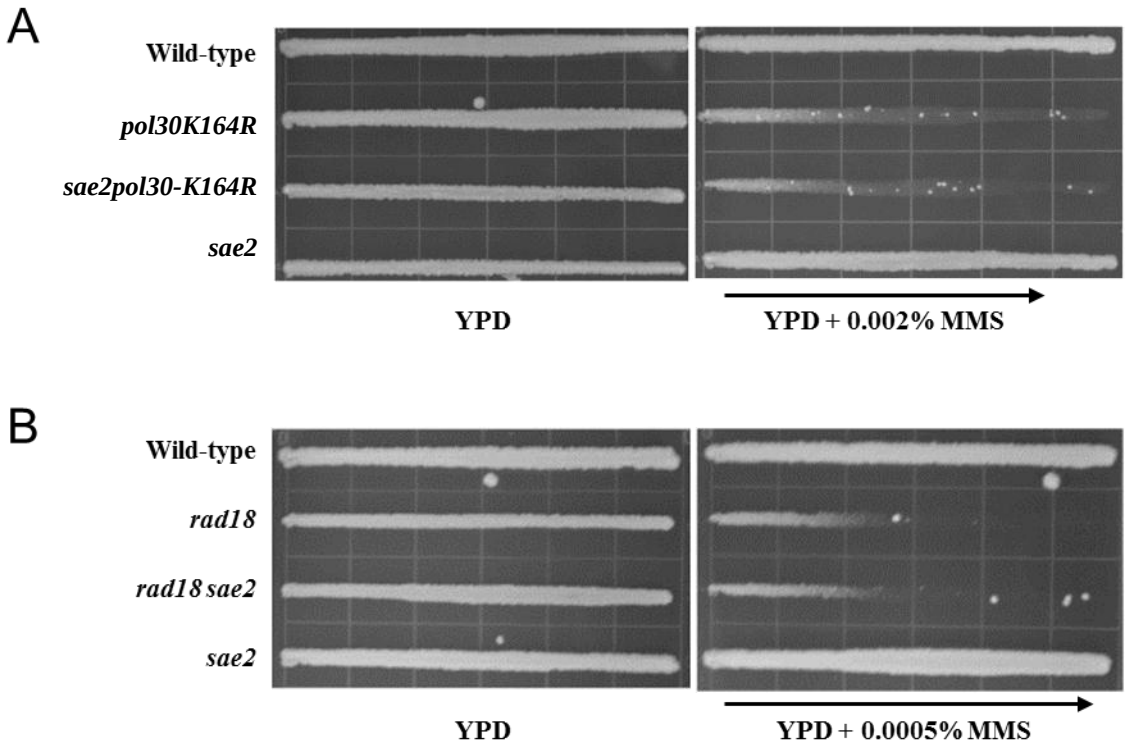

Figure 4.9 – *SAE2* Belongs to the Yeast PRR Pathway. (A-B) Overnight cell cultures were imprinted on YPD or YPD + MMS gradient plates at the given concentrations, and incubated at 30 °C for 2 days before being photographed. The arrow indicates the increasing MMS concentration. (A) *pol30-K164R* is epistatic to *sae2*Δ. Strains used were HK578-10A (Wild-type) and its isogenic derivatives WXY2975 (*sae2*Δ), WXY994 (*pol30-K164R*) and WXY3007 (*sae2*Δ *pol30-K164R*). (B) *rad18* is epistatic to *sae2*. Strains used were HK578-10A (wild-type), WXY930 (*rad18*Δ), WXY2975 (*sae2*Δ), and WXY3008 (*rad18*Δ *sae2*Δ). Results were observed a minimum of three times.

Error-free PRR is characterized by its enhanced spontaneous mutagenesis (Broomfield *et al.*, 1998). If *EXO1* is a member of error-free PRR, its inactivation would be expected to cause an increased spontaneous mutagenesis. Indeed, deletion of *EXO1* resulted in a 16-fold increase in spontaneous mutagenesis (Table 4.1). Two observations ruled out the possibility that this increase was due to the loss of the mismatch repair activity of *EXO1*. Firstly, the increased mutagenesis as seen in the *exo1* mutant was completely dependent on *REV3*, since the *exo1 rev3* double mutant has a spontaneous mutation rate comparable to that of wild-type cells. Secondly, the spontaneous mutation rate in the *exo1 mms2* double mutant is comparable to that of the *mms2* single mutant, which is consistent with a predicted outcome if the enhanced mutagenesis by *exo1* and *mms2* were due to the same mechanisms. Unlike *exo1*, deletion of *MRE11* or *SAE2* did not alter the spontaneous mutation rate over wild-types cells (Table 4.1), suggesting that if MRX and Sae2 function within PRR, they must play pivotal roles in the TLS pathway. This is in sharp contrast to *rad51*, which inactivates HR downstream of error-free PRR (Ball *et al.*, 2009) and results in a 30-fold increase in spontaneous mutagenesis over wild-type cells (Table 4.1).

Table 4.1 – *S. cerevisiae* Spontaneous Mutation Rates to Examine the *mrx* Complex, *exo1*, *sae2* and *sgs1*

Strain[a]	Key alleles	Rate (x 10^{-8})[b]	Fold[c]
DBY747	Wild-type	0.14 ± 0.12	1
WXY667	*rev3* Δ	0.031 ± 0.014	0.2
WXY2917	*exo1* Δ	2.27 ± 0.63	16.2
WXY644	*mms2* Δ	2.72 ± 0.64	19.4
WXY2394	*sae2* Δ	0.18 ± 0.08	1.3
WXY2397	*mre11* Δ	0.16 ± 0.07	1.1
WXY1164	*rad51* Δ	4.2 ± 0.6	30.0
WXY2392	*sgs1* Δ	0.044 ± 0.012	0.3
WXY2918	*exo1* Δ*mms2* Δ	3.33 ± 0.3	23.8
WXY2991	*exo1* Δ*rev3* Δ	0.12 ± 0.07	0.9

a. All strains are isogenic derivatives of DBY747.

b. The spontaneous mutation rates are the average of at least three independent experiments with standar deviation.

c. Relative to the wild-type mutation rate.

Results courtesy of Michelle Hanna

4.3.4 – Sgs1 Is Required for TLS

Based on the observations that the human Sgs1 homolog, BLM, dissociates D-loop and double-Holliday junction intermediates (Gangloff et al., 2000; Karmakar et al., 2006; van Brabant et al., 2000; Wu and Hickson, 2003), Sgs1 has been thought to function downstream of HR and upstream of Top3. Consistently, previous work from our laboratory demonstrated that *mms2* is epistatic to *sgs1* with respect to MMS sensitivity, placing *SGS1* downstream of *MMS2* for error-free lesion bypass via HR (Ball *et al.*, 2009). This model predicts that, like other HR mutations, *sgs1* is synergistic with TLS mutations. However, genetic analysis of the *sgs1 rev3* double mutant consistently shows that *sgs1* is completely epistatic to *rev3* (Figure 4.10) indicating that Sgs1 has a more complex function with respect to PRR than previously thought. This result suggests that Sgs1 functions in both branches of the PRR pathway, and is reminiscent of recent reports that Exo1 and Sgs1 function in different mechanisms for 5'-3' DSB processing (Bonetti et al., 2009; Mimitou and Symington, 2008; Zhu et al., 2008). To further confirm the involvement of Sgs1 in TLS, we examined the spontaneous mutation rate in an *sgs1* mutant and found that deletion of *SGS1* resulted in a spontaneous mutation rate comparable to that of *rev3* (Table 4.1), hence placing *SGS1* within the TLS pathway.

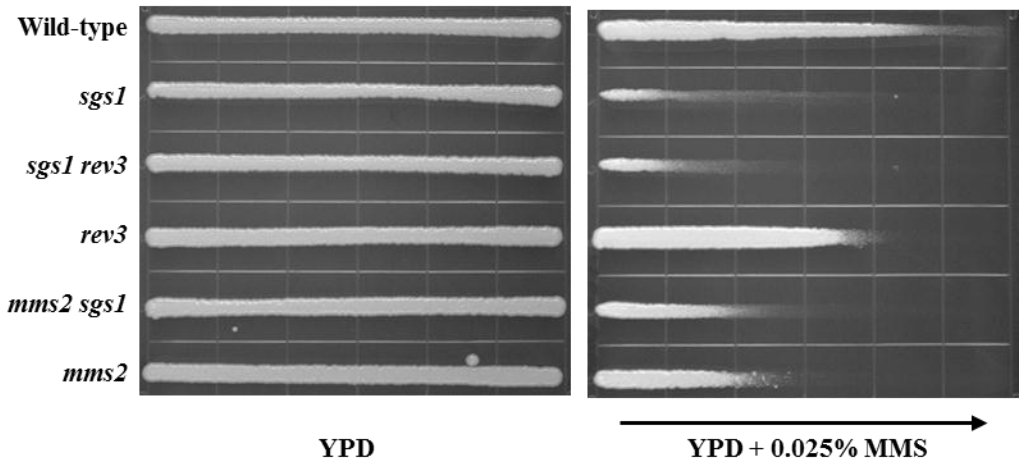

Figure 4.10 – Genetic Interactions Between *SGS1* and *REV3* or *MMS2*. Overnight cell cultures were imprinted on YPD or YPD + MMS gradient plates at the given concentrations, and incubated at 30°C for 2 days before being photographed. Arrows indicate the increasing MMS concentration. All strains used were isogenic to BY4741. *sgs1*Δ vs. *mms2*Δ or *rev3*Δ. Results were observed a minimum of three times, and in two different strain backgrounds.

4.3.5 – The Nuclease Activities of Mre11 and Sae2 Are Required for Their Functions in PRR

The MRX complex is well known for its structural function in maintaining sister chromatid cohesion during DNA metabolic events (Williams *et al.*, 2007). However Mre11 also maintains a nuclease activity responsible for processing DSB ends and hairpins (Connelly et al., 1999; Furuse et al., 1998; Lobachev et al., 2002; Paull and Gellert, 1998; Trujillo and Sung, 2001). The nuclease activity of Mre11 is not essential for some of its known functions including DNA damage sensitivity (Furuse *et al.*, 1998) and the stabilization of the replisome (Tittel-Elmer *et al.*, 2009). In order to determine whether the nuclease activity of Mre11 is required for its function in PRR, we compared the relative sensitivity of a nuclease deficient *mre11-3* (125-126$^{HD->LV}$) mutant with the *mre11-3 rev3* double mutant. It should be noted that this nuclease dead mutant is still proficient in allowing the MRX complex to assemble (Bressan *et al.*, 1998) and is much less sensitive to MMS than the *mre11* null mutant (Figure 4.11A). We argue that if the nuclease activity of Mre11 was not required for its function in PRR one would expect to see a synergistic interaction between *mre11-3* and *rev3*. In contrast, the *mre11-3 rev3* double mutant is nearly as sensitive to MMS as the *mre11-3* single mutant (Figure 4.11A), confirming that the nuclease activity of Mre11 is indeed required for its function in TLS.

Sae2 controls the initiation of DNA-end resection in meiotic and mitotic cells and was recently shown to be a DNA endonuclease (Lengsfeld *et al.*, 2007), a function that is

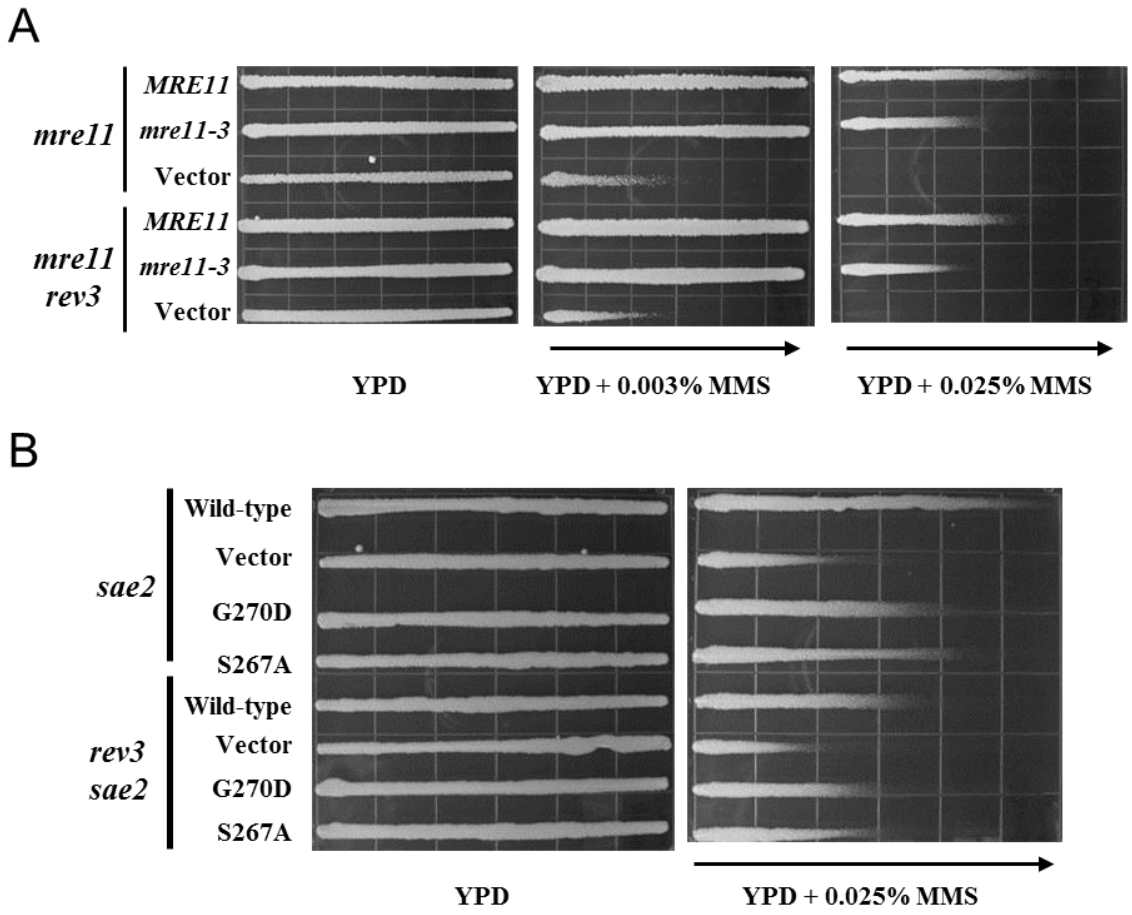

Figure 4.11 – Involvement of Nuclease Activities of Mre11 and Sae2 in TLS. Single and double mutants were transformed with plasmids carrying wild-type, the nuclease/helicase-dead mutations or the vector alone. Overnight cell cultures were imprinted on YPD or YPD + MMS at desired concentrations and incubated at 30 °C for 2 days before being photographed. (A) *mre11*Δ vs. *rev3*Δ, strains are isogenic to DBY747. (B) *sae2*Δ vs. *rev3*Δ, strains are isogenic to BY4741. Results were observed a minimum of three times. Results contributed by Ke Zhang.

abolished by a *sae2-G270D* mutation. Furthermore, it has been reported that a *sae2-S267A* point mutation, which prohibits the Cdc28-dependent phosphorylation of Sae2, displays a phenotype indistinguishable from the *sae2* null mutant (Huertas *et al.*, 2008). We found that *sae2-G270D* and *sae2-S267A* mutants displayed intermediate sensitivity to MMS; when combined with *rev3*, the double mutants were slightly more sensitive to MMS than the *rev3* single mutant (Figure 4.11B), suggesting that these activities are also required for the PRR function.

To determine whether the helicase activity of Sgs1 is important for DSB processing in PRR, we compared wild-type or the helicase-dead (*sgs1-hd*) mutant with *rev3* or the *rev3 sgs1-hd* mutant. As seen in Figure 4.12, the *sgs1-hd* mutant is as sensitive to MMS as the null mutant, and the *rev3 sgs1-hd* double mutant is no more resistant to MMS than the *rev3 sgs1* double mutant, which is consistent with a notion that the Sgs1 helicase activity is required for its function within PRR. The slightly increased sensitivity of *rev3 sgs1-hd* to MMS over the *rev3 sgs1* null mutant is probably due to a dominant-negative effect of Sgs1-hd protein on other pathway(s).

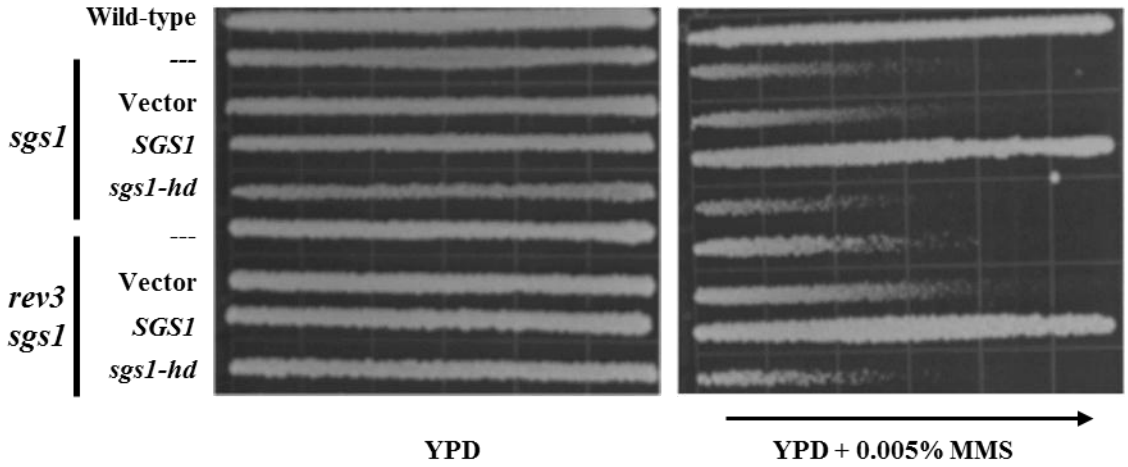

Figure 4.12 – Involvement of the Helicase Activity of Sgs1 in TLS. Single and double mutants were transformed with plasmids carrying wild-type, the nuclease/helicase-dead mutations or the vector alone. Overnight cell cultures were imprinted on YPD or YPD + MMS at desired concentrations and incubated at 30 °C for 2 days before being photographed. *sgs1*Δ vs. *rev3*Δ, strains are isogenic to DBY747. Results were observed a minimum of three times.

4.3.6 – Effects of *mre11*, *sae2*, *exo1*, and *sgs1* on PCNA Ubiquitination

TLS and error-free PRR are achieved by sequential ubiquitination of PCNA in response to DNA damage (Hoege *et al.*, 2002). To investigate how Mre11, Sae2, Exo1 and Sgs1 are involved in PRR, we endeavoured to detect both mono- and polyubiquitinated PCNA. As SUMOylation (SUMO - small ub-like modifier) of PCNA and diubiquitination of PCNA migrate similarly under our experimental conditions we introduced a *siz1* null mutation to our query strains to eliminate SUMOylation of PCNA. Siz1 is a SUMO ligase of the SIZ/PIAS family (Johnson and Gupta, 2001) and a null mutation of *siz1* abolishes SUMOylation of PCNA without affecting PCNA ubiquitination (Stelter and Ulrich, 2003). As seen in Figure 4.13A, SUMOylated PCNA is observed in the absence of MMS treatment (lanes 1 and 3), but it is dependent on the Pol30-K164 residue (lanes 2 and 4), as well as *SIZ1* (lane 5). Upon MMS treatment, the two prominent bands marked as Ub_1 and Ub_2 are deemed to be PCNA mono- and diubiquitinations, respectively, as they were shifted in the lane containing the Pol30-His_7 cell extract (Figure 4.13B, lane cf. lanes 1 and 3), and were abolished in the *pol30-K164R* mutations (lanes 2 and 4). As expected, they were not affected by deletion of *SIZ1* (lane 5) and only the diubiquitinated PCNA was abolished by the *mms2* null mutation (lane 6). We repeatedly observed a drastic decrease in monoubiquitinated PCNA in an *mre11 siz1* mutant compared to the *siz1* and *rad51* null mutants (Figure 4.14, cf. lanes 4, 5 and 8). *rad51* is not expected to alter the ubiquitination state of PCNA as it has only been suggested to function downstream of error-free PRR (Ball *et al.*, 2009). In addition *mre11* appears to reduce the level of detectable diubiquitinated

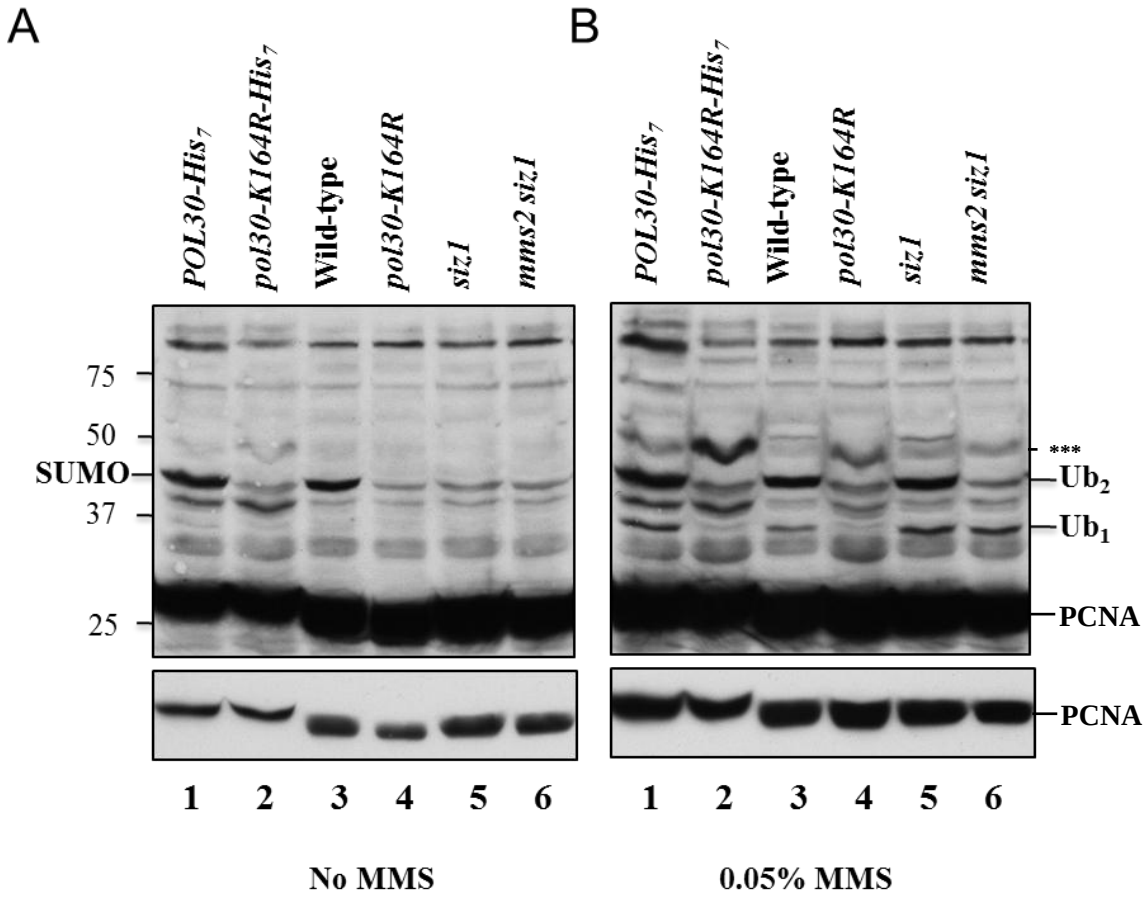

Figure 4.13 – Characterization of Diubiquitinated PCNA. (A) Western blot analysis with extracts from cells without DNA damage treatment. (B) Western blot analysis with extracts from cells treated with 0.05 % MMS for 90 minutes. A *siz1*Δ mutation was used to eliminate SUMOylation of PCNA in order to better detect diubiquitinated PCNA. Cell extracts were prepared as previously described and subject to western blot analyses with an in-house anti-Pol30 monoclonal antibody. Strains used were HK578-10A (wild-type), and its isogenic derivatives WXY994 (*pol30-K164R*), WXY989 (*POL30-HIS*$_7$), WXY990 (*pol30-K164R-His*$_7$), WXY2959 (*siz1*Δ) and WXY2960 (*mms2*Δ *siz1*Δ). Molecular size markers are labeled on left (in kD). Unmodified Pol30 protein is indicated by PCNA, and monoubiquitinated PCNA is indicated by Ub_1 and diubiquitinated PCNA is indicated by Ub_2. *** An unknown band that appears only in a *pol30-K164R* point mutation after MMS treatment, and may represent a different modification of PCNA. The lower box in both Figure A and B resulted from a shorter exposure time of the same western directly above. Results were observed a minimum of three times.

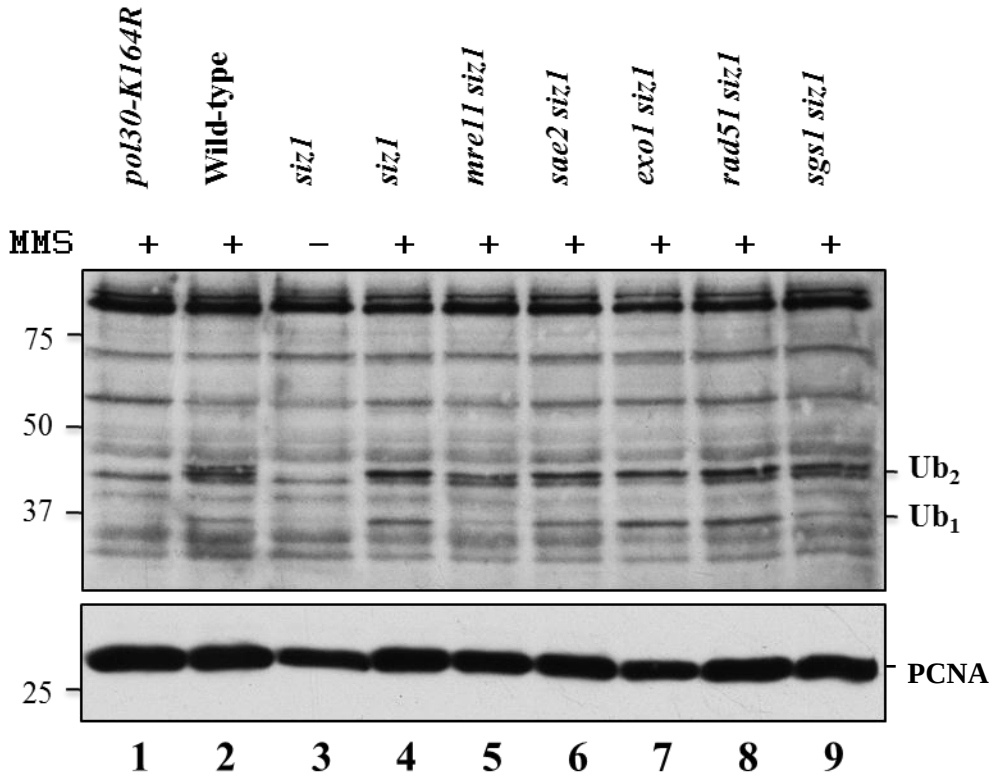

Figure 4.14 – Effects of *mre11, sae2, exo1, rad51* and *sgs1* on MMS-induced Mono- and Diubiquitination of PCNA. Overnight cultures were subcultured and allowed to grow to a cell count of approximately $1x10^7$ cells/mL before being treated with 0.05 % MMS (as indicated) for 90 minutes. Total cell extracts were obtained under denaturing conditions and analysed by SDS-PAGE and western blot. Cell extracts were prepared as previously described and subject to western blot analyses with an in-house anti-Pol30 monoclonal antibody. Strains used were HK578-10A (wild-type) and its isogenic derivatives WXY994 (*pol30-K164R*), WXY2959 (*siz1*Δ), WXY2995 (*mre11*Δ *siz1*Δ), WXY2962 (*sae2*Δ*siz1*Δ), WXY2963 (*exo1*Δ*siz1*Δ), WXY2994 (*rad51*Δ*siz1*Δ) and WXY2969 (*sgs1*Δ*siz1*Δ). Molecular size markers are labeled on left (in kD). Unmodified Pol30 protein is indicated by PCNA, and monoubiquitinated PCNA is indicated by Ub_1 and diubiquitinated PCNA is indicated by Ub_2. The lower box resulted from a shorter exposure time of the same western directly above. Results were observed a minimum of three times.

PCNA (Figure 4.13, lane 5). Although genetic analysis does not clearly assign Sae2 to the error-free or TLS PRR pathway, deletion of *SAE2* appears to decrease monoubiquitinated and possibly diubiquitinated PCNA (Figure 4.14, lane 6), further suggesting Sae2 functions in PRR, primarily in the TLS pathway. Deletion of *exo1* does not affect monoubiquitinated PCNA; however, it does appear to decrease the level of diubiquitinated PCNA (lane 7), lending further support to the notion that Exo1 plays an accessory role in error-free PRR. Finally, deletion of *SGS1* drastically decreases the level of monoubiquitinated PCNA without an apparent impact on diubiquitinated PCNA (lane 9). Collectively, the above observations allow us to conclude that MRX, Sae2 and Exo1 nucleases and the Sgs1 helicase involved in the processing of DSB ends are variably required for PCNA ubiquitination while some of them play multiple roles in PRR.

4.4 – Discussion

Here we report unexpected observations that MRX, Sae2 and Exo1 endo/exonucleases and the Sgs1 helicase are variably involved in the error-prone and error-free branches of PRR. This study gives a greater understanding of how TLS and error-free PRR are co-coordinately operated at the molecular level.

4.4.1 – MRX and Sae2

MRX has been implicated in numerous DNA damage response pathways specifically the processing of DSBs during meiosis and mitosis. It would be highly expected for MRX to play a role downstream of error-free PRR along with other HR

proteins (Ball *et al.*, 2009). However, in addition to its expected genetic interactions with members of error-free PRR, *mrx* mutations are surprisingly epistatic to mutations in the TLS pathway. The involvement of MRX was further confirmed by several observations. First of all, unlike other *HR* genes, none of the *MRX* genes were identified from a conditional synthetic lethal screen using either TLS or error-free PRR pathway mutants as queries, these absent synergistic interactions were later individually confirmed. Secondly, the *pol30-K164R* mutation is epistatic to *mre11*, indicating that the DNA damage tolerance to MMS conferred by the MRX complex is completely dependent on PCNA covalent modifications at the K164 residue. Thirdly, despite numerous roles played by MRX to maintain genomic stability, deletion of *MRE11* does not result in an increased spontaneous mutagenesis in a *trp1-289* reversion assay, which is tailored to base substitutions. This is in sharp contrast to the *hr* mutant *rad51*. Finally, deletion of *MRE11* noticeably reduces levels of both mono- and diubiquitination of PCNA, providing direct physical evidence that the MRX complex is required for both branches of PRR.

Sae2 is considered an accessory factor of the MRX complex during DSB resection. Although *sae2* does not display a clear epistatic relationship with either *mms2* or *rev3*, we argue that this observation is a result of Sae2 being partially required for both PRR pathways. This argument is further supported by several observations. Firstly, although *sae2* is slightly additive to *mms2* or *rev3*, when both *MMS2* and *REV3* are inactivated, further deletion of *SAE2* does not cause increase sensitivity to MMS. Secondly, both *rad18* and *pol30-K164R* are epistatic to *sae2*, indicating that once PCNA

cannot be ubiquitinated, *SAE2* plays no role in the protection of host cells from MMS-induced DNA damage. Thirdly, like *mre11*, the *sae2* mutant does not display an increased spontaneous mutagenesis, consistent with a role in TLS. Fourthly, *sae2* is epistatic to *exo1*, suggesting that Sae2 must play an overlapping role with Exo1 within error-free PRR. Finally, careful examination of PCNA ubiquitination indicates that deletion of *SAE2* partially reduces both mono- and diubiquitinated PCNA, albeit to a lesser extent than *mre11*. These observations are consistent with Sae2 being an accessory protein for MRX within PRR pathways.

4.4.2 – Exo1

The Exo1 exonuclease is also a multi-functional protein. Its involvement in error-free PRR was recently reported by means of epistasis analyses (Tran *et al.*, 2007). Supporting this conclusion was the observation that *exo1* and *rad9* were synergistic (Tran *et al.*, 2007), a characteristic trait of an error-free PRR component (Barbour *et al.*, 2006). We further extend this conclusion by providing additional experimental evidence. Deletion of *EXO1* resulted in a dramatic increase in spontaneous mutations in a *trp1-289* based mutagenesis assay and this increase was largely dependent on the functional *REV3* and due to defective error-free PRR. Remarkably, deletion of *EXO1* specifically compromises the relative level of diubiquitinated PCNA without affecting its monoubiquitination. Hence, Exo1 is exclusively involved in the error-free PRR branch. Given the fact that the *exo1* single mutant barely displays an increased sensitivity to

MMS, we suspect that Exo1 only plays an accessory role in the promotion of error-free PRR.

4.4.3 – Sgs1

It has previously been determined that Sgs1 plays a role downstream of the error-free PRR pathway in resolving the recombination intermediate (Ball *et al.*, 2009). Here we unequivocally demonstrate that Sgs1 also plays a role upstream of TLS. First of all, *sgs1* is completely epistatic to *rev3*, which is unexpected if Sgs1 were only required for the downstream events of error-free PRR. Secondly, deletion of *SGS1* resulted in a spontaneous mutation rate comparable to that of *rev3*, which is in sharp contrast to the fact that *sgs1* causes increased spontaneous gross chromosomal rearrangements (Myung *et al.*, 2001) and overall genomic instability (Chu and Hickson, 2009). Finally, deletion of *SGS1* specifically reduces monoubiquitinated PCNA without apparent alteration of diubiquitinated PCNA. Hence, Sgs1 must play dual roles in both TLS and error-free PRR via two distinct mechanisms.

4.4.4 – Comparison of ssDNA Gap Processing and DSB End Resection

The involvement of MRX, Sae2, Exo1 and Sgs1 in the different modes of PRR is highly surprising and unexpected. When this research was in progress, several laboratories independently reported the differential involvement of the above proteins in the sequential processing of DSB ends (Bonetti et al., 2009; Mimitou and Symington, 2008; Zhu et al., 2008), which shed light on the possible co-ordination of these proteins

in the PRR pathway. We argue that to apply the DSB processing model to PRR, one has to first ask whether the nuclease and helicase activities of the above proteins are required for PRR. Our experimental results, although preliminary, collectively suggest that these enzymatic activities are indeed required for PRR. Secondly, we envisage that the major difference between the DSB model and PRR is that the latter acts on ssDNA gaps. This may not impose a problem since based on the DSB processing model the above enzymes primarily act at the junction of single-double stranded DNA. Thirdly, the long-range DSB end processing model only deals with the 5'-3' resection, whereas it is unclear whether this is the only orientation of processing for PRR. Nevertheless, it is noticed that the Mre11 subunit of MRX possesses a 3'-5' exonuclease activity (Paull and Gellert, 1998), which has not been fully accounted for by the DSB processing model. By our genetic and physical analyses and inference to the DSB processing model, we propose that MRX and its accessory protein Sae2 participate in the initial processing of ssDNA gaps, which is required for efficient PCNA ubiquitination and lesion bypass. In contrast, Sgs1 and Exo1 promote TLS and error-free PRR, respectively, primarily by signalling for, or balancing between, mono- *vs*. polyubiquitination. Of great interest is the division of labour for Sgs1 and Exo1 to modulate the two alternative mechanisms of lesion bypass, whereas in the DSB processing model, the two proteins are known to play overlapping roles for long-range 5'-3' resection (Bonetti et al., 2009; Mimitou and Symington, 2008; Zhu et al., 2008); however, their division of labour at the molecular level is unclear to date. A working model of PRR based on previous reports and the above analyses is presented in Figure 4.15. Based on this model, we hypothesize the MRX complex functions upstream

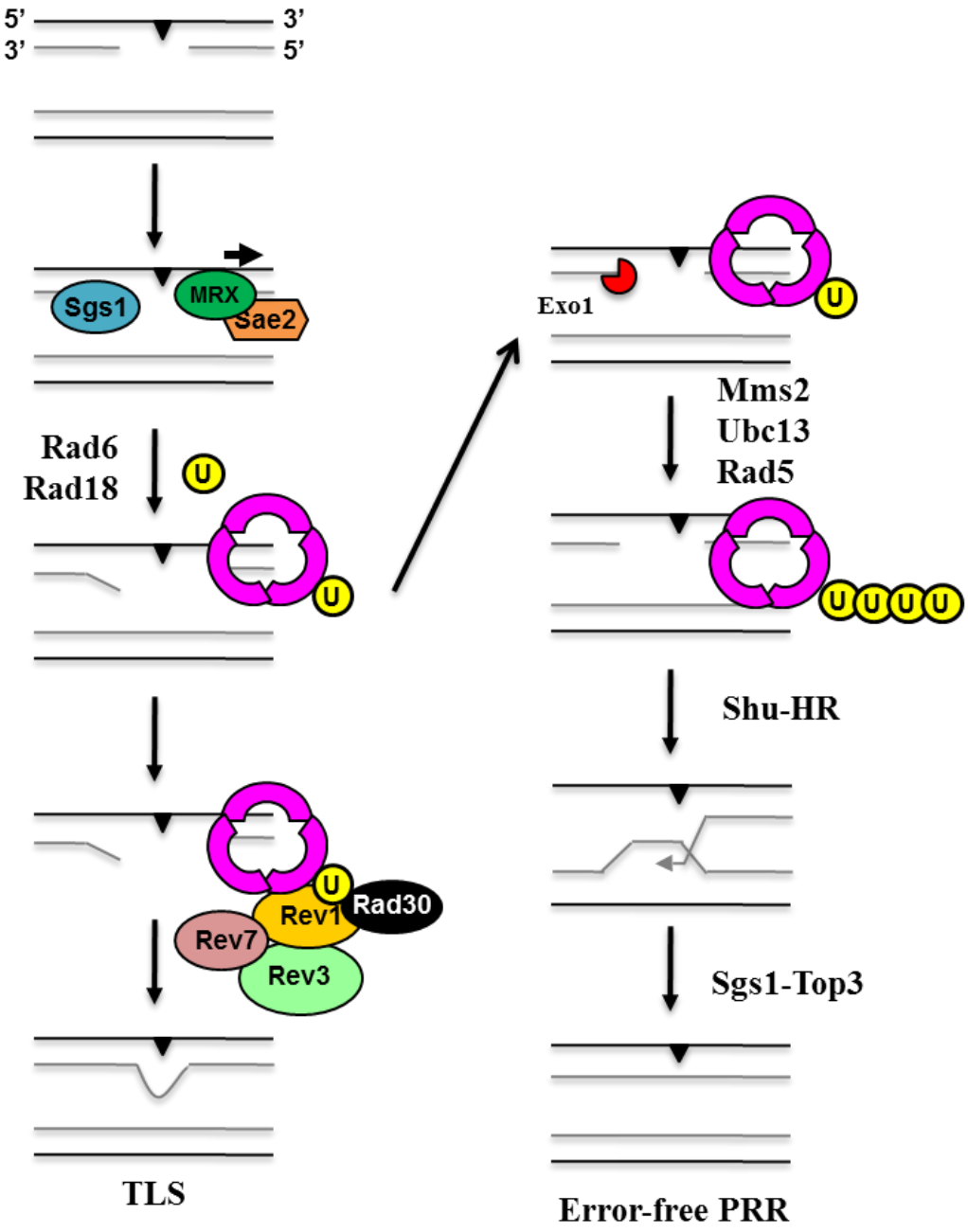

Figure 4.15 – Proposed Working Model for the Budding Yeast PRR Pathways. MRX in conjunction with Sae2 function upstream of PCNA monoubiquitination by ssDNA resection thus promoting Rad6-Rad18 to monoubiquitinate PCNA. Sgs1 is also required for Rad6-Rad18 mediated PCNA monoubiquitination, which allows for TLS in the presence of Polζ (Rev3 + Rev7) and Rev1. Exo1 processes ssDNA gaps at the 5'-3' direction, which facilitates PCNA polyubiquitination by Rad5-Ubc13-Mms2 and subsequent error-free lesion bypass mediated by the Shu complex, HR and Sgs1-Top3 resolution.

of PCNA to resect ssDNA at the stalled replication fork. Sae2 may facilitate MRX activity by removing DNA-binding proteins (Hartsuiker *et al.*, 2009) or secondary structures (Lengsfeld *et al.*, 2007). The resulting ssDNA may recruit RPA and lead to the recruitment of Rad6-Rad18 (Davies *et al.*, 2008), which, in conjunction with Sgs1, monoubiquitinates PCNA for efficient lesion bypass via TLS. On the other hand, the 5'-3' exonuclease activity of Exo1 causes further strand resection that favours the recruitment of Rad5-Ubc13-Mms2 to polyubiquitinate PCNA and allows for error-free PRR lesion bypass via the Shu complex, HR and Sgs1-Top3. As all the genes described in this report are conserved in eukaryotes, from yeast to human, it would be of great interest to determine if the same regulatory mechanisms occur in higher eukaryotes.

CHAPTER FIVE

THE HELICASE ACTIVITY OF Rad5 IS REQUIRED FOR ERROR-FREE POSTREPLICATION REPAIR

5.1 – Abstract

DNA postreplication repair (PRR) functions to bypass replication-blocking lesions and is subdivided into two parallel pathways: error-prone translesion synthesis (TLS) and error-free PRR. While both pathways are dependent on the ubiquitination of PCNA, error-free PRR utilizes non-canonical K63-linked polyubiquitinated PCNA to signal lesion bypass through template switching, a process thought to be dependent on Mms2-Ubc13 and a RING finger motif of the Rad5 Ub-ligase. Previous *in vitro* studies demonstrated the ability of Rad5 to promote replication fork regression, a function dependent on its helicase activity. To investigate the genetic and mechanistic relationship between fork regression and template switch, we created and characterized site-specific mutants defective in the Rad5 RING finger and/or helicase activity. Our results indicate that both the Rad5 Ub-ligase and the helicase activities are exclusively involved in error-free PRR. To our surprise, lack of the Rad5 helicase activity abolishes the K63-linked PCNA polyubiquitin chain assembly. Thereby suggesting that the Rad5 helicase activity functions upstream of Mms2-Ubc13-Rad5 assembly and PCNA polyubiquitination.

5.2 – Introduction

In addition to mechanisms that cells possess to remove DNA damage, they also possess the ability to bypass replication-blocking lesions. In *S. cerevisiae* this mechanism is termed PRR, which is mediated by the *RAD6* epistasis group of genes. PRR can be divided into two parallel pathways; the error-prone TLS pathway and the error-free PRR pathway. The stable complex formed between Rad6-Rad18 (Bailly *et al.*, 1994) is known to monoubiquitinate the *RAD30* gene product PCNA (Hoege *et al.*, 2002). The monoubiquitination of PCNA at K164 allows for TLS lesion bypass that requires a Y-family of polymerases Rev1 and a B-family polymerase Polζ, consisting of Rev3 and Rev7 (Nelson et al., 1996a, b). Inactivation of the TLS pathway abolishes DNA damage-induced mutagenesis and a moderate increase in the sensitivity to DNA-damaging agents (Lawrence, 2004).

Genetic characterization of the *mms2* null mutant demonstrated the existence of the error-free PRR branch (Broomfield et al., 1998; Xiao et al., 1999). *mms2* displays strong synergistic interaction with *rev3* and *REV3*-dependent increase in spontaneous mutagenesis. Although Mms2 encodes a Ubc-like protein it does not contain an active-site Cys residue essential for a Ub-conjugating enzyme (Ubc or E2). It turned out that Mms2 forms a stable complex with Ubc13 to promote non-canonical Lys63-linked polyubiquitination (Hofmann and Pickart, 1999) and that error-free PRR is dependent on the K63-linked polyubiquitination of PCNA by Mms2-Ubc13 and an E3 Ub-ligase Rad5

(Hoege *et al.*, 2002). Although *ubc13* is epistatic to *mms2* and they share all characteristic phenotypes (Brusky *et al.*, 2000), Rad5 appears to have additional activities.

Rad5 is a multifunctional protein known to prevent non-homologous end-joining (Ahne et al., 1997), promote instability of simple repetitive sequences (Johnson et al., 1992) and repair DNA DSBs (Chen et al., 2005). Rad5 is also implicated in the repair of DNA minor groove adducts in association with NER (Kiakos et al., 2002) and a potential role in TLS (Pages *et al.*, 2008a). Indeed, the *rad5* mutant is much more sensitive to killing by DNA-damaging agents than the *mms2/ubc13* mutants, particularly ionizing radiations (Friedl *et al.*, 2001), and demonstrates elevated rates of spontaneous mitotic recombination as well as GCR (Liefshitz et al., 1998; Smith et al., 2004). The current working model suggests that Rad5 interacts with Ubc13 (Ulrich and Jentsch, 2000) through its RING finger motif (Ulrich, 2003) and recruits Mms2-Ubc13 in close proximity to monoubiquitinated PCNA through its association with and PCNA (Hoege et al., 2002) and Rad18 (Ulrich and Jentsch, 2000), which facilitates the sequential polyubiquitination of PCNA. In addition to E3 Ub-ligase activity, Rad5 also contains a conserved helicase-like domain of the SWI/SNF family of ATPases (Johnson et al., 1992; Johnson et al., 1994). Previous *in vitro* experiments demonstrated the ability of Rad5 to promote replication fork regression, a function dependent on its helicase activity (Blastyak et al., 2007). However, there are two possible competing modes for error-free lesion bypass, namely replication fork regression and template switching (Figure 1.4), both gained recent experimental support (Ball et al., 2009; Blastyak et al., 2007). However, it remains plausible that fork regression followed by sister chromatid invasion

and resolution may allow for error-free bypass. Alternatively, error-free PRR may employ two parallel modes of lesion bypass. Furthermore, it is unclear whether Rad5-mediated fork regression promotes one or both error-prone and error-free pathways of lesion bypass. In order to address the above questions, yeast strains were created to characterize the *rad5* mutants defective in either RING finger and/or the DNA helicase activity. Genetic analyses clearly demonstrate that both the Rad5 E3 and helicase activities are exclusively involved in error-free PRR and their mutations are epistatic, indicating that the two activities act sequentially. Furthermore, lack of either one of these Rad5 functions abolishes the PCNA polyubiquitination chain formation, suggesting that the Rad5 helicase activity is required upstream of PCNA polyubiquitination.

5.3 – Results

5.3.1 – Experimental Design and Rationale

While molecular mechanisms of translesion DNA synthesis have been well characterized in recent years, little is known about the detailed molecular events leading to the error-free PRR in eukaryotes, despite the fact that two models of error-free lesion bypass, namely the template switch and the replication fork regression, have been proposed for many years (Broomfield et al., 2001). Recently, we provided experimental evidence suggesting that the HR machinery acts downstream of PCNA polyubiquitination to mediate error-free PRR (Chapter 3) (Ball et al., 2009), which favours the template switch model. Meanwhile, it was reported that Rad5 possesses a

helicase activity required for the fork reversal *in vitro* (Blastyak et al., 2007), which supports the fork regression model of error-free PRR.

It has been well established that the E2 complex Ubc13-Mms2 and the E3 protein Rad5 are required for the non-canonical K63-linked polyubiquitination of PCNA, which leads to the error-free mode of PRR (Hoege et al., 2002). However, unlike Ubc13 and Mms2, which are exclusively involved in the above E2 activity and error-free PRR, Rad5 has been implicated in several DNA repair/damage tolerance pathways. Indeed, although *rad5* is epistatic to *ubc13/mms2* (Ulrich and Jentsch, 2000), the *rad5* mutant is much more sensitive to DNA-damaging agents than the *ubc13* or *mms2* mutant (Xiao et al., 2000). Rad5 is a rather large protein and contains several putative functional domains (Figure 5.1). We reasoned that if the Rad5 RING finger E3 activity is required for PCNA polyubiquitination together with Ubc13-Mms2, this activity will be involved in signalling for the template switch. Meanwhile, if the Rad5 helicase activity acts in the same pathway as PCNA polyubiquitination, the helicase- and RING- (or *mms2/ubc13*) mutations will be epistatic. Alternative, if Rad5-mediated fork regression and PCNA polyubiquitination-mediated template switch constitute two means of lesion bypass, the above mutations will be additive or synergistic with respect to killing by DNA-damaging agents. Experiments were designed to critically test the above two hypotheses.

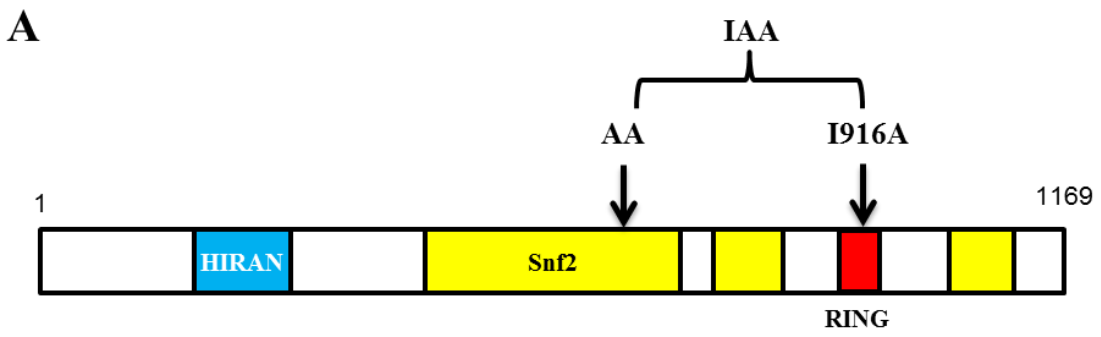

Figure 5.1 – A Schematic Representation of the Rad5 Domains in Budding Yeast *S. cerevisiae* and the Point Mutations Used in this Study.

5.3.2 – The Rad5 Helicase Mutation is Epistatic to the Rad5 RING Finger Mutation

To ask whether the Rad5 E3 activity is mediated by its RING finger motif, we initially created a *rad5-C914S* mutation known to inactivate its RING finger activity. Unfortunately, this mutant is much more sensitive to killing by MMS than *mms2* or *ubc13*, although it is epistatic to *mms2* (data not shown), suggesting that the *rad5-C914S* mutation affects other Rad5 functions, most likely its proper folding and/or stability. It was reported (Ulrich, 2003) that an adjacent *rad5-I916A* mutation abolished its interaction with Ubc13 and that cells carrying this mutation are epistatic to and indistinguishable from *ubc13*. Hence we created the same mutation and examined its genetic interaction with the *rad5-AA* mutation defective in the helicase activity (Blastyak et al., 2007).

A gradient plate assay (Figure 5.2A) shows the *rad5-AA* mutant is slightly more sensitive to MMS than the *rad5-I916A* mutant; nevertheless, the *rad5-IAA* double mutant is as sensitive to MMS as the *rad5-AA* single mutant, suggesting that the two Rad5 activities function in the same pathway. This observation was further confirmed by a quantitative killing experiment (Figure 5.2B), in which the *rad5-IAA* double mutant is as sensitive to MMS as the *rad5-AA* single mutant, clearly demonstrating that the double mutant displays a similar phenotype to the single mutant of *rad5-AA*. Furthermore, the *rad5-IAA* double mutant is no more sensitive than the *rad5-AA* single mutant to killing induced by UV irradiation (Figure 5.2C), indicating that the two Rad5 activities function in the same pathway.

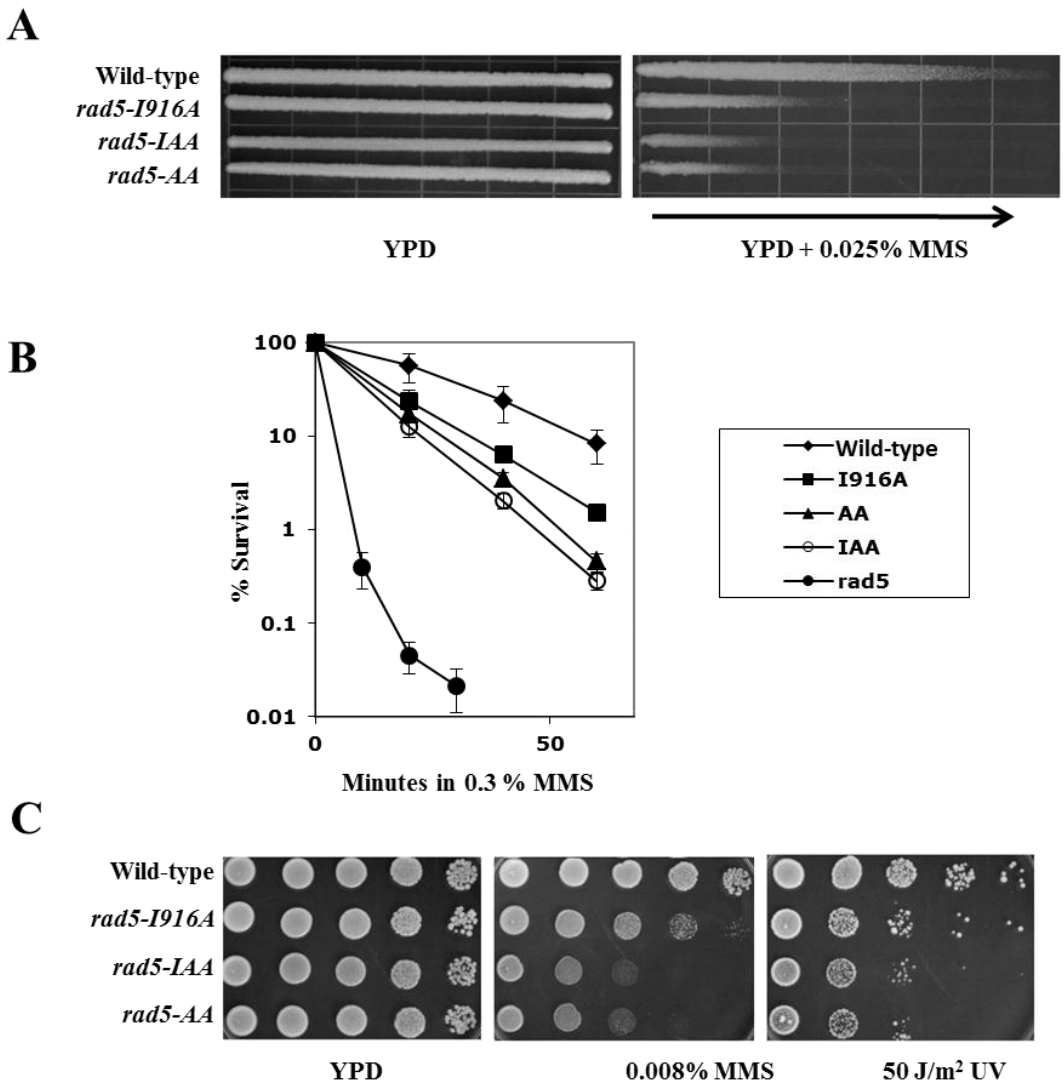

Figure 5.2 – The *rad5-AA* Mutation Displays a Similar Phenotype to the *rad5-IAA* Mutation. (A) A gradient plate assay demonstrating an epistatic relationship between *rad5-AA* and *rad5-I916A.* The gradient plate assay was performed as previously described and the plates were incubated for 2 days at 30ºC before being photographed. The arrow indicates the increasing concentration of MMS. Results were observed a minimum of three times. (B) A liquid killing experiment for the relative sensitivity to MMS. Results are the average of four independent experiments with standard deviations shown as error-bars. (C) A serial dilution assay to compare the relative sensitivity of wild-type (WT) and *rad5* mutants to MMS and UV irradiation. All strains are isogenic to HK578-10A (WT); HK578-2C (*rad5*Δ), WXY3001 (*rad5-I916A*), WXY2981 (*rad5-AA*), and WXY2982 (*rad5-AA*). Results were observed a minimum of three times. Figure 5.2B and 5.2C were completed in collaboration with Amanda Lambrecht.

5.3.3 – The Rad5 Helicase Activity is Exclusively Involved in the Error-Free PRR Pathway

During the above studies, we noticed that the *rad5-AA* mutant is more sensitive to MMS and UV-induced killing than the *rad5-I916A* mutant (Figure 5.2A, B, C), which can be explained by one of two possibilities: either the *rad5-I916A* mutation does not completely abolish its RING finger activity or the Rad5 helicase has functions beyond that of error-free PRR. To address the first possibility, we examined genetic interactions between *rad5-I916A* and *mms2*. As seen in Figure 5.3A, the *rad5-I916A* mutant is noticeably less sensitive to killing by MMS than the *mms2* mutant. Since Mms2 and Ubc13 are absolutely required for PCNA polyubiquitination and error-free PRR, and this function requires the Rad5 RING finger activity, we infer that the *rad5-I916A* point mutation may not completely abolish its RING finger E3 function. Nevertheless, the *mms2 rad5-I916A* double mutant is as sensitive to MMS as the *mms2* single mutant, and the *rev3 rad5-I916A* double mutant displays an extreme sensitivity to MMS (Figure 5.3A). These results reaffirm the exclusive role of Rad5 RING finger domain in error-free PRR.

To ask whether the Rad5 helicase activity is exclusively involved in error-free PRR, we examined genetic interactions between the Rad5 helicase function and both branches of PRR. It has been previously reported that the *rad5-AA* mutant is as sensitive to killing by UV as the *mms2* null mutant (Gangavarapu *et al.*, 2006). As seen in Figure 5.3B, the *rad5-AA* single mutant is as sensitive to MMS as the *mms2* mutant, and more importantly the corresponding double mutant is still as sensitive to MMS as the *rad5-AA*

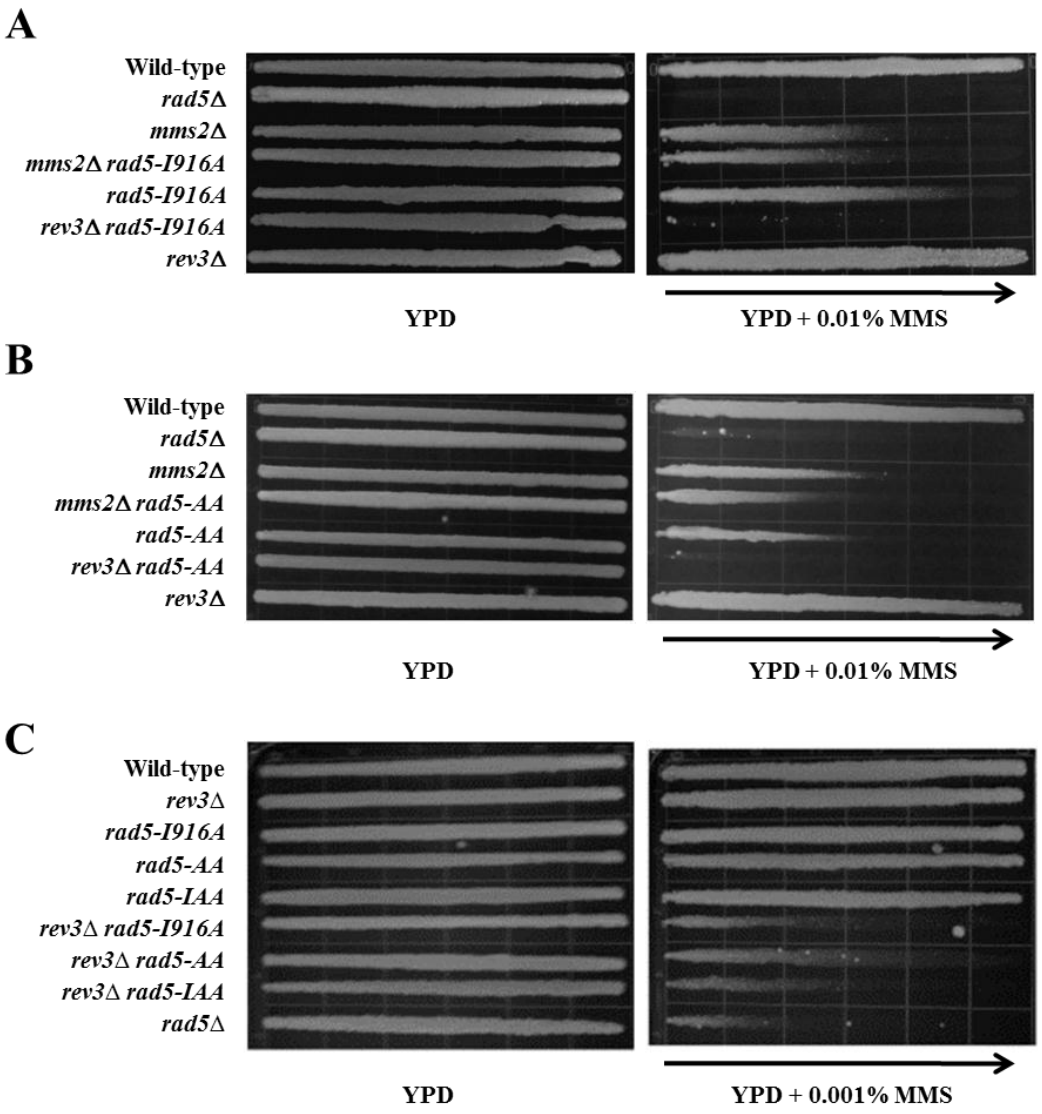

Figure 5.3 – Gradient Plate Assays to Assess Genetic Interactions Between *rad* Mutations and Error-Free PRR or Error-Prone TLS. (A) *mms2*Δ is epistatic to the *rad5-I916A* point mutation. (B) *mms2*Δ is epistatic to the *rad5-AA* point mutation. (C) Both *rad5-AA* and *rad5-I196A* point mutations are synergistic with *rev3*. The gradient plate assay was performed as previously described and the plates were incubated for 2 days at 30ºC before being photographed. The arrow indicates the increasing concentration of MMS. All strains used were isogenic to HK578-10A (WT), HK578-2C (*rad5*Δ), WXY901 (*mms2*Δ), WXY2998 (*rad5-AA mms2*Δ), WXY2981 (*rad5-AA*), WXY2996 (*rad5-AA rev3*Δ), WXY956 (*rev3*Δ), WXY3002 (*rad5-I916A mms2*Δ), and WXY2983 (*rad5-I916A rev3*Δ). Results were observed a minimum of three times.

or *mms2* single mutant, indicating that the two mutations are epistatic to each other. In sharp contrast, the *rad5-AA rev3* double mutant is extremely sensitive to MMS, and the genetic interaction is clearly synergistic, reminiscent of the *rad5-I916A rev3* or *mms2 rev3* double mutant (Figure 5.2C). The above observations suggest that the Rad5 helicase activity functions exclusively in the error-free branch of PRR and in the same pathway as Mms2.

A hallmark of faulty error-free PRR is an elevated spontaneous mutagenesis (Broomfield *et al.*, 1998). To ask whether the Rad5 helicase and RING finger activities inherit all error-free PRR functions within Rad5, we compared the spontaneous mutation rates of the above site-specific mutants with that of the *rad5* null mutant. This *trp1-289* reversion assay is particularly sensitive to error-free PRR defect, which channels replication-blocking lesions to Polζ-mediated translesion synthesis. As seen in Table 5.1, both *rad5-AA* and *rad5-I916A* mutants display strongly elevated spontaneous mutation rates, which are slightly higher than that of the *rad5* null mutant. Interestingly, the *rad5-IAA* double mutant has an elevated spontaneous mutation rate comparable to that of corresponding single mutant, once again confirming that the two activities represented by each mutation function in the same error-free PRR pathway.

Table 5.1 – *S. cerevisiae* Spontaneous Mutation Rates to Examine the *rad5* point mutations

Strain[a]	Key alleles	Rate (x 10^{-8})[b]	Fold[c]
DBY747	Wild-type	0.15 ± 0.07	1
WXY731	*rad5* Δ	1.61 ± 0.51	10.7
WXY2900	*rad5-AA*	2.24 ± 0.38	14.9
WXY2990	*rad5-IAA*	2.09 ± 0.05	13.9
WXY2974	*rad5-I916A*	1.90 ± 0.15	12.7

a. All strains are isogenic derivatives of DBY747.

b. The spontaneous mutation rates are the average of at least three independent experiments with standar deviation.

c. Relative to the wild-type mutation rate.

Results are courtesy of Michelle Hanna.

5.3.4 – The Rad5 Helicase Domain is Required for the Polyubiquitination of PCNA

After establishing that the *rad5-AA* mutation is specifically defective in the error-free PRR, we wished to investigate the molecular mechanism(s) by which this helicase activity is involved in the error-free lesion bypass. It is well established that Ubc13, Mms2 and Rad5 are required for PCNA polyubiquitination and the subsequent error-free lesion bypass. The current model predicts that the Rad5 RING finger motif is required for the E3 activity and hence the *rad5-I916A* mutation will affect PCNA polyubiquitination. On the other hand, it is unclear if the Rad5 helicase activity acts upstream or downstream of PCNA polyubiquitination. To critically address the above issue, we raised polyclonal antibodies against purified Pol30 expressed from bacterial cells, and further screened for monoclonal antibodies. Subsequently we verified our antibody for its ability to detect both mono- and diubiquitinated PCNA (as demonstrated in Chapter 3)(Ball *et al.*, 2009). Furthermore, we were able to verify monoubiquitinated PCNA following MMS treatment in wild-type yeast whole cell extracts without the need for His_n-affinity purification (Figure 5.4 lanes 2 and 3). Notably this modification is absent in a strain containing the *pol30-K164R* point mutation (cf. lanes 1 and 2, 3 and 4). The predicted PCNA-Ub band is slightly shifted up in the strain containing the Pol30-His_7 allele compared to the native Pol30 allele (cf. lanes 2 and 3), further confirming that this band contains modified PCNA. As PCNA sumoylation and diubiquitination at the K164 residue co-migrate under our experimental conditions we introduced a *siz1* null mutation to our query strains to eliminate this PCNA sumoylation. Siz1 is a SUMO ligase of the SIZ/PIAS family (Johnson and Gupta, 2001)

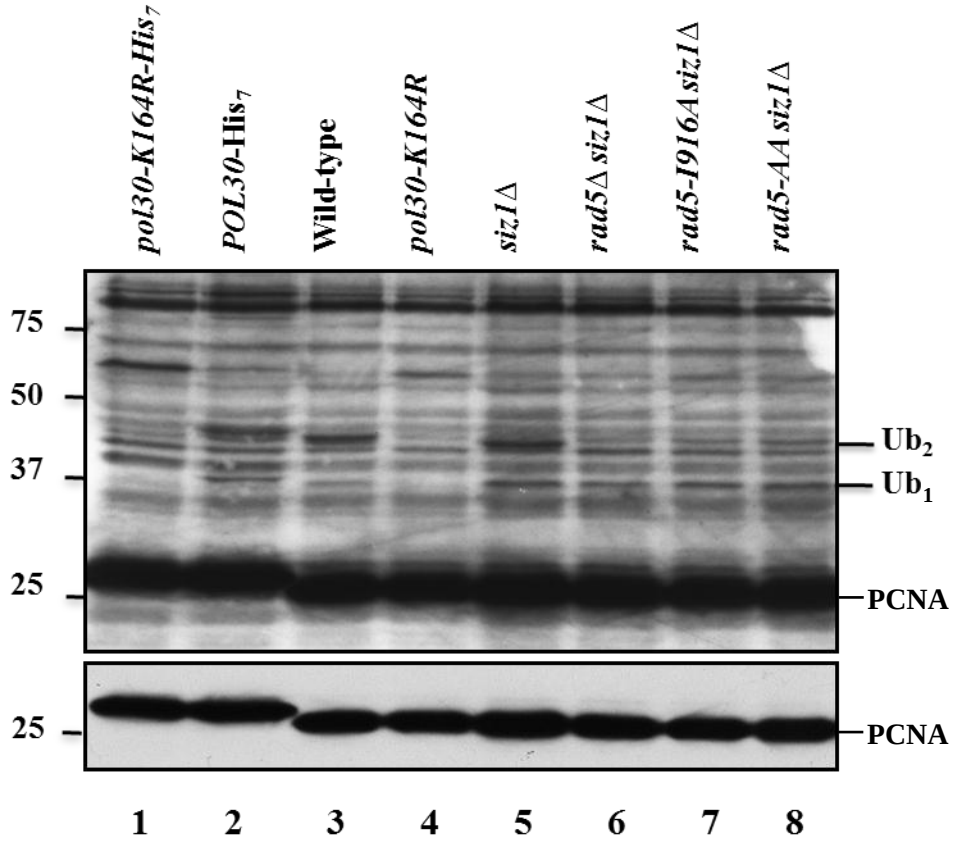

Figure 5.4 – The Effects of *rad5* Mutations on PCNA Ubiquitination. A PCNA ubiquitination assay showing mono- and diubiquitinations. Overnight cultures were subcultured and allowed to grow to a cell count of approximately $1x10^7$ cells/mL before being treated with 0.05% MMS for 90 minutes before harvesting proteins under denaturing conditions. Proteins were separated on an SDS-page gel and PCNA was identified by an anti-PCNA western blot. Molecular size markers are labeled on left (in kD) and monoubiquitinated and diubiquitinated PCNA are labeled on the right as Ub_1 and Ub_2, respectively. Unmodified Pol30 protein is indicated by PCNA. A short exposure of the same blot is shown in the lower panel. The blot containing cells extracts from untreated cells and other control blots to identify mono- and diubiquitinated PCNA bands are shown in Chapter 3. Strains used are isogenic to HK578-10A (WT), WXY994 (*pol30-K164R*), WXY989 (*pol30-His*$_7$), WXY990 (*pol30-K164R-His*$_7$), WXY2959 (*siz1*Δ), WXY2964 (*rad5*Δ *siz1*Δ), WXY2965 (*rad5-AA siz1*Δ), WXY2966 (*rad5-I916A siz1*Δ), HK578-2C (*rad5*Δ), WXY3001 (*rad5-I916A*), WXY2981 (*rad5-AA*). Results were observed a minimum of three times.

and thus a null mutation of *siz1* abolishes sumoylation of PCNA without affecting its ubiquitination (lane 5) (Stelter and Ulrich, 2003). As expected, a prominent Pol30-K164 dependent and *SIZ1*-independent band is noticed in the *siz1*Δ mutant (lane 5) but is absent in the *rad5*Δ*siz1*Δ double mutant (lane 6), which was also shifted in the Pol30-His7 allele (lane 2). This band was deemed to be diubiquitinated PCNA by this and other experimental observations (data not shown), which allowed us to examine the role of Rad5 RING finger and helicase motifs in DNA damage-induced PCNA polyubiquitination. As seen in Figure 5.4, while *rad5-I916A* (lane 7) and *rad5-AA* (lane 8) point mutations do not affect PCNA monoubiquitination, they both reduced (or eliminated) PCNA diubiquitination to the level indistinguishable from that of *rad5*Δ (lane 6). These observations indicate that both the RING finger and the helicase motifs are required for PCNA polyubiquitination.

5.3.5 – Suppression of *rad5* Mutations by *siz1*

It has been previously reported that the *siz1* mutation suppresses the severe DNA damage sensitivity phenotypes of *rad6* and *rad18* (Stelter and Ulrich, 2003). During the process of validating *rad5* and *siz1* mutant strains, we noticed that deletion of *SIZ1* also partially suppresses the *rad5* null mutant sensitivity to MMS (Figure 5.5). More interestingly, deletion of *SIZ1* brings *rad5-AA* and *rad5-I916A* point mutants to the same level of MMS sensitivity, although the two single mutants display different levels of MMS sensitivity (Figure 5.5). This observation further reinforces the notion that the

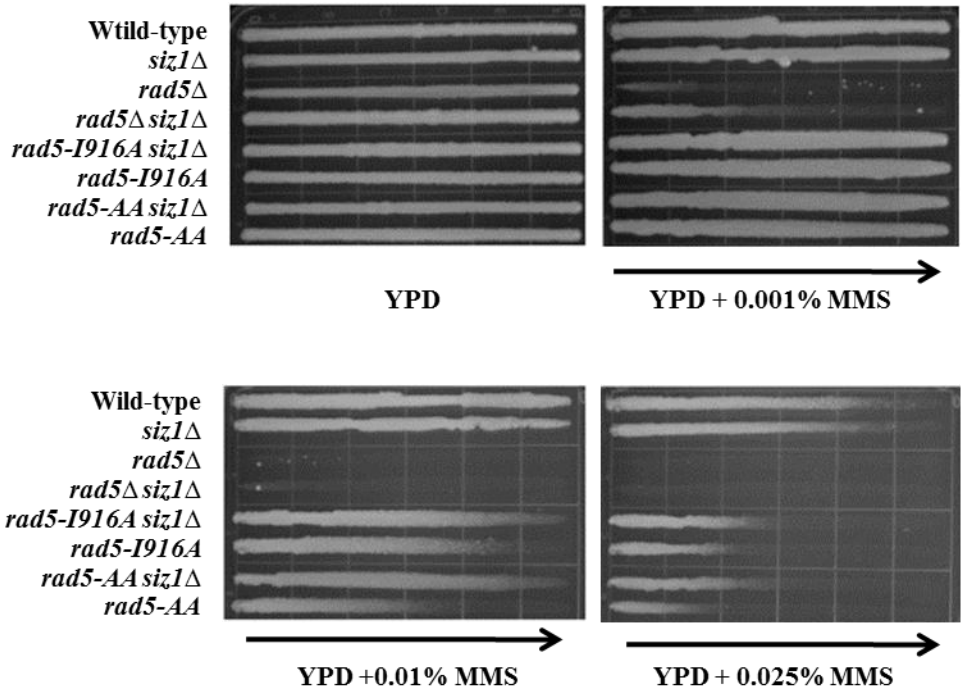

Figure 5.5 – Relative Sensitivity of the Strains Used in Figure 5.4 to Killing by MMS in a Gradient Plate Assay. Note that the *siz1* null mutation partially suppresses *rad5*Δ, *rad5-AA* and *rad5-I916A* sensitivity. The gradient plate assay was performed as previously described and the plates were incubated for 2 days at 30ºC before being photographed. The arrows indicate the increasing concentration of MMS. Strains used were isogenic to HK578-10A (wild-type), WXY2959 (*siz1*Δ), WXY2964 (*rad5*Δ *siz1*Δ), WXY2965 (*rad5-AA siz1*Δ), WXY2966 (*rad5-I916A siz1*Δ), HK578-2C (*rad5*Δ), WXY3001 (*rad5-I916A*), WXY2981 (*rad5-AA*). Results were observed a minimum of three times.

Rad5 RING finger E3 activity and helicase activity act in the same damage tolerance pathway.

5.4 - Discussion

Although it is well accepted that Rad5-Ubc13-Mms2 mediated PCNA polyubiquitination results in error-free PRR (Hoege *et al.*, 2002) the exact mechanism for the error-free lesion bypass is unclear. Historically two possible models have been proposed for error-free lesion bypass, namely replication fork regression (the chicken-foot model) and template switching (Broomfield *et al.*, 2001). Template switching would involve homologous sister chromatid invasion, high-fidelity DNA synthesis and Holliday junction resolution. Initial support for this model came from visualization of Holliday junctions, which were enhanced in temperature-sensitive DNA Polα and ζ mutants held at the restrictive temperature (Zou and Rothstein, 1997). Recently, template switching was characterized as an X-shaped replication intermediate in a 2-D gel electrophoresis assay (Branzei *et al.*, 2008; Minca and Kowalski, 2010). In addition, we recently demonstrated that error-free PRR does employ template switching via Ubc13-Mms2 and PCNA polyubiquitination, homologous recombination and Sgs1-Top3 resolution to bypass replication blocking lesions that arise during S-phase (Chapter 3) (Ball *et al.*, 2009). Meanwhile, a report by Blastyak *et al.* demonstrated *in vitro* that Rad5, through its intrinsic ATPase/helicase activity, promotes replication fork regression (Blastyak *et al.*, 2007). In this report, we examined the two competing models based on the *rad5* point mutations that specifically inactivate either the helicase or the RING finger activity. If the

two modes of error-free PRR functions separately, the *rad5* RING finger and helicase double mutant would display an additive or synergistic effect. Alternatively, if the two activities function in the same pathway, the *rad5* double mutant would be as sensitive to DNA damage as one of the single mutants. We found that both *rad5-I916A* and *rad5-AA* mutations exclusively affect error-free PRR and are synergistic to the TLS mutation. Furthermore, they are epistatic to each other and to the *mms2* mutation. Hence, our experimental results collectively support the latter prediction and confirm that the Rad5 helicase activity and PCNA polyubiquitination act sequentially for the error-free lesion bypass.

Based on the above observations and their enzymatic activities, the simplest model for error-free PRR would be; fork regression, PCNA polyubiquitination by Mms-Ubc13-Rad5 followed by sister chromatid invasion, synthesis and resolution (Figure 5.6). However, this model predicts that the fork regression event promotes, but may not be absolutely required for the strand invasion, yet the *rad5-AA* mutant is as sensitive to UV (Gangavarapu *et al.*, 2006) and MMS as the *mms2* mutant. In addition, to our complete surprise, the *rad5-AA* mutation actually reduced PCNA polyubiquitination to the same extend as the *rad5-I916A* mutation, suggesting that the helicase activity acts upstream of PCNA polyubiquitination. Nevertheless, the above observations suggest that the Rad5 "helicase motif" may play dual roles within error-free PRR, namely fork regression and the E2-E3 complex assembly.

It was noticed that a previous report by Chen *et al.* (Chen *et al.*, 2005) concluded that polyubiquitination of PCNA does not require the ATPase activity of Rad5. We also

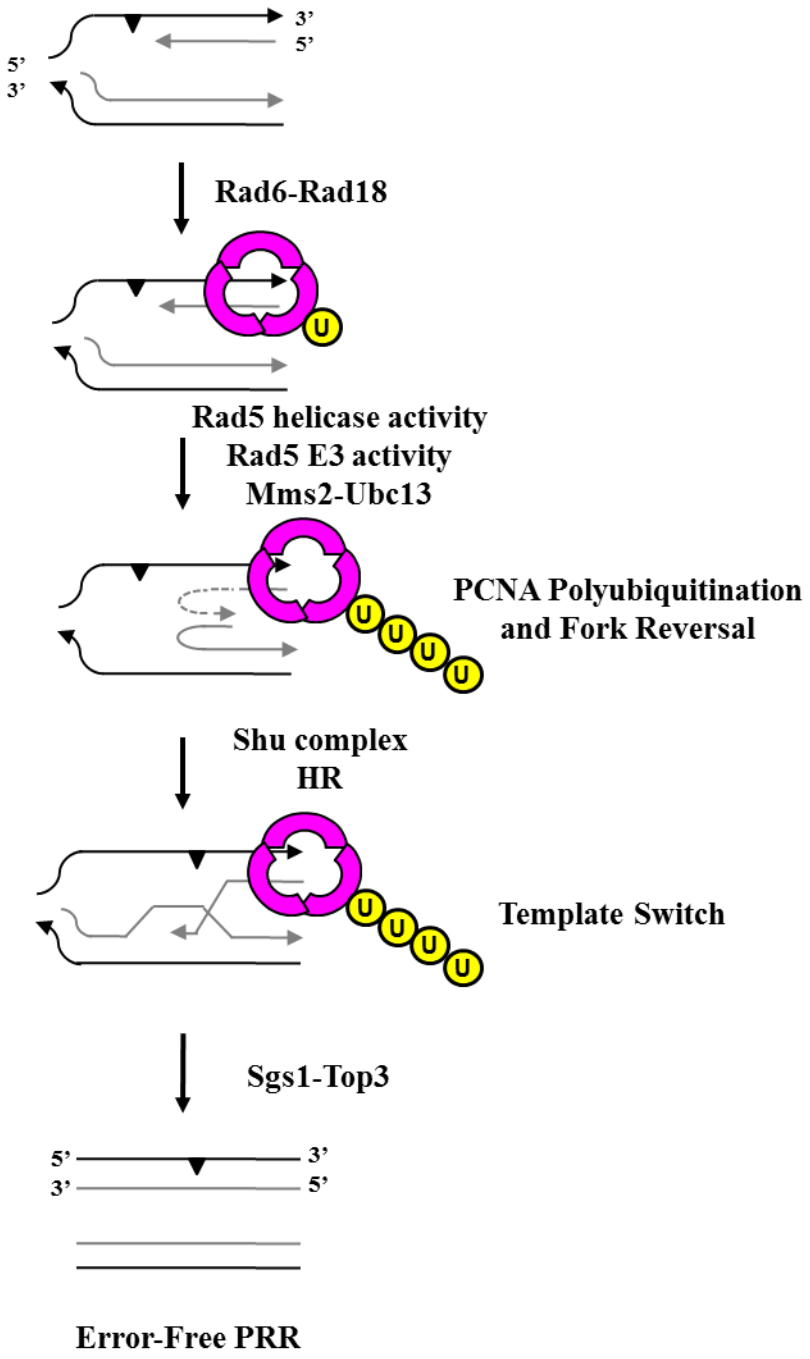

Figure 5.6 – A Proposed Working Model Depicting the Budding Yeast Error-Free PRR Pathway. Our results suggest that for error-free PRR the Rad5 helicase activity functions upstream of Mms2-Ubc13-Rad5 assembly and PCNA polyubiquitination. Following polyubiquitination of PCNA the Shu complex is thought to couple error-free PRR to HR for sister chromatid invasion, synthesis and resolution by Sgs1-Top3, thus completing error-free PRR and lesion bypass.

noticed that a recent report by Minca and Kowalski (Minca and Kowalski, 2010) found an additive effect between *rad5* RING finger mutation and the ATPase mutation. In both cases, the authors characterized a *rad5-KT538A,539AA* (GAA) mutation within a presumed "GKT" ATP-binding motif. Although these point mutations have been previously described to abolish all ATP-binding and hydrolytic activities of Rad5 (Davies *et al.*, 1998; Pause and Sonenberg, 1992; Richmond and Peterson, 1996), a subsequent report demonstrated that it is the *rad5-DE681,682AA* (AA) mutation that biochemically abolishes the ATPase activity of Rad5 in an *in vitro* assay (Gangavarapu *et al.*, 2006). The same *rad5-AA* mutation was found to abolish the fork regression helicase activity *in vitro* (Blastyak *et al.*, 2007) and was employed in this *in vivo* study. In addition, the *rad5-K538A* mutation confers much less sensitivity to DNA-damaging agents than *mms2* or *rad5-AA*, and does not have a clear synergistic effect with TLS mutations (data not shown), indicating that mutations at the Rad5 GKT motif are more complicated than we previously thought, and hence may not represent a true ATPase/helicase dead mutation. Alternatively, the ATPase activity conferred by the Rad5 GKT motif may not be required for its helicase activity as defined by Blastyak *et al*. (Blastyak *et al.*, 2007). Nonetheless, our results clearly suggest that the Rad5 helicase activity functions upstream of Mms2-Ubc13-Rad5 assembly and PCNA polyubiquitination to allow for lesion bypass.

CHAPTER 6

CONCLUSIONS AND FUTURE DIRECTIONS

6.1 – Conclusions

Overall, the purpose of this study was to identify novel genes and proteins involved in the PRR pathways. By initiating this study with a large-scale genomic SGA screen of all the non-essential genes in the *S. cerevisiae* genome, I believe that I was able to accomplish this task. The result is a new working model depicting the budding yeast DNA damage tolerance pathways (Figure 6.1). The new PRR model now begins with MRX. We propose that MRX and its accessory protein Sae2 participate in the initial processing of ssDNA gaps at stalled replication forks which may recruit RPA and lead to the recruitment of Rad6-Rad18 (Davies *et al.*, 2008) which is required for efficient PCNA monoubiquitination by Rad6-Rad18. Sae2 may facilitate MRX activity by removing DNA-binding proteins (Hartsuiker *et al.*, 2009) or secondary structures (Lengsfeld *et al.*, 2007). Our observations are consistent with Sae2 being an accessory protein for MRX within PRR pathways. In addition, Sgs1 is required for Rad6-Rad18-mediated PCNA monoubiquitination allowing for TLS DNA lesion bypass in the presence of Polζ (Rev3 + Rev7) and Rev1. Rad5 also appears to have a role in TLS, perhaps in a structural or recruiting role by initially binding to PCNA (Pol30) and Rad18 thus recruiting Rev1 and the TLS polymerases allowing for TLS lesion bypass. Epistasis

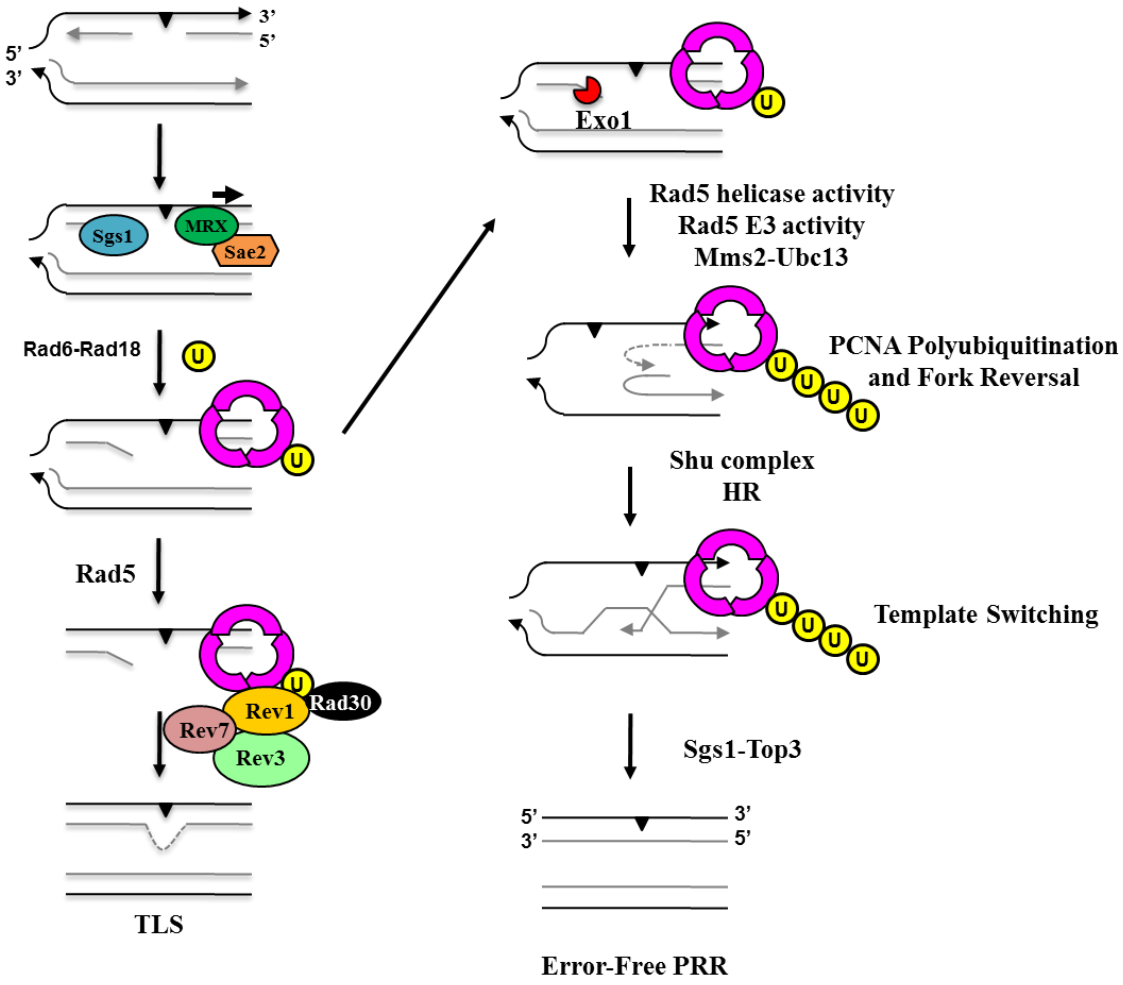

Figure 6.1 – A Proposed Working Model Depicting the Budding Yeast PRR Pathways. MRX and its accessory protein Sae2 participate in the initial processing of ssDNA gaps at stalled replication forks which may recruit RPA and lead to the recruitment of Rad6-Rad18. In addition, Sgs1 is required for Rad6-Rad18-mediated PCNA monoubiquitination allowing for TLS DNA lesion bypass. To continue, we suspect that Exo1 only plays an accessory role in the promotion of error-free PRR. We found that the helicase and RING finger function of Rad5 act sequentially in the same biochemical pathway, and that both functions are required with Mms2-Ubc13 for PCNA polyubiquitination. Subsequently we showed that the Shu complex couples error-free PRR to HR to allow for strand invasion and resolution by Sgs1-Top3.

analysis of the *exo1* mutant is difficult as it barely displays an increased sensitivity to MMS, however, we suspect that Exo1 only plays an accessory role in the promotion of error-free PRR as the double *exo1 rev3* mutant displays a much greater sensitivity to MMS than either corresponding single mutant, suggesting that *EXO1* functions in a pathway distinct from TLS. Along with the observation that *mms2* is epistatic to *exo1* we are able to conclude that Exo1 is exclusively involved in and perhaps plays an accessory role in the promotion of error-free PRR. The 5'-3' exonuclease activity of Exo1 causes further strand resection that favours the recruitment of Rad5-Ubc13-Mms2 to polyubiquitinate PCNA. Hence, Sgs1 and Exo1 promote TLS and error-free PRR, respectively, primarily by signalling for, or balancing between, mono- *vs*. polyubiquitination.

We also examined two competing models based on the *rad5* point mutations that specifically inactivate either the helicase or the RING finger activity. If the two modes of error-free PRR function separately, the *rad5* RING finger and helicase double mutant would display an additive or synergistic effect; however, we found that the double mutant is no more sensitive than the corresponding single point mutants indicating an epistatic interaction, suggesting that the helicase and RING finger functions of Rad5 act sequentially in the same biochemical pathway. The Rad5 helicase and RING finger domain together with Mms2-Ubc13 are all required for the polyubiquitination of PCNA. Following PCNA polyubiquitination, we demonstrated that it is the Shu complex that couples error-free PRR to HR to allow for strand invasion and resolution by Sgs1-Top3. Hence, Sgs1 plays dual roles in both TLS and error-free PRR at two distinct steps. This

study expands our understanding of how TLS and error-free PRR are coordinately operated at the molecular level.

As the majority of genes described in this report are conserved in eukaryotes, from yeast to humans, it would be of great interest to determine if the same regulatory mechanisms occur in higher eukaryotes to prevent genomic instability, a hallmark of cancer.

6.2 – Future Directions

6.2.1 - Roles of the Shu Complex in PCNA Polyubiquitination

Although this body of work identified and genetically characterized the Shu complex to function by coupling error-free PRR to HR, exactly how the Shu complex fulfills this role remains to be determined. Analysis of protein-protein interactions between members of the Shu complex and known error-free and HR proteins might give further insight into the function of the Shu complex. It may also help to pinpoint at which step(s) in error-free PRR the Shu complex functions. In addition, it is unclear whether the Shu complex functions upstream or downstream of polyubiquitinated PCNA, as mutations in the *shu* complex are not nearly as sensitive to MMS as *rad5*, *mms2* or *ubc13* mutation, which can be explained by either model. Analyzing the *shu* complex in the PCNA polyubiquitination assay (in a *siz1*Δ background) is expected to give a definitive answer as to whether the Shu complex functions upstream or downstream of PCNA polyubiquitination. This critical experiment was not performed or previously reported

(Ball *et al.*, 2009) because it was not until after publication that detection of PCNA polyubiquitination was established in my hands in our laboratory.

6.2.2 – Molecular Mechanisms of the *S. cerevisiae* Rad5 Helicase Domain in Error-free PRR

By utilising specific point mutations, genetic characterization and the PCNA ubiquitination assay, this study clearly demonstrates that the Rad5 helicase and E3 RING finger activities act in a sequential manner for error-free lesion bypass. Based on the above observations of Rad5 and its enzymatic activities, the preferred model is that the Rad5 helicase and RING finger domain together with Mms2-Ubc13 are all required for the polyubiquitination of PCNA which then allows for signalling fork regression followed by sister chromatid invasion, synthesis and resolution. However, it should be taken into account that Rad5 is known to bind to PCNA, Ubc13 and Rad18 (Ulrich and Jentsch, 2000). Therefore, it becomes essential to ensure that the *rad5-AA* point mutation is still able to bind to its targets. This will ensure that the loss of PCNA polyubiquitination demonstrated in the *rad5-AA* mutation is indeed completely dependent on the Rad5 helicase function and not due to a loss of interaction with PCNA, Ubc13 and/or Rad18. In order to accomplish this task a PCR product of the Rad5 genomic integration containing the point mutation could be cloned into a Y2H expression vector. The functionality of the fusion constructs can be assessed by functional complementation analysis in the *rad5* null mutant, and the ability of these Rad5 point mutations to interact with Rad5 binding partners can be determined by the Y2H assay through comparison

with wild-type Rad5. However, if a physical interaction is not seen in this Y2H experiment it does not mean the physical protein-protein interaction does not exist. The demonstration of a physical interaction in a Y2H experiment is a valid result; however, a negative result would be considered inconclusive. Nevertheless, the Y2H system itself may be altered, for example, by switching fusion partners or utilising different Y2H systems, to achieve enhanced detection sensitivity. In addition, it has been reported that some protein interactions are only identifiable in the presence of a DNA-damaging agent such as 4NQO (Zhang *et al.*, 2001). Therefore, by adding MMS or 4NQO to the Y2H selection media detection of a protein-protein interaction could be strengthened as this interaction would only be required for lesion bypass following DNA damage.

An alternative approach to Y2H would be utilising DNA constructs that exist for the genomic tagging of proteins for fluorescence or affinity tagging (Deng *et al.*, 2009). One possibility would be to tag Rad5, *rad5-I916A*, and *rad5-AA* and utilize affinity purification or co-immunoprecipitation to identify protein interactions. In theory Rad5, as an experimental control, and *rad5-AA* should still physically interact with PCNA, Ubc13 and Rad18; however, *rad5-I916A* should only interact with PCNA and Rad18, but not Ubc13.

6.2.3 – Roles of Rad5 in TLS

In addition to exploring Rad5 physical interactions for error-free PRR a recent report demonstrated the importance of Rad5 in TLS mediated by Polζ (Pages *et al.*, 2008a). Pages *et al*. suggest that because Rad5 binds to the Rad6-Rad18 complex, the

function of Rad6-Rad18-Rad5 is to promote assembly of the TLS polymerases through the binding of Rad5 to Rev1, thus targeting Polζ to the site of stalled replication. Although Rad5 has been shown to interact with Rev1 (Pages *et al.*, 2008a), a result which we have duplicated (data not shown), the exact region of Rad5 and Rev1 which are required for protein-protein interaction has not yet been mapped and may allow for further insight into the function of Rad5 in lesion bypass.

6.2.4 – How Does Rad5 Function When Error-free PRR Is Dissociated From Replication Forks?

A recent report adds a further level of complexity to our model presented in this study. Karras *et al*. found that limiting TLS or the error-free PRR pathway to the G2/M phase of the cell cycle allowed for efficient promotion of lesion bypass (Karras and Jentsch, 2010). One issue raised by this paper in association with our finding that the Rad5 RING finger and helicase activities act sequentially in error-free PRR is: how is the fork reversal structure able to form in the absence of a replication fork? Therefore, in the absence of a replication fork, are there other proteins able to promote replication-fork-independent fork reversal structures to allow for lesion bypass in the G2/M phase of the cell cycle? These are questions to be pondered and further investigated in the future.

6.2.5 – Roles of MRX and Sae2 in the Formation of ssDNA Gaps Near Replication Forks and Their Implication in PRR

Further investigation to expand on the genetic and ubiquitination analysis of the MRX complex explored in this body of work, by a more mechanistic means, might give further insight into the function of the MRX complex in PRR. Niu *et al*. recently demonstrated a system that can serve as a model for delineating the mechanistic intricacy of the DNA break resection process in eukaryotes (Niu *et al.*, 2010). Therefore, by utilising this system it would be possible to monitor DSBs and determine if they persisted in yeast strains containing mutations in known PRR genes, which would give us an additional tool to determine whether DSBs resected by MRX are processed by PRR. In addition to the helicases and nucleases discussed here, evidence has suggested that the heterodimer Ku regulates HR through inhibition of DNA end processing (Clerici *et al.*, 2008; Lee *et al.*, 1998; Zhang *et al.*, 2007). Furthermore, evidence indicates that DSB resection by Exo1 could be repressed by Ku (Wasko *et al.*, 2009). Exo1 performs resection at telomeric regions in the absence of Ku (Maringele and Lydall, 2002), and deletion of Ku suppresses the hypersensitivity of *mre11* and *rad50* mutants to DSBs in an Exo1-dependent manner (Tomita *et al.*, 2003). In addition, we found that deletion of *EXO1* specifically compromises the relative level of diubiquitinated PCNA without affecting its monoubiquitination. Therefore, the question becomes: is the function of Exo1 in relation to PRR affected by the heterodimer Ku? It is possible that if we utilize the PCNA ubiquitination assay, as previously described, with a *ku* mutant, we would see an increase in the relative level of diubiquitinated PCNA, compared to wild-type, as Exo1

would no longer be inhibited by Ku. However, it may not be possible to achieve, or detect, higher than wild-type levels of diubiquitination, even in a mutant strain. Therefore, it might be more relevant to overexpress Ku in a wild-type background to determine if the overexpression of Ku is sufficient to decrease diubiquitinated PCNA. If this is indeed the case, it would suggest that Ku plays a critical role in mediating DNA lesion bypass by PRR.

6.2.6 – A Search for the PCNA Deubiquitination Enzyme

Ubiquitination of PCNA has been shown in this body of work, and previously, to be vital for PRR and cell survival in *S. cerevisiae*. However, ubiquitination of any substrate is a covalent modification, and thought to be short-lived. As PCNA is constantly ubiquitinated, and is therefore in a "turned on" state so to speak, a constant state of DNA repair or DNA damage tolerance would ensue. Therefore it seems vital that at some point the cell would need to deubiquitinate Lys63-linked polyubiquitinated PCNA to return to a "normal" state following DNA lesion bypass. The non-processive, low-fidelity DNA polymerases must be removed rapidly from the replication fork following their required function in bypassing DNA lesions to ensure additional errors are not incorporated into the DNA, and that genomic stability is preserved. The question therefore becomes how does this occur, and what proteins are involved in the deubiquitination of PCNA to "turn off" PRR? A recent review explored this issue (Gallego-Sanchez *et al.*, 2010), and although *USP1* has been shown to deubiquitinate PCNA in cultured human cells the same conclusion has remained elusive in yeast. There

are 17 known genes in budding yeast that code for ubiquitin-specific proteases, some of which have been well characterized, while others remain unknown (Gallego-Sanchez *et al.*, 2010; Kvint *et al.*, 2008; Wilkinson, 1997). Analysis of the 17 putative ubiquitin-specific proteases has failed to locate a PIP (PCNA interacting protein) domain; however, this analysis assumes a direct interaction between PCNA and a putative ubiquitin-specific protease. Alternatively, analysis of PIP plain variant, which has been shown to be required for PCNA to interact with Eco1 (Moldovan *et al.*, 2006), reveals such a domain in 4 of the 17 putative ubiquitin-specific proteases (Gallego-Sanchez *et al.*, 2010). The 4 putative ubiquitin-specific proteases are: Ubp3, Doa4/Ubp4, Ubp8 and Dot4/Ubp10. As none of these 4 putative ubiquitin-specific proteases are essential, yeast strains containing null mutations of these genes could be run through our ubiquitination assay, (as described in Chapter 2 and further explored in Chapter 4). I hypothesize that in the absence of a ubiquitin-specific protease, detection of PCNA ubiquitination following DNA damage would be enhanced. Enhancement could be shown as total quantity of mono- and diubiquitinated PCNA or, in the number of ubiquitin moieties attached to PCNA in the non-canonical Lys63 linked chains. Alternatively, candidate genes could be cloned into yeast overexpression vectors, and screened for their ability to virtually eliminate detectable PCNA ubiqutination following DNA damage. Therefore, by employing these methods, there would be no dependence on direct physical interaction between PCNA and a putative deubiquitinating enzyme, which may or may not be essential. Should these initial 4 candidates show a lack of involvement in PCNA-deubiquitinating function, the remaining 13 putative ubiquitin-specific enzymes could be tested in a similar manner.

6.2.7 – Roles of Rad18 Phosphorylation in PRR

A recent study showed that Rad18 is phosphorylated in a Cdc7-mediated manner in cultured human cells (Day *et al.*, 2010). Rad18 is a highly conserved E3 ubiquitin ligase, and previous genetic studies have shown an interaction between Cdc7 and known members of the TLS pathway in *S. cerevisiae* (Pessoa-Brandao and Sclafani, 2004). *CDC7* was initially assigned to the *RAD6* epistasis group (Njagi and Kilbey, 1982), and subsequently shown to act with Dbf4 as a protein kinase required for DNA replication in eukaryotes from yeast to humans. In addition, Day *et al*. demonstrated that Cdc7-dependent Rad18 phosphorylation promotes recruitment of Polη to stalled replication forks after UV treatment (Day *et al.*, 2010). In *S. cerevisiae* Polη is encoded for by the *RAD30* gene (Andersen *et al.*, 2008), and it is one of three DNA polymerases utilized for TLS lesion bypass, and all three (including Rev1 and Pol ζ) have known human homologs (Reviewed in (Andersen *et al.*, 2008) and most recently discussed in (Wiltrout and Walker, 2010)). Studies with knockout mice have demonstrated the importance of Polη in tumour suppression, as 100% of mice with polη-/- develop epithelial tumours (Lin *et al.*, 2006). Therefore, the question becomes: is Rad18 phosphorylated in *S. cerevisiae* in order to recruit TLS polymerases? If so, is the phosphorylation of Rad18 only required to recruit Rad30, or all three TLS polymerases? In order to test this hypothesis Rad18 could be examined for phosphorylation via western blot analysis with specific antibodies to either a genomic integrated tag or Rad18 following DNA damage. Should phosphorylated Rad18 be detected, determining the site of Rad18 phosphorylation, by creating site specific mutations, could allow for further analysis to

determine the function of Rad18 phosphorylation. However, the serine residue that is phosphorylated in humans and conserved amongst orangutans, mice, dogs, rats, chickens and zebrafish (Gallego-Sanchez *et al.*, 2010) is not conserved in *S. cerevisiae* thus making this study a little more challenging.

S. cerevisiae has proven an excellent eukaryotic model to study DNA repair and mutagenesis. As many of the genes examined in this study have known human homologues, it is hopeful that gaining further insight into yeast PRR will guide our investigation into higher eukaryotes, including humans, for similar processes that function to maintain genomic stability and prevent the hallmark of genomic instability, cancer.

CHAPTER 7

REFERENCES

Acharya, N., Haracska, L., Johnson, R.E., Unk, I., Prakash, S., and Prakash, L. (2005). Complex formation of yeast Rev1 and Rev7 proteins: a novel role for the polymerase-associated domain. Mol Cell Biol *25*, 9734-9740.

Acharya, N., Johnson, R.E., Prakash, S., and Prakash, L. (2006). Complex formation with Rev1 enhances the proficiency of Saccharomyces cerevisiae DNA polymerase zeta for mismatch extension and for extension opposite from DNA lesions. Mol Cell Biol *26*, 9555-9563.

Adelman, R., Saul, R.L., and Ames, B.N. (1988). Oxidative damage to DNA: relation to species metabolic rate and life span. Proc Natl Acad Sci U S A *85*, 2706-2708.

Ahne, F., Jha, B., and Eckardt-Schupp, F. (1997). The RAD5 gene product is involved in the avoidance of non-homologous end-joining of DNA double strand breaks in the yeast Saccharomyces cerevisiae. Nucleic Acids Res *25*, 743-749.

Alani, E., Reenan, R.A., and Kolodner, R.D. (1994). Interaction between mismatch repair and genetic recombination in Saccharomyces cerevisiae. Genetics *137*, 19-39.

Albert, R.E., and Burns, F.J. (1977). Carcinogenic atmospheric pollutants and the nature of low-level risks.
(Cold Spring Harbor, N.Y., Cold Spring Harbor Laboratory).

Allen, R.G., and Tresini, M. (2000). Oxidative stress and gene regulation. Free Radic Biol Med *28*, 463-499.

Alvarez, M.E., Pennell, R.I., Meijer, P.J., Ishikawa, A., Dixon, R.A., and Lamb, C. (1998). Reactive oxygen intermediates mediate a systemic signal network in the establishment of plant immunity. Cell *92*, 773-784.

Ames, B.N., and Gold, L.S. (1991). Endogenous mutagens and the causes of aging and cancer. Mutat Res *250*, 3-16.

Ames, B.N., Shigenaga, M.K., and Hagen, T.M. (1993). Oxidants, antioxidants, and the degenerative diseases of aging. Proc Natl Acad Sci U S A *90*, 7915-7922.

Andersen, P.L. (2009). DNA Damage Tolerance in Mammalian Cells. In Microbiology and Immunology (Saskatoon, University of Saskatchewan), pp. 232.

Andersen, P.L., Xu, F., and Xiao, W. (2008). Eukaryotic DNA damage tolerance and translesion synthesis through covalent modifications of PCNA. Cell Res *18*, 162-173.

Andersen, P.L., Zhou, H., Pastushok, L., Moraes, T., McKenna, S., Ziola, B., Ellison, M.J., Dixit, V.M., and Xiao, W. (2005). Distinct regulation of Ubc13 functions by

the two ubiquitin-conjugating enzyme variants Mms2 and Uev1A. J Cell Biol *170*, 745-755.
Anderson, D.E., Trujillo, K.M., Sung, P., and Erickson, H.P. (2001). Structure of the Rad50 x Mre11 DNA repair complex from Saccharomyces cerevisiae by electron microscopy. J Biol Chem *276*, 37027-37033.
Arnason, T., and Ellison, M.J. (1994). Stress resistance in Saccharomyces cerevisiae is strongly correlated with assembly of a novel type of multiubiquitin chain. Mol Cell Biol *14*, 7876-7883.
Bailly, V., Lamb, J., Sung, P., Prakash, S., and Prakash, L. (1994). Specific complex formation between yeast RAD6 and RAD18 proteins: a potential mechanism for targeting RAD6 ubiquitin-conjugating activity to DNA damage sites. Genes Dev *8*, 811-820.
Bailly, V., Lauder, S., Prakash, S., and Prakash, L. (1997a). Yeast DNA repair proteins Rad6 and Rad18 form a heterodimer that has ubiquitin conjugating, DNA binding, and ATP hydrolytic activities. J Biol Chem *272*, 23360-23365.
Bailly, V., Prakash, S., and Prakash, L. (1997b). Domains required for dimerization of yeast Rad6 ubiquitin-conjugating enzyme and Rad18 DNA binding protein. Mol Cell Biol *17*, 4536-4543.
Ball, L.G., Zhang, K., Cobb, J.A., Boone, C., and Xiao, W. (2009). The yeast Shu complex couples error-free post-replication repair to homologous recombination. Mol Microbiol *73*, 89-102.
Barbour, L., Ball, L.G., Zhang, K., and Xiao, W. (2006). DNA damage checkpoints are involved in postreplication repair. Genetics *174*, 1789-1800.
Barbour, L., and Xiao, W. (2003). Regulation of alternative replication bypass pathways at stalled replication forks and its effects on genome stability: a yeast model. Mutat Res *532*, 137-155.
Barbour, L., and Xiao, W. (2006). Mating type regulation of cellular tolerance to DNA damage is specific to the DNA post-replication repair and mutagenesis pathway. Mol Microbiol *59*, 637-650.
Barbour, L., Zhu, Y., and Xiao, W. (2000). Improving synthetic lethal screens by regulating the yeast centromere sequence. Genome *43*, 910-917.
Bemark, M., Khamlichi, A.A., Davies, S.L., and Neuberger, M.S. (2000). Disruption of mouse polymerase zeta (Rev3) leads to embryonic lethality and impairs blastocyst development in vitro. Curr Biol *10*, 1213-1216.
Berben, G., Dumont, J., Gilliquet, V., Bolle, P.A., and Hilger, F. (1991). The YDp plasmids: a uniform set of vectors bearing versatile gene disruption cassettes for Saccharomyces cerevisiae. Yeast *7*, 475-477.
Bienko, M., Green, C.M., Crosetto, N., Rudolf, F., Zapart, G., Coull, B., Kannouche, P., Wider, G., Peter, M., Lehmann, A.R., *et al.* (2005). Ubiquitin-binding domains in Y-family polymerases regulate translesion synthesis. Science *310*, 1821-1824.
Bjelland, S., and Seeberg, E. (2003). Mutagenicity, toxicity and repair of DNA base damage induced by oxidation. Mutat Res *531*, 37-80.
Blackwell, L.J., Martik, D., Bjornson, K.P., Bjornson, E.S., and Modrich, P. (1998). Nucleotide-promoted release of hMutSalpha from heteroduplex DNA is

consistent with an ATP-dependent translocation mechanism. J Biol Chem *273*, 32055-32062.
Blaisdell, J.O., and Wallace, S.S. (2001). Abortive base-excision repair of radiation-induced clustered DNA lesions in Escherichia coli. Proc Natl Acad Sci U S A *98*, 7426-7430.
Blastyak, A., Pinter, L., Unk, I., Prakash, L., Prakash, S., and Haracska, L. (2007). Yeast Rad5 protein required for postreplication repair has a DNA helicase activity specific for replication fork regression. Mol Cell *28*, 167-175.
Bonetti, D., Martina, M., Clerici, M., Lucchini, G., and Longhese, M.P. (2009). Multiple pathways regulate 3' overhang generation at S. cerevisiae telomeres. Mol Cell *35*, 70-81.
Borts, R.H., Chambers, S.R., and Abdullah, M.F. (2000). The many faces of mismatch repair in meiosis. Mutat Res *451*, 129-150.
Branzei, D., Vanoli, F., and Foiani, M. (2008). SUMOylation regulates Rad18-mediated template switch. Nature *456*, 915-920.
Breen, A.P., and Murphy, J.A. (1995). Reactions of oxyl radicals with DNA. Free Radic Biol Med *18*, 1033-1077.
Bressan, D.A., Olivares, H.A., Nelms, B.E., and Petrini, J.H. (1998). Alteration of N-terminal phosphoesterase signature motifs inactivates Saccharomyces cerevisiae Mre11. Genetics *150*, 591-600.
Broomfield, S., Chow, B.L., and Xiao, W. (1998). MMS2, encoding a ubiquitin-conjugating-enzyme-like protein, is a member of the yeast error-free postreplication repair pathway. Proc Natl Acad Sci U S A *95*, 5678-5683.
Broomfield, S., Hryciw, T., and Xiao, W. (2001). DNA postreplication repair and mutagenesis in Saccharomyces cerevisiae. Mutat Res *486*, 167-184.
Broomfield, S., and Xiao, W. (2002). Suppression of genetic defects within the RAD6 pathway by srs2 is specific for error-free post-replication repair but not for damage-induced mutagenesis. Nucleic Acids Res *30*, 732-739.
Brown, M., Zhu, Y., Hemmingsen, S.M., and Xiao, W. (2002). Structural and functional conservation of error-free DNA postreplication repair in Schizosaccharomyces pombe. DNA Repair (Amst) *1*, 869-880.
Bruck, I., Woodgate, R., McEntee, K., and Goodman, M.F. (1996). Purification of a soluble UmuD'C complex from Escherichia coli. Cooperative binding of UmuD'C to single-stranded DNA. J Biol Chem *271*, 10767-10774.
Brusky, J., Zhu, Y., and Xiao, W. (2000). UBC13, a DNA-damage-inducible gene, is a member of the error-free postreplication repair pathway in Saccharomyces cerevisiae. Curr Genet *37*, 168-174.
Buonocore, G., and Bellieni, C. (2010). Neonatal pain and oxidative stress. Minerva Pediatr *62*, 59-60.
Chen, S., Davies, A.A., Sagan, D., and Ulrich, H.D. (2005). The RING finger ATPase Rad5p of Saccharomyces cerevisiae contributes to DNA double-strand break repair in a ubiquitin-independent manner. Nucleic Acids Res *33*, 5878-5886.

Cheng, K.C., Cahill, D.S., Kasai, H., Nishimura, S., and Loeb, L.A. (1992). 8-Hydroxyguanine, an abundant form of oxidative DNA damage, causes G----T and A----C substitutions. J Biol Chem *267*, 166-172.

Chi, N.W., and Kolodner, R.D. (1994). The effect of DNA mismatches on the ATPase activity of MSH1, a protein in yeast mitochondria that recognizes DNA mismatches. J Biol Chem *269*, 29993-29997.

Chu, W.K., and Hickson, I.D. (2009). RecQ helicases: multifunctional genome caretakers. Nat Rev Cancer *9*, 644-654.

Chung, C.T., Niemela, S.L., and Miller, R.H. (1989). One-step preparation of competent Escherichia coli: transformation and storage of bacterial cells in the same solution. Proc Natl Acad Sci U S A *86*, 2172-2175.

Cleaver, J.E. (2003). Photoreactivation. DNA Repair (Amst) *2*, 629, 637-628.

Clerici, M., Mantiero, D., Guerini, I., Lucchini, G., and Longhese, M.P. (2008). The Yku70-Yku80 complex contributes to regulate double-strand break processing and checkpoint activation during the cell cycle. EMBO Rep *9*, 810-818.

Clerici, M., Mantiero, D., Lucchini, G., and Longhese, M.P. (2005). The Saccharomyces cerevisiae Sae2 protein promotes resection and bridging of double strand break ends. J Biol Chem *280*, 38631-38638.

Connelly, J.C., de Leau, E.S., and Leach, D.R. (1999). DNA cleavage and degradation by the SbcCD protein complex from Escherichia coli. Nucleic Acids Res *27*, 1039-1046.

Courcelle, J., Khodursky, A., Peter, B., Brown, P.O., and Hanawalt, P.C. (2001). Comparative gene expression profiles following UV exposure in wild-type and SOS-deficient Escherichia coli. Genetics *158*, 41-64.

Craig, N.L., and Roberts, J.W. (1980). E. coli recA protein-directed cleavage of phage lambda repressor requires polynucleotide. Nature *283*, 26-30.

D'Amours, D., and Jackson, S.P. (2002). The Mre11 complex: at the crossroads of dna repair and checkpoint signalling. Nat Rev Mol Cell Biol *3*, 317-327.

Daley, J.M., Palmbos, P.L., Wu, D., and Wilson, T.E. (2005). Nonhomologous end joining in yeast. Annu Rev Genet *39*, 431-451.

Davies, A.A., Huttner, D., Daigaku, Y., Chen, S., and Ulrich, H.D. (2008). Activation of ubiquitin-dependent DNA damage bypass is mediated by replication protein a. Mol Cell *29*, 625-636.

Davies, G.P., Powell, L.M., Webb, J.L., Cooper, L.P., and Murray, N.E. (1998). EcoKI with an amino acid substitution in any one of seven DEAD-box motifs has impaired ATPase and endonuclease activities. Nucleic Acids Res *26*, 4828-4836.

Day, T.A., Palle, K., Barkley, L.R., Kakusho, N., Zou, Y., Tateishi, S., Verreault, A., Masai, H., and Vaziri, C. (2010). Phosphorylated Rad18 directs DNA Polymerase {eta} to sites of stalled replication. J Cell Biol *191*, 953-966.

de Jager, M., van Noort, J., van Gent, D.C., Dekker, C., Kanaar, R., and Wyman, C. (2001). Human Rad50/Mre11 is a flexible complex that can tether DNA ends. Mol Cell *8*, 1129-1135.

Demple, B., and DeMott, M.S. (2002). Dynamics and diversions in base excision DNA repair of oxidized abasic lesions. Oncogene *21*, 8926-8934.

Deng, C., Xiong, X., and Krutchinsky, A.N. (2009). Unifying fluorescence microscopy and mass spectrometry for studying protein complexes in cells. Mol Cell Proteomics *8*, 1413-1423.
di Caprio, L., and Cox, B.S. (1981). DNA synthesis in UV-irradiated yeast. Mutat Res *82*, 69-85.
Doetsch, P.W., Morey, N.J., Swanson, R.L., and Jinks-Robertson, S. (2001). Yeast base excision repair: interconnections and networks. Prog Nucleic Acid Res Mol Biol *68*, 29-39.
Doherty, A.J., Serpell, L.C., and Ponting, C.P. (1996). The helix-hairpin-helix DNA-binding motif: a structural basis for non-sequence-specific recognition of DNA. Nucleic Acids Res *24*, 2488-2497.
Dzierzbicki, P., Koprowski, P., Fikus, M.U., Malc, E., and Ciesla, Z. (2004). Repair of oxidative damage in mitochondrial DNA of Saccharomyces cerevisiae: involvement of the MSH1-dependent pathway. DNA Repair (Amst) *3*, 403-411.
Earley, M.C., and Crouse, G.F. (1998). The role of mismatch repair in the prevention of base pair mutations in Saccharomyces cerevisiae. Proc Natl Acad Sci U S A *95*, 15487-15491.
Esposito, G., Godindagger, I., Klein, U., Yaspo, M.L., Cumano, A., and Rajewsky, K. (2000). Disruption of the Rev3l-encoded catalytic subunit of polymerase zeta in mice results in early embryonic lethality. Curr Biol *10*, 1221-1224.
Feldmann, E., Schmiemann, V., Goedecke, W., Reichenberger, S., and Pfeiffer, P. (2000). DNA double-strand break repair in cell-free extracts from Ku80-deficient cells: implications for Ku serving as an alignment factor in non-homologous DNA end joining. Nucleic Acids Res *28*, 2585-2596.
Fenton, H.J.H. (1894). Oxidation of tatraric acid in the presence of iron. . J Chem Soc Trans *65*, 899-905.
Ferguson, L.R., and Baguley, B.C. (1996). Mutagenicity of anticancer drugs that inhibit topoisomerase enzymes. Mutat Res *355*, 91-101.
Fields, S., and Song, O. (1989). A novel genetic system to detect protein-protein interactions. Nature *340*, 245-246.
Finley, D., Sadis, S., Monia, B.P., Boucher, P., Ecker, D.J., Crooke, S.T., and Chau, V. (1994). Inhibition of proteolysis and cell cycle progression in a multiubiquitination-deficient yeast mutant. Mol Cell Biol *14*, 5501-5509.
Flores-Rozas, H., and Kolodner, R.D. (1998). The Saccharomyces cerevisiae MLH3 gene functions in MSH3-dependent suppression of frameshift mutations. Proc Natl Acad Sci U S A *95*, 12404-12409.
Frei, C., and Gasser, S.M. (2000). The yeast Sgs1p helicase acts upstream of Rad53p in the DNA replication checkpoint and colocalizes with Rad53p in S-phase-specific foci. Genes Dev *14*, 81-96.
Friedberg, E.C. (1988). Deoxyribonucleic acid repair in the yeast Saccharomyces cerevisiae. Microbiol Rev *52*, 70-102.
Friedberg, E.C., Walker, G.C., Siede, W., Wood, R.D., Schultz, R.A., and Ellenberger, T. (2006). DNA Repair and Mutagenesis, Vol Second Edition (Washington, DC, ASM Press).

Friedl, A.A., Liefshitz, B., Steinlauf, R., and Kupiec, M. (2001). Deletion of the SRS2 gene suppresses elevated recombination and DNA damage sensitivity in rad5 and rad18 mutants of Saccharomyces cerevisiae. Mutat Res *486*, 137-146.

Froelich-Ammon, S.J., and Osheroff, N. (1995). Topoisomerase poisons: harnessing the dark side of enzyme mechanism. J Biol Chem *270*, 21429-21432.

Fu, Y., Zhu, Y., Zhang, K., Yeung, M., Durocher, D., and Xiao, W. (2008). Rad6-Rad18 mediates a eukaryotic SOS response by ubiquitinating the 9-1-1 checkpoint clamp. Cell *133*, 601-611.

Fung, C.W., Mozlin, A.M., and Symington, L.S. (2009). Suppression of the double-strand-break-repair defect of the Saccharomyces cerevisiae rad57 mutant. Genetics *181*, 1195-1206.

Furuse, M., Nagase, Y., Tsubouchi, H., Murakami-Murofushi, K., Shibata, T., and Ohta, K. (1998). Distinct roles of two separable in vitro activities of yeast Mre11 in mitotic and meiotic recombination. EMBO J *17*, 6412-6425.

Gallego-Sanchez, A., Conde, F., San Segundo, P., and Bueno, A. (2010). Control of PCNA deubiquitylation in yeast. Biochem Soc Trans *38*, 104-109.

Game, J.C., and Mortimer, R.K. (1974). A genetic study of x-ray sensitive mutants in yeast. Mutat Res *24*, 281-292.

Ganesan, A.K. (1974). Persistence of pyrimidine dimers during post-replication repair in ultraviolet light-irradiated Escherichia coli K12. J Mol Biol *87*, 103-119.

Gangavarapu, V., Haracska, L., Unk, I., Johnson, R.E., Prakash, S., and Prakash, L. (2006). Mms2-Ubc13-dependent and -independent roles of Rad5 ubiquitin ligase in postreplication repair and translesion DNA synthesis in Saccharomyces cerevisiae. Mol Cell Biol *26*, 7783-7790.

Gangloff, S., Soustelle, C., and Fabre, F. (2000). Homologous recombination is responsible for cell death in the absence of the Sgs1 and Srs2 helicases. Nat Genet *25*, 192-194.

Gellon, L., Barbey, R., Auffret van der Kemp, P., Thomas, D., and Boiteux, S. (2001). Synergism between base excision repair, mediated by the DNA glycosylases Ntg1 and Ntg2, and nucleotide excision repair in the removal of oxidatively damaged DNA bases in Saccharomyces cerevisiae. Mol Genet Genomics *265*, 1087-1096.

Gietz, R.D., and Sugino, A. (1988). New yeast-Escherichia coli shuttle vectors constructed with in vitro mutagenized yeast genes lacking six-base pair restriction sites. Gene *74*, 527-534.

Gottlich, B., Reichenberger, S., Feldmann, E., and Pfeiffer, P. (1998). Rejoining of DNA double-strand breaks in vitro by single-strand annealing. Eur J Biochem *258*, 387-395.

Gradia, S., Subramanian, D., Wilson, T., Acharya, S., Makhov, A., Griffith, J., and Fishel, R. (1999). hMSH2-hMSH6 forms a hydrolysis-independent sliding clamp on mismatched DNA. Mol Cell *3*, 255-261.

Grenon, M., Gilbert, C., and Lowndes, N.F. (2001). Checkpoint activation in response to double-strand breaks requires the Mre11/Rad50/Xrs2 complex. Nat Cell Biol *3*, 844-847.

Grilley, M., Welsh, K.M., Su, S.S., and Modrich, P. (1989). Isolation and characterization of the Escherichia coli mutL gene product. J Biol Chem *264*, 1000-1004.

Guarente, L. (1993). Synthetic enhancement in gene interaction: a genetic tool come of age. Trends Genet *9*, 362-366.

Guillet, M., and Boiteux, S. (2003). Origin of endogenous DNA abasic sites in Saccharomyces cerevisiae. Mol Cell Biol *23*, 8386-8394.

Guo, C., Fischhaber, P.L., Luk-Paszyc, M.J., Masuda, Y., Zhou, J., Kamiya, K., Kisker, C., and Friedberg, E.C. (2003). Mouse Rev1 protein interacts with multiple DNA polymerases involved in translesion DNA synthesis. EMBO J *22*, 6621-6630.

Guo, C., Sonoda, E., Tang, T.S., Parker, J.L., Bielen, A.B., Takeda, S., Ulrich, H.D., and Friedberg, E.C. (2006). REV1 protein interacts with PCNA: significance of the REV1 BRCT domain in vitro and in vivo. Mol Cell *23*, 265-271.

Haber, F., and Weiss, J.J. (1939). The catalytic decomposition of hydrogen peroxide by iron salts. . Proc R Soc Lond Ser A *147*, 332-351.

Harfe, B.D., Minesinger, B.K., and Jinks-Robertson, S. (2000). Discrete in vivo roles for the MutL homologs Mlh2p and Mlh3p in the removal of frameshift intermediates in budding yeast. Curr Biol *10*, 145-148.

Hartman, J.L.t., Garvik, B., and Hartwell, L. (2001). Principles for the buffering of genetic variation. Science *291*, 1001-1004.

Hartsuiker, E., Neale, M.J., and Carr, A.M. (2009). Distinct requirements for the Rad32(Mre11) nuclease and Ctp1(CtIP) in the removal of covalently bound topoisomerase I and II from DNA. Mol Cell *33*, 117-123.

Hearst, J.E., Isaacs, S.T., Kanne, D., Rapoport, H., and Straub, K. (1984). The reaction of the psoralens with deoxyribonucleic acid. Q Rev Biophys *17*, 1-44.

Hershko, A., Ciechanover, A., Heller, H., Haas, A.L., and Rose, I.A. (1980). Proposed role of ATP in protein breakdown: conjugation of protein with multiple chains of the polypeptide of ATP-dependent proteolysis. Proc Natl Acad Sci U S A *77*, 1783-1786.

Heude, M., and Fabre, F. (1993). a/alpha-control of DNA repair in the yeast Saccharomyces cerevisiae: genetic and physiological aspects. Genetics *133*, 489-498.

Hicke, L., and Dunn, R. (2003). Regulation of membrane protein transport by ubiquitin and ubiquitin-binding proteins. Annu Rev Cell Dev Biol *19*, 141-172.

Hochstrasser, M. (1996). Ubiquitin-dependent protein degradation. Annu Rev Genet *30*, 405-439.

Hoege, C., Pfander, B., Moldovan, G.L., Pyrowolakis, G., and Jentsch, S. (2002). RAD6-dependent DNA repair is linked to modification of PCNA by ubiquitin and SUMO. Nature *419*, 135-141.

Hoffman, C.S., and Winston, F. (1987). A ten-minute DNA preparation from yeast efficiently releases autonomous plasmids for transformation of Escherichia coli. Gene *57*, 267-272.

Hofmann, R.M., and Pickart, C.M. (1999). Noncanonical MMS2-encoded ubiquitin-conjugating enzyme functions in assembly of novel polyubiquitin chains for DNA repair. Cell *96*, 645-653.

Hollingsworth, N.M., Ponte, L., and Halsey, C. (1995). MSH5, a novel MutS homolog, facilitates meiotic reciprocal recombination between homologs in Saccharomyces cerevisiae but not mismatch repair. Genes Dev *9*, 1728-1739.

Hopfner, K.P., Craig, L., Moncalian, G., Zinkel, R.A., Usui, T., Owen, B.A., Karcher, A., Henderson, B., Bodmer, J.L., McMurray, C.T., *et al.* (2002). The Rad50 zinc-hook is a structure joining Mre11 complexes in DNA recombination and repair. Nature *418*, 562-566.

Hough, R., Pratt, G., and Rechsteiner, M. (1987). Purification of two high molecular weight proteases from rabbit reticulocyte lysate. J Biol Chem *262*, 8303-8313.

Huang, M.E., Rio, A.G., Nicolas, A., and Kolodner, R.D. (2003). A genomewide screen in Saccharomyces cerevisiae for genes that suppress the accumulation of mutations. Proc Natl Acad Sci U S A *100*, 11529-11534.

Huertas, P., Cortes-Ledesma, F., Sartori, A.A., Aguilera, A., and Jackson, S.P. (2008). CDK targets Sae2 to control DNA-end resection and homologous recombination. Nature *455*, 689-692.

Iaccarino, I., Marra, G., Dufner, P., and Jiricny, J. (2000). Mutation in the magnesium binding site of hMSH6 disables the hMutSalpha sliding clamp from translocating along DNA. J Biol Chem *275*, 2080-2086.

Ito, H., Fukuda, Y., Murata, K., and Kimura, A. (1983). Transformation of intact yeast cells treated with alkali cations. J Bacteriol *153*, 163-168.

Ito, T., Chiba, T., Ozawa, R., Yoshida, M., Hattori, M., and Sakaki, Y. (2001). A comprehensive two-hybrid analysis to explore the yeast protein interactome. Proc Natl Acad Sci U S A *98*, 4569-4574.

Ivanov, E.L., Sugawara, N., White, C.I., Fabre, F., and Haber, J.E. (1994). Mutations in XRS2 and RAD50 delay but do not prevent mating-type switching in Saccharomyces cerevisiae. Mol Cell Biol *14*, 3414-3425.

Jacobs, A., Bopp, A., and Hagen, U. (1972). In vitro repair of single-strand breaks in -irradiated DNA by polynucleotide ligase. Int J Radiat Biol Relat Stud Phys Chem Med *22*, 431-435.

James, P., Halladay, J., and Craig, E.A. (1996). Genomic libraries and a host strain designed for highly efficient two-hybrid selection in yeast. Genetics *144*, 1425-1436.

Jentsch, S., McGrath, J.P., and Varshavsky, A. (1987). The yeast DNA repair gene RAD6 encodes a ubiquitin-conjugating enzyme. Nature *329*, 131-134.

Johnson, E.S., and Gupta, A.A. (2001). An E3-like factor that promotes SUMO conjugation to the yeast septins. Cell *106*, 735-744.

Johnson, R.E., Henderson, S.T., Petes, T.D., Prakash, S., Bankmann, M., and Prakash, L. (1992). Saccharomyces cerevisiae RAD5-encoded DNA repair protein contains DNA helicase and zinc-binding sequence motifs and affects the stability of simple repetitive sequences in the genome. Mol Cell Biol *12*, 3807-3818.

Johnson, R.E., Kovvali, G.K., Prakash, L., and Prakash, S. (1996). Requirement of the yeast MSH3 and MSH6 genes for MSH2-dependent genomic stability. J Biol Chem *271*, 7285-7288.

Johnson, R.E., Prakash, S., and Prakash, L. (1994). Yeast DNA repair protein RAD5 that promotes instability of simple repetitive sequences is a DNA-dependent ATPase. J Biol Chem *269*, 28259-28262.

Johnson, R.E., Torres-Ramos, C.A., Izumi, T., Mitra, S., Prakash, S., and Prakash, L. (1998). Identification of APN2, the Saccharomyces cerevisiae homolog of the major human AP endonuclease HAP1, and its role in the repair of abasic sites. Genes Dev *12*, 3137-3143.

Jones, J.S., Weber, S., and Prakash, L. (1988). The Saccharomyces cerevisiae RAD18 gene encodes a protein that contains potential zinc finger domains for nucleic acid binding and a putative nucleotide binding sequence. Nucleic Acids Res *16*, 7119-7131.

Kaiser, P., and Tagwerker, C. (2005). Is this protein ubiquitinated? Methods Enzymol *399*, 243-248.

Karmakar, P., Seki, M., Kanamori, M., Hashiguchi, K., Ohtsuki, M., Murata, E., Inoue, E., Tada, S., Lan, L., Yasui, A., *et al.* (2006). BLM is an early responder to DNA double-strand breaks. Biochem Biophys Res Commun *348*, 62-69.

Karras, G.I., and Jentsch, S. (2010). The RAD6 DNA damage tolerance pathway operates uncoupled from the replication fork and is functional beyond S phase. Cell *141*, 255-267.

Ke, S.H., and Madison, E.L. (1997). Rapid and efficient site-directed mutagenesis by single-tube 'megaprimer' PCR method. Nucleic Acids Res *25*, 3371-3372.

Kelner, A. (1949). Effect of visible light on the recovery of Streptomyces griseus conidia from ultraviolet irradiation injury. Proc Natl Acad Sci U S A *35*, 73-79.

Kiakos, K., Howard, T.T., Lee, M., Hartley, J.A., and McHugh, P.J. (2002). Saccharomyces cerevisiae RAD5 influences the excision repair of DNA minor groove adducts. J Biol Chem *277*, 44576-44581.

Knop, M., Siegers, K., Pereira, G., Zachariae, W., Winsor, B., Nasmyth, K., and Schiebel, E. (1999). Epitope tagging of yeast genes using a PCR-based strategy: more tags and improved practical routines. Yeast *15*, 963-972.

Koppenol, W.H. (2001). The Haber-Weiss cycle--70 years later. Redox Rep *6*, 229-234.

Kozekov, I.D., Nechev, L.V., Moseley, M.S., Harris, C.M., Rizzo, C.J., Stone, M.P., and Harris, T.M. (2003). DNA interchain cross-links formed by acrolein and crotonaldehyde. J Am Chem Soc *125*, 50-61.

Krejci, L., Van Komen, S., Li, Y., Villemain, J., Reddy, M.S., Klein, H., Ellenberger, T., and Sung, P. (2003). DNA helicase Srs2 disrupts the Rad51 presynaptic filament. Nature *423*, 305-309.

Krogh, B.O., and Symington, L.S. (2004). Recombination proteins in yeast. Annu Rev Genet *38*, 233-271.

Kuchino, Y., Mori, F., Kasai, H., Inoue, H., Iwai, S., Miura, K., Ohtsuka, E., and Nishimura, S. (1987). Misreading of DNA templates containing 8-

hydroxydeoxyguanosine at the modified base and at adjacent residues. Nature *327*, 77-79.
Kurtz, A.J., and Lloyd, R.S. (2003). 1,N2-deoxyguanosine adducts of acrolein, crotonaldehyde, and trans-4-hydroxynonenal cross-link to peptides via Schiff base linkage. J Biol Chem *278*, 5970-5976.
Kvint, K., Uhler, J.P., Taschner, M.J., Sigurdsson, S., Erdjument-Bromage, H., Tempst, P., and Svejstrup, J.Q. (2008). Reversal of RNA polymerase II ubiquitylation by the ubiquitin protease Ubp3. Mol Cell *30*, 498-506.
Laemmli, U.K. (1970). Cleavage of structural proteins during the assembly of the head of bacteriophage T4. Nature *227*, 680-685.
Laterjet, R., and Ephrussi, B. (1949). Courbes de survie de levures haloides et diploides soumises aux rayon X. C. R. . Acad Sci *229*, 306-308.
Lawrence, C. (1994). The RAD6 DNA repair pathway in Saccharomyces cerevisiae: what does it do, and how does it do it? Bioessays *16*, 253-258.
Lawrence, C.W. (2004). Cellular functions of DNA polymerase zeta and Rev1 protein. Adv Protein Chem *69*, 167-203.
Lee, S.E., Moore, J.K., Holmes, A., Umezu, K., Kolodner, R.D., and Haber, J.E. (1998). Saccharomyces Ku70, mre11/rad50 and RPA proteins regulate adaptation to G2/M arrest after DNA damage. Cell *94*, 399-409.
Lemontt, J.F. (1971a). Mutants of yeast defective in mutation induced by ultraviolet light. Genetics *68*, 21-33.
Lemontt, J.F. (1971b). Pathways of ultraviolet mutability in Saccharomyces cerevisiae. II. The effect of rev genes on recombination. Mutat Res *13*, 319-326.
Lengsfeld, B.M., Rattray, A.J., Bhaskara, V., Ghirlando, R., and Paull, T.T. (2007). Sae2 is an endonuclease that processes hairpin DNA cooperatively with the Mre11/Rad50/Xrs2 complex. Mol Cell *28*, 638-651.
Lett, J.T., Stacey, K.A., and Alexander, P. (1961). Crosslinking of dry deoxyribonucleic acids by electrons. Radiat Res *14*, 349-362.
Li, Z., Xiao, W., McCormick, J.J., and Maher, V.M. (2002). Identification of a protein essential for a major pathway used by human cells to avoid UV- induced DNA damage. Proc Natl Acad Sci U S A *99*, 4459-4464.
Liang, F., and Jasin, M. (1996). Ku80-deficient cells exhibit excess degradation of extrachromosomal DNA. J Biol Chem *271*, 14405-14411.
Liberi, G., Maffioletti, G., Lucca, C., Chiolo, I., Baryshnikova, A., Cotta-Ramusino, C., Lopes, M., Pellicioli, A., Haber, J.E., and Foiani, M. (2005). Rad51-dependent DNA structures accumulate at damaged replication forks in sgs1 mutants defective in the yeast ortholog of BLM RecQ helicase. Genes Dev *19*, 339-350.
Liberti, S.E., and Rasmussen, L.J. (2004). Is hEXO1 a cancer predisposing gene? Mol Cancer Res *2*, 427-432.
Liefshitz, B., Steinlauf, R., Friedl, A., Eckardt-Schupp, F., and Kupiec, M. (1998). Genetic interactions between mutants of the 'error-prone' repair group of Saccharomyces cerevisiae and their effect on recombination and mutagenesis. Mutat Res *407*, 135-145.

Limbo, O., Chahwan, C., Yamada, Y., de Bruin, R.A., Wittenberg, C., and Russell, P. (2007). Ctp1 is a cell-cycle-regulated protein that functions with Mre11 complex to control double-strand break repair by homologous recombination. Mol Cell *28*, 134-146.

Lin, Q., Clark, A.B., McCulloch, S.D., Yuan, T., Bronson, R.T., Kunkel, T.A., and Kucherlapati, R. (2006). Increased susceptibility to UV-induced skin carcinogenesis in polymerase eta-deficient mice. Cancer Res *66*, 87-94.

Lindahl, T. (1993). Instability and decay of the primary structure of DNA. Nature *362*, 709-715.

Lisby, M., Barlow, J.H., Burgess, R.C., and Rothstein, R. (2004). Choreography of the DNA damage response: spatiotemporal relationships among checkpoint and repair proteins. Cell *118*, 699-713.

Little, J.W. (1984). Autodigestion of lexA and phage lambda repressors. Proc Natl Acad Sci U S A *81*, 1375-1379.

Little, J.W., Mount, D.W., and Yanisch-Perron, C.R. (1981). Purified lexA protein is a repressor of the recA and lexA genes. Proc Natl Acad Sci U S A *78*, 4199-4203.

Lobachev, K.S., Gordenin, D.A., and Resnick, M.A. (2002). The Mre11 complex is required for repair of hairpin-capped double-strand breaks and prevention of chromosome rearrangements. Cell *108*, 183-193.

Loeb, L.A., and Preston, B.D. (1986). Mutagenesis by apurinic/apyrimidinic sites. Annu Rev Genet *20*, 201-230.

Love, J.D., Nguyen, H.T., Or, A., Attri, A.K., and Minton, K.W. (1986). UV-induced interstrand cross-linking of d(GT)n.d(CA)n is facilitated by a structural transition. J Biol Chem *261*, 10051-10057.

Maniatis, T., Fritsch, E.F., and Sambrook, J. (1982). *Molecular cloning: A laboratory manual* (Cold Spring Harbor, New York, Cold Spring Harbor Laboratory).

Maniatis, T., Fritsch, E.F., and Sambrook, J. (1989). *Molecular cloning; A laboratory manual*, Vol Second edition (Cold Spring Harbor, New York, Cold Spring Harbor Laboratory).

Mankouri, H.W., Ngo, H.P., and Hickson, I.D. (2007). Shu proteins promote the formation of homologous recombination intermediates that are processed by Sgs1-Rmi1-Top3. Mol Biol Cell *18*, 4062-4073.

Marmur, J., and Grossman, L. (1961). Ultraviolet light induced linking of deoxyribonucleic acid strands and its reversal by photoreactivating enzyme. Proc Natl Acad Sci U S A *47*, 778-787.

Marsischky, G.T., Filosi, N., Kane, M.F., and Kolodner, R. (1996). Redundancy of Saccharomyces cerevisiae MSH3 and MSH6 in MSH2-dependent mismatch repair. Genes Dev *10*, 407-420.

Martin, V., Chahwan, C., Gao, H., Blais, V., Wohlschlegel, J., Yates, J.R., 3rd, McGowan, C.H., and Russell, P. (2006). Sws1 is a conserved regulator of homologous recombination in eukaryotic cells. EMBO J *25*, 2564-2574.

Matyskiela, M.E., Rodrigo-Brenni, M.C., and Morgan, D.O. (2009). Mechanisms of ubiquitin transfer by the anaphase-promoting complex. J Biol *8*, 92.

McKee, A.H., and Kleckner, N. (1997). A general method for identifying recessive diploid-specific mutations in Saccharomyces cerevisiae, its application to the isolation of mutants blocked at intermediate stages of meiotic prophase and characterization of a new gene SAE2. Genetics *146*, 797-816.
Mimitou, E.P., and Symington, L.S. (2008). Sae2, Exo1 and Sgs1 collaborate in DNA double-strand break processing. Nature *455*, 770-774.
Mimitou, E.P., and Symington, L.S. (2009). DNA end resection: many nucleases make light work. DNA Repair (Amst) *8*, 983-995.
Minca, E.C., and Kowalski, D. (2010). Multiple Rad5 activities mediate sister chromatid recombination to bypass DNA damage at stalled replication forks. Mol Cell *38*, 649-661.
Modrich, P., and Lahue, R. (1996). Mismatch repair in replication fidelity, genetic recombination, and cancer biology. Annu Rev Biochem *65*, 101-133.
Moldovan, G.L., Pfander, B., and Jentsch, S. (2006). PCNA controls establishment of sister chromatid cohesion during S phase. Mol Cell *23*, 723-732.
Myung, K., Datta, A., Chen, C., and Kolodner, R.D. (2001). SGS1, the Saccharomyces cerevisiae homologue of BLM and WRN, suppresses genome instability and homeologous recombination. Nat Genet *27*, 113-116.
Nakai, S., and Matsumoto, S. (1967). Two types of radiation-sensitive mutant in yeast. Mutat Res *4*, 129-136.
Nelms, B.E., Maser, R.S., MacKay, J.F., Lagally, M.G., and Petrini, J.H. (1998). In situ visualization of DNA double-strand break repair in human fibroblasts. Science *280*, 590-592.
Nelson, J.R., Lawrence, C.W., and Hinkle, D.C. (1996a). Deoxycytidyl transferase activity of yeast REV1 protein. Nature *382*, 729-731.
Nelson, J.R., Lawrence, C.W., and Hinkle, D.C. (1996b). Thymine-thymine dimer bypass by yeast DNA polymerase zeta. Science *272*, 1646-1649.
Niu, H., Chung, W.H., Zhu, Z., Kwon, Y., Zhao, W., Chi, P., Prakash, R., Seong, C., Liu, D., Lu, L., *et al.* (2010). Mechanism of the ATP-dependent DNA end-resection machinery from Saccharomyces cerevisiae. Nature *467*, 108-111.
Njagi, G.D., and Kilbey, B.J. (1982). cdc7-1 a temperature sensitive cell-cycle mutant which interferes with induced mutagenesis in Saccharomyces cerevisiae. Mol Gen Genet *186*, 478-481.
Oakley, T.J., Goodwin, A., Chakraverty, R.K., and Hickson, I.D. (2002). Inactivation of homologous recombination suppresses defects in topoisomerase III-deficient mutants. DNA Repair (Amst) *1*, 463-482.
Pages, V., Bresson, A., Acharya, N., Prakash, S., Fuchs, R.P., and Prakash, L. (2008a). Requirement of Rad5 for DNA polymerase zeta-dependent translesion synthesis in Saccharomyces cerevisiae. Genetics *180*, 73-82.
Pages, V., Johnson, R.E., Prakash, L., and Prakash, S. (2008b). Mutational specificity and genetic control of replicative bypass of an abasic site in yeast. Proc Natl Acad Sci U S A *105*, 1170-1175.

Paques, F., and Haber, J.E. (1999). Multiple pathways of recombination induced by double-strand breaks in Saccharomyces cerevisiae. Microbiol Mol Biol Rev *63*, 349-404.
Paull, T.T., and Gellert, M. (1998). The 3' to 5' exonuclease activity of Mre 11 facilitates repair of DNA double-strand breaks. Mol Cell *1*, 969-979.
Paull, T.T., and Gellert, M. (1999). Nbs1 potentiates ATP-driven DNA unwinding and endonuclease cleavage by the Mre11/Rad50 complex. Genes Dev *13*, 1276-1288.
Pause, A., and Sonenberg, N. (1992). Mutational analysis of a DEAD box RNA helicase: the mammalian translation initiation factor eIF-4A. EMBO J *11*, 2643-2654.
Pearlman, D.A., Holbrook, S.R., Pirkle, D.H., and Kim, S.H. (1985). Molecular models for DNA damaged by photoreaction. Science *227*, 1304-1308.
Peng, J., Schwartz, D., Elias, J.E., Thoreen, C.C., Cheng, D., Marsischky, G., Roelofs, J., Finley, D., and Gygi, S.P. (2003). A proteomics approach to understanding protein ubiquitination. Nat Biotechnol *21*, 921-926.
Pessoa-Brandao, L., and Sclafani, R.A. (2004). CDC7/DBF4 functions in the translesion synthesis branch of the RAD6 epistasis group in Saccharomyces cerevisiae. Genetics *167*, 1597-1610.
Pickart, C.M. (1997). Targeting of substrates to the 26S proteasome. FASEB J *11*, 1055-1066.
Povirk, L.F. (1996). DNA damage and mutagenesis by radiomimetic DNA-cleaving agents: bleomycin, neocarzinostatin and other enediynes. Mutat Res *355*, 71-89.
Prakash, L. (1981). Characterization of postreplication repair in Saccharomyces cerevisiae and effects of rad6, rad18, rev3 and rad52 mutations. Mol Gen Genet *184*, 471-478.
Prakash, S., Sung, P., and Prakash, L. (1993). DNA repair genes and proteins of Saccharomyces cerevisiae. Annu Rev Genet *27*, 33-70.
Prinz, S., Amon, A., and Klein, F. (1997). Isolation of COM1, a new gene required to complete meiotic double-strand break-induced recombination in Saccharomyces cerevisiae. Genetics *146*, 781-795.
Prise, K.M., Folkard, M., Newman, H.C., and Michael, B.D. (1994). Effect of radiation quality on lesion complexity in cellular DNA. Int J Radiat Biol *66*, 537-542.
Prolla, T.A., Christie, D.M., and Liskay, R.M. (1994a). Dual requirement in yeast DNA mismatch repair for MLH1 and PMS1, two homologs of the bacterial mutL gene. Mol Cell Biol *14*, 407-415.
Prolla, T.A., Pang, Q., Alani, E., Kolodner, R.D., and Liskay, R.M. (1994b). MLH1, PMS1, and MSH2 interactions during the initiation of DNA mismatch repair in yeast. Science *265*, 1091-1093.
Rabitsch, K.P., Toth, A., Galova, M., Schleiffer, A., Schaffner, G., Aigner, E., Rupp, C., Penkner, A.M., Moreno-Borchart, A.C., Primig, M., *et al.* (2001). A screen for genes required for meiosis and spore formation based on whole-genome expression. Curr Biol *11*, 1001-1009.
Reenan, R.A., and Kolodner, R.D. (1992). Characterization of insertion mutations in the Saccharomyces cerevisiae MSH1 and MSH2 genes: evidence for separate mitochondrial and nuclear functions. Genetics *132*, 975-985.

Richmond, E., and Peterson, C.L. (1996). Functional analysis of the DNA-stimulated ATPase domain of yeast SWI2/SNF2. Nucleic Acids Res *24*, 3685-3692.
Roche, H., Gietz, R.D., and Kunz, B.A. (1994). Specificity of the yeast rev3 delta antimutator and REV3 dependency of the mutator resulting from a defect (rad1 delta) in nucleotide excision repair. Genetics *137*, 637-646.
Rong, L., and Klein, H.L. (1993). Purification and characterization of the SRS2 DNA helicase of the yeast Saccharomyces cerevisiae. J Biol Chem *268*, 1252-1259.
Ross-Macdonald, P., and Roeder, G.S. (1994). Mutation of a meiosis-specific MutS homolog decreases crossing over but not mismatch correction. Cell *79*, 1069-1080.
Sancar, A. (2003). Structure and function of DNA photolyase and cryptochrome blue-light photoreceptors. Chem Rev *103*, 2203-2237.
Sarasin, A.R., and Hanawalt, P.C. (1980). Replication of ultraviolet-irradiated simian virus 40 in monkey kidney cells. J Mol Biol *138*, 299-319.
Sartori, A.A., Lukas, C., Coates, J., Mistrik, M., Fu, S., Bartek, J., Baer, R., Lukas, J., and Jackson, S.P. (2007). Human CtIP promotes DNA end resection. Nature *450*, 509-514.
Segal, A.W., and Shatwell, K.P. (1997). The NADPH oxidase of phagocytic leukocytes. Ann N Y Acad Sci *832*, 215-222.
Sherman, F., Fink, G.R., and Hicks, J. (1983). (Cold Spring Harbor, NY: Cold Spring Harbor Laboratory Press.).
Shibutani, S., Takeshita, M., and Grollman, A.P. (1991). Insertion of specific bases during DNA synthesis past the oxidation-damaged base 8-oxodG. Nature *349*, 431-434.
Shor, E., Gangloff, S., Wagner, M., Weinstein, J., Price, G., and Rothstein, R. (2002). Mutations in homologous recombination genes rescue top3 slow growth in Saccharomyces cerevisiae. Genetics *162*, 647-662.
Shor, E., Weinstein, J., and Rothstein, R. (2005). A genetic screen for top3 suppressors in Saccharomyces cerevisiae identifies SHU1, SHU2, PSY3 and CSM2: four genes involved in error-free DNA repair. Genetics *169*, 1275-1289.
Smith, S., Hwang, J.Y., Banerjee, S., Majeed, A., Gupta, A., and Myung, K. (2004). Mutator genes for suppression of gross chromosomal rearrangements identified by a genome-wide screening in Saccharomyces cerevisiae. Proc Natl Acad Sci U S A *101*, 9039-9044.
Spence, J., Gali, R.R., Dittmar, G., Sherman, F., Karin, M., and Finley, D. (2000). Cell cycle-regulated modification of the ribosome by a variant multiubiquitin chain. Cell *102*, 67-76.
Spence, J., Sadis, S., Haas, A.L., and Finley, D. (1995). A ubiquitin mutant with specific defects in DNA repair and multiubiquitination. Mol Cell Biol *15*, 1265-1273.
St Onge, R.P., Mani, R., Oh, J., Proctor, M., Fung, E., Davis, R.W., Nislow, C., Roth, F.P., and Giaever, G. (2007). Systematic pathway analysis using high-resolution fitness profiling of combinatorial gene deletions. Nat Genet *39*, 199-206.

Steininger, S., Ahne, F., Winkler, K., Kleinschmidt, A., Eckardt-Schupp, F., and Moertl, S. A novel function for the Mre11-Rad50-Xrs2 complex in base excision repair. Nucleic Acids Res *38*, 1853-1865.

Steininger, S., Gomez-Paramio, I., Braselmann, H., Fellerhoff, B., Dittberner, D., Eckardt-Schupp, F., and Moertl, S. (2008). Xrs2 facilitates crossovers during DNA double-strand gap repair in yeast. DNA Repair (Amst) *7*, 1563-1577.

Stelter, P., and Ulrich, H.D. (2003). Control of spontaneous and damage-induced mutagenesis by SUMO and ubiquitin conjugation. Nature *425*, 188-191.

Sun, L., and Chen, Z.J. (2004). The novel functions of ubiquitination in signaling. Curr Opin Cell Biol *16*, 119-126.

Sung, P., Prakash, S., and Prakash, L. (1990). Mutation of cysteine-88 in the Saccharomyces cerevisiae RAD6 protein abolishes its ubiquitin-conjugating activity and its various biological functions. Proc Natl Acad Sci U S A *87*, 2695-2699.

Sutherland, B.M., Bennett, P.V., Sutherland, J.C., and Laval, J. (2002). Clustered DNA damages induced by x rays in human cells. Radiat Res *157*, 611-616.

Swanson, R.L., Morey, N.J., Doetsch, P.W., and Jinks-Robertson, S. (1999). Overlapping specificities of base excision repair, nucleotide excision repair, recombination, and translesion synthesis pathways for DNA base damage in Saccharomyces cerevisiae. Mol Cell Biol *19*, 2929-2935.

Symington, L.S. (2002). Role of RAD52 epistasis group genes in homologous recombination and double-strand break repair. Microbiol Mol Biol Rev *66*, 630-670, table of contents.

Tishkoff, D.X., Boerger, A.L., Bertrand, P., Filosi, N., Gaida, G.M., Kane, M.F., and Kolodner, R.D. (1997). Identification and characterization of Saccharomyces cerevisiae EXO1, a gene encoding an exonuclease that interacts with MSH2. Proc Natl Acad Sci U S A *94*, 7487-7492.

Tittel-Elmer, M., Alabert, C., Pasero, P., and Cobb, J.A. (2009). The MRX complex stabilizes the replisome independently of the S phase checkpoint during replication stress. EMBO J *28*, 1142-1156.

Tomita, K., Matsuura, A., Caspari, T., Carr, A.M., Akamatsu, Y., Iwasaki, H., Mizuno, K., Ohta, K., Uritani, M., Ushimaru, T., *et al.* (2003). Competition between the Rad50 complex and the Ku heterodimer reveals a role for Exo1 in processing double-strand breaks but not telomeres. Mol Cell Biol *23*, 5186-5197.

Tong, A.H., and Boone, C. (2006). Synthetic genetic array analysis in Saccharomyces cerevisiae. Methods Mol Biol *313*, 171-192.

Tong, A.H., Evangelista, M., Parsons, A.B., Xu, H., Bader, G.D., Page, N., Robinson, M., Raghibizadeh, S., Hogue, C.W., Bussey, H., *et al.* (2001). Systematic genetic analysis with ordered arrays of yeast deletion mutants. Science *294*, 2364-2368.

Tran, P.T., Erdeniz, N., Symington, L.S., and Liskay, R.M. (2004). EXO1-A multi-tasking eukaryotic nuclease. DNA Repair (Amst) *3*, 1549-1559.

Tran, P.T., Fey, J.P., Erdeniz, N., Gellon, L., Boiteux, S., and Liskay, R.M. (2007). A mutation in EXO1 defines separable roles in DNA mismatch repair and post-replication repair. DNA Repair (Amst) *6*, 1572-1583.

Trujillo, K.M., and Sung, P. (2001). DNA structure-specific nuclease activities in the Saccharomyces cerevisiae Rad50*Mre11 complex. J Biol Chem *276*, 35458-35464.

Tsukamoto, Y., Mitsuoka, C., Terasawa, M., Ogawa, H., and Ogawa, T. (2005). Xrs2p regulates Mre11p translocation to the nucleus and plays a role in telomere elongation and meiotic recombination. Mol Biol Cell *16*, 597-608.

Tsukuda, T., Fleming, A.B., Nickoloff, J.A., and Osley, M.A. (2005). Chromatin remodelling at a DNA double-strand break site in Saccharomyces cerevisiae. Nature *438*, 379-383.

Tsuzuki, T., Fujii, Y., Sakumi, K., Tominaga, Y., Nakao, K., Sekiguchi, M., Matsushiro, A., Yoshimura, Y., and MoritaT (1996). Targeted disruption of the Rad51 gene leads to lethality in embryonic mice. Proc Natl Acad Sci U S A *93*, 6236-6240.

Ulrich, H.D. (2001). The srs2 suppressor of UV sensitivity acts specifically on the RAD5- and MMS2-dependent branch of the RAD6 pathway. Nucleic Acids Res *29*, 3487-3494.

Ulrich, H.D. (2002). Degradation or maintenance: actions of the ubiquitin system on eukaryotic chromatin. Eukaryot Cell *1*, 1-10.

Ulrich, H.D. (2003). Protein-protein interactions within an E2-RING finger complex. Implications for ubiquitin-dependent DNA damage repair. J Biol Chem *278*, 7051-7058.

Ulrich, H.D., and Jentsch, S. (2000). Two RING finger proteins mediate cooperation between ubiquitin-conjugating enzymes in DNA repair. EMBO J *19*, 3388-3397.

van Brabant, A.J., Ye, T., Sanz, M., German, I.J., Ellis, N.A., and Holloman, W.K. (2000). Binding and melting of D-loops by the Bloom syndrome helicase. Biochemistry *39*, 14617-14625.

Vance, J.R., and Wilson, T.E. (2001). Repair of DNA strand breaks by the overlapping functions of lesion-specific and non-lesion-specific DNA 3' phosphatases. Mol Cell Biol *21*, 7191-7198.

Vazquez-Torres, A., Fantuzzi, G., Edwards, C.K., 3rd, Dinarello, C.A., and Fang, F.C. (2001). Defective localization of the NADPH phagocyte oxidase to Salmonella-containing phagosomes in tumor necrosis factor p55 receptor-deficient macrophages. Proc Natl Acad Sci U S A *98*, 2561-2565.

Veaute, X., Jeusset, J., Soustelle, C., Kowalczykowski, S.C., Le Cam, E., and Fabre, F. (2003). The Srs2 helicase prevents recombination by disrupting Rad51 nucleoprotein filaments. Nature *423*, 309-312.

Walker, G.C. (1995). SOS-regulated proteins in translesion DNA synthesis and mutagenesis. Trends Biochem Sci *20*, 416-420.

Wallace, S.S. (2002). Biological consequences of free radical-damaged DNA bases. Free Radic Biol Med *33*, 1-14.

Wang, T.F., Kleckner, N., and Hunter, N. (1999). Functional specificity of MutL homologs in yeast: evidence for three Mlh1-based heterocomplexes with distinct roles during meiosis in recombination and mismatch correction. Proc Natl Acad Sci U S A *96*, 13914-13919.

Wasko, B.M., Holland, C.L., Resnick, M.A., and Lewis, L.K. (2009). Inhibition of DNA double-strand break repair by the Ku heterodimer in mrx mutants of Saccharomyces cerevisiae. DNA Repair (Amst) *8*, 162-169.

Watt, P.M., Louis, E.J., Borts, R.H., and Hickson, I.D. (1995). Sgs1: a eukaryotic homolog of E. coli RecQ that interacts with topoisomerase II in vivo and is required for faithful chromosome segregation. Cell *81*, 253-260.

Wilkinson, K.D. (1997). Regulation of ubiquitin-dependent processes by deubiquitinating enzymes. FASEB J *11*, 1245-1256.

Williams, R.S., Williams, J.S., and Tainer, J.A. (2007). Mre11-Rad50-Nbs1 is a keystone complex connecting DNA repair machinery, double-strand break signaling, and the chromatin template. Biochem Cell Biol *85*, 509-520.

Williamson, M.S., Game, J.C., and Fogel, S. (1985). Meiotic gene conversion mutants in Saccharomyces cerevisiae. I. Isolation and characterization of pms1-1 and pms1-2. Genetics *110*, 609-646.

Wiltrout, M.E., and Walker, G.C. (2010). The DNA Polymerase Activity of Saccharomyces cerevisiae Rev1 is Biologically Significant. Genetics.

Wittschieben, J., Shivji, M.K., Lalani, E., Jacobs, M.A., Marini, F., Gearhart, P.J., Rosewell, I., Stamp, G., and Wood, R.D. (2000). Disruption of the developmentally regulated Rev3l gene causes embryonic lethality. Curr Biol *10*, 1217-1220.

Woodgate, R., Rajagopalan, M., Lu, C., and Echols, H. (1989). UmuC mutagenesis protein of Escherichia coli: purification and interaction with UmuD and UmuD'. Proc Natl Acad Sci U S A *86*, 7301-7305.

Wright, A.P., Bruns, M., and Hartley, B.S. (1989). Extraction and rapid inactivation of proteins from Saccharomyces cerevisiae by trichloroacetic acid precipitation. Yeast *5*, 51-53.

Wu, H.I., Brown, J.A., Dorie, M.J., Lazzeroni, L., and Brown, J.M. (2004). Genome-wide identification of genes conferring resistance to the anticancer agents cisplatin, oxaliplatin, and mitomycin C. Cancer Res *64*, 3940-3948.

Wu, L., and Hickson, I.D. (2003). The Bloom's syndrome helicase suppresses crossing over during homologous recombination. Nature *426*, 870-874.

Xiao, W., Chow, B.L., Broomfield, S., and Hanna, M. (2000). The Saccharomyces cerevisiae RAD6 group is composed of an error-prone and two error-free postreplication repair pathways. Genetics *155*, 1633-1641.

Xiao, W., Chow, B.L., Fontanie, T., Ma, L., Bacchetti, S., Hryciw, T., and Broomfield, S. (1999). Genetic interactions between error-prone and error-free postreplication repair pathways in Saccharomyces cerevisiae. Mutat Res *435*, 1-11.

Xiao, W., Chow, B.L., and Rathgeber, L. (1996). The repair of DNA methylation damage in Saccharomyces cerevisiae. Curr Genet *30*, 461-468.

Zhang, H., and Lawrence, C.W. (2005). The error-free component of the RAD6/RAD18 DNA damage tolerance pathway of budding yeast employs sister-strand recombination. Proc Natl Acad Sci U S A *102*, 15954-15959.

Zhang, H., Zhu, Z., Vidanes, G., Mbangkollo, D., Liu, Y., and Siede, W. (2001). Characterization of DNA damage-stimulated self-interaction of Saccharomyces cerevisiae checkpoint protein Rad17p. J Biol Chem *276*, 26715-26723.

Zhang, Y., Hefferin, M.L., Chen, L., Shim, E.Y., Tseng, H.M., Kwon, Y., Sung, P., Lee, S.E., and Tomkinson, A.E. (2007). Role of Dnl4-Lif1 in nonhomologous end-joining repair complex assembly and suppression of homologous recombination. Nat Struct Mol Biol *14*, 639-646.

Zhu, Z., Chung, W.H., Shim, E.Y., Lee, S.E., and Ira, G. (2008). Sgs1 helicase and two nucleases Dna2 and Exo1 resect DNA double-strand break ends. Cell *134*, 981-994.

Zou, H., and Rothstein, R. (1997). Holliday junctions accumulate in replication mutants via a RecA homolog-independent mechanism. Cell *90*, 87-96.